UNIVERSITY OF ALBERTA

Predicting the Axial Capacity of Screw Piles Installed in Western Canadian Soils

By

Kristen M. Tappenden

A thesis submitted to the Faculty of Graduate Studies and Research
in partial fulfillment of the requirements for the degree of

MASTER OF SCIENCE

In

GEOTECHNICAL ENGINEERING

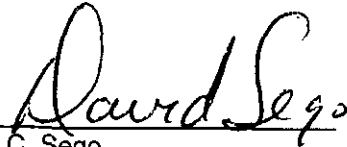**Department of Civil and Environmental Engineering**
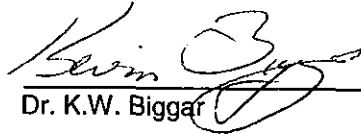
Edmonton, Alberta

Spring 2007

UNIVERSITY OF ALBERTA

Faculty of Graduate Studies and Research

The undersigned certify that they have read, and recommend to the Faculty of Graduate Studies and Research for acceptance, a thesis entitled **Predicting the Axial Capacity of Screw Piles Installed in Western Canadian Soils** submitted by **Kristen Michelle Tappenden** in partial fulfillment of the requirements for the degree of **Master of Science**.
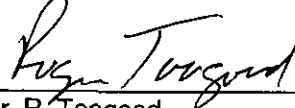
Dr. D.C. Sego

Dr. K.W. Biggar

Dr. D. Chan

Dr. M. Al-Hussein

Dr. R. Toogood

UNIVERSITY OF ALBERTA

Library Release Form

Name of Author: Kristen Michelle Tappenden

Title of Thesis: Predicting the Axial Capacity of Screw Piles Installed in Western Canadian Soils

Degree: Master of Science

Year this Degree Granted: 2007

_____

Abstract

Screw piles are deep foundations constructed of one or more steel helical plates affixed to a central steel shaft, embedded into the ground by the application of a turning moment to the pile head. This thesis evaluates the effectiveness of the LCPC direct pile design method and selected empirical torque correlations for predicting the capacity of screw piles loaded in static axial tension and compression. The results of 29 full-scale axial load tests conducted on screw piles installed in Western Canada are presented. The LCPC method is applied in conjunction with the results of site-specific cone penetration testing to 23 of the 29 documented screw piles, and empirical correlations of installation torque to ultimate axial capacity are examined for all 29 test piles. In addition, a light-weight apparatus is presented for conducting cone penetration tests in softer soils, as an alternative to commercial rig-mounted equipment.

Acknowledgments

Table of Contents

List of Tables

List of Figures

List of Symbols

a	constant equal to 1.5 times the pile diameter (LCPC method), m
A	surface area of helical plate (screw blade), m^2
C1, C2, etc.	designation for screw pile load-tested in compression
c_1	slope of straight line through data points (Brinch-Hansen method), $kN^{-1} \cdot mm^{-1/2}$
c_2	y-intercept of straight line through data points (Brinch-Hansen method), $kN^{-1} \cdot mm^{1/2}$
D	average helix diameter, m
d	diameter of screw pile shaft, m
D_1	diameter of first (uppermost) helix, m
D_2	diameter of second helix, located beneath first helix, m
D_3	diameter of third helix, located beneath second helix, m
D_p	pile diameter (LCPC method), m
f_s	sleeve friction measured by cone penetration test, kPa
F_t	non-dimensional torque factor
H	embedment depth (depth of uppermost helix below ground surface), m
h	piezometric head measured by cone penetration test, m
H/D_1	embedment ratio
H_{eff}	effective shaft length, m
k_c	penetrometer bearing capacity factor (LCPC method)
K_t	empirical torque correlation factor, m^{-1}
l_i	thickness of the layer i (LCPC method), m
$(N_1)_{60}$	corrected SPT blow count
N_k	empirical cone factor
N_q	empirical bearing capacity factor
N_u	empirical uplift capacity factor
p	pitch of the helical plate (screw blade), m

q_c	tip resistance measured by cone penetration test, kPa
q_c	uncorrected tip resistance obtained from a cone penetration test (CPT), kPa
q_{ca}	equivalent cone tip resistance at the depth of the pile point (LCPC method), kPa
q'_{ca}	mean value of the cone tip resistance, q_c, averaged over a length of $+a$ above the location of the pile tip to a distance of $-a$ below the pile tip (LCPC method), kPa
Q_L	*ultimate axial pile capacity predicted by the LCPC direct design method, kN*
Q_L^F	ultimate (limit) resistance along the pile shaft, kN
Q_L^P	ultimate (limit) resistance under the pile point, kN
Q_P	ultimate axial screw pile capacity predicted by the non-dimensional torque correlation of Ghaly and Hanna (1991), kN
q_{si}	limit unit skin friction at the depth of the layer i (LCPC method), kN/m^2
q_{smax}	maximum limit unit skin friction allowable at depth of layer i (LCPC method), kN/m^2
Q_T	ultimate axial screw pile capacity predicted by direct correlation with the required installation torque, kN
Q_u	ultimate axial screw pile capacity determined from full-scale load test, kN
R_f	friction ratio measured by cone penetration test, equal to $f_s/q_c \cdot 100\%$
S	spacing between adjacent helical plates, m
S/D	interhelix spacing ratio
s_u	undrained shear strength, kPa
T	screw pile installation torque, $kN \cdot m$
T1, T2, etc.	designation for screw pile load-tested in tension
Δ_u	*pile head movement at failure (Brinch-Hansen method), mm*
π	the constant, pi (approximately equal to 3.14159)
σ_{vo}	total in-situ vertical stress, kPa
γ	unit weight of soil, kN/m^3

1 Introduction

1.1 General Description of Screw Piles and Their Uses

Screw piles, also known as helical piles or screw anchors, are structural, deep foundation elements used to provide stability against forces exerted by axial compression, tension, and/or lateral loading (Bradka 1997). They consist of one or more circular, helical plates affixed to a central shaft of smaller diameter. For screw piles with multiple helices, the helices may be of equal diameters or have diameters tapered towards the pile tip. Screw piles are usually fabricated from steel, and may be galvanized for extra protection against corrosion. The helices are generally attached to the shaft by welding, but may also be bolted to, riveted to, or monolithically made with the shaft (Bradka 1997). Representative photographs of screw piles used in Western Canadian applications are shown in Figure 1-1. Screw piles are embedded into the soil by applying a turning moment to the head of the central shaft, which causes the helix or helices to penetrate the ground in a "screwing" motion. A downward force may also be applied to the screw pile during installation to facilitate the helices in "biting" into the soil and advancing the downward movement of the pile. To minimize disturbance to the soil during installation, the screw pile should be advanced into the ground at a rate of one pitch per revolution, and multiple helices should be spaced along the shaft in increments of the pitch, such that subsequent helices follow the same path as the initial helix when penetrating the ground. (Ghaly et al. 1991). Installation may be accomplished using standard truck or trailer-mounted augering equipment (Hoyt and Clemence 1989). In Western Canada, a torque head is frequently seen attached to a trailer-mounted hydraulic boom or mounted to the arm of a backhoe for installation of screw piles, as shown in Figure 1-2. Screw piles are installed in segments of length corresponding to the height of the torque head above the ground surface. If more than one length is required, additional shaft lengths are simply welded or threaded onto the pile as installation progresses. To ensure verticality of the screw pile, a level can be manually held against the central shaft during installation and hand directions given to the operator. Screw piles are typically installed to depths

of less than 10 meters, and installation usually requires only two people on a crew and approximately 30 minutes per pile.

Screw piles have traditionally been used as anchors in applications where resistance to significant uplift or lateral forces is required, such as for transmission tower and utility pole foundations, guyed tower anchorages, buried pipeline anchors, and for earth-bracing systems. In Alberta, screw piles have frequently been used in applications associated with hydrocarbon exploration, providing tensile, compressive, and lateral foundation support for drill rigs, pump jacks, pipelines, and temporary structures (Bradka 1997). While the capacity of screw piles to carry axial compression loading has historically been under-utilized, screw piles have recently begun serving in many of the same capacities as conventional concrete piles, and have been used to provide axial compression capacities in excess of 1000 kN (225,000 lbs) for permanent structures. Examples of compression-loaded screw pile projects currently under construction or recently completed in Western Canada include foundations for multi-family housing developments in Ft. St. John, British Columbia, and Saskatoon, Saskatchewan, warehouse facilities in the Alberta towns of Lamont and Hythe, and a commercial banking facility constructed in Ft. Nelson, British Columbia. Screw piles were also used as the foundation elements for an award-winning power transmission line recently constructed in Northern Alberta, near the city of Ft. McMurray. Photographs of selected structures founded on screw piles are shown in Figure 1-3.

Screw piles hold several distinct advantages over conventional piles for applications in soil conditions which permit their installation. The main advantages associated with the use of screw piles are that they can be loaded to their full capacity immediately after installation, they may be installed rapidly with very little noise or vibration, and may be installed using various sizes of lightweight equipment which makes them especially suited for use on soft or marshy terrain or in areas of restricted access, including the interior of existing buildings. Screw piles can be particularly cost-effective in cases of high groundwater tables, as dewatering is not required, and may also be removed after installation and re-used, which can create significant economic and

environmental advantages in the construction of temporary structures. Screw piles are not particularly well-suited for use in very hard or gravelly soils, and may sustain damage to the helical plates during installation under such conditions.

Screw piles can be fabricated in a wide variety of sizes and configurations, depending on the proposed application and the likely soil conditions to be encountered. Standard steel pipe sizes are used for the screw pile shaft—diameters of 11.4 cm (4 ½ in) to 32.0 cm (12 ¾ in) are typical in Western Canada. Helices in the range of 30.5 cm (12 in) to 91.4 cm (36 in) in diameter are commonly attached to the pipe shaft, usually as a single helix or in double or triple configurations; installation depths of 6 to 8 meters below ground are common. Screw piles installed in Western Canada are frequently used in oil field applications; the 11.4 cm (4 ½ in) shaft variety are commonly fitted with a 30.5 cm (12 in) helix and installed about 6 meters (20 ft) deep as support for flow lines and small buildings. Pump jacks and 400 barrel tanks are commonly founded on screw piles having a 17.8 cm (7 in) shaft fitted with a 40.6 cm (16 in) helix, installed to a depth of approximately 7.6 meters (25 ft). For larger pump jacks, compressors, and 400 to 750 barrel tanks, the screw pile shaft diameter is commonly increased to 21.9 cm (8 ⅝ in) with a 45.7 cm (18 in) helix. The small, 11.4 cm (4 ½ in) shaft screw piles affixed with one 30.5 cm (12 in) helix are also commonly used as foundations for modular homes, and commercial buildings are frequently founded on the 17.8 cm (7 in) shaft by 40.6 cm (16 in) helix variety (M. Schuhman, personal communication, 2006). The test piles investigated in this thesis are of commercially fabricated dimensions, having shaft diameters ranging from 11.4 cm (4 ½ in) to 40.6 cm (16 in), and helices between 40.0 cm (15 ¾ in) and 91.2 cm (36 in) in diameter; single-, double-, and triple-helix screw piles of both uniform and tapered helix diameters are included among the piles documented.

A review of the literature suggests that previous research regarding the engineering design of screw piles has focused mainly on predicting the pile capacity in uplift through the use of indirect theoretical approaches, or using empirical equations relating the torque required for installation to

the expected uplift capacity. As part of recent research at the University of Alberta, direct design approaches used for conventional pile design were applied to the design of screw piles, based on the results of site-specific cone penetration testing (Zhang 1999). Although of limited scope, the results of Zhang's (1999) research show promise for using cone penetration test (CPT) results to predict the capacity of screw piles loaded in tension or compression, with many calculated capacities falling within 30 percent of the actual screw pile capacities. CPT-based direct design methods are considered advantageous in that they eliminate the need for intermediate determination of soil strength properties by way of laboratory or field testing, and also remove the uncertainties related to soil sampling disturbance and soil testing under artificial laboratory conditions.

1.2 Thesis Objective and Testing Program

The objective of this thesis was to evaluate the effectiveness of the CPT-based LCPC direct design method (Bustamante and Gianeselli 1982) and selected empirical torque correlations (Ghaly and Hanna 1991; Hoyt and Clemence 1989) for predicting the capacity of screw piles loaded in static axial tension and compression. While Zhang's (1999) research touched on the use of the LCPC method for predicting axial screw pile capacity, only two test sites were considered in her work. This thesis compiles many more screw pile load test results conducted in a variety of subsurface conditions, to provide a more comprehensive indication of the validity of using the LCPC method and selected empirical torque correlations for predicting the axial capacity of screw piles. The results of 29 axial load tests are documented in this thesis, conducted on single-, double-, and triple-helix screw piles of varying geometries and lengths, installed at 10 different test sites located in the Western Canadian provinces of Alberta, Saskatchewan, and British Columbia. The varying surficial geology at each of the test sites consists mainly of glacially-derived materials typical of the Western Canadian landscape, including sand, lacustrine clay, and glacial till, as well as clay shale bedrock. Nine of the 29 screw piles tested were loaded in tension and the remaining 20 screw piles were loaded in compression, according to the "Quick Test" procedure documented in the respective ASTM standards (ASTM Designation: D1143 1981; ASTM Designation: D3689 1990). Although many of

the screw pile load tests were conducted in years prior to the undertaking of this thesis work, the detailed test results were graciously made available by the industrial companies and researchers involved. The 29 load test results will be compared with the axial capacity predictions made by the LCPC and empirical torque methods to evaluate the effectiveness of each approach.

The site investigation program within this thesis project was aimed at the procurement of cone penetration profiles at as many of the screw pile load test sites as possible, for use with the CPT-based LCPC direct design method. CPT results will be presented for seven of the 10 test sites, obtained using either commercial rig-mounted equipment, or using a light-weight modified cone penetration apparatus that was fabricated for this thesis project. The modified cone penetration apparatus was designed and tested as a portable and inexpensive alternative to commercial rig-mounted CPT equipment, for use in softer soil conditions.

1.3 Thesis Organization

The thesis is organized into seven chapters. Chapter 1 constitutes the introduction, followed by a literature review in Chapter 2, detailing failure models that have been proposed for embedded screw piles, direct and empirical approaches which may be used for screw pile design, as well as a general description of cone penetration testing (CPT) equipment and procedures, and a summary of the preliminary results obtained by Zhang (1999) regarding the adequacy of direct design methods for predicting the uniaxial capacity of screw piles installed in Alberta soils. Chapter 3 describes the fabrication and calibration of the modified cone penetration equipment that was developed for use in this thesis project as an alternative to the commercial, rig-mounted CPT equipment. Chapter 4 details the test sites where screw pile load tests and subsequent cone penetration tests were performed, describing the nature of the surficial soils within the context of the regional geology, including the detailed stratigraphy at each site where soil reports were available. The results of the cone penetration tests performed at each site are also reported in Chapter 4. Chapter 5 contains the results of the 29 screw pile load tests performed at the 10 Western Canadian test sites, including a description of the variety of screw pile geometries tested, the recorded installation torques, and the ultimate axial capacities that were measured.

Chapter 6 of the thesis presents capacity predictions for each of the test piles in tension or compression, made using the LCPC direct pile design method (Bustamante and Gianeselli 1982), and empirical torque correlations (Ghaly and Hanna 1991; Hoyt and Clemence 1989). The axial pile capacities predicted by the methods are compared to the measured pile capacities for assessing the validity of using the LCPC and torque design methods for screw piles installed in Western Canadian soils. Chapter 7 closes the thesis, with a summary of conclusions drawn from the results and recommendations for future research. Six Appendices, designated A through E, are attached to this report. In particular, Appendix A includes a compact disc containing electronically all of the raw data and subsequent calculations performed in generating this thesis report, as well as an electronic copy of the finished document.

1.4 Limitations of the Investigation

This thesis does not address the lateral load-carrying capacity of screw piles, but focuses solely on the determination of static axial (tensile or compressive) screw pile capacity. For preliminary results regarding the calculation of lateral screw pile capacity, the reader is referred to Zhang (1999). Regarding the prediction of axial screw pile capacity, the methods considered within this thesis are limited to the CPT-based direct pile design approach known as the LCPC method (Bustamante and Gianeselli 1982), and empirical torque correlation methods taken from the work of Hoyt and Clemence (1989) and Ghaly and Hanna (1991). No theoretical design methods based on the intermediate calculation of soil strength parameters are considered in this thesis, and the reader is again referred to Zhang (1999) for an overview of the available theoretical approaches.

A considerable amount of literature exists regarding various methods that have been proposed for the design of screw piles under uniaxial and lateral loading conditions. The complex load-transfer mechanism which exists between any type of pile and the surrounding soil is still not fully understood by researchers, and methods available for the design of deep foundations all contain a certain degree of empirical approximation. Therefore, full-scale load tests are periodically

required on pile installations for most projects in order to verify the predicted load-carrying capacity (Zhang 1999).

1.5   Symbols and Abbreviations

Symbols used in the text of the thesis are explained in the List of Symbols, and are defined the first time they appear in the text. The symbols used are not necessarily those used by their originator, but represent the same entities. All abbreviations are written out in full the first time they appear in the text. In general, the terms used in the thesis are as recommended by the American Society of Civil Engineers (ASCE) or by the American Society for Testing and Materials (ASTM: D653-64).

Figure 1-1: Typical Screw Piles: (a) Single-Helix; (b) Double-Helix, Galvanized
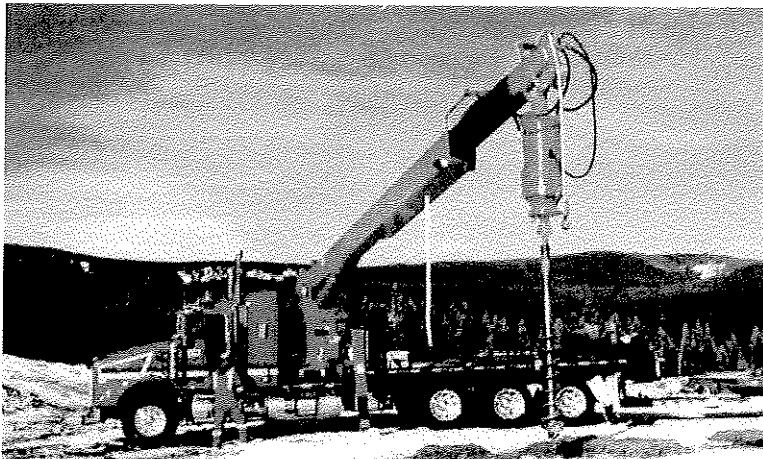
Figure 1-2: Common Methods for Screw Pile Installation: (a) Torque Head Affixed to Trailer-Mounted Hydraulic Boom; (b) Torque Head Affixed to Arm of Backhoe.
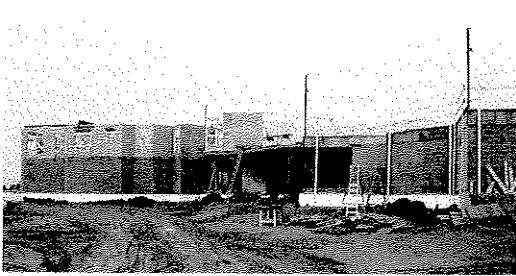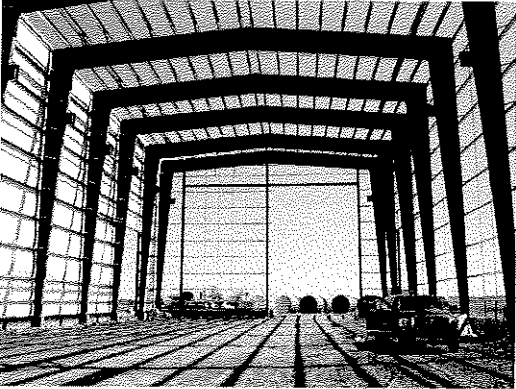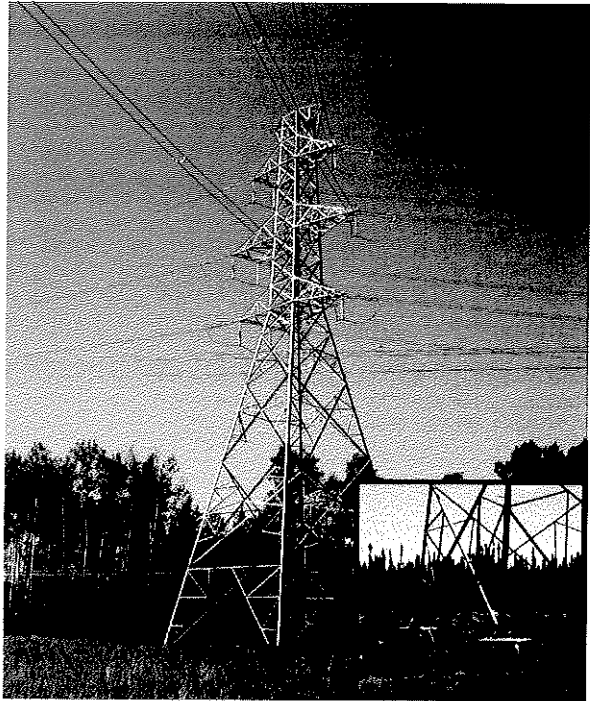
Figure 1-3: Structures Founded on Screw Piles: (a) Three-Storey Housing Complex, Under Construction in Saskatoon, Saskatchewan; (b) Warehouse Shop Facility, Under Construction in Hythe, Alberta; (c) Power Transmission Towers, Near Ft. McMurray, Alberta (With Detail of Battered Foundations Inset).

1.6 References

ASTM Designation: D1143 1981. Standard test method for piles under static axial compressive load. American Society for Testing and Materials.

ASTM Designation: D3689 1990. Standard test method for individual piles under static axial tensile load. American Society for Testing and Materials.

Bradka, T.D. 1997. Vertical Capacity of Helical Screw Anchor Piles. Masters of Engineering Report, Department of Civil and Environmental Engineering, University of Alberta, Edmonton, Alberta.

Bustamante, M., and Gianeselli, L. 1982. Pile bearing capacity prediction by means of static penetrometer CPT. *In* Proceedings of the 2nd European Symposium on Penetration Testing, ESOPT-II. Amsterdam. Balkema Publisher, Rotterdam, Vol.2, pp. 493-500.

Ghaly, A., and Hanna, A. 1991. Experimental and theoretical studies on installation torque of screw anchors. Canadian Geotechnical Journal, **28**(3): 353-364.

Ghaly, A., Hanna, A., and Hanna, M. 1991. Uplift behaviour of screw anchors in sand. I: Dry sand. Canadian Geotechnical Journal, **117**(5): 773-793.

Hoyt, R.M., and Clemence, S.P. 1989. Uplift capacity of helical anchors in soil. *In* Proceedings of the 12th International Conference on Soil Mechanics and Foundation Engineering. Rio de Janeiro, Brazil, Vol.2, pp. 1019-1022.

Zhang, D. 1999. Predicting capacity of helical screw piles in Alberta soils. M.Sc. thesis, Department of Civil and Environmental Engineering, University of Alberta, Edmonton, Alberta.

2 Literature Review

2.1 Introduction

This chapter provides background information on the current understanding of how embedded screw piles interact with the subsurface, including their mode of failure and prediction of ultimate capacity under uniaxial loading. The failure modes discussed in this chapter represent the two primary models currently established in the literature—the cylindrical shear model, and the individual plate bearing model. In terms of predicting the ultimate capacity of axially-loaded screw piles, emphasis is placed on a direct design approach rather than theoretical calculations, and the LCPC direct design method (Bustamante and Gianeselli 1982) is described in detail. The empirical torque correlations of Hoyt and Clemence (1989) and Ghaly and Hanna (1991) are also discussed. In addition, a description of standard cone penetration testing (CPT) procedures and equipment is included, as the LCPC design method is based on the results of a site-specific cone penetration profile. The modified cone penetration apparatus developed as part of this thesis project is modeled after the standard full-scale equipment and procedures, and will be described in detail in the Chapter 3.

The LCPC method is termed a direct design approach because it forgoes the need for the intermediate calculation of soil strength parameters, and directly calculates the capacity of piles from the in-situ cone penetration test. Direct design approaches therefore eliminate the time and costs associated with laboratory soil testing, and are considered by the author to be amenable to use in the screw pile industry as it currently is practiced. Screw piles are often installed over long distances in varying geologic conditions, such as for pipeline or transmission tower foundations, and therefore a design method which can directly size the pile based on an in-situ cone penetration profile is considered to be of primary interest. For an overview of the indirect, theoretical approaches which may be used to determine pile capacities based on traditional geotechnical parameters, the reader is referred to Zhang (1999).

2.2.2 Individual Plate Bearing Model

The failure model known as the individual plate bearing model describes the screw pile as a series of independent plate anchors embedded at different depths. Bearing failure is assumed to occur above or below each individual helix when the pile is loaded in tension or compression. As discussed above, the applicability of the individual plate bearing model is determined by the inter-helix spacing ratio (S/D) of the pile. The pile's capacity is considered to be the sum of the bearing capacity of the soil above each helix (in uplift) or below each helix (in compression), plus the adhesion acting along an effective shaft length above each helix. Narasimha Rao et al. (1993) suggested that above each plate, adhesion over a shaft length of 1.5D to 2.5D be considered for multi-helix screw piles installed in cohesive soil, when using the individual plate bearing method of analysis. However, based on full-scale load tests conducted on instrumented multi-helix screw piles in sand and clay, Zhang (1999) recommended an effective shaft length, H_{eff}, between adjacent helices equal to the available shaft length minus twice the helix diameter, regardless of loading direction or soil type. This reduction in the available shaft length is due to the interference caused by the formation of a compaction zone above (below) the helical plate and the formation of a hollow below (above) the helical plate when the screw pile is loaded in tension (compression).

The individual plate bearing model is an extension of earlier work done on the analysis and design of embedded plate anchors and shallow foundations subject to uplift forces (Adams and Hayes 1967; Meyerhof and Adams 1968; Vesic 1971). The method has reportedly been used in conjunction with traditional bearing capacity theory to analyze full-scale capacities of screw piles in the field. The uplift capacity of both multi-helix (Adams and Klym 1972; Hoyt and Clemence 1989; Narasimha Rao et al. 1991) and single-helix (Johnston and Ladanyi 1974) screw piles has been successfully described using the individual plate bearing model in conjunction with modified bearing capacity theory in which the empirical uplift capacity factor, N_u, replaces the bearing capacity factor, N_q, in the calculations. Hoyt and Clemence (1989) analyzed 91 load tests

conducted on multi-helix anchors with spacing ratios of S/D between 1.55 and 4.50. The ultimate pile capacities (Q_u) as determined from the load tests were compared to predicted capacities (Q_{calc}) based on the individual plate bearing model. The resulting Q_u/Q_{calc} ratios were statistically analyzed, and found to exhibit a mean value of 1.56 and a standard deviation of 1.28 (Hoyt and Clemence 1989). The above studies encompass both cohesive and cohesionless soil conditions.

2.3 Direct Methods for Screw Pile Design

Direct design methods allow the designer to take raw data obtained on-site, such as from a cone penetration test, and use it to directly design a structure, without the intermediate step of attempting to determine specific geotechnical parameters. Direct design methods, when successful, capture the nature of the soil and design the structure around the in-situ properties, avoiding the misrepresentations which may occur when soil properties used for design are determined from laboratory samples. Certain soil properties can also prove very difficult or expensive to determine, whether in the laboratory or on the site, and therefore direct design approaches hold an advantage in foregoing the need for intermediate calculation of representative soil parameters. The design strategies discussed in this section will be limited to direct design approaches which rely on information obtained from a cone penetration test (CPT). The cone penetration test is fast, repeatable, and provides a continuous soil profile from which a correlation can be made between the tip resistance and sleeve friction on the cone and the toe resistance and shaft friction on the pile. Reduction factors are applied to the measured cone penetration values when used for direct pile design, due to the differences in scale, loading rate, insertion technique, position of the CPT friction sleeve, and difference in horizontal soil displacement (Lunne et al. 1997).

There exist a number of direct methods for the design of piles which incorporate the results of cone penetration testing. The approach that will be utilized in this thesis is the LCPC method as documented by Bustamante and Gianeselli (1982). Although a number of direct approaches exist for the design of piles, the rationale for selecting the LCPC method is based on a review conducted by Lunne et al. (1997). The review compared several case studies in which the CPT

was used in conjunction with different direct design methods to predict the ultimate capacity of single piles. The authors of the case studies, including Robertson et al. (1988), Briaud (1988), Tand and Funegard (1989), and Sharp et al. (1988), all came to the same conclusion based on a substantial number of load test results—the LCPC method gave the most accurate prediction of pile load-carrying capacity, compared to the other available direct design approaches. Hence, it is the LCPC method which is chosen for discussion and subsequent use in this thesis.

2.3.1   LCPC Method

The LCPC Method is so named for the *Laboratoire Central des Ponts et Chaussees* in Paris, which was responsible for carrying out the bulk of the full-scale pile load tests on which the method was founded. The LCPC method was derived from the interpretation of 197 static loading (or extraction) tests conducted on many pile varieties, mostly of the bored or the driven type, including cast screwed piles. Almost all of the piles were installed by specialized foundation firms in accordance with the usual construction techniques of the time in order to achieve optimum results for the design of deep foundations for actual structures (Bustamante and Gianeselli 1982). Forty-eight test sites were involved in the research program, consisting of varied materials, including clay, silt, sand, gravel, and weathered rock, as well as mud, peat, weathered chalk, and marl. However, of the 39 sites at which the *Laboratoire des Ponts et Chausees* was responsible for conducting the site investigation, cone penetration testing was only performed at 21 of them. The nature of many of the soils found in France, because of their structural complexities (nodules or boulders, partial cementation) and their high degree of compactness (stiff marl or clay, gravel and weathered rock), account for the difficulties encountered in implementing the cone penetration tests (Bustamante and Gianeselli 1982).

Under the LCPC method, the calculated limit load, Q_L, of a deep foundation is taken as the sum of the limit resistance under the pile point, Q_L^P, and the limit skin friction along the height of the pile shaft, Q_L^F. Scaling coefficients are applied to a representative CPT profile of tip resistance, q_c, to obtain appropriate values of Q_L^P and Q_L^F. The cone penetration tip resistance profile is divided into layers when calculating Q_L^F, such that the skin friction along the height of the pile

shaft may be determined incrementally for multi-layered formations. The fact that the LCPC method makes use only of the cone tip resistance, q_c, for the calculation of pile capacity is generally considered to be advantageous, as the sleeve friction obtained from a CPT is often difficult to interpret and can be less reliable (Lunne et al. 1997). In the general case of a multi-layered formation for which the profile of cone tip resistance, q_c, is known, the pile point resistance and the total skin friction are calculated by equations [2-4] and [2-5], respectively (Bustamante and Gianeselli 1982):

[2-4]
$$Q_L^P = q_{ca} \cdot k_c \cdot \frac{\pi(D_p)^2}{4} \qquad (kN)$$

[2-5]
$$Q_L^F = \sum_1^i Q_{Li}^F = \sum_1^i q_{si} \cdot \pi D_p \, l_i \qquad (kN)$$

where successively,

q_{ca} is the equivalent cone tip resistance at the depth of the pile point (kN/m^2)

k_c is the penetrometer bearing capacity factor

D_p is the pile diameter (m)

q_{si} is the limit unit skin fiction at the depth of the layer i (kN/m^2)

l_i is the thickness of the layer i (m)

The unit skin friction, q_{si}, is calculated based on the average cone tip resistance measured over the height of the selected interval, divided by a scaling coefficient, α. The value of α varies between 30 and 150 for screwed or bored (uncased) piles, depending on the soil type and the magnitude of the average cone tip resistance measured over the interval depth. Table 2-1 displays the values of α for use within the LCPC Method. Additionally, the value of the unit skin friction is limited to a maximum value, q_{smax}, as shown in Table 2-1.

The unit bearing resistance at the depth of the pile point is calculated by multiplying the equivalent cone tip resistance, q_{ca}, by the scaling coefficient k_c, known as the penetrometer bearing capacity factor. The values of k_c applicable to screwed or bored (uncased) piles are

listed in Table 2-1. k_c varies between 0.30 and 0.50 depending on the soil type and measured cone tip resistance at the pile point.

The equivalent cone resistance, q_{ca}, at the depth of the pile point is determined from the CPT profile in several steps which are best carried out by a computer. First, values of the cone tip resistance, q_c, are averaged over a length of +a above the location of the pile tip to a distance of −a below the pile tip, where a is equal to 1.5 times the pile diameter. This average value is termed q'_{ca}. Next, the equivalent cone resistance, q_{ca}, is calculated after clipping the q_c profile (see Figure 2-8). This clipping is carried out so as to eliminate the values higher than $1.3·q'_{ca}$ along the distance a both above and below the pile point, while values lower than $0.7·q'_{ca}$ above the pile point are also eliminated over the length a.

The ultimate pile capacity, then, is the sum of the pile point load and the total skin friction (equations [2-4] and [2-5]). Bustamante and Gianeselli (1982) recommend that the allowable load for the pile be determined by applying a safety factor of 3 to the point resistance, and a safety factor of 2 to the skin friction.

2.3.2   Use of Direct Design Approaches in Alberta Soils

Recently, research conducted by Zhang (1999) at the University of Alberta in Edmonton, Alberta examined the accuracy of using CPT-based direct design approaches for predicting the capacities of screw piles installed at two Alberta test sites. Zhang (1999) conducted 12 full-scale load tests on instrumented screw piles installed at two sites in the Edmonton area, and compared the results with capacity predictions made using the LCPC method and another CPT-based direct design approach known as the European method. A detailed description of the European method is given by De Ruiter and Beringen (1979). Zhang (1999) conducted six load tests in tension and six load tests in compression on screw piles with geometries as shown in Figure 2-9, labeled as "short", "long", and "production" piles. At the two test sites, representing a cohesive and a cohesionless material respectively, a pile of each type was loaded to failure in tension and in compression. Figure 2-10 compares the pile capacities predicted by the LCPC method with the

actual measured capacities. In Figure 2-11, capacity predictions made by the European method are compared with the measured capacities. The cohesive material referred to in Figure 2-10 and Figure 2-11 is the Glacial Lake Edmonton sediment, which was deposited by a large proglacial lake at the close of the Wisconsin glacial period (Bayrock and Hughes 1962). The sediment generally consists of varved silts and clays, with pockets of till, sand, and sandy gravel (Godfrey 1993). The test site used by Zhang (1999) is located on the University of Alberta Farm in Edmonton, Alberta, near 115 Street and 58 Avenue. The cohesionless material referred to in Figure 2-10 and Figure 2-11 represents sand dunes of minor loess that consist of medium- to fine-grained sand with silt. The material is composed of dried sediments from Glacial Lake Edmonton, which were transported by wind and re-deposited in a nearby sand dune field after drainage of the glacial lake (Zhang 1999). The test site used by Zhang (1999) for the sand material is located outside of the town of Bruderheim, Alberta, approximately 60 km northeast of Edmonton.

The results of Zhang's (1999) work show promise for the direct design of screw piles using the LCPC and/or European methods. By selecting the appropriate failure model based on the geometry of the screw pile, the direct design method may be used in conjunction with a representative CPT profile to determine realistic values of shaft or cylindrical friction and bearing or uplift resistance for the pile. Zhang (1999) concluded that "both methods provided reasonable results with best predictions given by the LCPC method." Using the LCPC method for capacity prediction, the ratios of predicted to measured capacity reported by Zhang (1999) range from 0.70 for the short pile loaded in compression in clay to 2.26 for the short pile loaded in tension in sand. These ratios represent an under-prediction of 30 percent an over-prediction of 126 percent, respectively. The spread in the ratios of predicted to measured capacity for the screw piles tested by Zhang (1999) was well-distributed above and below the actual capacities, with the average ratio equal to 1.07. In the case of the shallow pile in tension in the sand, Zhang (1999) considered the significant over-prediction of 126 percent to most likely be the result of unreliably high cone penetration values obtained in the upper soil crust due to its dessicated state, which in

turn produced unrealistic in-situ strength predictions for the shallow pile. In contrast, at the clay site, it may be noted from Figure 2-10 that reasonable predictions of uplift capacity were made for all three screw piles using the LCPC method. It is also worth mentioning that the design of any type of pile is still not fully understood, and the complexity of the interaction between the pile and the subsurface cannot currently be described with complete confidence. In light of the significant amount of uncertainty which exists in the design of piles, whether screw piles or more conventional pile types, large safety factors are applied to the calculated capacities, and load testing of selected piles is often performed after installation, to ensure the adequacy of the piles as designed. In view then of the current state-of-the-art, the screw pile capacity predictions made by Zhang (1999) using the LCPC method (Figure 2-10) can be looked upon as holding reasonable promise.

2.4 Empirical Methods: Torque Relationship

The concept of correlating installation torque to axial capacity for screw piles is analogous to the relationship of pile driving effort to pile capacity (Hoyt and Clemence 1989). Several authors have attempted to express an empirical relationship relating the torque of installation to the ultimate screw pile capacity (Ghaly and Hanna 1991; Hoyt and Clemence 1989; Narasimha Rao et al. 1989; Perko 2000). Torque relationships have been used in the screw pile industry for many years; however, because most relate installation torque directly to pile capacity, they do not explicitly consider any geotechnical concepts or parameters, and so lack geotechnical explanation. The concept of a unique relationship between installation torque and screw pile capacity has not generally been accepted by the engineering community. The torque method is also disadvantaged by the fact that it cannot be used to predict screw pile capacity until after the installation has taken place; in other words, it is best used for on-site production control than for the actual design of piles in the office (Hoyt and Clemence 1989).

Hoyt and Clemence (1989) suggested a direct empirical relationship between installation torque and screw pile uplift capacity such that:

[2-6]
$$Q_u = K_t \cdot T$$

Where

K_t = empirical factor (m^{-1})

Q_u = uplift capacity

T = average installation torque (kN·m)

In an analysis of 91 screw pile load tests from the published literature and the authors' private file, Hoyt and Clemence (1989) obtained good approximations of ultimate axial screw pile capacities using K_t equal to 33 m^{-1} for all square shaft screw piles and round shaft piles less than 89 mm (3.5 in) in diameter, 23 m^{-1} for round shaft piles 89 mm in diameter, and 9.8 m^{-1} for round, 89-mm-diameter pile with 219 mm diameter extension shafts (extending from the top helix to the surface). The installation torque was averaged over the final distance of penetration equal to three times the largest helix diameter, and all piles were multi-helix (Hoyt and Clemence 1989). The torque relationship suggested by Hoyt and Clemence only provides empirical K_t factors for a limited selection of pile geometries, and therefore is of little practical value unless project-specific load testing is done to establish relevant empirical factors.

Two years later, Ghaly and Hanna (1991), published a more detailed relationship between the measured uplift capacity of screw piles installed in sand and the final installation torque achieved. The relationship is based on a rigorous theoretical analysis of the forces involved in resisting the insertion of the screw pile into the sand, thus determining the torque required for installation. The theory proposed for torque determination was employed in combination with experimental uplift capacity results to develop a correlation between the installation torque and the ultimate capacity of screw piles in tension. A torque factor, F_t, similar to the well-known uplift capacity factor, N_u, was introduced in order to express the installation torque in a non-dimensional form. This torque factor incorporates the three key parameters that were found to affect the installation torque magnitude: the pile geometry, the installation depth, and the unit weight of the sand (Ghaly and Hanna 1991). The torque factor, F_t, and uplift capacity factor, N_u, are defined by equations [2-7] and [2-8].

[2-7]
$$F_t = \frac{T}{\gamma A H p}$$

[2-8]
$$N_u = \frac{Q_u}{\gamma A H}$$

Where

T = installation torque measured at final pile depth (kN·m)

γ = unit weight of the sand (kN/m^3)

A = surface area of helical plate (m^2)

H = pile embedment depth (m)

p = pitch of the helix (m)

Q_u = ultimate pullout load (kN)

Ghaly and Hanna (1991) found that for all types of single-helix screw piles installed to varying depths in a range of sand deposits, there existed a unique relationship between N_u and F_t, approximated by the logarithmic equation [2-9].

[2-9]
$$N_u = 2 F_t^{(1.1)}$$

Substituting equations [2-7] and [2-8] into equation [2-9], the resulting equation may be manipulated to explicitly solve for the ultimate uplift capacity in terms of the installation torque (equation [2-10]).

[2-10]
$$Q_u = 2(\gamma A H) \left[\frac{T}{\gamma A H p} \right]^{(1.1)}$$

Equation [2-10] was developed based on the formulation of forces acting on a single-helix screw pile; however, the equation is equally applicable to the case of a multi-helix screw pile of constant diameter and pitch (Ghaly and Hanna 1991). Ghaly and Hanna (1991) explain that the distribution of forces acting on a multi-helix screw pile of constant diameter and pitch is essentially equivalent to the force distribution acting on a single-helix screw pile of the same diameter and pitch. That is, all the forces acting on the upper surface of the blade of the single-

helix screw pile are equally acting on the upper surface of the uppermost blade of the multi-helix screw pile; whereas the forces acting on the lower surface of the blade of the single-helix screw pile are equally acting on the lower surface of the lowermost blade of the multi-helix screw pile (Ghaly and Hanna 1991). The theoretical force distribution is more complex for multi-helix screw piles of tapered configurations, having either equal or variable pitch. Based on experimental findings and theoretical analysis, Ghaly and Hanna (1991) suggest that the torque value required to install a tapered, multi-helix screw pile of constant pitch is approximately 10 to 15 percent higher than the torque required to install a single-helix screw pile having the same pitch and blade diameter equal to that of the uppermost blade of multi-helix anchor. For a tapered, multi-helix screw pile of variable pitch, Ghaly and Hanna (1991) suggest that the torque value should be 10 to 15 percent lower than the value required to install a single-helix screw pile with blade diameter and pitch equal to that of the uppermost blade on the tapered pile. Thus when dealing with tapered screw piles of equal or variable pitch, the appropriate factor of increase or reduction should be applied, respectively, to the torque value used in equation [2-10]. The need for this correction vanishes for the case of a multi-helix screw pile of constant diameter and pitch (Ghaly and Hanna 1991).

2.5 Overview of the Cone Penetration Test (CPT)

2.5.1 Introduction to Cone Penetration Testing

In a cone penetration test (CPT), a cone (also called a cone penetrometer), consisting of a conical metal tip on the end of a metal cylinder, is attached to a drill rod and pushed into the ground at a constant rate as additional rods are added to the push system. Continuous or closely-spaced intermittent readings are taken of the resistance to penetration encountered by the cone as it descends into the soil. The test results provide a continuous profile of the stress acting on the conical tip due to displacement of the soil, and the friction measured on the lead segment of the rod, known as the sleeve. Pore pressure measurements, verticality of the rods, and temperature readings are also often recorded with depth. Figure 2-12 depicts a typical cone penetrometer and the associated terminology. The primary purpose of the cone penetration test is for stratigraphic logging and preliminary evaluation of geotechnical parameters (Robertson and

Campanella 1988). The results of a cone penetration test may also be used for direct design purposes, such as for determining the necessary dimensions for a deep foundation, without the need for intermediate calculation of geotechnical parameters. Within the cone penetrometer housing, resistance data is collected via load cells as the cone advances into the soil. Wiring from the load cells may be extended through the drill rods attached to the cone and delivered to a data collector at the surface. Measurements are made of the resistance to penetration of the conical tip, as well as the combined resistance to penetration of the cone tip and outer friction sleeve (subtraction cone), or of the friction sleeve resistance separately. The cone may also measure the pore pressure in the soil with the inclusion of an internal pore pressure transducer and an external porous element located at one of the three positions shown in Figure 2-13. A cone having a 10 cm^2 projected area and apex angle of 60 degrees is specified as the standard size in both the American and European Standards. The friction sleeve, located behind the conical tip, has a standard surface area of 150 cm^2 (Campanella and Robertson 1988).

The cone penetration test was first introduced in the Netherlands in 1934, and has been less-frequently referred to by several other names, including the Static Penetration Test, Quasi-static Penetration Test, Dutch Sounding Test, and Dutch Deep Sounding Test. The first electronic cone was developed in 1948 and later improved in 1971 (De Ruiter 1971; Robertson and Campanella 1988). The incorporation of a pore pressure transducer into the standard electronic cone penetrometer was achieved in the early 1980's, and the result referred to as the piezocone (Robertson and Campanella 1988). Today, cones exist which are capable of measuring inclination and temperature, in addition to tip resistance, sleeve friction, and pore pressure at several locations on the cone (Campanella and Robertson 1988). Penetration depths in excess of 100 meters have been achieved in soft soils (Robertson and Campanella 1988). Although cone penetration testing can be applied to many soil types, the system is relatively delicate and susceptible to damage by certain subsurface conditions. Gravel layers and boulders, heavily cemented zones and dense sand layers can severely restrict penetration and cause deflection and damage to the cone. The series of rods to which the cone is attached may also be in danger

of buckling when encountering a stiff layer overlain by very soft soils which are unable to provide the necessary lateral support to the rods (Robertson and Campanella 1988).

With the addition of pore pressure measurements to the CPT, the test may be more specifically referred to as the CPT(U). The addition of pore pressure readings opens up a new dimension for the interpretation of geotechnical parameters, particularly in loose or soft saturated deposits. Robertson and Campanella (1988) consider the main advantages of the CPT(U) or piezocone over the basic CPT to be:

- the ability to distinguish between drained, partially drained, and undrained penetration
- the ability to correct measured cone tip data to account for unbalanced water forces due to unequal end areas in cone design
- the ability to evaluate flow and consolidation characteristics
- the ability to assess equilibrium groundwater conditions
- improved soil profiling and identification
- improved evaluation of geotechnical parameters

At sites where the geology is variable and not well-characterized, or on high-risk projects, the CPT(U) can be used to identify critical locations and elevations at which other, more suitable in-situ tests or sampling for laboratory testing should be carried out. At sites with uniform geology that is well-understood, and for which local correlations exist between CPT(U) results and structural performance, the cone penetration test can be used alone for the direct design of structural components. However, it may still be deemed valuable to couple CPT(U) results with boreholes, sampling, and testing for one or more of the following reasons (Robertson and Campanella 1988):

- to clarify identification of soil type
- to verify local correlations
- to assist where interpretation of CPT(U) data is difficult due to partial drainage conditions or problem soils

27

- to assist in determining the effects of future changes in soil loading that are not represented by the CPT(U)

2.5.2 Standard CPT(U) Equipment and Procedures

2.5.2.1 Pushing Equipment

Rigs consisting of a hydraulic jacking system and reaction system are typically used to perform cone penetration testing. Generally, the rigs are built especially for this purpose; however the push-down of an anchored drill rig can also be used (Lunne et al., 1997). Land-based rigs are usually mounted inside of heavy duty trucks, as shown in Figure 2-14. The trucks are ballasted to a total dead weight of 150 kN or more, with power usually supplied to the jacking system through the truck motor. Screw piles can also be used as anchors to provide additional reaction, if necessary. The truck enclosure provides an ideal space for installation of all electronic equipment needed for data acquisition during the test (Lunne et al. 1997). To perform the test, the cone penetrometer is attached to a series of threaded rods which are typically pushed into the ground in 1-meter strokes, with successive push rods added after each pass. The thrust capacity required for cone testing generally varies between 100 and 200 kN, although lower capacities of 20 and 50 kN are also common for use in soft soils. A 200 kN thrust will normally result in about 30 meters of penetration in dense to medium dense sands and stiff clays, and also constitutes the maximum allowable thrust for use with standard 35.7 mm diameter high-tensile steel push rods; exceeding this load can result in buckling or damage to the rods (Lunne et al., 1997). Penetration can be increased by the installation of a friction reducer on the push rod behind the cone. The purpose is to expand the diameter of the hole created behind the advancing cone in order to reduce the friction generated between the rods and the soil. The friction reducer used, such as an expanded coupling, should be installed at 0.3 to 1.0 meters behind the cone (Lunne et al., 1997).

2.5.2.2 Dimensioning of Sleeve and Tip

Standards for cone penetration equipment duly apply to both the CPT and CPT(U) systems, as the CPT(U) is simply regarded as a basic cone with the addition of a porous element and

transducer. As previously mentioned, a cone of 10 cm^2 base area with an apex angle of 60 degrees is generally accepted as the standard for both American and European testing (ASTM Designation: D3441 1986; ISSMFE 1977). The friction sleeve, to be located directly behind the base of the cone, has a standard area of 150 cm^2. The friction sleeve and conical tip have the same diameter as the drill rods used to push the cone, which is 35.7 mm. Bonded strain gauges are most commonly used as the load cells for recording tip and sleeve resistances in electronic cone penetrometers. Experience has shown that strain gauges make for high precision load cells, in addition to their innate simplicity, ruggedness, and zero stability (Robertson and Campanella 1988).

2.5.2.3   Selection and Location of Porous Element

Measurement of pore pressures during cone penetration testing requires that careful consideration be given to the probe design, choice and location of the porous element, and method of probe saturation (Robertson and Campanella 1988). The design of the cone must be such that when stress is applied to the cone tip, the pore pressure response is not affected; it must therefore be ensured that no load is transferred from the tip to the pore pressure transducer, porous element, or fluid volume. Essential requirements for the measurement of pore pressure are to incorporate small fluid cavity, a low compressibility of saturating fluid, and a rigid or low compliance transducer. In selecting the type of porous filter element to be used, a compromise must be reached between the rapid response time provided by a highly-permeable filter and the ability of a low-permeability filter to resist air entry and maintain saturation. The filter can be made from porous plastic, ceramic, or stainless steel. A porous polypropylene filter is best able to survive adverse soil conditions such as dense sand, which can cause significant damage to a ceramic filter and clog a stainless steel filter (Robertson and Campanella 1988).

The placement of the porous filter element should also be given due consideration, as its location on the cone can have an important effect on the interpretation of the data (Robertson and Campanella 1988). No agreed standard exists for the location of the porous element, but it is usually placed at one of two locations: on the cone face or immediately behind the cone tip. Pore

pressures measured on the face of the tip are consistently 10 to 20 percent higher than those measured immediately behind the tip in normally-consolidated soft clays and silts. In fine sands and over-consolidated clays and silts, pore pressures on the face of the tip tend to be large and positive, while those measured immediately behind the tip can be considerably smaller, and even negative. No single filter location will provide information for all applications of pore pressure interpretation, and for this reason cones exist which allow the location of the porous element to be changed in the field, or which record pore pressures at both locations simultaneously (Robertson and Campanella 1988). However, locating a single pore pressure element behind the cone tip is arguably the most practical arrangement for maintaining saturation and protecting the filter from damage and abrasion. Other advantages of placement immediately behind the tip include measurements less affected by element compressibility, positioning appropriate for data correction due to the effect of unequal end areas, and procurement of good stratigraphic detail (Robertson and Campanella 1988). Regardless of where the pore pressure element is located, complete saturation of the element and the cavity are essential for the procurement of accurate measurements. Sluggish or inaccurate pore pressure readings can be the result of poorly saturated CPT(U) systems (Robertson and Campanella 1988).

Table 2-1: Scaling Coefficients for Use in LCPC Method (after Bustamante and Gianeselli 1982)

Soil Type	Average CPT tip resistance over layer i q_c (kPa)	Bearing capacity factor k_c	Skin friction factor α	Maximum unit skin friction q_{smax} (kPa)
Soft clay and mud	<1,000	0.50	30	15
Moderately compact clay	1,000 to 5,000	0.45	40	35
Silt and loose sand	≤ 5,000	0.50	60	35
Compact to stiff clay and compact silt	> 5,000	0.55	60	35
Soft chalk	≤ 5,000	0.30	100	35
Moderately compact sand and gravel	5,000 to 12,000	0.50	100	80
Weathered to fragmented chalk	> 5,000	0.40	60	120
Compact to very compact sand and gravel	12,000	0.40	150	120
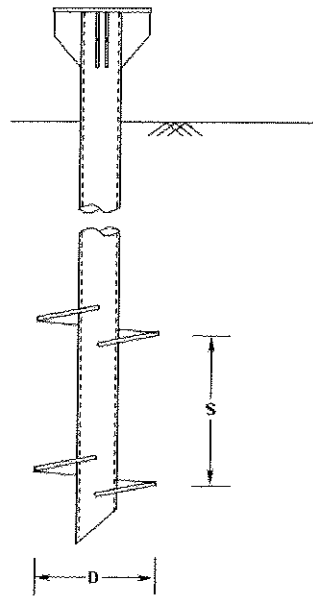
Figure 2-1: Illustration of Geometrical Parameters S (Inter-Helix Spacing) and D (Helix Diameter)
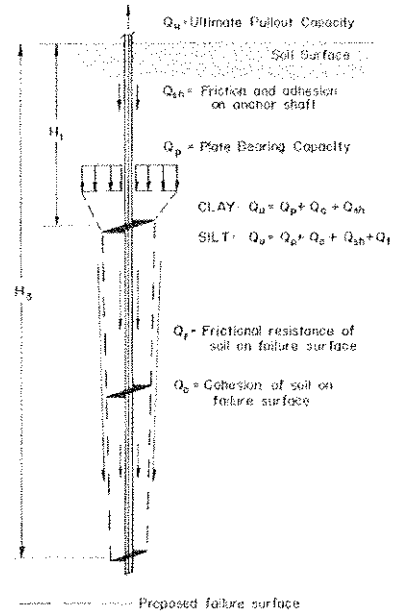
Figure 2-2: Cylindrical Failure Model for Screw Pile in Uplift (Mooney et al. 1985)

(a)　　　　　　　　(b)　　　　　　　　(c)
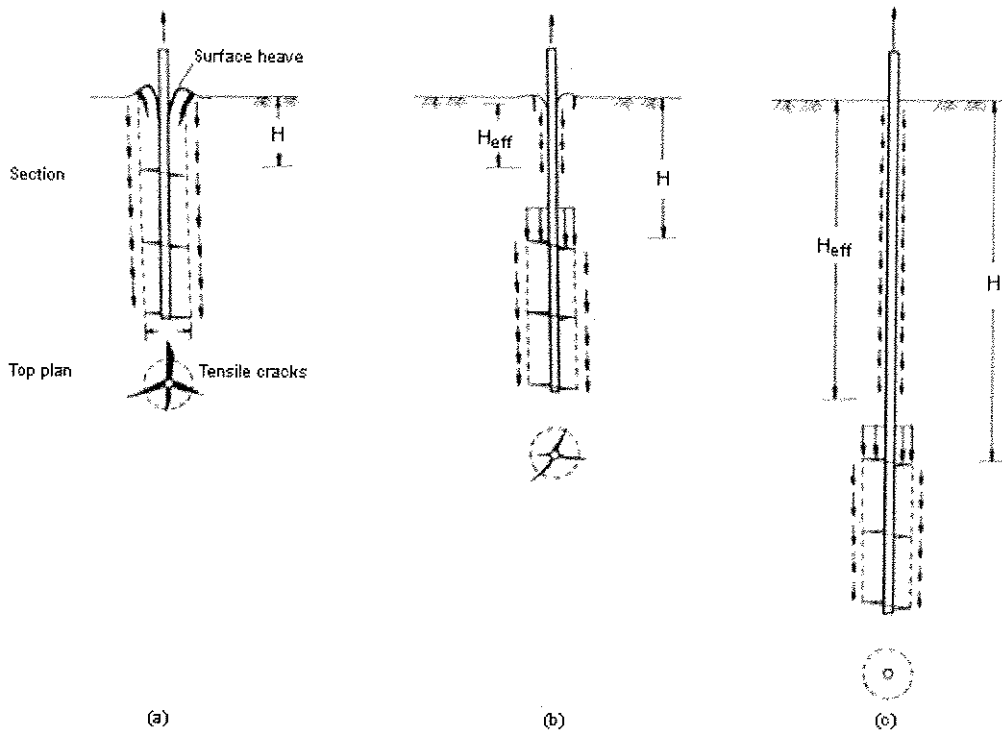
Figure 2-3: Behavior of Screw Pile in Tension at Various Embedment Ratios in Clay: (a) Shallow; (b) Transition; (c) Deep. (Narasimha Rao et al. 1993)
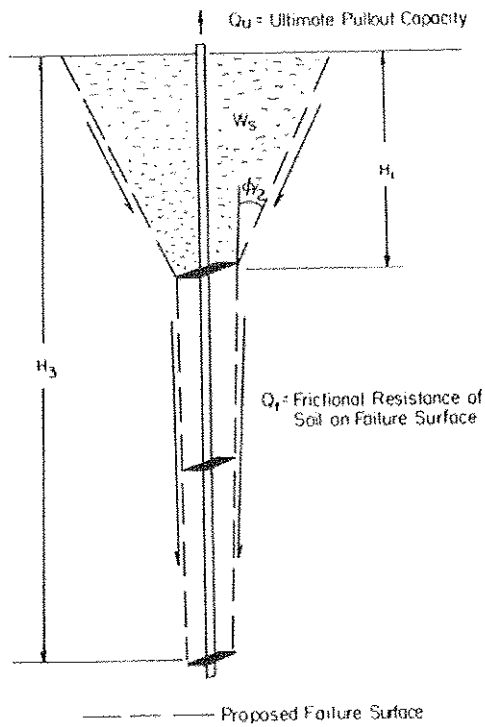
Figure 2-4: Failure Surface for Shallow Multi-Helix Screw Pile Under Uplift in Sand (Mitsch and Clemence 1985)
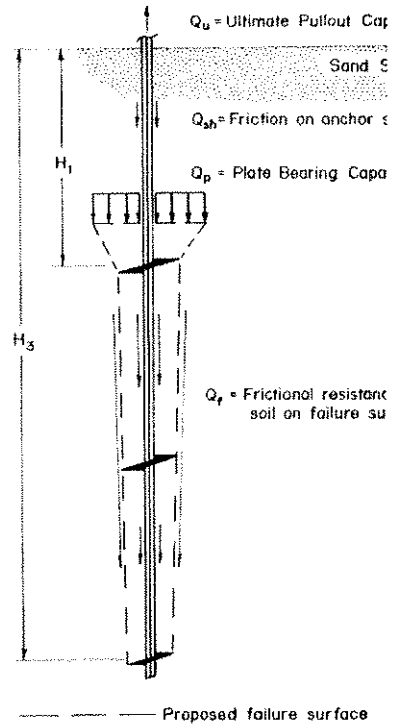
Figure 2-5: Failure Surface for Deep Multi-Helix Screw Pile Under Uplift in Sand (Mitsch and Clemence 1985)
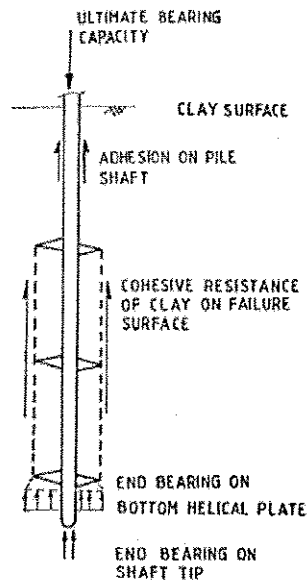
Figure 2-6: Cylindrical Shear Model for Screw Pile in Compression (Narasimha Rao et al. 1991)

33

Figure 2-7: Pulled-Out Model Screw Piles With Spacing Ratios (L-R) of 1.5, 2.3, and 4.6 (Narasimha Rao et al. 1989)
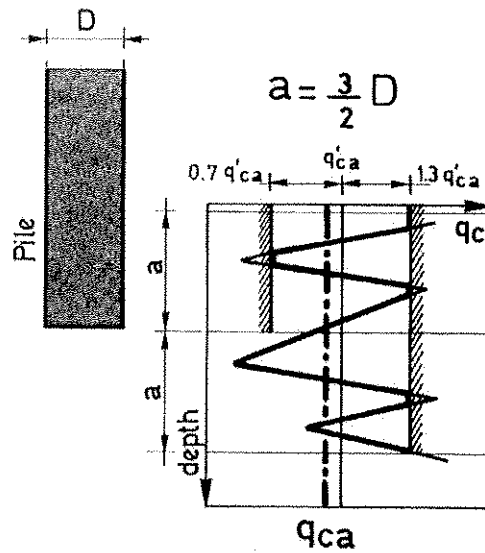
Figure 2-8: Procedure for the Determination of Equivalent Cone Resistance, LCPC Method (Bustamante and Gianeselli 1982)
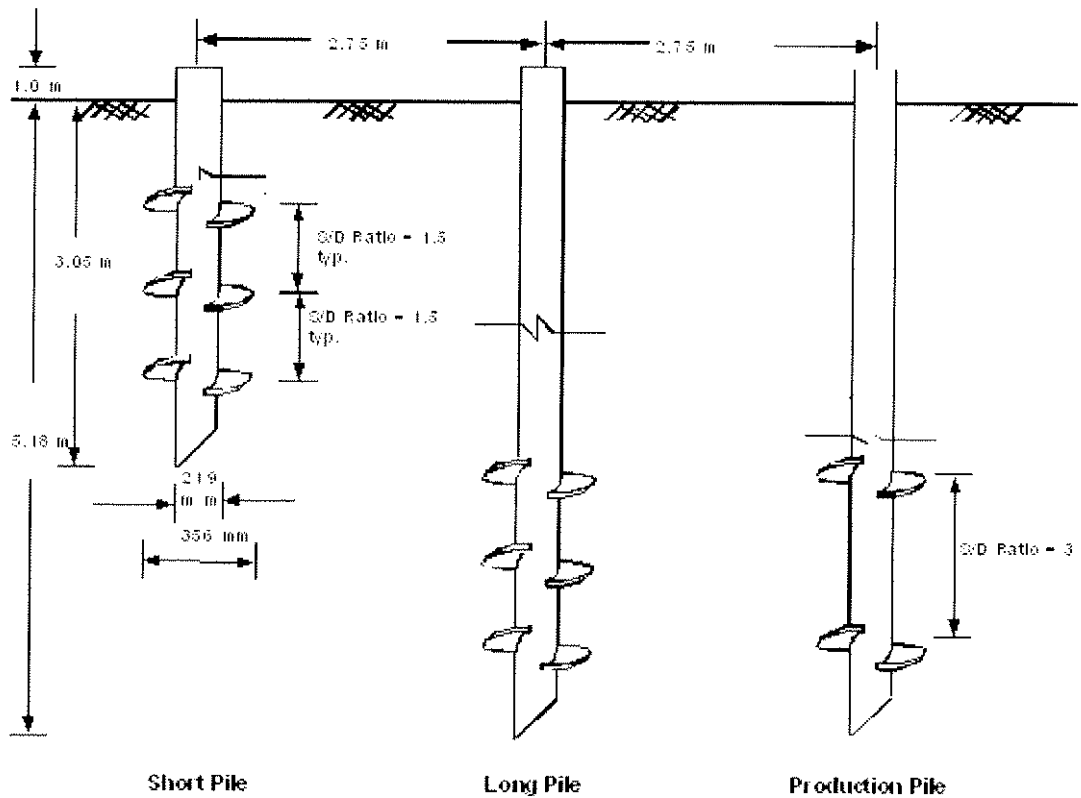
Figure 2-9: Pile Geometries used by Zhang (after Zhang 1999)
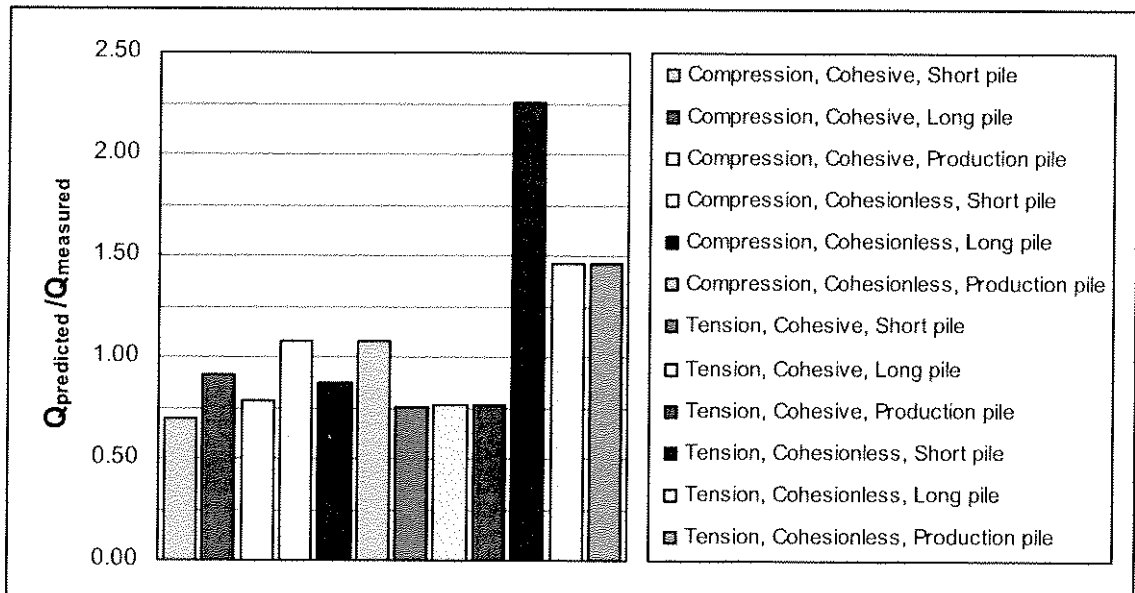
Figure 2-10: Ratio of Zhang's (1999) Measured to Predicted Screw Pile Capacity, LCPC Method
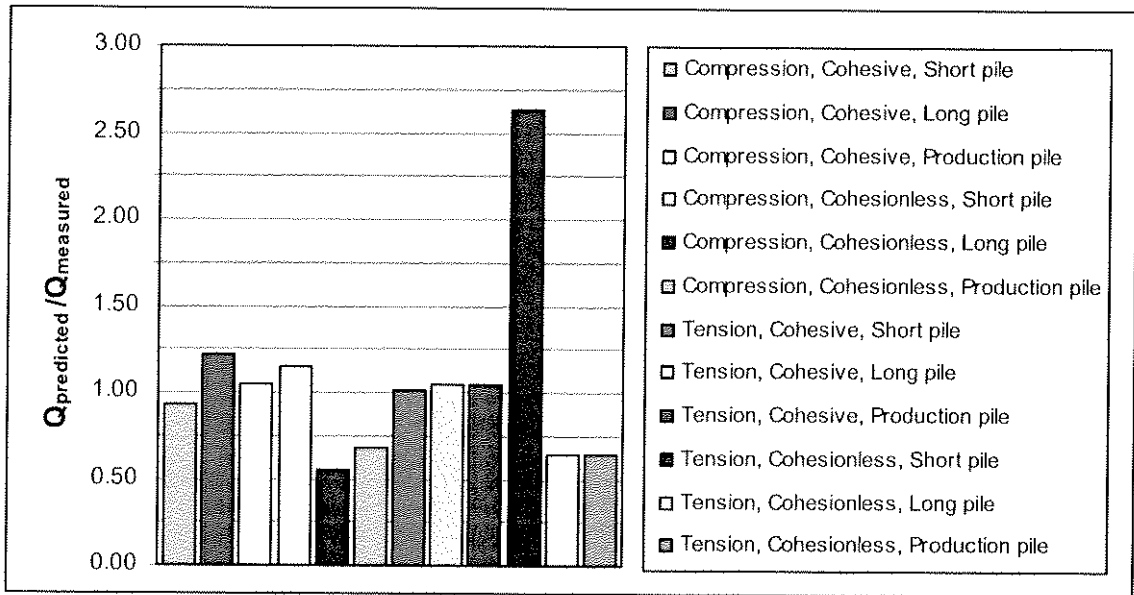
Figure 2-11: Ratio of Zhang's (1999) Measured to Predicted Screw Pile Capacity, European Method
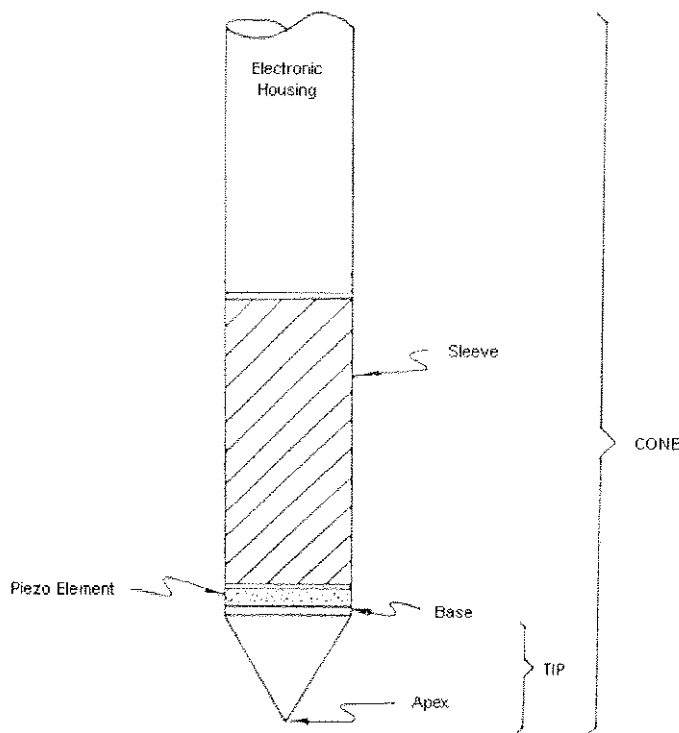
Figure 2-12: Cone Penetrometer Terminology (after Robertson and Campanella 1988)
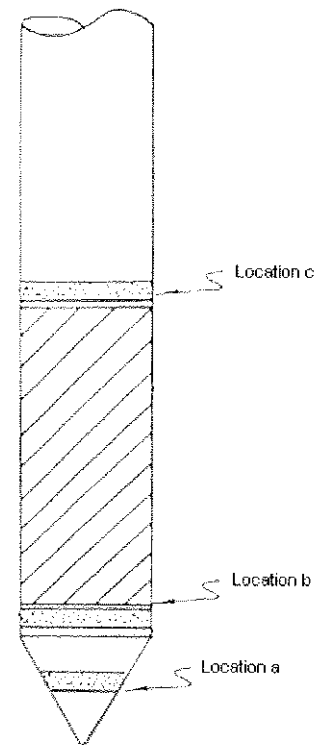
Figure 2-13: Common Piezo Element Locations: (a) On the Face; (b) Directly Behind the Tip; (c) Directly Behind the Friction Sleeve (after Robertson and Campanella 1988)
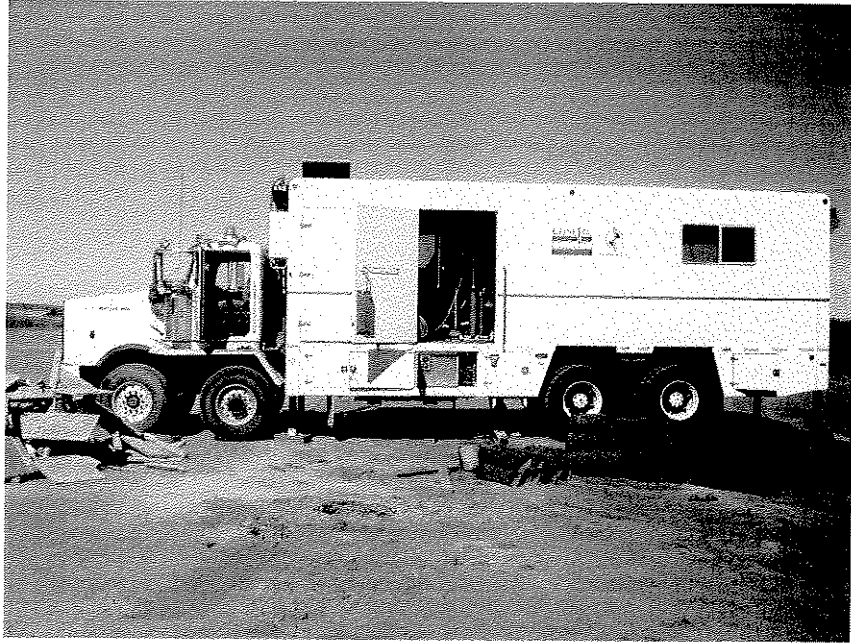
(a)
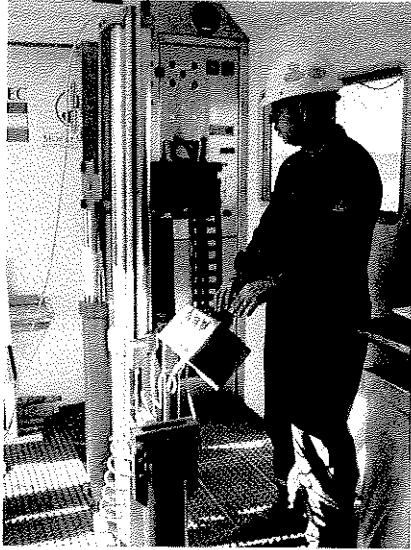
(b)

(c)

Figure 2-14: Typical CPT Truck: (a) Exterior View; (b), (c) Interior Views (Courtesy of ConeTec Inc)

2.6 References

Adams, J.I., and Hayes, D.C. 1967. The uplift capacity of shallow foundations. Ontario Hydro Research Quarterly, **19**: 1-13.

Adams, J.I., and Klym, T.W. 1972. A study of anchors for transmission tower foundations. Canadian Geotechnical Journal, **8**: 452-462.

ASTM Designation: D3441 1986. Standard method for deep quasi-static, cone and friction -cone penetration tests of soil. American Society for Testing and Materials.

Bayrock, L.A., and Hughes, G.M. 1962. Surficial geology of the Edmonton district, Alberta. Research Council of Alberta, Preliminary Report 62-6, Edmonton, Alberta.

Briaud, J.L. 1988. Evaluation of cone penetration test methods using 98 pile load tests. *In* Proceedings of the International Symposium on Penetration Testing, ISOPT-1. Orlando, Florida. Balkema Publisher, Rotterdam, Vol.2, pp. 687-697.

Bustamante, M., and Gianeselli, L. 1982. Pile bearing capacity prediction by means of static penetrometer CPT. *In* Proceedings of the 2nd European Symposium on Penetration Testing, ESOPT-II. Amsterdam. Balkema Publisher, Rotterdam, Vol.2, pp. 493-500.

Campanella, R.G., and Robertson, P.K. 1988. Current status of the piezocone test. *In* First Internation Symposium on Penetration Testing, ISOPT-I. Florida. March 1988.

Clemence, S.P., and Pepe, F.D., Jr. 1984. Measurement of lateral stress around multi-helix anchors in sand. Geotechnical Testing Journal, **7**(3): 145-152.

De Ruiter, J. 1971. Elastic penetrometer for site investigations. Journal of soil Mechanics and Foundation Division, ASCE, SM 2, **97**: 457-472.

De Ruiter, J., and Beringen, G.L. 1979. Pile foundations for large North Sea structures. Marine Geotechnology, **3**(3): 267-314.

Ghaly, A., and Hanna, A. 1991. Experimental and theoretical studies on installation torque of screw anchors. Canadian Geotechnical Journal, **28**(3): 353-364.

Godfrey, J.D. 1993. Edmonton beneath our feet: a guide to the geology of the Edmonton region. Edmonton Geological Society, Edmonton, Alberta.

Hoyt, R.M., and Clemence, S.P. 1989. Uplift capacity of helical anchors in soil. *In* Proceedings of the 12th International Conference on Soil Mechanics and Foundation Engineering. Rio de Janeiro, Brazil, Vol.2, pp. 1019-1022.

ISSMFE 1977. Report of the subcommittee on standardization of penetrometer testing in Europe. *In* Proceedings of the 9th International Conference on Soil Mechanics and Foundation Engineering. Tokyo. International Society for Soil Mechanics and Foundation Engineering, Vol.3, Appendix 5, pp. 95-152.

Johnston, G.H., and Ladanyi, B. 1974. Field tests of deep-installed screw anchors in permafrost. Canadian Geotechnical Journal, **11**(3): 348-358.

Lunne, T., Robertson, P.K., and Powell, J.J.M. 1997. Cone penetration testing in geotechnical practice. Blackie Academic & Professional.

Meyerhof, G.G., and Adams, J.I. 1968. The ulitmate uplift capacity of foundations. Canadian Geotechnical Journal, **5**(4): 224-244.

Mitsch, M.P., and Clemence, S.P. 1985. The uplift capacity of helix anchors in sand. *In* Uplift Behaviour of Anchor Foundations in Soil: Proceedings of ASCE. New York, New York, pp. 26-47.

Mooney, J.M., Adamczad, S., and Clemence, S.P. 1985. Uplift capacity of helix anchors in clay and silt. *In* Uplift Behaviour of Anchor Foundations in Soil: Proceedings of ASCE. New York, New York, pp. 48-72.

Narasimha Rao, S., and Prasad, Y.V.S.N. 1993. Estimation of uplift capacity of helical anchors in clays. Journal of Geotechnical Engineering, **119**(2): 352-357.

Narasimha Rao, S., Prasad, Y.V.S.N., and Prasad, C.V. 1990. Experimental studies on model screw pile anchors. *In* Proceedings of the Indian Geotechnical Conference. Bombay, pp. 465-468.

Narasimha Rao, S., Prasad, Y.V.S.N., and Shetty, M.D. 1991. The behaviour of model screw piles in cohesive soils. Journal of Soils and Foundations, Japanese Society of Soil Mechanics and Foundation Engineering, **31**(2): 35-50.

Narasimha Rao, S., Prasad, Y.V.S.N., and Veeresh, C. 1993. Behaviour of embedded model screw anchors in soft clays. Geotechnique, **43**: 605-614.

Narasimha Rao, S., Prasad, Y.V.S.N., Shetty, M.D., and Joshi, V.V. 1989. Uplift capacity of screw pile anchors. Geotechnical Engineering, **20**(2): 139-159.

Perko, H.A. 2000. Energy method for predicting installation torque of helical foundations and anchors. *In* New technological and design developments in deep foundations. ASCE, Special Publication no. 100, Denver, Colorado. p. 490.

Robertson, P.K., and Campanella, R.G. 1988. Guidelines for geotechnical design using CPT and CPTU. Civil Engineering Department, University of British Columbia.

Robertson, P.K., Campanella, R.G., Davies, M.G., and Sy, A. 1988. Axial capacity of driven piles in detaic soils using CPT. *In* Proceedings of the International Symposium on Penetration Testing, ISOPT-1. Orlando, Florida. Balkema Publisher, Rotterdam, Vol.2, pp. 919-928.

Sharp, M.R., McVey, M.C., Townsend, F.C., and Basnett, C.R. 1988. Evaluation of pile capacity from in situ tests. *In* Soil Properties Evaluation from Centrifugal Models and Field Performance: Session at the ASCE National Convention. Nashville, Tennessee. American Society of Civil Engineers (ASCE), pp. 135-156.

Tand, K.E., and Funegard, E.G. 1989. Pile capacity in stiff clays--CPT method. *In* Proceedings of the 12th International Conference on Soil Mechanics and Foundation Engineering. Rio de Janeiro. Balkema Publisher, Rotterdam, Vol.1, pp. 349-352.

Trofimenkov, J.G., and Mariupolskii, L.G. 1965. Screw piles used for mast and tower foundations. *In* Proceedings of the 6th International Conference on Soil Mechanics and Foundation Engineering. Montreal, Quebec, Vol.1, pp. 328-332.

Vesic, A.S. 1971. Breakout resistance of objects embedded in ocean bottom. Journal of Soil Mechanics and Foundation Division, ASCE, SM 9, **97**: 1183-1205.

Zeevaert, L. 1983. Foundation engineering for difficult subsoil conditions. Van Norstrand Reinhold, New York.

Zhang, D. 1999. Predicting capacity of helical screw piles in Alberta soils. M.Sc. thesis, Department of Civil and Environmental Engineering, University of Alberta, Edmonton, Alberta.

3 Modified Cone Penetration Equipment

3.1 Introduction

Cone penetration testing is generally performed by a specialty contractor using equipment, described in Chapter 2, that is mounted inside of a large rig ballasted to 150 kN or more. The capital investment required to procure such a system is significant, and the mobilization cost of having a test performed on-site can be substantial. The objective of this thesis being the prediction of screw pile capacity using the LCPC direct design approach, cone penetration testing was desired at each site where the screw piles were load tested to failure. With the limited resources available for this project, it was necessary that an alternative system be developed for conducting some of the required cone penetration tests. It was decided that a rectangular steel frame could be fabricated which would be assembled on the ground by nut-and-bolt construction, with hydraulic cylinders mounted to it for the purpose of pushing the cone penetrometer into the soil. Counterweight would be delivered to the system by parking the rear axle of a one-ton truck at one end of the frame, and adding steel weights to the other end. This modified push system would be inexpensive to manufacture, and easily transported in the back of a pickup truck to the desired test sites around Western Canada. The modified cone penetration system would be restricted to use in softer soils, due to the limited amount of push force which could be generated before lifting of the counterweights or bending of the steel frame occurred. For test sites where hard material would be encountered under the ground, the conventional rig-mounted cone penetration test (CPT) would have to be arranged. The modified cone penetration system developed for this thesis project is described in detail in the following sections, with equipment operation and critical dimensions discussed in terms of the currently accepted CPT guidelines and standards.

3.2 Pushing Apparatus

The purpose of developing and building a modified cone penetration apparatus as part of this thesis project was to obtain cone penetration profiles in soils of soft to medium consistency at a lower cost than mobilizing a rig-mounted system. A back-of-the-pickup-truck setup for the

modified CPT equipment was chosen for ease of transportability, which is ideal for typical locations of screw pile installations, as the piles are often used in soft terrain and areas of restricted access. The components of the modified cone penetration apparatus are shown schematically in Figure 3-1. The equipment arrangement as a whole basically consists of a steel frame assembled on the ground to which hydraulic rams are mounted for pushing the cone, a control station for regulating the flow of hydraulic fluid to the rams, and a motor-powered pump for delivering fluid to the system. The assembly of the frame is shown in the sequential photographs of Figure 3-2. The frame is weighted at both ends in order to provide the necessary ballast to the system. The rear axle of a one-ton truck may be conveniently backed onto one end of the frame, and steel weights stacked onto the other end to provide enough ballast for the cone to penetrate most soft- to medium-consistency soils. The steel weights added in this testing program provided approximately 10 kN of counterweight. Mounted on the push frame are two upright hydraulic cylinders of 6.35 cm (2 ½ in) bore and 1.22 m (48 in) stroke. The cone penetrometer itself is threaded onto a 3.54 cm diameter drill rod and positioned midway between the two hydraulic cylinders as shown in Figure 3-1. A "T"-shaped cap is threaded onto the top of the drill rod to assist in pushing and retracting the rods. When the cylinders are raised, the "T"-shaped cap is first manually detached from the mounted cone rod, and an additional rod segment threaded onto the existing sequence. The "T" cap is then reattached to the uppermost rod, and the cone is pushed into the ground by the abutment of the cap against the upper cross-piece as the hydraulic cylinders are slowly retracted (Figure 3-3). The sequence of removing the cap, raising the cylinders, adding an additional rod segment, and retracting the cylinders is repeated until the desired depth of penetration by the cone has been achieved. The amount of time required to push the cone to a typical depth of 8 meters is approximately 30 minutes using a two-man crew. An additional 30 minutes or so is required to retrieve the rods from the ground after termination of the test.

The depth of ground penetrated by the cone is electronically recorded by a linear potentiometer (LP) affixed to one of the hydraulic cylinders (Figure 3-4). The inner rod of the LP is attached to

the upper cross-piece of the apparatus, and is raised and lowered with the action of the hydraulic cylinders. The movement of the cylinders is fed by upper and lower hydraulic hoses which stem from a simple control station, where the flow of hydraulic fluid is manipulated by a single spool with a built-in flow meter (Figure 3-5). The pressure input to the hydraulic cylinders is monitored at the control station by an analogue gauge reading. The system is driven by a 5.5 horsepower gasoline motor affixed to a two-stage pump, which is supplied with hydraulic fluid from a small storage tank (Figure 3-6). Used hydraulic fluid is returned from the control station to the storage tank from which it originated after passing through a hydraulic filter mounted on the return hose.

The rate at which the cone descends into the ground is manually regulated using the single spool at the control station. Although the exact rate of penetration with depth cannot be determined until after the test is complete and the electronic data is fully generated, the rate of penetration is monitored manually as the test progresses by taking time readings at the beginning and end of each push, which is equal to the length of one drill rod (3 ft or 0.91 m). In this manner, the penetration rate may be controlled to a reasonable degree. The International Reference Test Procedure (ISOPT 1988) and most national standards or guidelines require that a constant penetration rate of 20 mm/s be maintained throughout the cone penetration test, with a narrow tolerance of typically about ± 5 mm/s (Lunne et al. 1997). Varying the penetration rate affects the rate of strain induced in the soil as it is deformed by the cone, and the drainage conditions within intermediate soil may effectively change from fully drained, to partly drained, to undrained as the penetration rate increases, which will significantly affect the soil behavior. On the basis of an extensive literature survey, Lunne et al. (1997) cite the work of Bemben and Myers (1974) as being especially helpful in exemplifying the response of a cohesive material to different rates of cone penetration. Bemben and Myers (1974) performed tests in a lightly overconsolidated varved clay using nine rates of penetration between 0.2 and 200 mm/s; the resulting variation in measured cone resistances is shown in Figure 3-7 (Lunne et al. 1997). A minimum cone tip resistance was obtained at a penetration rate of 2 mm/s. The authors attributed the shape of the curve to a combination of viscosity and pore pressure effects. As summarized by Lunne et al.

(1997), the curve represents a general response for clays, where at very slow rates of penetration, tip resistance, q_c, is generally of a drained nature. As the rate of penetration increases, excess pore pressures begin to develop and q_c decreases due to the decrease in effective stress and reduction in strength. As the penetration rate continues to increase, the viscous forces will begin to offset the reduction in strength and the cone resistance will pass through a minimum before increasing again as viscous forces become large enough to dominate the process (Lunne et al. 1997). However, as seen in Figure 3-7, the rate of penetration must change by several orders of magnitude in order for the cone resistance curve to pass through the stages of behavior identified above. Similar results were obtained by Roy et al. (1982) for tests performed in a sensitive, soft, slightly overconsolidated silty clay (Lunne et al. 1997). For testing in sands, Lunne et al. (1997) state that there is little effect on the cone resistance for penetration rates a little slower than 20 mm/s. Higher rates of penetration may produce an increase in cone resistance due to dilatancy and higher negative pore water pressures.

3.3 Cone Penetrometer Configuration and Dimensions

Three cone penetrometers were fabricated for this thesis project, each capable of measuring tip resistance and sleeve friction when connected to an electronic data acquisition system, such as the *Data Dolphin Model 400* (Figure 3-8). Two full-wheatstone-bridge load cells were placed inside the metal cone casing, the first located behind the tip of the cone to record the tip resistance encountered with depth, and the second behind the internal shoulder of the friction sleeve, to record the combined load of tip resistance and sleeve friction. This configuration is known as a subtraction cone, because the tip resistance recorded by the lower load cell must be subtracted from the resistance recorded by the upper load cell in order to obtain the sleeve friction value. The diameter of the cone tip measures 3.54 cm, with a projected area of 9.84 cm^2. Behind the cone tip the friction sleeve is located, measuring 14.82 cm in length and 3.54 cm in diameter. The assembly of the cone is shown in Figure 3-9, pictures (a) to (d). The cone may be conveniently threaded to locally-available drill rod sections, which are 3.49 cm (1 ⅜ inches) in diameter and 0.91 meters (3 feet) long.

As mentioned in Chapter 2, the accepted standard for the projected cone tip area is 10 cm^2, which is equivalent to a diameter of 3.57 cm. The slight difference between the diameter of the cone fabricated for this project and the standard diameter is not considered to be significant. Based on a literature survey of reported results for measured tip resistances using non-standard cones, Lunne et al. (1997) concluded that cone penetrometers ranging in cross section from 5 cm^2 to 15 cm^2 will yield essentially equivalent corrected cone resistances in most soils. The cone penetrometers used in this study were fabricated with the standard apex angle of 60 degrees. The International Reference Test Procedure (ISOPT 1988) also requires that the length of the cylindrical portion attached to the removable cone tip, included in the measured q_c, should be between 7 and 10 mm (Lunne et al. 1997). Tests in overconsolidated stiff to very stiff clays in the U.K. conducted by Lunne et al. (1986a) show that including a longer cylindrical portion in the measured tip resistance can have significant effects—a higher measured q_c is attributed to the friction acting on the longer cylindrical section. The cone tip fabricated for this research was made with a standard 8 mm cylindrical portion attached to the tip.

The dimensions and position of the friction sleeve on the cone are also important parameters which should be standardized for the accruement of comparable data. According to the International Reference Test Procedure (ISOPT 1988), the friction sleeve should be located immediately behind the cylindrical part of the cone, with an intermediate distance for slots and dirt seals of up to 5 mm (Lunne et al. 1997). Under the current investigation, the friction sleeve fabricated for the cone was placed immediately behind the cone tip, as required, except for the allowable 5 mm gap. The standard surface area required for the friction sleeve is 150 cm^2, with a length of 13.37 cm, and a circumference of 11.22 cm in accordance with a 3.57 cm-diameter rod (Lunne et al. 1997). The standard drill rods available for this undertaking were of 3.49 cm in diameter, and the friction sleeve was fabricated to a 3.54 cm diameter, equal to the diameter of the cone tip. The length of the friction sleeve was selected as 14.82 cm, resulting in a surface area of 164.82 cm^2. Unfortunately, the anomaly in the size of the friction sleeve was not observed until after completion of the field testing program. Lunne et al. (1997) insist that even

small deviations from the standard size of friction sleeve may cause significant differences in the data retrieved, and the minor over-sizing of the friction sleeve in this project may have slightly affected the sleeve readings obtained. The accuracy of the sleeve friction results will be discussed further in the following section.

3.4 Accuracy of Results using Modified Cone Penetration Equipment

3.4.1 Introduction

After fabrication of the modified cone penetration equipment described above, the task was undertaken of ensuring the accuracy of the data collected by the system. The University of Alberta Farm site, located at 115 Street and 58 Avenue in Edmonton, Alberta, was selected as the location to be used for preliminary testing and evaluation of the modified cone equipment. The University Farm has been often used for geotechnical research undertakings in the past, and three commercial rig-mounted CPT profiles have been documented at the site, taken in the year 1997 (Zhang 1999). It was therefore decided that under the current investigation, modified cone penetration tests would be carried out at the University Farm site, and the results compared to the earlier CPT data for verification.

The existing CPT profiles for the University Farm site are shown in Figure 3-10 (Zhang 1999). Each of Zhang's (1999) cone penetration tests were conducted to a minimum depth of 7.5 meters, with measurements taken of tip resistance, sleeve friction, and pore pressure. The measured cone tip resistance profile of Figure 3-10(a) is generally in the order of 1500 to 2000 kPa, while the friction ratio is approximately equal to 5 percent for most of the depth investigated (Figure 3-10(b)). The water table at the University Farm site was located at an approximate depth of 3.0 meters below the ground surface, as can be deduced from Figure 3-10(c) (Zhang 1999). As discussed in Chapter 3, by normalizing the CPT measurements of tip resistance and friction ratio with depth, a soil type profile may be generated for the test site using Robertson's (1990) soil behavior type chart. The CPT profiles of Figure 3-10 describe the University Farm site as consisting of 4.0 meters uniform clay underlain by 3.5 meters of interbedded clay and silt; at the time of the testing, the top 0.45 meters of soil consisted of clay mixed with gravels that were

the result of the site having been used as a snow dump for the University of Alberta (Zhang 1999).

Several penetration tests using the modified cone equipment were performed at the University of Alberta Farm site between December 16, 2005, and January 18, 2006. Figure 3-11 shows the tip resistance profile for a typical modified cone penetration test conducted at the University Farm site under the current investigation, compared to Zhang's (1999) previous CPT profiles. The upper 30 cm of the tip resistance profile for the modified cone test is interpolated in Figure 3-11, because this section of soil was frozen during the period of testing and had to be augured through. It can be seen from Figure 3-11 that the modified cone penetration test yielded significantly higher values of tip resistance compared to Zhang's (1999) prior CPT work; this was consistently the case for all of the modified cone tests that were initially carried out at the University Farm under the current investigation. In addition, the measurements of sleeve friction obtained using the modified cone penetration equipment were inevitably plagued by the same discrepancies as the tip resistance readings, because the configuration of load cells within a subtraction cone necessitates the calculation of sleeve friction be dependent upon the simultaneously measured tip resistance value.

3.4.2 Comparison of Soil Properties: Previous and Current Investigations

The discrepancies between the initial tip resistance profiles obtained under the current investigation and the tip resistance profiles recorded by Zhang's (1999) CPT work created immediate concern as to the accuracy of the results obtained using the modified cone penetration equipment. By way of justifying the current tip resistance results, it was at first thought that perhaps the properties of the soil at the University Farm site had changed since the time Zhang's (1999) CPT profiles were obtained in October of 1997, over eight years prior to the current investigation. In order to determine whether this was indeed the case, Shelby tube samples were taken from various depths at the University Farm site, and laboratory strength testing performed. Laboratory vane and field vane tests were conducted on the Shelby samples before extrusion, and unconfined compressive strength (UCS) tests were performed on representative samples

after extrusion. Standard Penetration Testing (SPT) was also conducted at the University Farm site, and corrected blow counts converted to an approximation of undrained shear strength using the empirical relationship given by Terzaghi and Peck (1967), equation [3-1]:

[3-1]
$$s_u = 0.87 \cdot (N_1)_{60} \quad (psi)$$

Or, in metric units as equation [3-2]:

[3-2]
$$s_u = 6.0 \cdot (N_1)_{60} \quad (kPa)$$

where

s_u = undrained shear strength

$(N_1)_{60}$ = corrected SPT blow count

For the purpose of comparison with the soil strength determinations discussed above, the CPT profiles of tip resistance reported by Zhang (1999) for the University Farm site were converted to profiles of shear strength using the well-known empirical correlation of equation [3-3] (Lunne et al. 1997):

[3-3]
$$s_u = \frac{(q_c - \sigma_{vo})}{N_k}$$

where

s_u = undrained shear strength (kPa)

q_c = measured cone tip resistance (kPa)

σ_{vo} = total in-situ vertical stress (kPa)

N_k = empirical cone factor

An N_k factor of 19 was used in equation [3-3]. Lunne and Kleven (1981) compiled empirical cone factors for 12 sites consisting of very soft to medium normally consolidated clays, and using the field vane as a reference test the cone factor, N_k, was found to vary between 11 and 19 with an average value of 15. Lunne and Kleven (1981) therefore recommended that for sites where no local correlations exist, a cone factor of 19 be used for computing average undrained shear strength for bearing capacity or stability problems. The undrained shear strength profiles thus

derived from Zhang's (1999) CPT profiles were plotted against the laboratory shear strength determinations from the current investigation, and the two sets of data showed very good correlation (Figure 3-12). Therefore, it was established that the current soil properties at the University Farm site were essentially equivalent to what they were at the time of Zhang's (1999) prior cone penetration testing, and that another reason must exist for the discrepancy between the earlier cone tip resistance profiles and those obtained during the current investigation using the modified cone penetration equipment (Figure 3-11).

3.4.3 Temperature Correction to Load Cell Output

Having determined that the soil properties at the University Farm site had not changed since the time of Zhang's (1999) prior investigation, it was hypothesized that perhaps changes in temperature were affecting the output of the load cells contained in the cone penetrometer fabricated for the current project. Lunne et al. (1997) state that, as for any device containing load cells, temperature can have a significant effect on the measurements obtained—the main reason being that a change in temperature can cause a shift in the load cell output at zero load. In particular, Lunne et al. (1986b) conducted a study of commercially available piezocones and found that temperature changes may indeed have significant effects on the measurements obtained. The temperature issue, as related to the current University Farm investigation, is based on the fact that the cone was routinely zeroed at the ambient air temperature above ground before testing, but the load cell readings taken during the course of the cone penetration tests were obtained below the surface, at different temperatures than above ground.

In order to determine whether differences between the ambient air temperature and the temperature in the ground were the cause of the inaccurate modified cone penetration results, Carslaw's solution (see Jumikis 1977) was used to formulate a temperature profile for the University Farm site for each of the days on which cone tests had been conducted. Carslaw's solution was used in conjunction with hourly average ambient air temperature readings collected for the year by Environment Canada at the Edmonton International Airport, located approximately 25 km south of the University Farm. The temperature profiles for the times at which the modified

cone tests were carried out, along with the theoretical yearly maximum and minimum boundaries of temperature fluctuation below the ground surface at the University Farm site are shown in Figure 3-13. It can be seen from Figure 3-13 that there exists a significant temperature variation with depth. The hourly average ambient air temperature readings taken by Environment Canada for the dates of the cone testing performed at the University Farm were also used to determine the temperature at which the cone was calibrated above ground, corresponding to the time of day immediately prior to commencement of the test. In this way, the initial zero readings on the cone were correlated with the ambient air temperature present at the beginning of the tests, and the zero readings then adjusted as the cone penetrated the ground according to the Carslaw temperature at depth.

Temperature zero shifts may be avoided by making sure that instrument zero readings are taken at the same temperature as in the ground (Lunne et al. 1997). However, for the upper several meters of ground below surface, there does not exist a constant ground temperature, but rather a temperature curve which approaches a constant value at some depth, typically 5 to 8 °C in northern climates, at several meters deep. The second option therefore, is to mount a temperature sensor on the cone penetrometer, and then to correct the measured cone penetration results based on laboratory calibrations (Lunne et al. 1997). Because the screw piles under consideration for this thesis project were typically installed to less than eight meters in depth, it was decided that the latter option of obtaining a temperature profile at the time of the cone tests and then correcting the penetration results for changes in temperature with depth would yield the most reliable results. However, the fabrication of the cone penetrometers being already complete meant that a thermistor could not easily be installed into the existing cones. A replacement cone tip of identical dimensions was therefore produced with the sole capability of temperature measurement. The temperature cone tip was made to be threaded onto a segment of drill rod and pushed into the ground in the same manner as the cone penetrometer for future tests. The thermistor device supplies temperature readings, recorded at three second intervals, to the electronic data logger at the surface, creating a near-continuous profile of ground

temperature with depth. The difference between the surface air temperature at which the initial zero readings for the cone are recorded and the temperature measured by the thermistor at any given depth allow the cone penetration test results to be corrected in terms of the temperature sensitivity of the individual load cells. Ideally, a thermistor should have been included in the fabrication of the cone penetrometer from the beginning, rather than inserted into a separate cone tip. However, the solution at hand serves the purpose of allowing for a temperature profile to be obtained with depth, but necessitates that two separate tests, a cone penetration test and a temperature test, be conducted in the place of one comprehensive test.

In order to establish the correction factor to be applied to the zero load readings, the cone penetrometer was taken back to the laboratory and subjected to changes in ambient temperature under controlled conditions and zero load. The correlations developed between the ambient temperature and the zero-load outputs of the cone tip load cell and sleeve load cell are included in Appendix B. Three cone penetrometers of identical dimensions were used in the course of this thesis project, and each was tested independently for sensitivity of zero load outputs to changes in ambient temperature. Cone No. 1 was used for all preliminary testing at the University Farm site; the temperature sensitivity factors determined for Cone No. 1 were 0.0328 mV/°C for the tip resistance load cell, and 0.0037 mV/°C for the sleeve friction load cell. Figure 3-14 (a) and (b) shows the profiles of a typical modified cone penetration test performed at the University Farm site, before and after application of the appropriate temperature correction factors to the two load cells. While the temperature correction with depth made only a negligible difference to the sleeve friction profile, a very significant adjustment is visible in the profile of tip resistance after application of the temperature correction. The tip resistance profile is the only information from the CPT which is used in the LCPC method for pile capacity prediction, and therefore its accuracy is of critical importance. When the temperature correction factor was applied to all of the tip resistance profiles obtained at the University Farm site using the Carslaw temperature profiles, the results of the current investigation fell into very good alignment with the CPT tip resistance profiles obtained at the site by Zhang (1999), as evidenced by Figure 3-15.

After correction of the tip resistance measurements for temperature sensitivity, the sleeve friction profiles obtained using the modified cone penetration equipment at the University Farm site naturally fell into alignment with expected values. The subtraction configuration of the load cells in the cone meant that the temperature sensitivity of the tip resistance measurements necessarily affected the corresponding values of sleeve friction. Therefore, once the tip resistance data were corrected for the effects of temperature, the sleeve friction data, being the difference between the measured loading on the upper (sleeve plus tip) and lower (tip only) load cells, naturally fell into alignment with expected values. Figure 3-16 shows the sleeve friction results obtained using the modified cone penetration equipment at the University of Alberta Farm site, after applying the temperature correction to the corresponding tip resistance results. It is evident that when compared to the results obtained by Zhang (1999) at the same site using conventional CPT equipment, the data from the current investigation gives somewhat higher readings of sleeve friction, the difference being in the order of 30 percent. This discrepancy may be related to the difference in size of the friction sleeves used under the two separate projects; however, a definite conclusion cannot be drawn. As previously mentioned, the standard surface area used for the friction sleeve is 150 cm^2, with a 3.57 cm diameter (Lunne et al. 1997). The friction sleeve for the cone penetrometers used for this thesis project measured 3.54 cm in diameter, and 14.82 cm in length, resulting in a surface area of 164.82 cm^2; unfortunately, this anomaly in the size of the friction sleeve was not observed until after completion of the field testing program. Lunne et al. (1997) insist that even small deviations from the standard size of friction sleeve may cause significant differences in the data retrieved, and this may explain the discrepancy between Zhang's (1999) sleeve friction profile and the results obtained under the current investigation (Figure 3-16). However, Lunne et al. (1997) also note that as a general rule for cone penetration testing, sleeve friction readings do tend to be less reliable than tip resistance readings. In the broader picture, the purpose of this thesis project was to obtain predictions of screw pile axial load capacities using the LCPC direct design method, which requires only the input of the CPT tip resistance profile for the test sites. Therefore, the degree of accuracy in the sleeve friction results

achieved using the slightly larger-sized friction sleeve is considered adequate for the purposes of this thesis, as the sleeve friction profiles obtained were limited to use as a tool in conjunction with the tip resistance profiles for describing only the general nature of the soil deposits encountered, and not for use in the detailed calculations regarding screw pile capacity prediction.
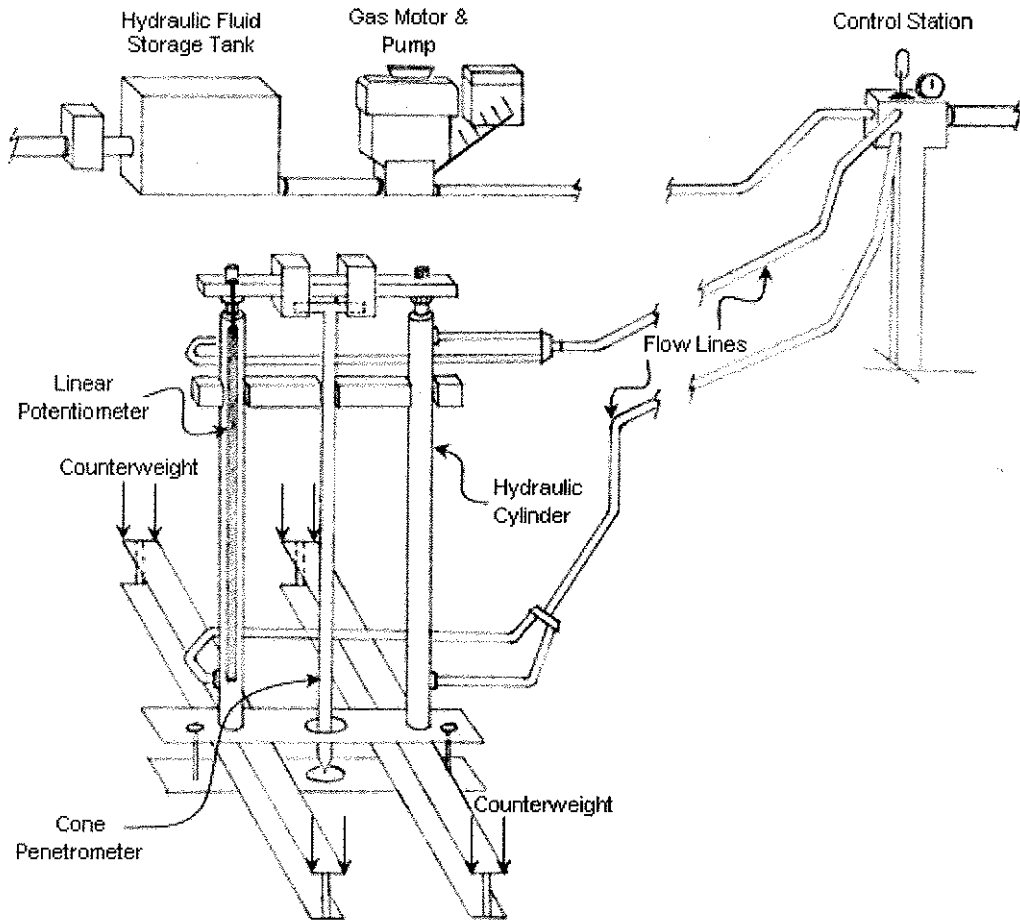
Figure 3-1: Schematic Drawing of Modified Cone Penetration Apparatus (Not To Scale)
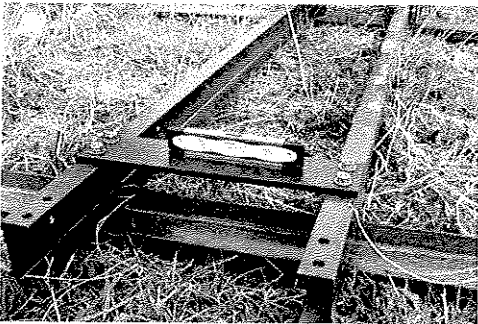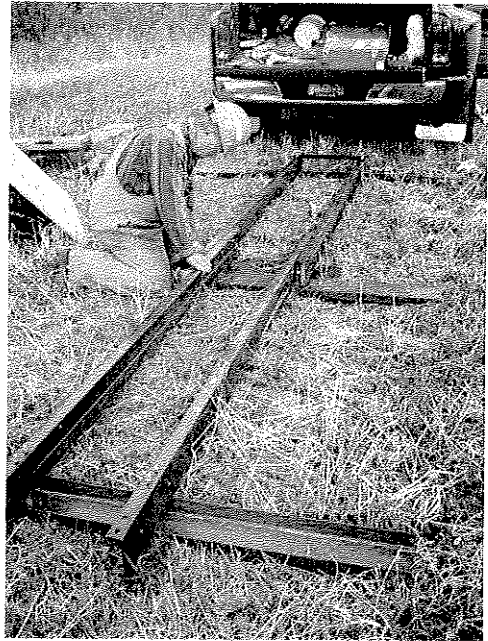
Figure 3-2: Assembling the Cone Penetrometer Push Frame

Figure 3-3: Pushing the Cone
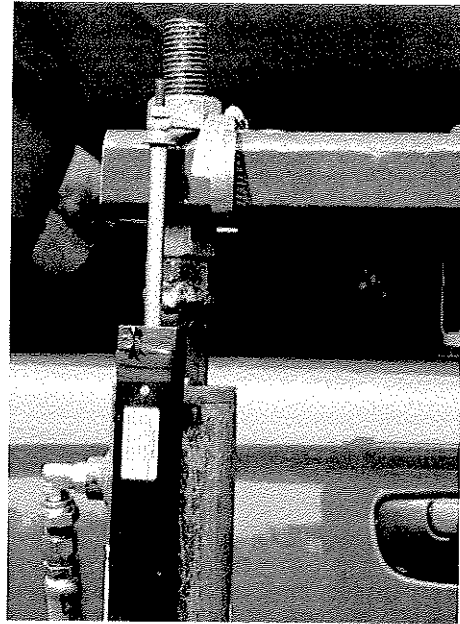
Figure 3-4: Linear Potentiometer Affixed to Push Frame
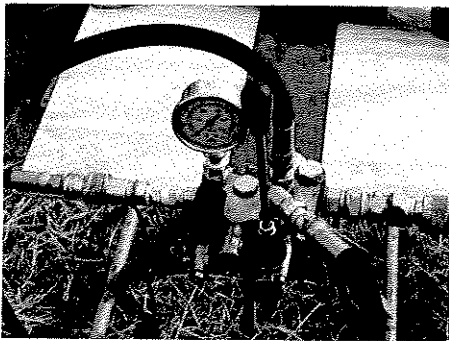
Figure 3-5: Single Spool Control Station
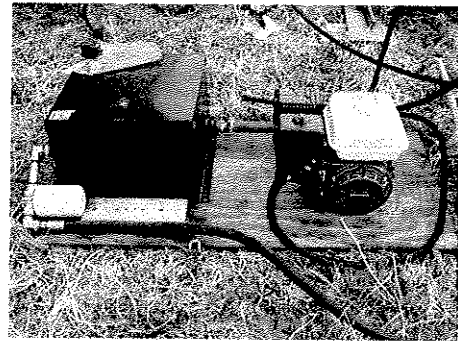
Figure 3-6: Hydraulic Fluid Tank and Gas Motor
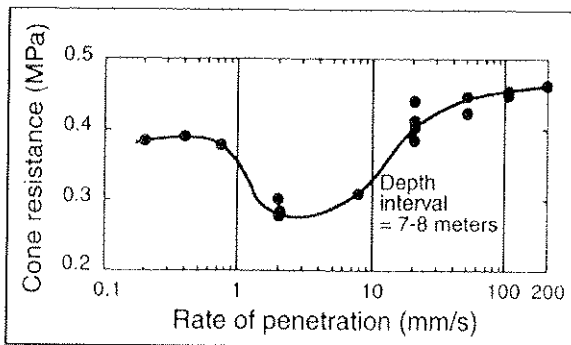
Figure 3-7: Influence of Penetration Rate on Cone Tip Resistance (Bemben and Meyers 1974; Lunne et al. 1997)
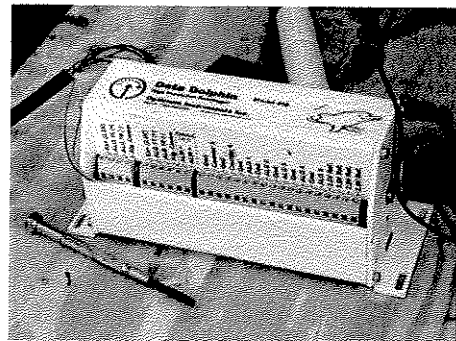
Figure 3-8: High Resolution Datalogger

(a)   (b)   (c)   (d)
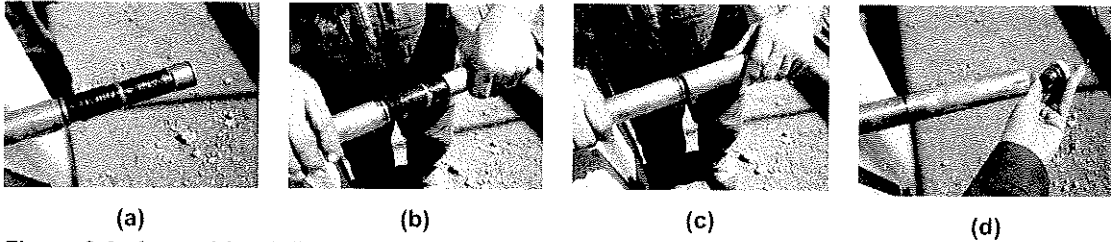
Figure 3-9: Assembly of Cone Penetrometer; (a) Location of Load Cells; (b), (c) Placement of Friction Sleeve; (d) Threaded Attachment of the Cone Tip.

(a)   (b)   (c)
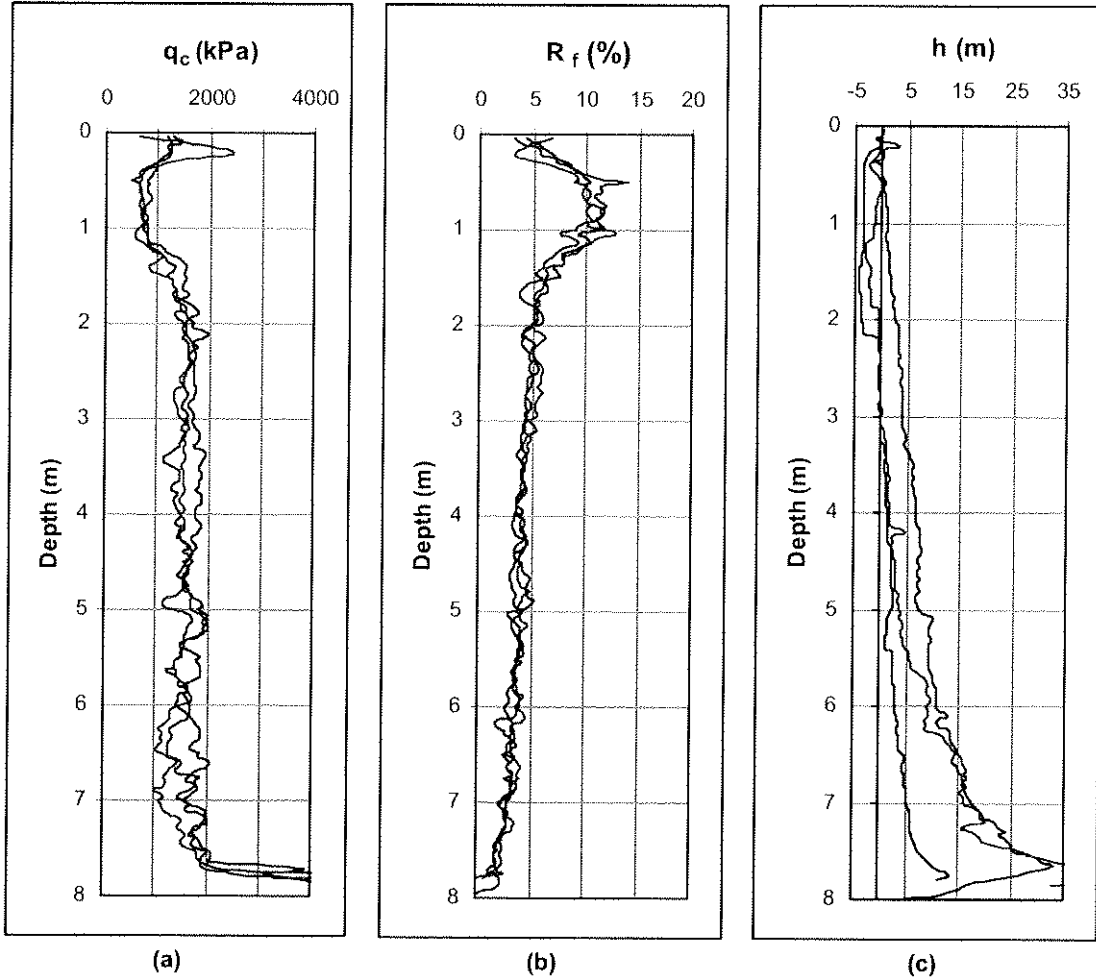
Figure 3-10: Existing CPT Profiles for University Farm Site: (a) Cone Tip Resistance, q_c; (b) Friction Ratio, R_f; (c) Piezometric Head, h (after Zhang 1999)
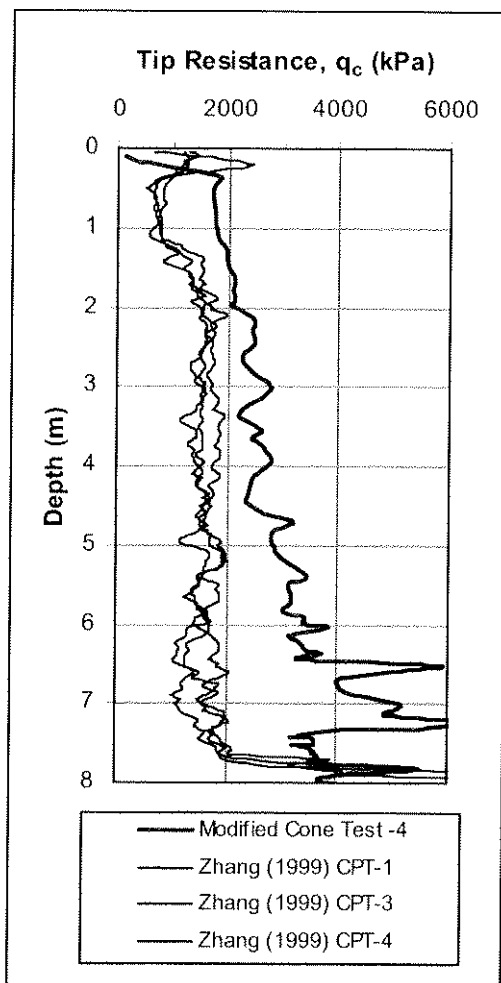
Figure 3-11: Comparison of Tip Resistance Profiles, University Farm Site
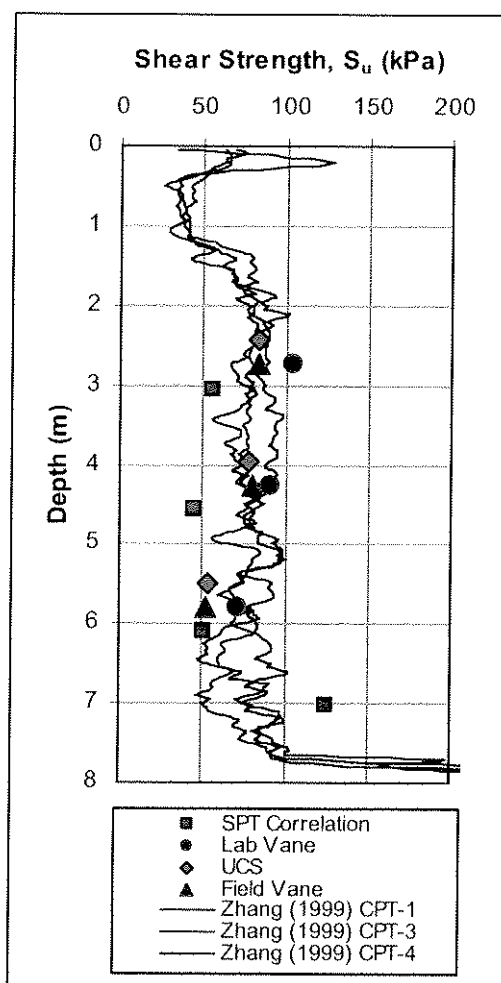
Figure 3-12: Shear Strength Profile from Laboratory Testing and Local Correlations, University Farm Site
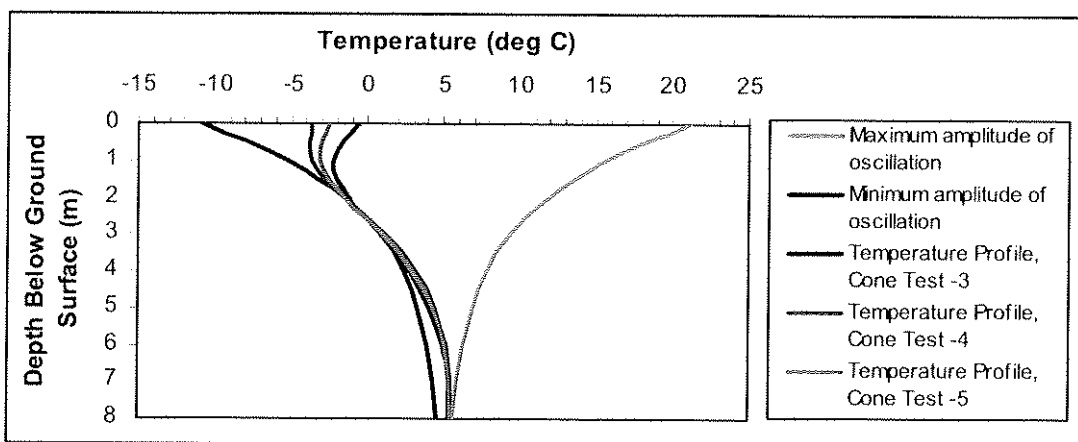
Figure 3-13: Carslaw Temperature Profiles for University Farm Site
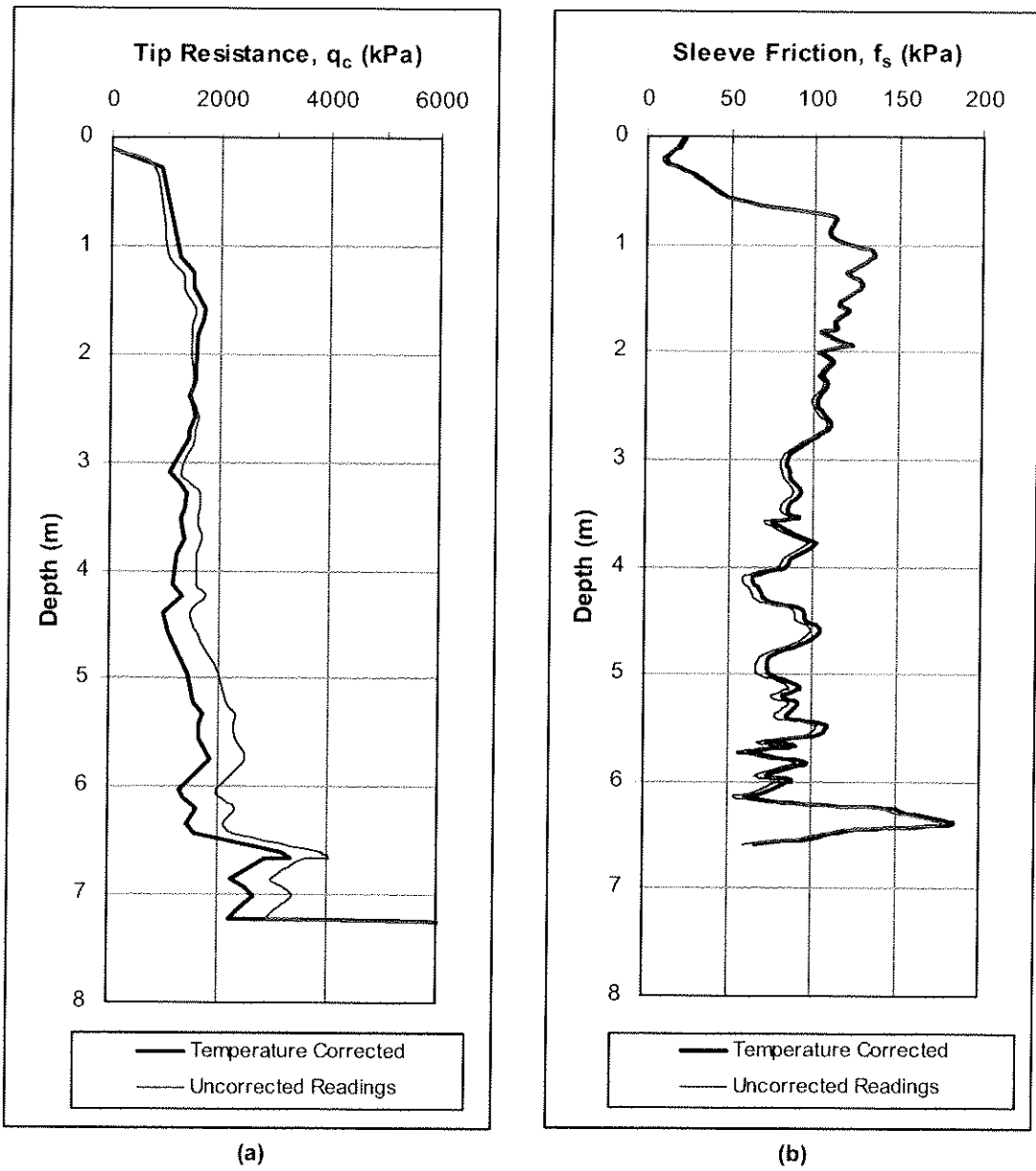
Figure 3-14: Modified Cone Penetration Profiles Before and After Temperature Correction, University Farm Site: (a) Tip Resistance, q_c; (b) Sleeve Friction, f_s
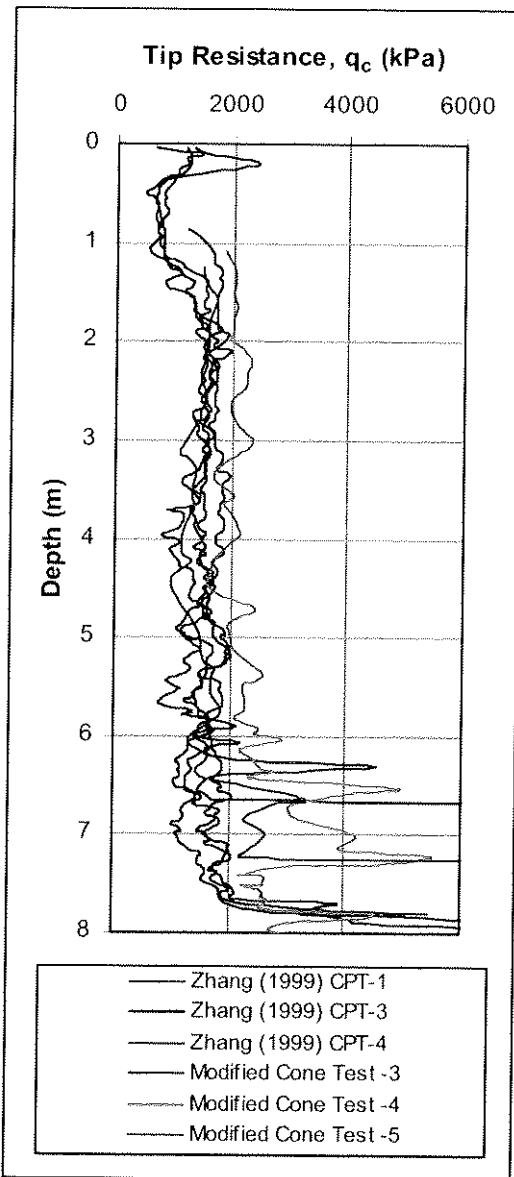
Figure 3-15: Comparison of Tip Resistance Profiles After Temperature Correction, University Farm Site
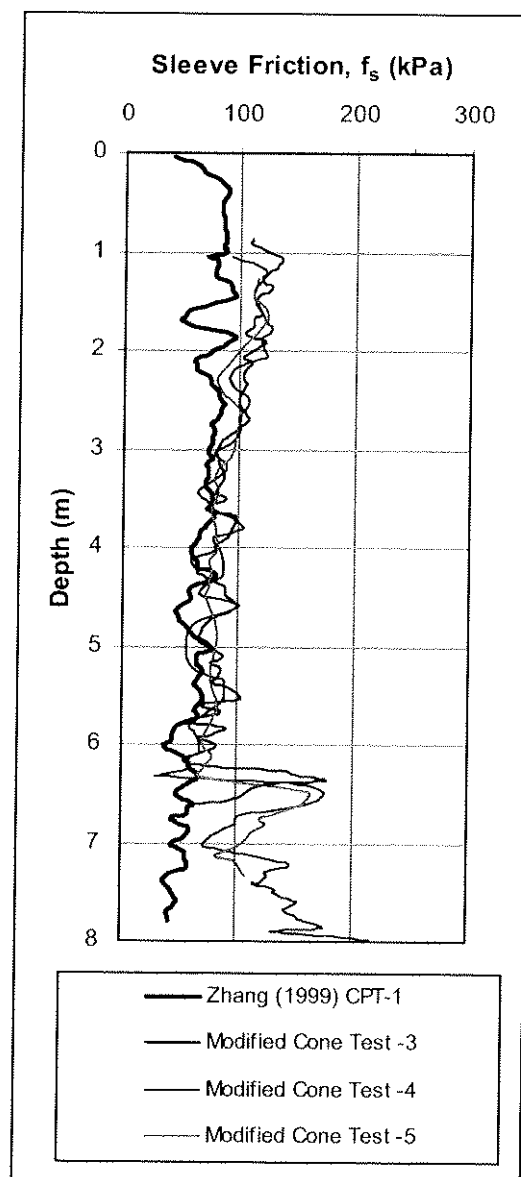
Figure 3-16: Comparison of Sleeve Friction Profiles, University Farm Site

3.5 References

Bemben, S.M., and Meyers, H.J. 1974. The influence of rate of penetration on static cone resistance in Connecticut River Valley varved clay. *In* Proceedings of the European Symposium on Cone Penetration Testing, ESOPT. Stockholm, Vol.2.2, pp. 33-34.

ISOPT 1988. Internation Symposium on Penetration Testing. Report of the ISSMFE Technical Committee on Penetration Testing. *In* Working party, pp. 27-51.

Jumikis, A.R. 1977. Thermal Geotechnics. Rutgers University Press, New Jersey.

Lunne, T., and Kleven, A. 1981. Role of CPT in North Sea foundation engineering. *In* Cone Penetration Testing and Experience: Proceedings of a Session Sponsored by the Geotechnical Engineering Division at the ASCE National Convention, St. Louis, Missouri, pp. 76-107.

Lunne, T., Robertson, P.K., and Powell, J.J.M. 1997. Cone penetration testing in geotechnical practice. Blackie Academic & Professional.

Lunne, T., Eidsmoen, T., Powell, J.J.M., and Quaterman, R.S.T. 1986a. Piezocone testing in overconsolidated clays. *In* Proceedings of the 39th Canadian Geotechnical Conference. Ottawa. Canadian Geotechnical Society, Preprint Volume, pp. 209-218.

Lunne, T., Eidsmoen, T., Gillespie, D., and Howland, J.D. 1986b. Laboratory and field evaluation of cone penetrometers. *In* Proceedings of the ASCE Specialty Conference in Situ '86: Use of In Situ Tests in Geotechnical Engineering. Blacksburg. American Society of Engineers (ASCE), pp. 714-729.

Robertson, P.K. 1990. Soil classification using the CPT. Canadian Geotechnical Journal, **27**(1): 151-158.

Roy, M., Tremblay, M., Tavenas, F., and La Rochelle, P. 1982. Development of pore pressures in quasi-static penetration tests in sensitive clay. Canadian Geotechnical Journal, **19**(2): 124-138.

Terzaghi, K., and Peck, R.B. 1967. Soil mechanics in engineering practice. John Wiley and Sons, New York.

Zhang, D. 1999. Predicting capacity of helical screw piles in Alberta soils. M.Sc. thesis, Department of Civil and Environmental Engineering, University of Alberta, Edmonton, Alberta.

4 Geology of Screw Pile Load Test Sites

4.1 Introduction

The following chapter provides a brief overview of the geology and glacial processes related to each of the five vicinities in Western Canada in which the documented screw pile axial load tests were carried out by industry partners. The results of 29 screw pile load tests have been made available for presentation in this thesis, conducted at 10 different test sites located in the five broad locales of Ft. St. John, British Columbia, Edmonton, Alberta, Ft. McMurray, Alberta, Beaverlodge, Alberta, and Saskatoon, Saskatchewan. The stratigraphy of the individual test sites will be discussed in detail under the heading of the appropriate locale; many of the test sites were subject to an engineering site investigation at the time of the screw pile installations and load testing. The site investigation program performed for this thesis project was aimed at revisiting as many of the test sites as possible for the procurement of relevant cone penetration profiles. The CPT profiles obtained during the site investigation program will also be presented in this chapter, and subsequently used in conjunction with the LCPC direct pile design method (Bustamante and Gianeselli 1982) in an attempt to predict the ultimate axial screw pile capacities, as determined by the documented load test results. At as many sites as possible, the modified cone penetration equipment described in Chapter 3 was used to perform the cone penetration testing, due to the financial savings which could be incurred; however, as previously mentioned, the modified equipment was restricted to use in softer soils due to the limited capacity of the push system. For sites where screw pile load tests had been performed in harder soils, commercial, rig-mounted cone penetration tests were commissioned where possible. All in all, cone penetration profiles are presented for seven of the 10 test sites, with two sites tested using the modified cone penetration equipment, four sites tested using the commercial, rig-mounted equipment, and one site tested using both types of equipment.

4.2 Surficial Geology of the Edmonton Area, Alberta

The surficial geology of the Edmonton district is mainly derived from the glaciation which occurred during the late Wisconsin period, covering most of Alberta at the time of its maximum extent.

During the recession of the glacier, many large, short-lived glacial lakes were produced due to the impounding of meltwaters flowing northeast towards Hudson's Bay. The proglacial Lake Edmonton, since vanished, once covered much of the area now comprising the City of Edmonton. The lacustrine sediments deposited by Glacial Lake Edmonton consist of varved silts and clays, becoming more clayey towards the top of the deposit. The lower lake sediment consists of fine- to medium-grained sand and silt, with some till inclusions, pebbles, and boulders believed to be the result of ice-rafting (Bayrock and Hughes 1962). Because of the rapid lowering of the lake during the recession of the glacier, there are no beaches associated with Glacial Lake Edmonton. The lacustrine sediments deposited by Glacial Lake Edmonton are underlain by stiff glacial till. The till is comprised of unsorted, unstratified deposits of sand, silt, and clay, in fractions of approximately 41%, 31% and 28% respectively (Bayrock and Hughes 1962). In addition, sporadic occurrences of Saskatchewan sands and gravels can be found throughout the Edmonton area. The origin of the Saskatchewan sands and gravels is complex, and involves more than one depositional cycle. The Saskatchewan sands and gravels are differentiated from glacial gravels in that their lithology is clearly derived from the quartzite and cherts of the Rocky Mountains, as opposed to the metamorphic and igneous rocks of the Canadian Shield (Bayrock and Hughes 1962). Saskatchewan sands and gravels occur in the Edmonton district as channel fill in preglacial valleys incised in the bedrock beneath the glacial till, and also form the cores of various hills in the vicinity, including the Mount Pleasant Cemetery in southwest Edmonton (Bayrock and Hughes 1962).

4.2.1   Test Site No. 1: Edmonton, Alberta

The Edmonton test site is located on the University of Alberta Farm in the southwest area of the city, at approximately 115 Street and 69 Avenue. Six screw pile load tests, three in compression and three in tension, were performed at the University Farm site in February 1998 and documented by Zhang (1999). The site stratigraphy was described by Zhang (1999) using the results of commercial cone penetration tests in conjunction with the soil classification chart developed by Robertson (1990). Beneath the topsoil, the CPT profiles classify the upper 4.0 m of soil as uniform clay. From 4.0 m to 7.5 m below the surface, the soil consists of interbedded silty

clay and clayey silt, becoming more silty and sandy beyond 7.5 meters. The material is described as slightly overconsolidated in nature, and is of proglacial lacustrine origin, deposited by the former Lake Edmonton. The Edmonton till was encountered at a depth of approximately 8.0 meters below the surface, and the groundwater table was located at a depth of 3.0 meters (Zhang 1999).

As part of the current investigation, it was undertaken to determine the approximate undrained shear strength (s_u) of the lacustrine material with depth at the University Farm site in Edmonton. This information was obtained for use in verifying the results of the modified cone penetration tests which were performed at the site. Shelby tube samples were taken from the University Farm site for undisturbed strength testing, and before extracting the tubes, vane shear tests were performed on the open ends using a field vane and a laboratory vane of appropriate dimensions. After extraction of the Shelby samples, representative specimens were obtained for unconfined compressive strength (UCS) testing in the University of Alberta laboratory. Standard Penetration Testing was also carried out on site, and the corrected blow counts were used to provide additional estimates of shear strength with depth using the relationship given by Terzaghi and Peck (1967) and cited by Bhanot (1968) for the prediction of shear strength in clays using the SPT blow count (equations [3-1] and [3-2]). Based on the results of the methods described above, Figure 4-1 depicts the approximate undrained shear strength with depth for the Lake Edmonton Clay at the University of Alberta Farm site. It may be seen from the figure that the undrained strength of the lacustrine material is quite uniform over the depth of the investigation, and lies in the range of 50 to 100 kPa.

Cone penetration testing has twice been conducted at the University Farm site under separate investigations. First, in October 1997, commercial, rig-mounted CPT profiles were obtained at the site and documented by Zhang (1999), and second, under the current investigation, cone penetration testing using the modified equipment developed for this thesis project was conducted in January 2006. The profiles of tip resistance, friction ratio, and piezometric head obtained by

the commercial CPT(U) testing are shown in Figure 4-2, followed by the tip resistance and friction ratio results of the modified cone penetration tests in Figure 4-3.

4.2.2 Test Site No. 2: Bruderheim, Alberta

The town of Bruderheim is located in central Alberta, approximately 60 km northeast of the city of Edmonton. Six screw pile load tests, three in compression and three in tension, were conducted in May 1998 at a sand pit site near Bruderheim, Alberta, and documented by Zhang (1999). The test site is located approximately 7.5 km north of Bruderheim town center. The general stratigraphy of the Bruderheim site consists of clean sand to silty sand, formed by sand dunes of minor loess. The dunes were produced from dried sediments of the Glacial Lake Edmonton which were transported by wind after the drainage of the lake (Zhang 1999). Based on the results of three commercial cone penetration tests documented by Zhang (1999) at the Bruderheim test site, the soil profile is described using Robertson's (1990) soil behaviour type chart as clean sand to a depth of 0.75 m, underlain by medium-grained sand to silty sand to a depth of 2.75 m. From 2.75 m to 5.0 m, the soil is classified as silty sand to sandy silt, beyond which it is described as clayey silt to silty clay to the final depth investigated, 6.5 m. The groundwater table was encountered at approximately 4.5 m below the surface. The tip resistance and friction ratio profiles obtained by cone penetration testing at the Bruderheim test site in November 1997 are shown in Figure 4-4, (a) and (b) (after Zhang 1999).

4.2.3 Test Site No. 3: Ft. Saskatchewan, Alberta

The city of Ft. Saskatchewan is located approximately 30 km northeast of the city of Edmonton, in Alberta. Three axial compression tests were conducted in the fall of 2001 on screw piles installed at a commercial piling yard located in Ft. Saskatchewan at 86 Avenue and 111 Street. At the time of the screw pile load tests, the Ft. Saskatchewan location was subject to an engineering site investigation consisting of two boreholes augered to respective depths of 9.0 m and 10.5 m below the surface. Beneath a layer of topsoil, the stratigraphy was determined to uniformly consist of silty, stiff to very stiff clay extending to the depth investigated. Pocket penetrometer readings showed the unconfined compressive strength of the material to generally lie between 150 and

250 kPa. The boreholes included in Appendix C may be viewed for further detail regarding moisture content determinations and pocket penetrometer readings with depth. The test hole was dry upon completion of the drilling.

Two cone penetration tests were conducted at the Ft. Saskatchewan site in June 2006 using the modified equipment described in Chapter 3. The cone holes were pushed within a few meters of where the screw piles had been installed for load testing in 2001. The profiles of tip resistance obtained are shown in Figure 4-5. The sleeve friction readings measured by the modified equipment at the Ft. Saskatchewan site yielded a friction ratio profile that was very nearly equal to zero or even negative for most of the depth penetrated; it is suspected that the sleeve readings taken at the site were in error, perhaps due to sticking of the sleeve, and the friction ratio profiles have therefore been omitted.

4.2.4   Test Site No. 4: Lamont, Alberta

The town of Lamont, Alberta, is situated approximately 65 km northeast of the city of Edmonton, nearly 35 km eastbound from the city of Ft. Saskatchewan. An undeveloped site located just west of Lamont, near the intersection of Highway 15 and Secondary Highway 637, was selected for the construction of a warehouse fabricating facility, to be built on screw pile foundations. A single load test in compression was performed at the site on the screw pile design selected to form the building foundations in June of 2006. An engineering site investigation was conducted a month prior, consisting of two boreholes augered to depths of approximately 9 meters each. Based on examination of the disturbed cuttings, the subsurface was characterized as consisting of a thin layer of topsoil above clay till, underlain by a discontinuous layer of sand over clay shale bedrock. The clay till was described as silty, hard to very hard in consistency, and extended to depths of 3.4 m and 1.7 m in the two boreholes, respectively. A layer of sand was encountered beneath the till in the second borehole only, lying between 1.7 m and 3.6 m below surface. The remaining 5.5 m investigated turned up clay shale in both test holes, described as silty, highly-weathered, hard to very hard consistency bedrock. No evidence of groundwater seepage was detected after drilling. The two boreholes are included for reference in Appendix C, with soil

classifications, moisture content determinations, and pocket penetrometer readings recorded with depth.

Two commercial cone penetration tests were commissioned at the Lamont test site under the current investigation in August 2006. The tests were conducted within about 6 meters of the spot where the screw pile load test was conducted 2 months prior. The resulting profiles of tip resistance, friction ratio, and piezometric head are shown in Figure 4-6; the water table was located at a depth of approximately 8.0 m during cone penetration testing. Measurements of seismic shear wave velocities were also taken at 1-m increments during the cone tests, utilizing a geophone embedded in the commercial cone penetrometer. A summary of the shear wave velocity results is given in Table 4-1.

4.3 Surficial Geology of the Ft. McMurray Area, Alberta

The city of Ft. McMurray is located in northern Alberta where the Clearwater River meets the Athabasca River flowing north. The region is famous for its vast deposits of natural oil sands, which rise as black cliffs along the banks of the Athabasca. The oil sand deposits are classified as Lower Cretaceous, and of the McMurray Formation. The oil sands were formed by sediment deposited in an extensive drainage basin created in the area by the solution of a large volume of salts from buried evaporites, causing collapse of the overlying Upper Devonian limestone beds. The sand grains of the McMurray formation are primarily quartz, believed to be derived from the Canadian Shield to the northeast, and from sandstones to the south. The bitumen is thought to have migrated updip, eastward, from source rock shales in the central Alberta Basin (O'Donnell 2006). Overlying the McMurray Formation are Cretaceous clays and shales of the Clearwater formation, followed by a variety of glacial, glaciofluvial, and glaciolacustrine sediments (till, gravel, sand, and clay) (Carrigy 1959; O'Donnell 2006). In the downtown area of Ft. McMurray, erosion has removed the Cretaceous sedimentary rocks, so that three to fifteen meters of floodplain alluvium rests directly on the Devonian limestone. Extensive coarse gravel and sand deposits are distributed downstream from Ft. McMurray, due to catastrophic late-glacial flooding that

partially drained Glacial Lake Agassiz and discharged down the Clearwater and Athabasca River valleys nearly 10,000 years ago (O'Donnell 2006).

4.3.1   Test Site No. 5: Ruth Lake Substation Near Ft. McMurray, Alberta

The Ruth Lake test site is located approximately 40 km northwest of the city of Ft. McMurray, next to the electrical substation at NE-16-92-10-W4M. Four screw pile load tests, two in compression and two in tension, were performed at this location in November of 2001. The geology of the Ruth Lake site was determined by an engineering site investigation in the same year, consisting of two boreholes drilled near the test pile locations to depths of 10.2 m and 9.3 m, respectively. Appendix C shows the two bore logs obtained, with classification of disturbed soil samples and measured SPT blow counts and moisture content determinations taken at regular intervals. The dominant soil conditions within the zone of influence of the test piles consist of very stiff to hard clay till, encountered from approximately 2.0 m to 6.5 m below surface. Glaciofluvial outwash or meltwater channel sand with discontinuous glaciolacustrine clay layers was encountered above the clay till deposit, and a rafted oilsand layer of the McMurray formation was encountered below the clay till strata in one of the two boreholes, before reaching the very stiff to hard Clearwater Clay soils which extend to the ultimate depth of investigation. Groundwater levels of 2.4 m and 2.7 m were observed in the two boreholes following completion of the drilling, and 17 days later, a longer-term groundwater level was detected at 1.1 meters below surface.

The Ruth Lake Substation site was revisited in August 2006 as part of the current investigation, and two commercial cone penetration tests were carried out several meters north of the substation, near the spot where the prior screw pile load tests were done. In addition to the measurement of tip resistance and sleeve friction with depth, the commercial cone penetration tests included the continuous measurement of pore pressure with depth and the recording of seismic shear wave velocities at each 1-m increment. The profiles of tip resistance, sleeve friction, and piezometric head obtained are shown in Figure 4-7. Based on the pore pressure dissipation response and the profile of piezometric head measured during the cone penetration

tests, the current water table was placed at approximately 2 m below the surface. A summary of the seismic shear wave velocities at the Ruth Lake Substation site is given in Table 4-2.

4.3.2   Test Site No. 6: Dover Substation Near Ft. McMurray, Alberta

A single screw pile was installed and load tested in axial tension in January 2004, at a second site in the vicinity of Ft. McMurray, Alberta, near the Dover electrical substation located about 80 km northwest of the city, at NE-31-92-12-W4M. The engineering site investigation conducted at the Dover substation consisted of a single, 6.4 m test boring, from which the subsurface profile was found to be essentially comprised of very dense sand, described as possible sand till, overlain by 1.2 m of clay till followed by 1.2 m of sand to the surface. SPT counts of 50 blows for 75 mm and 89 blows for 150 mm were recorded in the lower sand layer, indicating a very dense state. The test hole was dry on completion. The detailed bore log showing the classifications of the soil cuttings, along with intermittent records of moisture content and SPT blow counts is included in Appendix C.

One commercial cone penetration test was conducted beside the Dover substation when the site was revisited in August 2006 under the current investigation. The test was carried out near the transmission line to the south of the substation, close to the spot where the screw pile was previously loaded in tension to failure. The results of the cone penetration test at the Dover substation site consist of profiles of tip resistance, friction ratio, and piezometric head to a depth of 6.0 m, shown in Figure 4-8, and a summary of seismic shear wave velocities shown in Table 4-3.

4.4   Surficial Geology of the Beaverlodge Area, Alberta

The town of Beaverlodge, Alberta, is located near the British Columbia border approximately 45 km northwest of the city of Grande Prairie, Alberta. The surficial geology of the area is dealt with in a thesis work by Jones (1961); he observed buried gravels, probably of preglacial origin, located in a broad valley trending westerly and northwesterly through Beaverlodge. The preglacial landscape was subsequently overrun by Wisconsin ice from the north and northeast,

filling the broad valleys with glacial debris composed mainly of till (Jones 1961). The ice advance over the Beaverlodge map-area appears to have followed the local bedrock topography, leaving thick deposits of till up to 60 meters deep in the preglacial valleys, but only a thin layer of till or none at all on the highlands (Jones 1961). While some of the preglacial gravels were incorporated into the advancing ice, considerable amounts were left undisturbed, buried at their site of original deposition. Jones (1961) also noted that high carbonate percentages were lacking in the till of the Beaverlodge district, indicating that the area was never reached by the Cordilleran glaciation. This observation is in agreement with the findings of Mathews (1963) who positioned the termination of the Cordilleran glaciation somewhat to the west of the town of Ft. St. John, B.C., which in turn lies about 165 km to the northwest of Beaverlodge, Alberta.

As the continental ice sheet overlying the Beaverlodge district began to recede, highlands in the area were the first features to emerge. The topographic highs were exposed to wind and wave action by surrounding meltwater ponded on top of the remaining ice, and well-developed beach deposits of sand and gravel may be found northeast of the hamlet of La Glace, near Beaverlodge (Jones 1961). Following this initial period of ablation, a minor re-advance of ice outside the Beaverlodge map-area caused the local meltwaters to become impounded, depositing lacustrine sediments atop the till, their boundary marked by a sharp disconformity (Jones 1961). This impounded water was part of the glacial Lake Peace, also referred to by Mathews (1963) in his discussion of the glacial history of the Ft. St. John area, British Columbia. The waters of Lake Peace slowly receded and eventually disappeared from the area with the final retreat of Continental ice.

4.4.1   Test Site No. 7: Hythe, Alberta

The village of Hythe is located in northwestern Alberta near the town of Beaverlodge, 15 km to the southeast, and is approximately 60 km northwest of the city Grande Prairie. A screw pile installed at the site of a proposed shop facility in the village of Hythe was load tested under axial compression in December 2005, to verify the capacity of the screw pile foundations selected for the proposed facility. Three test holes were drilled at the site in May 2005 as part of an

engineering investigation to delineate the surficial geology, to depths of up to 6.8 m. The borehole logs, including soil classification, moisture content determinations, and SPT blow counts are included in Appendix C. The soil profile generally consists of a thin layer of stiff clay below the topsoil, of less than 1 meter in thickness, followed by a section of silty clay overlying stiff clay till to a depth of approximately 3.5 to 4.5 m. The water table was detected approximately 2.5 m to 3.0 m below surface, midway through the silty clay/clay till section. Beneath the clay till, discontinuous layers of hard sandstone, stiff to very stiff clay shale, and dense, water-bearing sand were detected, if at all, in differing order and thickness under each borehole. The three test holes were terminated due to refusal at depths of 5.2 m, 6.2 m, and 6.8 m below surface, respectively. Immediate sloughing and rapid ingress of water was observed where the sand layer was encountered in drilling, and for this reason it was recommended that casing be readily available on-site if poured concrete piles were to be installed. However, the selection of screw piles for use at the site precluded the need for casing, thereby eliminating much of the associated cost and effort.

Cone penetration testing using the modified equipment described in Chapter 3 was attempted at the Hythe site in May 2006, but due to the hard nature of the subsurface the cone could not be pushed beyond about 3 m deep. Since the screw pile load tested at the site was installed to a depth of 7.5 m, the cone penetration data obtained was not considered sufficient for analysis.

4.5   Surficial Geology of the Ft. St. John Area, British Columbia

The town of Fort St. John is located on the Great Plains in northeastern British Columbia, lying about 80 km to the east of the Rocky Mountain front. The town is the central community for one of the northernmost farming areas in Canada (Mathews 1963). Ft. St. John lies within the limits reached by the Laurentide glaciation which advanced from the Canadian Shield, and is positioned just beyond the eastern limit of the Cordilleran ice sheet which subsequently advanced from the west (Mathews 1963). The surficial geology of the area is quite complex, comprising, in order of decreasing age, an old layer of glacial till attributable to an early advance of Laurentide ice, overlain by interglacial river and lake deposits, the latter being a result of river ponding due to

advancing ice, a subsequent layer of glacial till deposited by the last major advance of Laurentide ice in the area, and finally, late glacial deposits including lacustrine silt and clay, and near-shore sand and gravel occurring as a result of persistent ice-dammed lakes. To the west of Ft. St. John, overlying sand and till attributed to the advance of the Cordilleran ice sheet may also be found (Mathews 1963).

The first and oldest layer of glacial till is a massive unit at least 15 meters thick containing scattered pebbles, some of which are derived from the Canadian Shield (Mathews 1963). The old glacial till has been detected to the southeast of Ft. St. John, and the early glaciation to which it is linked is also indicated by the varved and pebbly silts which can be found southwest of the town. Presumably, an early Laurentide ice sheet moved in from the north or east, and proceeded to dam the ancestral Peace River, creating an environment for the deposition of the lacustrine sediments and the early till layer in their respective areas of extent (Mathews 1963). A well-defined erosional interval followed the early glaciation, leading to the development of the interglacial Peace River near Ft. St. John. A period of sedimentation terminated the interglacial erosional interval, and during this time, the gravel-floored trenches were covered by alluvium and lacustrine deposits, the latter presumably as a result of ponding due to advancing ice from the east (Mathews 1963). The arrival of the second ice sheet to reach the Ft. St. John area is clearly indicated by the younger till formation left behind and associated glacial grooves (Mathews 1963). During the retreat of this second glaciation, there developed a series of ice-dammed lakes referred to as Glacial Lake Peace. As the glacial lake slowly receded, a lower and younger stage of Lake Peace left a strip of gravel beach in the Ft. St. John area, as well as extensive lacustrine clay deposits.

4.5.1   Test Site No. 8: Town of Ft. St. John, British Columbia

Two screw pile load tests were performed at the site of a proposed development in the town of Ft. St. John, British Columbia, near 93 Avenue and 96 Street. Two separate manufacturers installed screw piles at the site in August 2005 and tested them under static compressive load for the purpose of procuring the foundation contract for a planned two-storey commercial/condominium

project. An engineering investigation of the test site was commissioned by the developer prior to the load testing of the piles. Several test holes were augered into the subsurface and indicated that below a thin layer of topsoil, the soil uniformly consisted of glaciolacustrine silty clay to the maximum depth investigated, 10.4 m. The consistency of the silty clay was described as firm to stiff, with an average moisture content of 25 percent, and blow counts of less than 10 recorded to the depth of boring. The clay was determined to be sensitive in nature, exhibiting volume change upon variation in moisture content. The depth of the water table was not identified.

The condominium site in Ft. St. John could not be accessed for cone penetration testing under the current investigation, as the land had since been turned over to private ownership.

4.5.2   Test Site No. 9: Farmland Near Ft. St. John, British Columbia

A second screw pile load test site located in the vicinity of Ft. St. John, British Columbia, is situated on a privately-owned plot of farmland, approximately 10 km northeast of the town. Two screw piles were tested at the site under axial compression in September 2006. Although no subsoil report is available for the location, two cone penetration tests were performed at the test site in May 2006 under the current investigation, using the modified equipment described in Chapter 3. Figure 4-9 shows the profiles of tip resistance and friction ratio obtained at the farm site. The profiles may be used in conjunction with the soil behavior chart developed by Robertson et al. (1986) to describe the surficial geology at the site. The cone penetration testing shows that beneath a layer of topsoil, the subsurface may be uniformly described as clay to a depth of approximately 6.2 m, beyond which the deposit becomes more silty, and is classified as silty clay to clayey silt to the final depth penetrated, 6.6 m. The reason for the significant discrepancy visible between the two profiles of friction ratio presented in Figure 4-9 is not known.

4.6   Surficial Geology of the Saskatoon Area, Saskatchewan

The city of Saskatoon, located in southern Saskatchewan, is underlain by till and stratified drift glacially deposited during Pleistocene time (Christiansen 1968). The sediments are subdivided, in ascending order, into the Sutherland and Saskatoon Groups on the basis of dolomite content of

the tills. The Saskatoon Group is further divided into two tills, the Floral Formation and the overlying Battleford Formation.

The Sutherland Group is composed of till and stratified drift, and ranges in thickness from 40 to 85 meters. The dominant clay minerals present are montmorillonite, illite, kaolinite, and minor amounts of chlorite. The tills are dense, and grey in colour where unoxidized, light olive to olive where oxidized (Christiansen 1968). As noted by Christiansen (1968), leaching of the till where it forms the uppermost part of the Sutherland Group indicates an interglacial hiatus between the Sutherland and Saskatoon Groups. The Saskatoon Group lies between the Sutherland Group and the present ground surface. It is comprised of stratified drift and till of a more sandy, less clayey nature, and represents a higher resistivity when compared to the Sutherland Group below (Christiansen 1968). The Floral Formation forms the bottom 32 meters of the Saskatoon Group, composed of dense till interbedded with sand and gravel. The upper portion of the Floral Formation is oxidized, jointed, and stained with iron and manganese oxide, suggesting only a partial truncation of the weathered surface during the last glaciation (Christiansen 1968). The overlying Battleford Formation is comprised of soft, massive, unstained till interbedded locally with sand and gravel. The Battleford Formation is of 0 to 45 meters in thickness, lying between the Floral Formation and the ground surface. The base of the formation is commonly marked by a boulder pavement, and the surface may be overlain by a thin layer of stratified drift (Christiansen 1968).

4.6.1   Test Site No. 10: Saskatoon, Saskatchewan

At the location of a prospective multi-family housing development inside the city of Saskatoon, Saskatchewan, three screw piles of differing geometry were installed and axially load tested under static compression in October 2005. As part of the proposed development of the large, low-rise condominium project, an engineering investigation of the site was carried out in April 2005 to determine the subsoil conditions. Eight test holes were drilled on-site to a depth of up to 18.3 m, and soil classification and moisture contents determined from disturbed cuttings. The stratigraphy at the subject site was thus determined to consist of a layer of sand and clay fill

underlain by variable fluvial-lacustrine deposits of silt, sand, and clay to the depth investigated. The one borehole included in Appendix C is that which was drilled nearest to the location of the screw pile load tests, and shows approximately 1.7 m of fill, followed by compact, silty sand to a depth of about 12.6 m, underlain by stiff clay to the final depth investigated, 15 m. The water table was detected immediately after drilling at 2.3 m below the ground surface.

Due to the compact nature of the sand deposit located beneath the Saskatoon site, it was not possible to conduct cone penetration testing using the modified equipment developed for this thesis project. The results of the screw pile load tests at the Saskatoon site will therefore be discussed in terms of how they relate to the pile geometries and installation torques achieved, but the lack of CPT results for the site precludes analysis using the LCPC direct design method.

Table 4-1: Shear Wave Velocity Measurements, Lamont Site, Alberta

Tip Depth (m)	Geophone Depth (m)	Ray Path (m)	V_s (m/s)	Mid-Layer Depth (m)
1.00	0.80	1.20	--	--
2.00	1.80	2.01	162	1.30
3.00	2.80	2.94	272	2.30
4.00	3.80	3.91	222	3.30
5.00	4.80	4.88	260	4.30
6.00	5.80	5.87	250	5.30
7.00	6.80	6.86	249	6.30
8.00	7.80	7.85	236	7.30
9.00	8.80	8.85	242	8.30
10.00	9.80	9.84	251	9.30

Table 4-2: Shear Wave Velocity Measurements, Ruth Lake Substation Site, Alberta

Tip Depth (m)	Geophone Depth (m)	Ray Path (m)	V_s (m/s)	Mid-Layer Depth (m)
1.00	0.80	1.20	--	--
2.00	1.80	2.01	126	1.30
3.00	2.80	2.94	193	2.30
4.00	3.80	3.91	202	3.30
5.00	4.80	4.88	187	4.30
6.00	5.80	5.87	222	5.30
7.00	6.80	6.86	222	6.30
8.00	7.80	7.85	237	7.30

Table 4-3: Shear Wave Velocity Measurements, Dover Substation Site, Alberta

Tip Depth (m)	Geophone Depth (m)	Ray Path (m)	V_s (m/s)	Mid-Layer Depth (m)
1.00	0.80	1.20	--	--
2.00	1.80	2.01	174	1.30
3.00	2.80	2.94	300	2.30
4.00	3.80	3.91	348	3.30
5.00	4.80	4.88	376	4.30
6.00	5.80	5.87	620	5.30
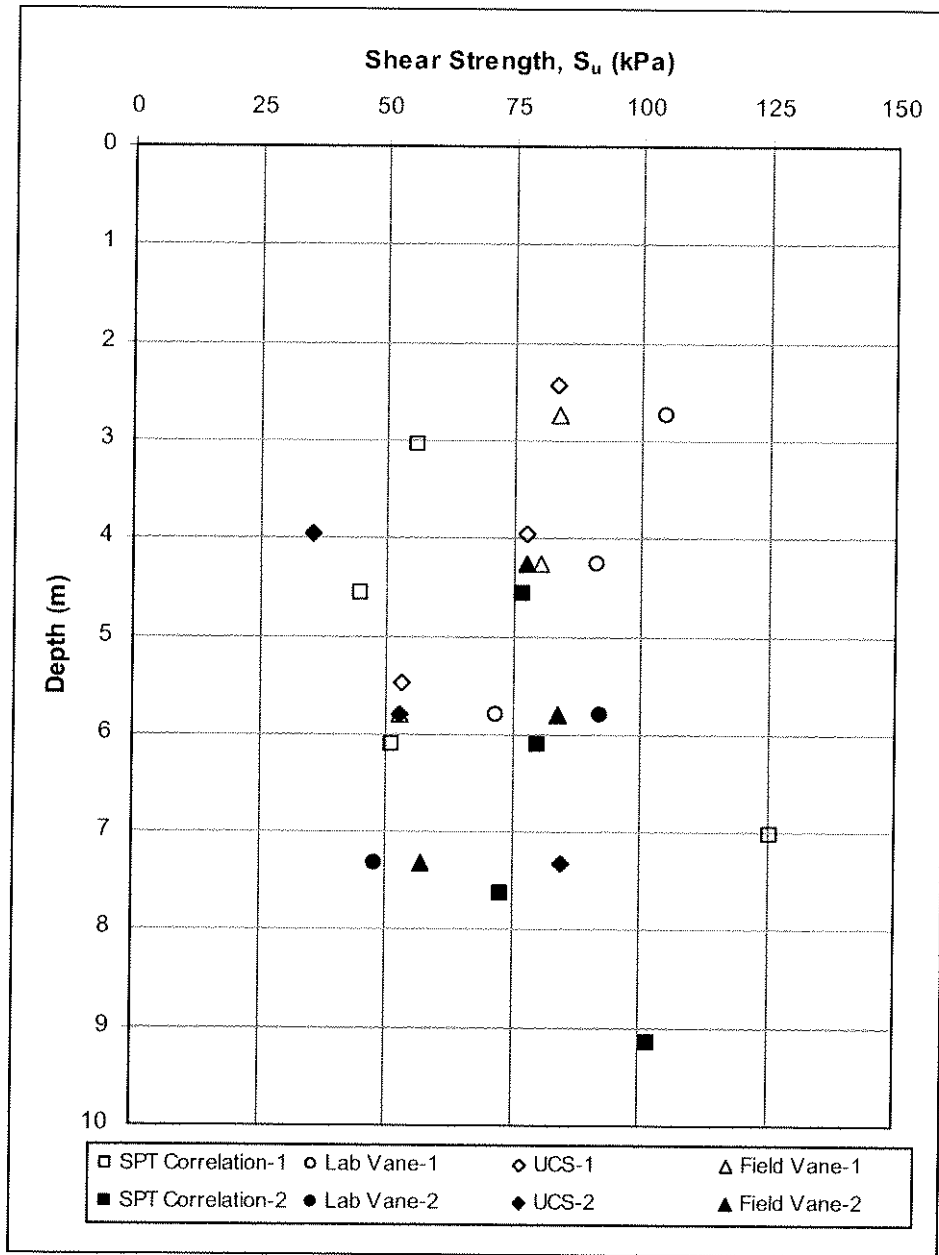
Figure 4-1: Shear Strength Profile, University Farm Site, Edmonton, Alberta
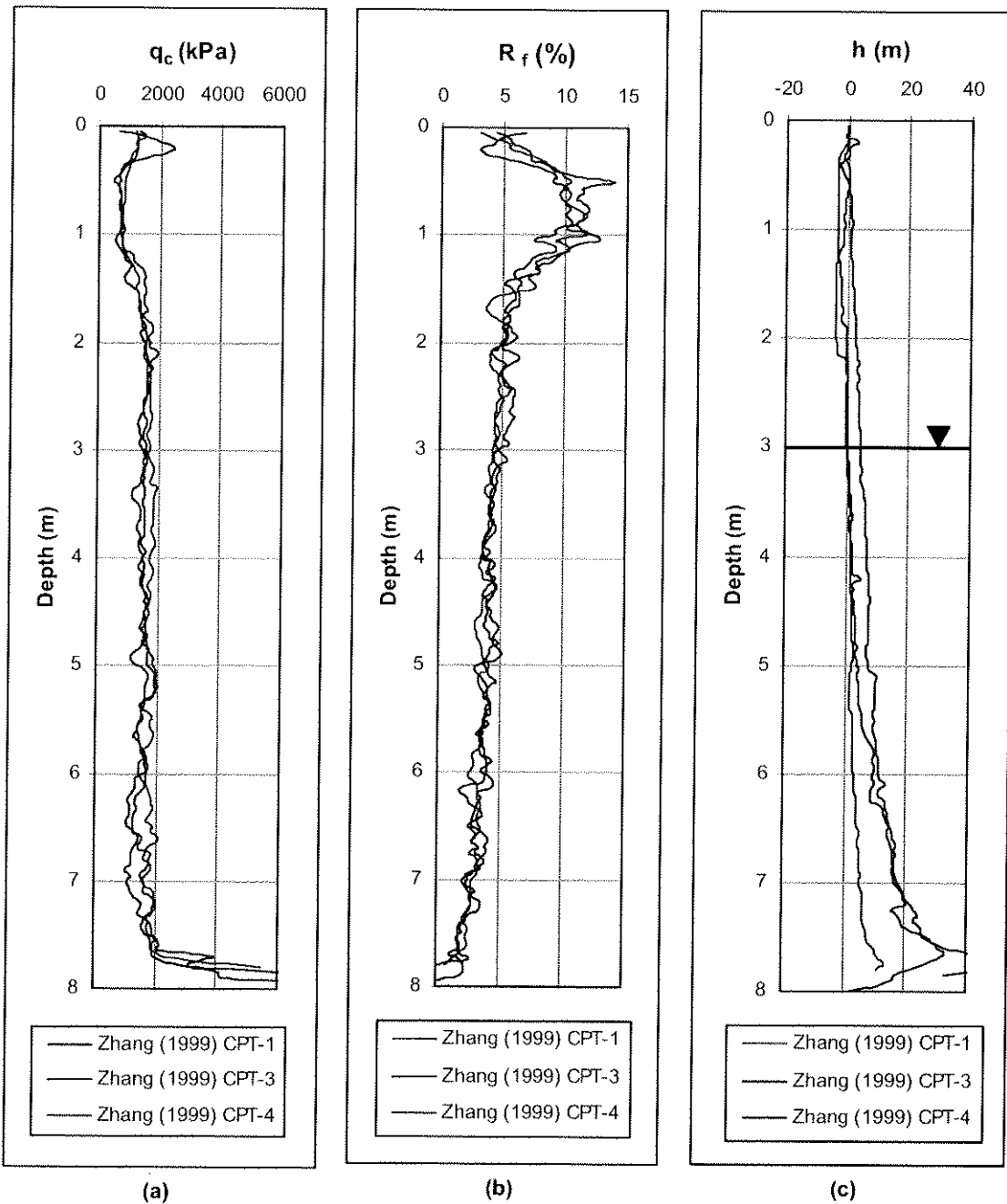
Figure 4-2: Cone Penetration Profiles, University Farm Site (after Zhang 1999): (a) Tip Resistance, q_c; (b) Sleeve Friction, R_f; (c) Piezometric Head, h
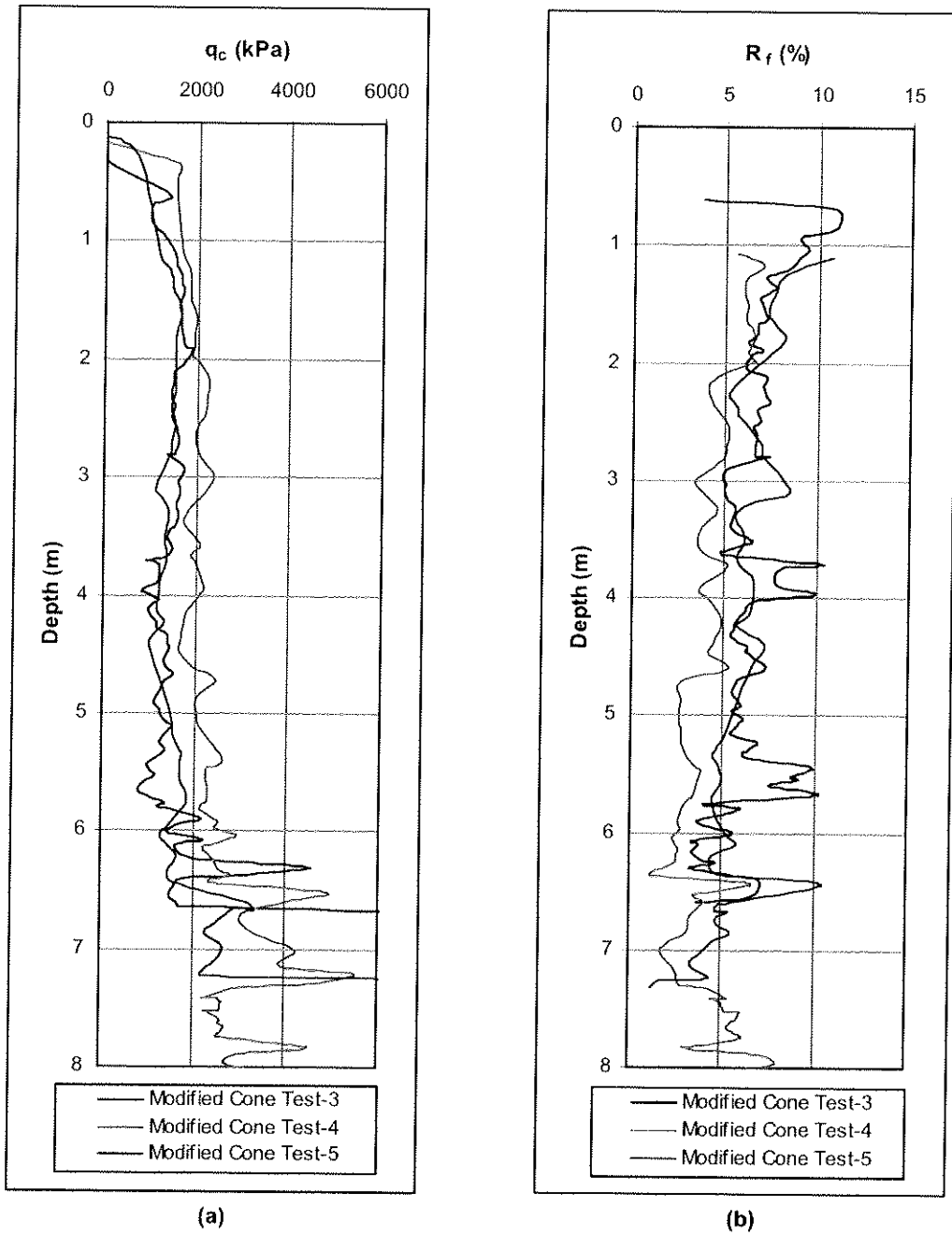
Figure 4-3: Cone Penetration Profiles, University Farm Site, Current Investigation: (a) Tip Resistance, q_c; (b) Friction Ratio, R_f
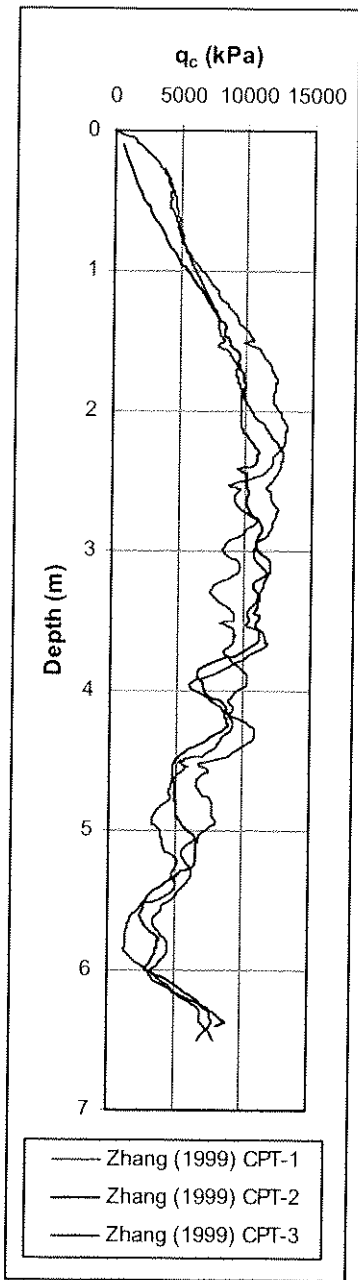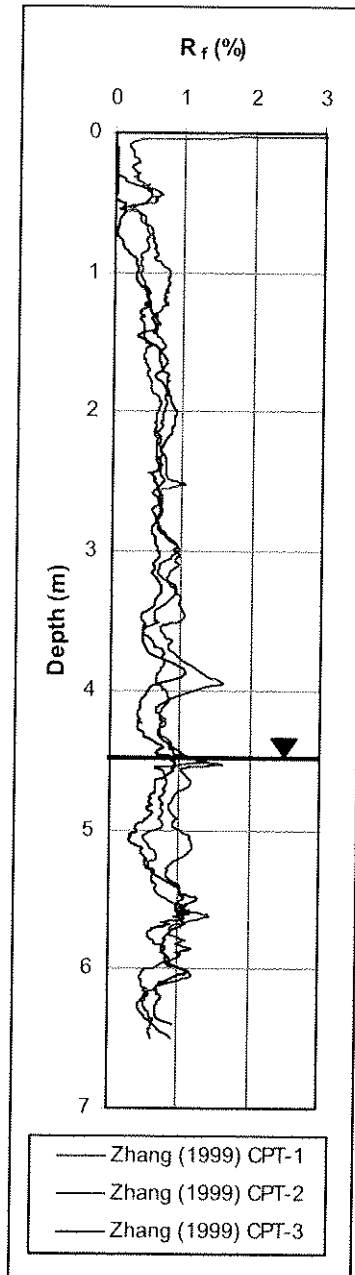
Figure 4-4: Cone Penetration Profiles, Bruderheim Site (after Zhang 1999): (a) Tip Resistance, q_c; (b) Friction Ratio, R_f
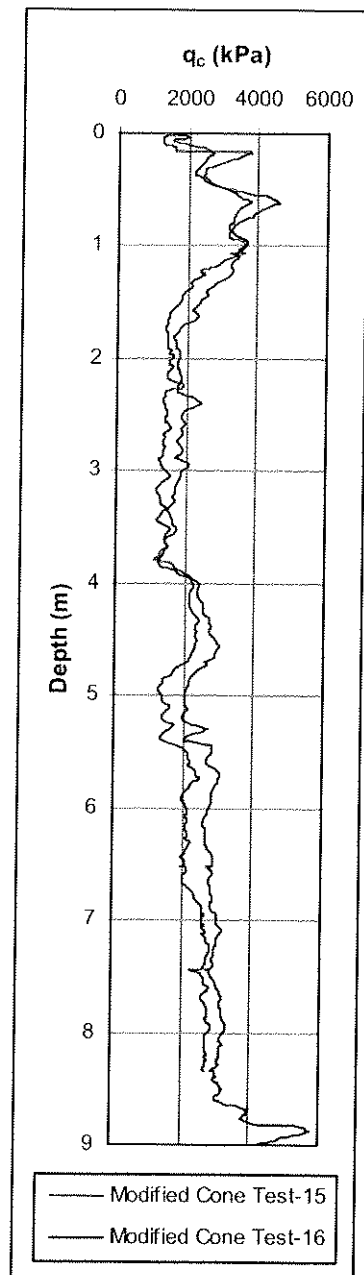
Figure 4-5: Cone Penetration Profiles, Ft. Saskatchewan Site: Tip Resistance, q_c
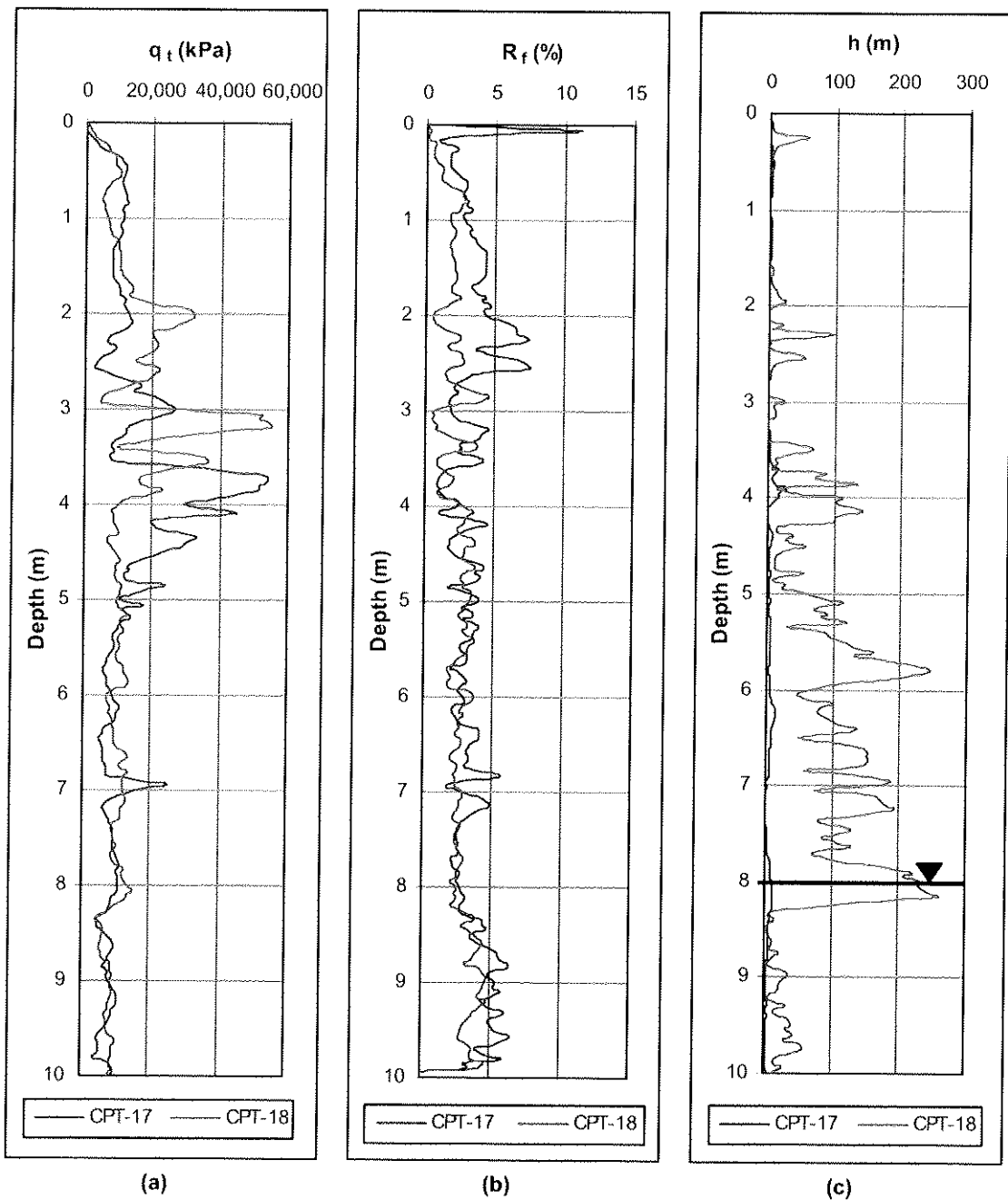
Figure 4-6: Cone Penetration Profiles, Lamont Site: (a) Tip Resistance, q_c; (b) Friction Ratio, R_f; (c) Piezometric Head, h
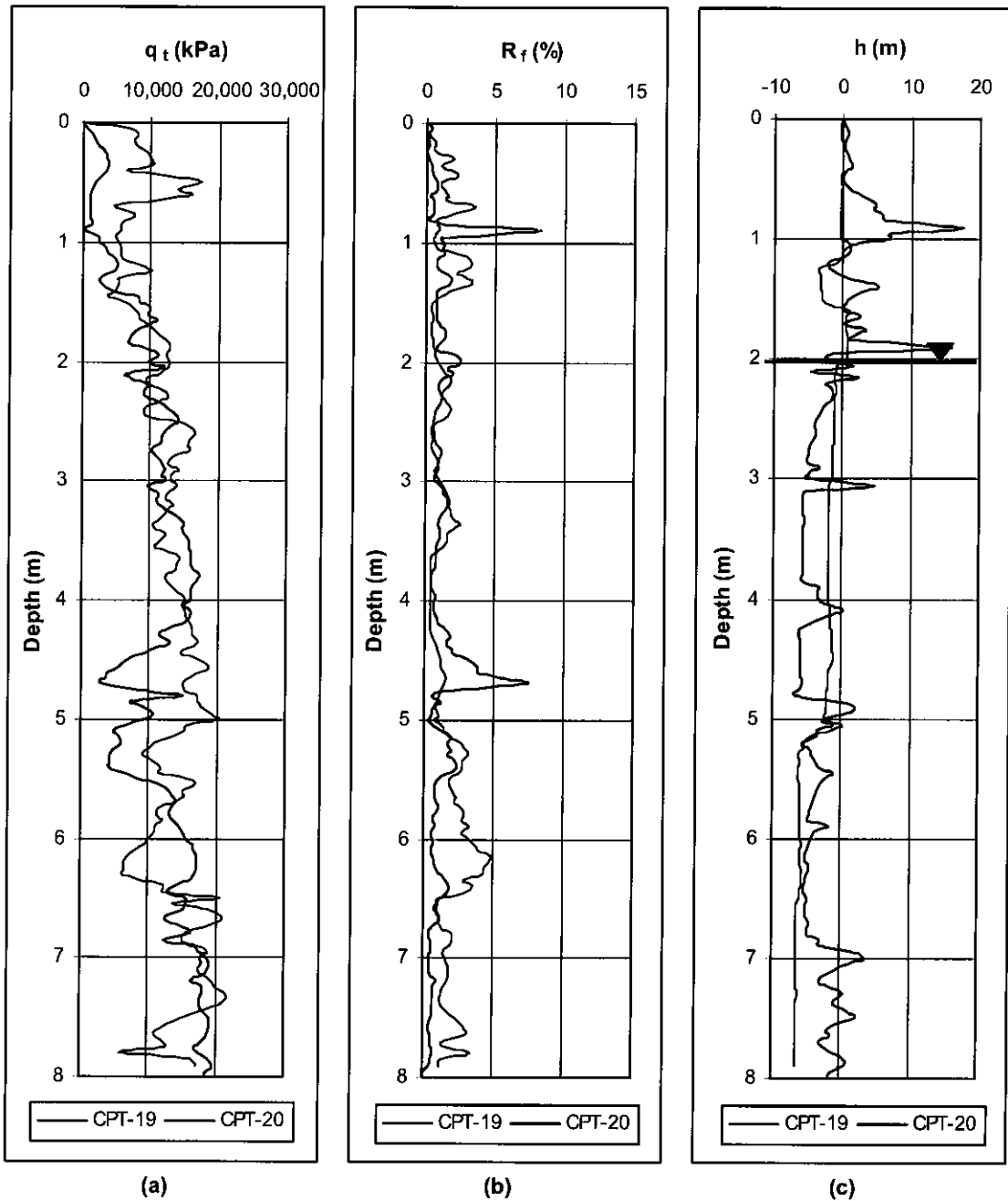
Figure 4-7: Cone Penetration Profiles, Ruth Lake Site: (a) Tip Resistance, q_c; (b) Friction Ratio, R_f; (c) Piezometric Head, h
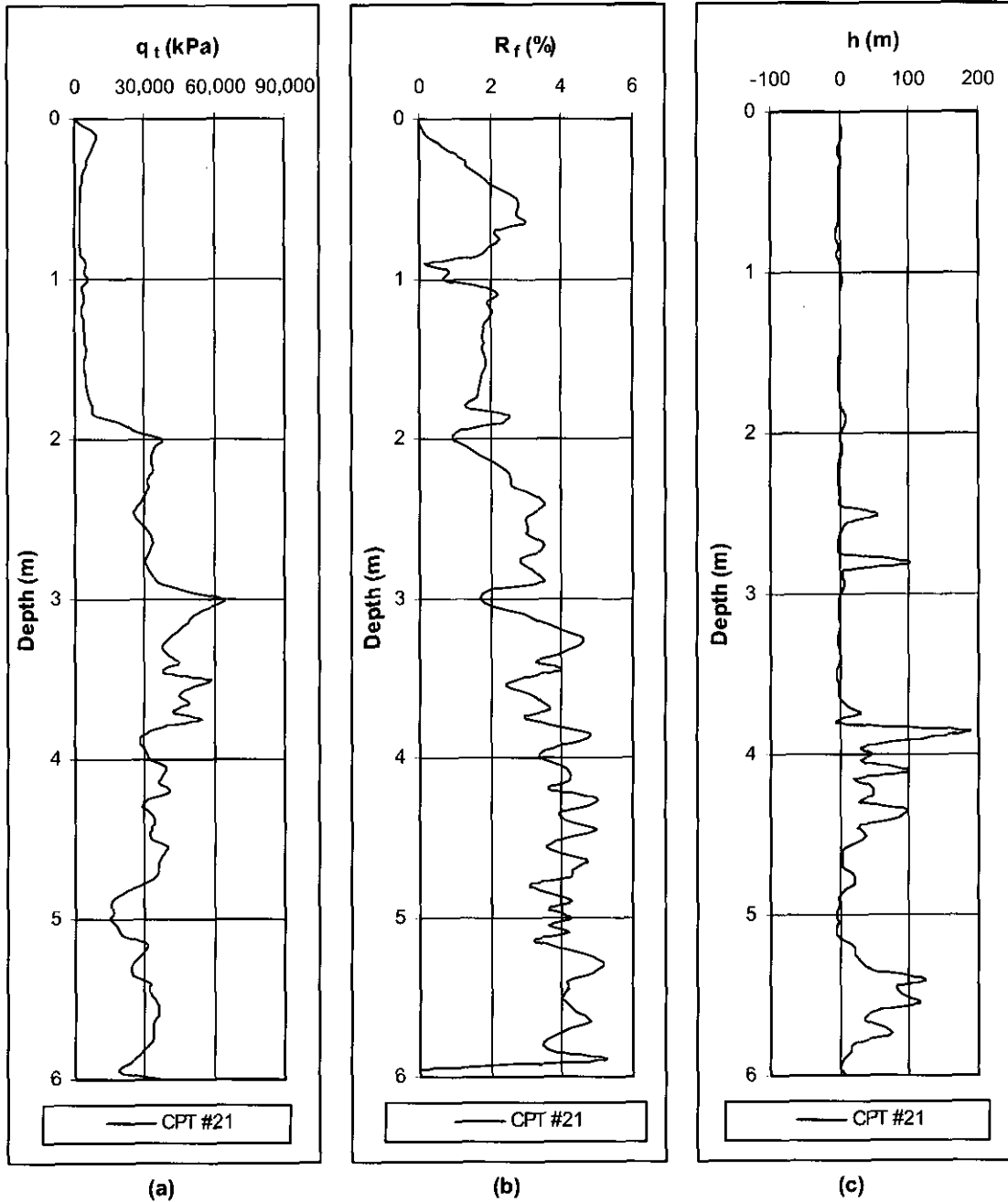
Figure 4-8: Cone Penetration Profiles, Dover Site: (a) Tip Resistance, q_c; (b) Friction Ratio, R_f; (c) Piezometric Head, h
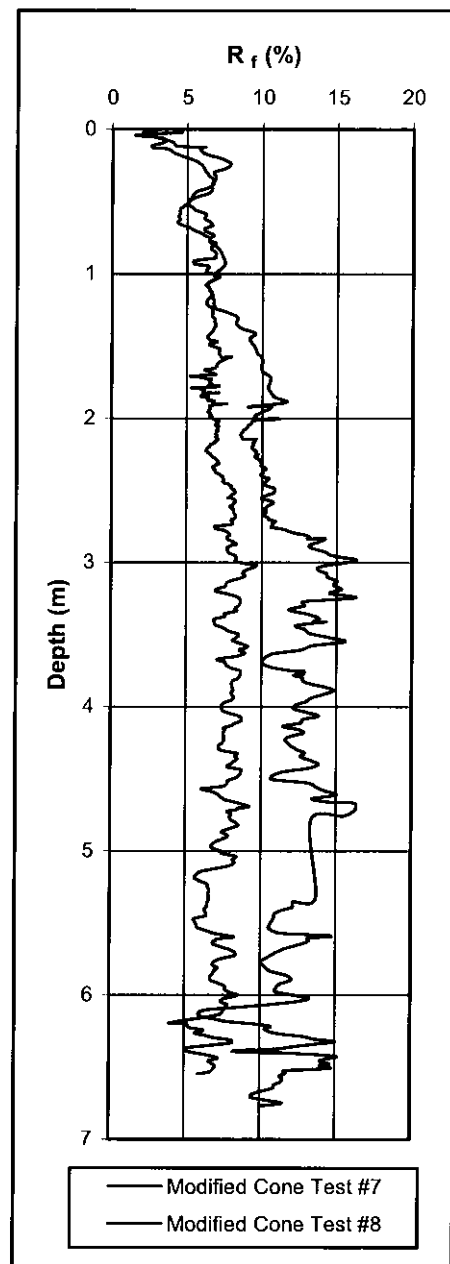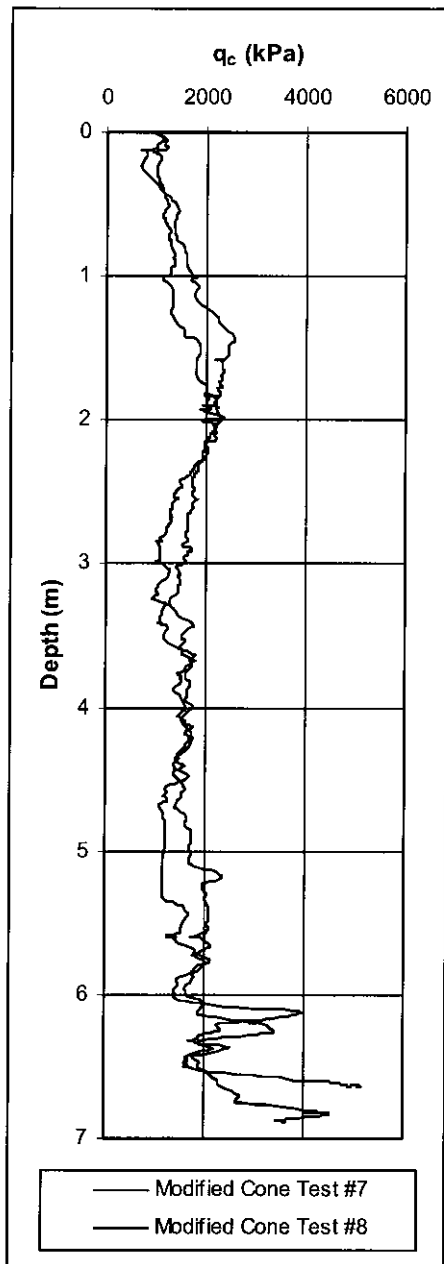
Figure 4-9: Cone Penetration Profiles, Ft. St. John Farm Site: (a) Tip Resistance, q_c; (b) Friction Ratio, R_f

4.7 References

Bayrock, L.A., and Hughes, G.M. 1962. Surficial geology of the Edmonton district, Alberta. Research Council of Alberta, Preliminary Report 62-6, Edmonton, Alberta.

Bhanot, K.L. 1968. Behaviour of scaled and full-length cast-in-place concrete piles. Ph.D. thesis, Department of Civil Engineering, University of Alberta, Edmonton, Alberta.

Bustamante, M., and Gianeselli, L. 1982. Pile bearing capacity prediction by means of static penetrometer CPT. *In* Proceedings of the 2nd European Symposium on Penetration Testing, ESOPT-II. Amsterdam. Balkema Publisher, Rotterdam, Vol.2, pp. 493-500.

Carrigy, M.A. 1959. Geology of the McMurray Formation. Part III. General geology of the McMurray area. Alberta Research Council Memoir 1.

Christiansen, E.A. 1968. Pleistocene stratigraphy of the Saskatoon area, Saskatchewan, Canada. Canadian Journal of Earth Sciences, 5(5): 1167-1173.

Jones, J.F. 1961. Surficial geology and related problems, Beaverlodge district, northwestern Alberta. M.Sc. thesis, Department of Geology, The University of Western Ontario, London, Canada.

Mathews, W.H. 1963. Quaternary stratigraphy and geomorphology of the Fort St. John area, northeastern British Columbia. Department of Mines and Petroleum Resources, Victoria, B.C.

O'Donnell, N. 2006. Fort McMurray. *In* Alberta beneath our feet: the story of our rocks and fossils. Geoscience Publishing. p. 248.

Robertson, P.K. 1990. Soil classification using the CPT. Canadian Geotechnical Journal, 27(1): 151-158.

Robertson, P.K., Campanella, R.G., Gillespie, D., and Grieg, J. 1986. Use of piezometer cone data. *In* Proceedings, In-situ '86: ASCE Specialty Conference. Blacksburg, Virginia.

Terzaghi, K., and Peck, R.B. 1967. Soil mechanics in engineering practice. John Wiley and Sons, New York.

Zhang, D. 1999. Predicting capacity of helical screw piles in Alberta soils. M.Sc. thesis, Department of Civil and Environmental Engineering, University of Alberta, Edmonton, Alberta.

5 Screw Pile Load Test Results

5.1 Introduction

The following chapter provides a synopsis of results for 29 screw pile axial load tests performed at 10 sites throughout Western Canada. The sites are located in or near Edmonton, Alberta, Bruderheim, Alberta, Ft. Saskatchewan, Alberta, Lamont, Alberta, Ft. McMurray, Alberta, Hythe, Alberta, Ft. St. John, British Columbia, and Saskatoon, Saskatchewan. This chapter will describe the specific geometries of the test piles, the installation torques recorded at the finished screw pile depths, and the ultimate measured capacities of the test piles in axial tension or compression. The screw piles tested were all constructed of one, two, or three steel helices welded to a hollow, circular steel shaft. While most of the pile load tests were performed in years prior to the undertaking of the current thesis work, the results of the tests have been made available by the companies and researchers involved for the purpose of furthering scientific understanding of screw pile capacity prediction and design. All screw pile load tests were conducted in accordance with the respective ASTM standards for individual piles loaded in compression and tension (ASTM Designation: D1143 1981; ASTM Designation: D3689 1990). The incremental application of load to the test piles was applied at constant, short intervals of time, in accordance with the "Quick Test" procedure described in the above standards.

Table 5-1 summarizes the locations and predominant subsoil conditions at each of the ten load test sites, and provides an indication of which load tests were supervised by the author, and which load tests were supervised by Zhang (1999). Table 5-1 also indicates at which sites cone penetration testing was performed, and the supervisor of the test, whether the author or Zhang (1999). In light of the ultimate screw pile capacity results, a discussion will be made in the next chapter regarding a possible relationship between the installation torque and ultimate screw pile capacity, as well as the accuracy with which the cone penetration tip resistance profile may be used in conjunction with the LCPC method for screw pile capacity prediction. The specific

stratigraphy of each test site and the relevant cone penetration profiles, if obtained at the site, have already been discussed within the context of the regional geology in Chapter 4.

5.2 Determination of Ultimate Pile Capacity

Ultimate pile capacity is commonly defined as the load required to achieve a displacement equal to 10-percent of the pile diameter. Among the screw pile load tests presented in the following sections, those which were carried out to large displacements are said to have reached ultimate capacity at a displacement equal to 10-percent of the bearing helix diameter, unless the onset of plunging failure was observed to occur prior to this point (i.e., continuous jacking required to maintain the applied load). For the documented screw pile load tests which were not carried out to plunging failure or to displacements equaling 10-percent of their respective helix diameters, the ultimate pile capacity is taken as the average value indicated by the Brinch-Hansen and Mazurkiewicz Methods, detailed in Fellenius (1990).

The Brinch-Hansen method, also known as the 80% criterion, defines the failure load as the load the gives four times the movement of the pile head as obtained for 80% of that load (Fellenius 1990). In order to mathematically determine the failure load by the Brinch Hansen method, the pile load test data is plotted as the square root of each movement value divided by its corresponding load, versus the pile movement. A straight line can then be plotted through the latter portion of the data points, having a slope, c_1, and a y-intercept, c_2. The following simple relations can be derived for computing the ultimate filure load, Q_u, based on the straight-line portion of the data plot:

[5-1]
$$Q_u = \frac{1}{2\sqrt{c_1 c_2}}$$

[5-2]
$$\Delta_u = \frac{c_2}{c_1}$$

where:

Q_u = ultimate axial load (kN)

Δ_u = pile head movement at failure (mm)

c_1 = slope of straight line through latter data points ($kN^{-1} \cdot mm^{-1/2}$)

c_2 = y-intercept of straight line through latter data points ($kN^{-1} \cdot mm^{1/2}$)

When using the Brinch-Hansen 80% criterion, it must be checked that the point 0.80 Q_u/0.25 Δ_u indeed lies on or near the measured load-movement curve (Fellenius 1990). Mazurkiewicz's method, on the other hand, is a graphical approach for extrapolating the ultimate pile capacity from a plot of the applied load versus measured pile movement. First, a series of equally spaced lines are drawn parallel to the load axis to intersect with the load-movement curve. The, from each intersection, a line is drawn parallel to the movement axis, crossing the load axis. At the point of intersection between each such line and the load axis, a 45-degree line is drawn to intersect with the line above. These intersections approximately define a straight line, whose own intersection with the load axis defines the failure or ultimate load. Maxurkiewicz's method is also aptly called "the method of multiple intersections" (Fellenius 1990).

5.3 Screw Pile Geometries, Installations, and Ultimate Capacities

The following section presents the geometries, measured installation torques, and ultimate axial load-carrying capacities of 29 vertically-installed screw piles located at 10 different sites throughout Western Canada, in the eight vicinities of Edmonton, Alberta, Bruderheim, Alberta, Ft. Saskatchewan, Alberta, Lamont, Alberta, Ft. McMurray, Alberta, Hythe, Alberta, Ft. St. John, British Columbia, and Saskatoon, Saskatchewan. Nine of the 29 documented test piles were loaded in static axial tension, and the remaining 20 test piles were loaded in static axial compression. The specific geometries, installation torque records, and ultimate measured capacities of the screw piles are summarized below under the heading of the appropriate test site, followed by the presentation of a tabular synopsis of results in Table 5-2.

5.3.1   Test Site No. 1: Edmonton, Alberta

At the University of Alberta Farm site, located in the city of Edmonton, Alberta at approximately 115 Street and 69 Avenue, six screw piles were load tested in February 1998 as part of Zhang's (1999) Masters thesis work; three screw piles were loaded in compression, and three piles were

loaded in tension. The specific screw pile geometries tested by Zhang (1999) and the installation torques achieved at the University Farm site are described below; all of the test piles were fabricated with a shaft diameter of 21.9 cm (8 ⅝ in), and helix diameters of 35.6 cm (14 in). The first pile tested in compression, C1, consisting of three helices spaced at 0.53 m center-to-center, yielding an inter-helix spacing ratio (S/D) of 1.5, was installed to a depth of 5.0 m (17 ft) with a torque of 20.3 kN·m (15,000 lb·ft). The ultimate capacity of pile C1, determined as the load applied to attain settlement equal to 10-percent of the helix diameter (3.56 cm or 1.4 in), was 180 kN (40,500 lbs). The second compression pile, C2, was identical in geometry to pile C1, but was installed to a shallower depth of only 3.0 m (10 ft), requiring 15.6 kN·m (11,500 lb·ft) of torque. The ultimate measured capacity of pile C2 was 160 kN (36,000 lbs), occurring at settlement equal to 10-percent of the helix diameter (3.56 cm or 1.4 in). The third screw pile tested in compression at the University Farm site by Zhang (1999), denoted C3, consisted of two helices spaced at 1.07 m (3.5 ft), such that S/D = 3.0, and was installed with 19.5 kN·m (14,375 lb·ft) of torque to a depth of 5.0 m (17 ft). Zhang (1999) reported that pile C3 failed in plunging at an applied load of 210 kN (47,200 lbs) prior to attaining settlement equal to 10 percent its helix diameter, so 210 kN (47,200 lbs) was taken as the ultimate load for pile C3. The load-displacement curves for piles C1, C2, and C3 can be seen in Figure 5-1.

The first screw pile tested in tension by Zhang (1999) at the University Farm site, T1, was installed to a depth of 5.0 m (17 ft), requiring a torque of 22.0 kN·m (16,300 lb·ft), having three helices affixed to the shaft at 0.53 m (1.75 ft) spacing, such that S/D = 1.5. The ultimate tensile capacity of pile T1 was reached with the onset of plunging failure, as reported by Zhang (1999), at 210 kN (47,200 lbs). The second screw pile tested in tension at the site, T2, consisted again of three helices spaced at 0.533 m (1.75 ft) center-to-center (S/D = 1.5), but this time installed with a torque of 20.3 kN·m (15,000 lb·ft) to a depth of 3.0 m (10 ft). The capacity of pile T2 was reported by Zhang (1999) to be 140 kN (31,500 lbs), the applied load which initiated plunging failure prior to the pile attaining settlement equal to 10-percent of the helix diameter. The final load test documented by Zhang (1999) for the University Farm site was for a 5.0 m (17 ft) screw pile, T3,

having two helices spaced at 1.07 m (3.5 ft), such that S/D = 3.0. Pile T3 required 22.9 kN·m (16,900 lb·ft) of torque for installation, and reached plunging failure at 210 kN (47,200 lbs) (Zhang 1999). The results of the screw pile load tests in tension at the University Farm site are illustrated by the load-displacement curves shown in Figure 5-2.

5.3.2   Test Site No. 2: Bruderheim, Alberta

The town of Bruderheim is situated 60 km northeast of the city of Edmonton in Alberta. At a sand pit site located approximately 7.5 km north of Bruderheim town center, six screw pile load tests, three in compression and three in tension, were conducted and documented in May 1998 by Zhang (1999) as part of her Masters thesis work. All of the test piles were fabricated with a shaft diameter of 21.9 cm (8 ⅝ in), and helix diameters of 35.6 cm (14 in). The first compression pile, C4, consisted of three helices spaced at 0.53 m center-to-center, yielding an inter-helix spacing ratio (S/D) of 1.5, installed to a depth of 5.0 m (17 ft) with an installation torque of 44.7 kN·m (33,000 lb·ft). The ultimate capacity of pile C4, as recorded by Zhang (1999) at the onset of observed plunging failure, was 470 kN (106,000 lbs). The second compression pile, C5, was identical in geometry to pile C4, but was installed to a shallower depth of only 3.0 m (10 ft), requiring 40.7 kN·m (30,000 lb·ft) of torque. Plunging failure of Pile C5 was initiated at an applied load of 420 kN (94,400 lbs) (Zhang 1999). The third compression pile, C6, consisted of two helices spaced at 1.07 m (3.5 ft), such that S/D = 3, installed with 44.7 kN·m (33,000 lb·ft) of torque to a depth of 5.0 m (17 ft). The ultimate capacity of pile C6 was marked by the onset of plunging failure at an applied load of 380 kN (85,400 lbs) (Zhang 1999). The load-displacement curves for compression piles C4, C5, and C6 are shown in Figure 5-3.

The three screw piles installed and loaded in tension at the Bruderheim site by Zhang (1999) were also fabricated with a shaft diameters of 21.9 cm (8 ⅝ in), and helix diameters of 35.6 cm (14 in). The construction of the first tension pile, T4, consisted of three helices affixed to the shaft at 0.53 m spacing, creating an inter-helix spacing ratio (S/D) of 1.5. Pile T4 was installed to a depth of 5.0 m (17 ft) requiring 50.8 kN·m (37,500 lb·ft) of torque, and reached its ultimate capacity upon attaining uplift equal to 3.56 cm (1.4 in) or 10-percent of its helix diameter, at an

applied load of 360 kN (80,900 lbs). The second tension screw pile, T5, tested at the site by Zhang (1999) was of the same dimensions as pile T4, but installed to a depth of only 3.0 m (10 ft). The installation torque recorded for pile T5 at the finished depth was 42.7 kN·m (31,500 lb·ft), and the pile was reported to fail in plunging at an applied load of 190 kN (42,700 lb·ft) before reaching uplift equal to 10-percent of the helix diameter (Zhang 1999). Screw pile T6, the third pile tested in tension by Zhang (1999) at the Bruderheim site, was constructed of two helices affixed to the central shaft at a spacing of 1.07 m, such that S/D = 3.0. Pile T6 was installed 5.0 m (17 ft) deep using 47.8 kN·m (35,300 lb·ft) of torque, and the ultimate tensile capacity of the pile was reached upon incurring 3.56 cm (1.4 in) of uplift, under 360 kN of applied load. Figure 5-4 shows the load-displacement results for tension piles T4, T5, and T6 at the Bruderheim sand pit site.

5.3.3   Test Site No. 3: Ft. Saskatchewan, Alberta

At a commercial building site located in the city of Ft. Saskatchewan, Alberta, approximately 25 km northeast of Edmonton, three screw piles were load tested under static compression in the fall of 2001. The test piles are designated as C7, C8, and C9, respectively. The first pile, C7, consisted of a 17.8 cm (7 in) diameter shaft, fitted with one 46 cm (18 in) helix, installed 4.6 m (15 ft) deep with a final installation torque of 25.6 kN·m (18,900 lb·ft). The second test pile, C8, having a 21.9 cm (8 ⅝ in) shaft diameter, affixed with one 46 cm (18 in) helix, was installed 4.6 m (15 ft) deep with a measured torque of 34.9 kN·m (25,700 lb·ft). The third test pile, C9, consisted of a tapered, double-helix configuration, with the lower, 46 cm (18 in) helix and upper, 51 cm (20 in) helix affixed to a 17.8 cm (7 in) shaft, at a spacing of 1.5 m (5 ft) or S/D = 3.1, installed with 31.4 kN·m (23,200 lb·ft) of torque to a finished depth of 5.5 m (18 ft). Based on the load test results, the respective ultimate capacities of the screw piles were calculated as the average of the values interpolated by the Brinch-Hansen and Mazurkiewicz Methods. The ultimate capacity of pile C7 was determined to be approximately 212 kN, pile C8, 268 kN, and pile C9, 372 kN. The load-displacement curves for piles C7, C8, and C9 are shown in Figure 5-5. The graphical constructions of the Brinch-Hansen and Mazurkiewicz methods are shown in Appendix D using the pile load test results from Ft. Saskatchewan.

5.3.4   Test Site No. 4: Lamont, Alberta

A single screw pile was installed and load tested under axial compression at the site of a proposed fabricating facility near the town of Lamont, Alberta. The tapered test pile, designated C10, consisted of two helices, 45 cm (17.7 in) and 50 cm (19.7 in) in respective diameter, affixed to a 24 cm (9 ⅜ in) shaft. The spacing between the helices was equal to 1.5 m (5 ft), yielding an inter-helix spacing ratio (S/D) of 3.2. The final torque measurement recorded during installation of the test pile was 119 kN·m (87,500 lb·ft), at the finished depth of 9.25 m (30 ft). Figure 5-6 shows the load-displacement curve for test pile C10. The ultimate capacity of pile C10 in compression was found to be approximately 1177 kN (264,600 lbs), determined by averaging the results obtained using the Brinch-Hansen and Mazurkiewicz methods in conjunction with the load test data. The graphical constructions of the Brinch-Hansen and Mazurkiewicz methods for pile C10 may be viewed in Appendix D.

5.3.5   Test Site No. 5: Ruth Lake Substation Near Ft. McMurray, Alberta

Two locations in the vicinity of Ft. McMurray, Alberta, are included in this thesis as documented sites of screw pile load testing. The first site is located approximately 40 km northwest of the city of Ft. McMurray, outside the Ruth Lake Substation at NE-16-92-10-W4M. Two axial tension tests and two axial compression tests were conducted on screw piles installed at the Ruth Lake site in November 2001. Two pile configurations were used in the four tests, the first consisting of a single, 76.2 cm (30 in) helix welded to a 27.3 cm (10 ¾ in) shaft, and the second being a double-helix test pile, with a 27.3 cm (10 ¾ in) shaft affixed with two 76.2 cm (30 in) helices at a spacing of 2.3 m (7.5 ft), or S/D = 3.0. The first compression test was performed on a screw pile of the single-helix configuration, C11, installed to a depth of 5.9 m (19.5 ft), at which point a torque of 85.4 kN·m (63,000 lb·ft) was achieved. The ultimate capacity of pile C11 in compression was determined by the onset of plunging failure to be 1094 kN (246,000 lbs). The second compression test was performed on the double-helix screw pile, C12, installed to a depth of 6.0 m (19.6 ft), with the required torque of installation equal to 97.6 kN·m (72,000 lb·ft). Pile C12 reached plunging failure at an applied load of 1375 kN (309,000 lbs). The load-displacement curves for the piles C11 and C12 are shown in Figure 5-7.

The first tension test performed at the Ruth Lake site was conducted on a screw pile of the single-helix configuration, denoted T7, installed to a depth of 5.9 m (19.5 ft), with a torque of 81.3 kN·m (60,000 lb·ft). The second tension test was performed on a double-helix test pile, T8, installed to a depth of 6.0 m (19.6 ft) at which point a torque of 122 kN·m (90,000 lb·ft) was recorded. The ultimate capacities of piles T7 and T8 were determined to be 800 kN (180,000 lbs) and 1325 kN (298,000 lbs), respectively, as marked by the onset of plunging failure during testing. The load-displacement curves for pile T7 and T8, tested in tension at the Ruth Lake site, may be viewed in Figure 5-8.

5.3.6   Test Site No. 6: Dover Substation Near Ft. McMurray, Alberta

A single screw pile was installed and load-tested in axial tension at a second site in the vicinity of Ft. McMurray, Alberta, beside the Dover Substation about 80 km northwest of the city, at NE-31-92-12-W4M. This test pile, T9, was constructed of a single, 76.2 cm (30 in) diameter helix welded to a 40.6 cm (16 in) shaft, installed to a depth of 4.9 m (16 ft) below grade. The torque achieved at the final depth of installation was a substantial 257 kN·m (190,000 lb·ft). In order to install the screw pile in the very dense soil conditions encountered, an incremental process of rotating the pile into the ground for a limited distance, removing the soil plug from inside the pile shaft by drilling, and then resuming the rotation of the pile was carried out. The ultimate tensile capacity of pile T9 was not reached during the load testing procedure, but was subsequently determined by the Mazurkiewicz method to equal approximately 2025 kN or 455,000 lbs (see Appendix D). The load-displacement relationship recorded for pile T9 is shown in Figure 5-9.

5.3.7   Test Site No. 7: Hythe, Alberta

A single screw pile was installed and tested under static compression at the site of a prospective shop facility in the town of Hythe, Alberta. The test pile, C13, consisted of one 40 cm (15 ¾ in) diameter helix welded to a circular steel shaft of 21.9 cm (8 ⅝ in) diameter. The pile was installed to a depth of 7.5 meters (24.6 ft), at which time a torque value of 121,000 N·m (89,200 lb·ft) was recorded. The load-displacement relationship from the compression test on pile C13 is shown in

Figure 5-10. The ultimate capacity of the pile was subsequently determined by taking the average of values yielded by the Brinch-Hansen and Mazurkiewicz methods, approximately 1075 kN (242,000 lbs), as detailed in Appendix D.

5.3.8   Test Site No. 8: Town of Ft. St. John, British Columbia

Two different locations in the vicinity of Ft. St. John, British Columbia, were used as sites for the testing of three different screw piles loaded in compression. The first test site was located at 93 Avenue and 96 Street in the town Ft. St. John. Two separate screw piles were installed at the site in August 2005 and tested under static compressive load for the purpose of selecting a foundation for a proposed multi-family housing development. Each of the two screw piles were installed and tested by separate manufacturers. Pile C14 consisted of two 91.4 cm (36 in) diameter helices welded to a circular shaft 32.4 cm (12 ¾ in) in diameter. The inter-helix spacing was 1.6 m (5.3 ft), resulting in an inter-helix spacing ration (S/D) of 1.75. The pile was installed to a finished depth of 10.4 meters (34 ft), upon which an installation torque of 79.1 kN·m (58,300 lb·ft) was achieved. The load displacement curve for test pile C14 is shown in Figure 5-11, from which the ultimate capacity of 634 kN (143,000 lbs) was estimated using the average values determined by the Brinch-Hansen and Mazurkiewicz methods (see Appendix D). The second test pile, C15, consisted of three helices, each of 50.8 cm (20 in) in diameter, welded to a 14.0 cm (5 ½ in) diameter circular steel shaft. The inter-helix spacing was equal to 3.0D (1.5 m or 5 ft), and the screw pile was installed to a depth of 6.1 meters (20 ft) using a torque of 19.7 kN·m (14,500 lb·ft). The ultimate compressive capacity of pile C15 was approximately 270 kN (60,700 lbs), as determined by subsequent analysis of the load test results using the Brinch-Hansen and Mazurkiewicz methods (see Appendix D). The load-displacement curve for the compression load test performed on pile C15 is shown in Figure 5-11.

5.3.9   Test Site No. 9: Farmland Near Ft. St. John, British Columbia

The second screw pile load test site in the vicinity of Ft. St. John was a private farm located approximately 10 km northeast of the town. Two screw piles were load tested at the site under axial compression in September 2006. The first test pile, C16, was constructed of two 45.7 cm

(18 in) helices spaced at 1.5 m (S/D = 3.3) on an 11.4 cm (4 ½ in) diameter shaft. Pile C16 was installed 5.0 m deep, requiring 13.5 kN·m (9990 ft·lbs) of torque. The second test pile, C17, consisted of a single 45.7 cm (18 in) helix affixed to a 11.4 cm (4 ½ in) shaft, installed 4.0 m deep using 8.0 kN·m (5920 ft·lbs) of torque. The ultimate capacities of piles C16 and C17 in compression were determined from the load test results to equal approximately 245 kN (55,200 lbs) and 169 kN (37,900 lbs) respectively, based on the average values calculated by the Brinch-Hansen and Mazurkiewicz methods (Appendix D). The load displacement curves for piles C16 and C17 are shown in Figure 5-12.

5.3.10 Test Site No. 10: Saskatoon, Saskatchewan

At the location of a prospective multi-family housing development inside the city of Saskatoon, Saskatchewan, three screw piles of differing configuration were installed and axially load tested under static compression. All of the piles were constructed with a hollow steel shaft 11.4 cm (4 ½ in) in diameter. The first test pile, C18, consisted of a single, 45 cm (17.7 in) helix welded to the shaft, installed to a depth of 5.0 m (16.4 ft), at which time a torque of 11.0 kN·m (8140 lb·ft) was recorded. The second test pile, C19, was made from a single, 40 cm (15 ¾ in) helix welded to the central shaft, also installed 5.0 m (16.4 ft) deep, with an ultimate measured installation torque of 9.5 kN·m (7030 lb·ft). The third screw pile tested, C20, was composed of two helices affixed to the central shaft in a tapered configuration, whereby the lower helix was 40 cm (15 ¾ in) in diameter, and the upper, 45 cm (17.7 in) in diameter; the spacing between the helices was 1.5 m (5.0 ft), generating an inter-helix spacing ratio of S/D = 3.6. The pile was installed to 5.9 m (19.4 ft) below the surface, and achieved a torque of 9.5 kN·m (7030 lb·ft) at the finished depth. The load-displacement curves obtained at the Saskatoon site from the compression testing of screw piles C18, C19, and C20 are shown in Figure 5-13. Based on the analysis of the load-displacement curves using the Brinch-Hansen and Mazurkiewicz methods, the ultimate compressive capacity of pile C18 was estimated to be 203 kN (45,600 lbs), and pile C19, 148 kN (33,300 lbs). Pile C20 could not be analyzed using the Brinch-Hansen method, so the ultimate capacity of 200 kN (45,000 lbs) was approximated using the Mazurkiewicz method only. The

detailed Brinch-Hansen and Mazurkiewicz analyses of the Saskatoon load test results are included in Appendix D.

Table 5-1: Summary of Test Site Stratigraphies, In-Situ Testing and Supervision

Test Site No.	Location	Predominant Soil Conditions	Tension Tests	Compression Tests	Date	Supervised / Observed By	In-Situ Soil Test	Date	Supervised / Observed By
1	U of A Farm, Edmonton, AB	Stiff silty clay	3	3	Feb 1998	Zhang (1999)	CPT	Oct 1997 and Jan 2006	Zhang (1999) and Tappenden
2	Bruderheim, AB	Loose to compact silty sand	3	3	May 1998	Zhang (1999)	CPT	Nov 1997	Zhang (1999)
3	Ft. Saskatchewan, AB	Stiff silty clay	0	3	Fall 2001	--	CPT	Jun 2006	Tappenden
4	Lamont, AB	Hard clay till over hard clay shale bedrock	0	1	June 2006	Tappenden	CPT	Aug 2006	Tappenden
5	Ruth Lake, Ft. McMurray, AB	Hard clay till	2	2	Nov 2001	--	CPT	Aug 2006	Tappenden
6	Dover, Ft. McMurray, AB	Very dense sand till	1	0	Jan 2004	--	CPT	Aug 2006	Tappenden
7	Hythe, AB	Firm to stiff clay/clay till, hard clay shale, very dense sand/sandstone	0	1	Dec 2005	--	SPT	May 2005	--
8	Ft. St. John, BC	Firm to stiff silty clay	0	2	Aug 2005	Tappenden	None	--	--
9	Farmland, Ft. St. John, BC	Stiff silty clay	0	2	Sep 2006	--	CPT	May 2006	Tappenden
10	Saskatoon, SK	Compact sand	0	3	Oct 2005	Tappenden	SPT	Apr 2005	--

Table 5-2: Summary of Test Pile Geometries and Ultimate Axial Capacities

Test Site No.	Test Pile Designation (Tension, T, or Compression, C)	Installation Depth (m)	No. of Helices	Helix Diameter(s) D_1 (cm)	D_2 (cm)	D_3 (cm)	Inter-Helix Spacing Ratio S/D	Shaft Diameter d (cm)	Installation Torque lb·ft	kN·m	Ultimate Measured Capacity, Q_u lbs	kN
1	C1	5.0	3	35.6	35.6	35.6	1.5	21.9	15 000	20.3	40 500	180
1	C2	3.0	3	35.6	35.6	35.6	1.5	21.9	11 500	15.6	36 000	160
1	C3	5.0	2	35.6	35.6	--	3.0	21.9	14 400	19.5	47 200	210
1	T1	5.0	3	35.6	35.6	35.6	1.5	21.9	16 300	22.1	47 200	210
1	T2	3.0	3	35.6	35.6	35.6	1.5	21.9	15 000	20.3	31 500	140
1	T3	5.0	2	35.6	35.6	--	3.0	21.9	16 900	22.9	47 200	210
2	C4	5.0	3	35.6	35.6	35.6	1.5	21.9	33 000	44.7	106 000	470
2	C5	3.0	3	35.6	35.6	35.6	1.5	21.9	30 000	40.7	94 400	420
2	C6	5.0	2	35.6	35.6	--	3.0	21.9	33 000	44.7	85 400	380
2	T4	5.0	3	35.6	35.6	35.6	1.5	21.9	37 500	50.8	80 900	360
2	T5	3.0	3	35.6	35.6	35.6	1.5	21.9	31 500	42.7	42 700	190
2	T6	5.0	2	35.6	35.6	--	3.0	21.9	35 300	47.9	80 900	360
3	C7	4.6	1	45.7	--	--	--	17.8	18 900	25.6	47 700	212
3	C8	4.6	1	45.7	--	--	--	21.9	25 700	34.8	60 300	268
3	C9	5.5	2	50.8	45.7	--	3.1	17.8	23 200	31.5	83 600	372
4	C10	9.3	2	50.8	45.7	--	3.2	24.4	87 500	118.6	265 000	1177
5	C11	5.9	1	76.2	--	--	--	27.3	63 000	85.4	246 000	1094
5	C12	6.0	2	76.2	76.2	--	3.0	27.3	72 000	97.6	309 000	1375
5	T7	5.9	1	76.2	--	--	--	27.3	60 000	81.3	180 000	800
5	T8	6.0	2	76.2	76.2	--	3.0	27.3	90 000	122.0	298 000	1325
6	T9	4.9	1	76.2	--	--	--	40.6	190 000	257.6	455 000	2025
7	C13	7.5	1	40.0	--	--	--	21.9	89 200	120.9	242 000	1075
8	C14	10.4	2	91.4	91.4	--	1.8	32.4	58 300	79.0	143 000	634
8	C15	6.1	3	50.8	50.8	50.8	3.0	14.0	14 500	19.7	60 700	270
9	C16	5.0	2	45.7	45.7	--	3.3	11.4	9 990	13.5	55 200	245
9	C17	4.0	1	45.7	--	--	--	11.4	5 920	8.0	37 900	169
10	C18	5.0	1	45.7	--	--	--	11.4	8 140	11.0	45 600	203
10	C19	5.0	1	40.0	--	--	--	11.4	7 030	9.5	33 300	148
10	C20	5.9	2	45.7	40.0	--	3.4	11.4	7 030	9.5	45 000	200
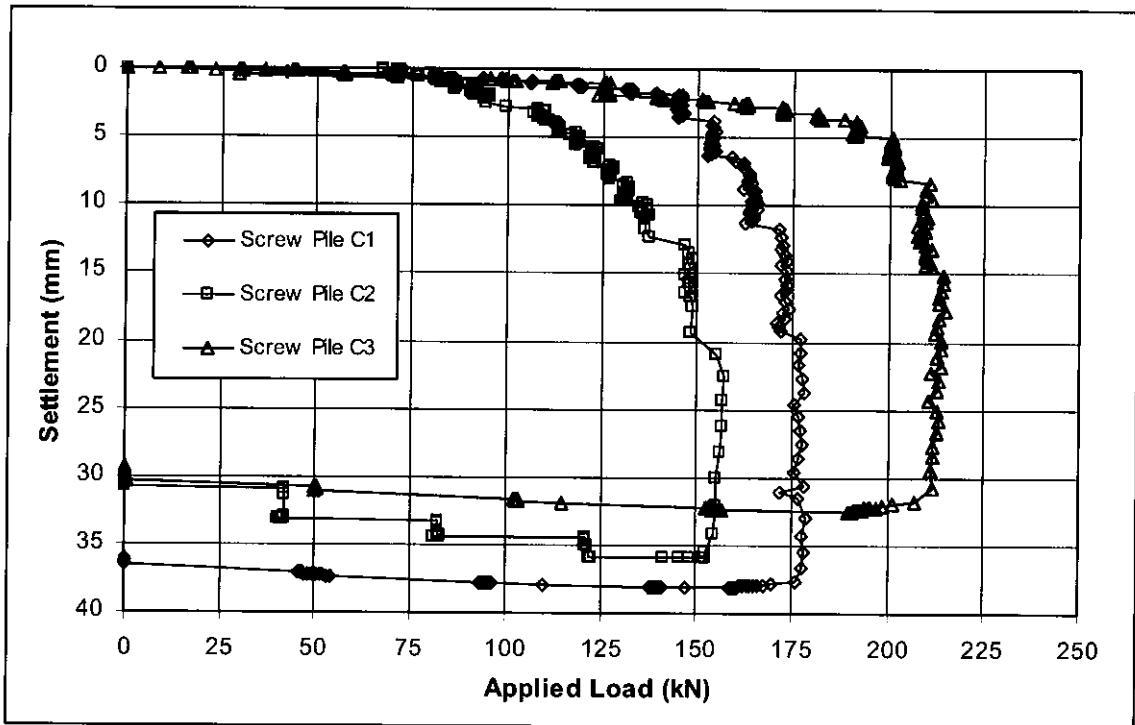
Figure 5-1: Load-Displacement Curves, Compression Tests at University Farm (after Zhang 1999)
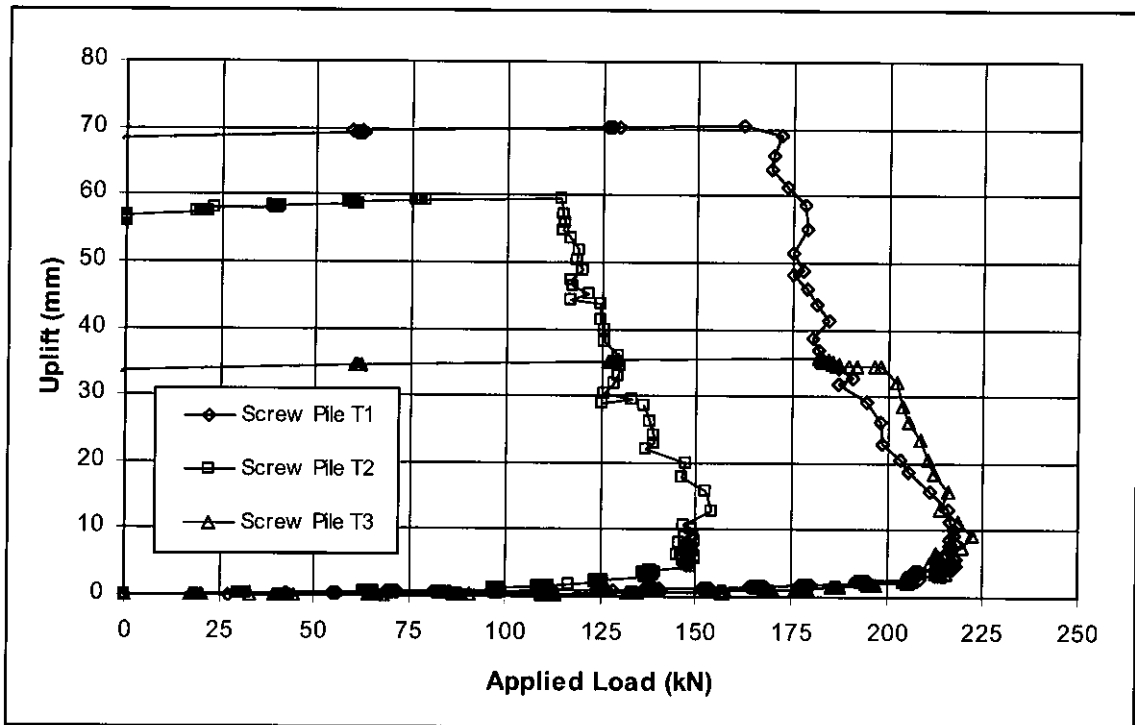
Figure 5-2: Load-Displacement Curves, Tension Tests at University Farm (after Zhang 1999)
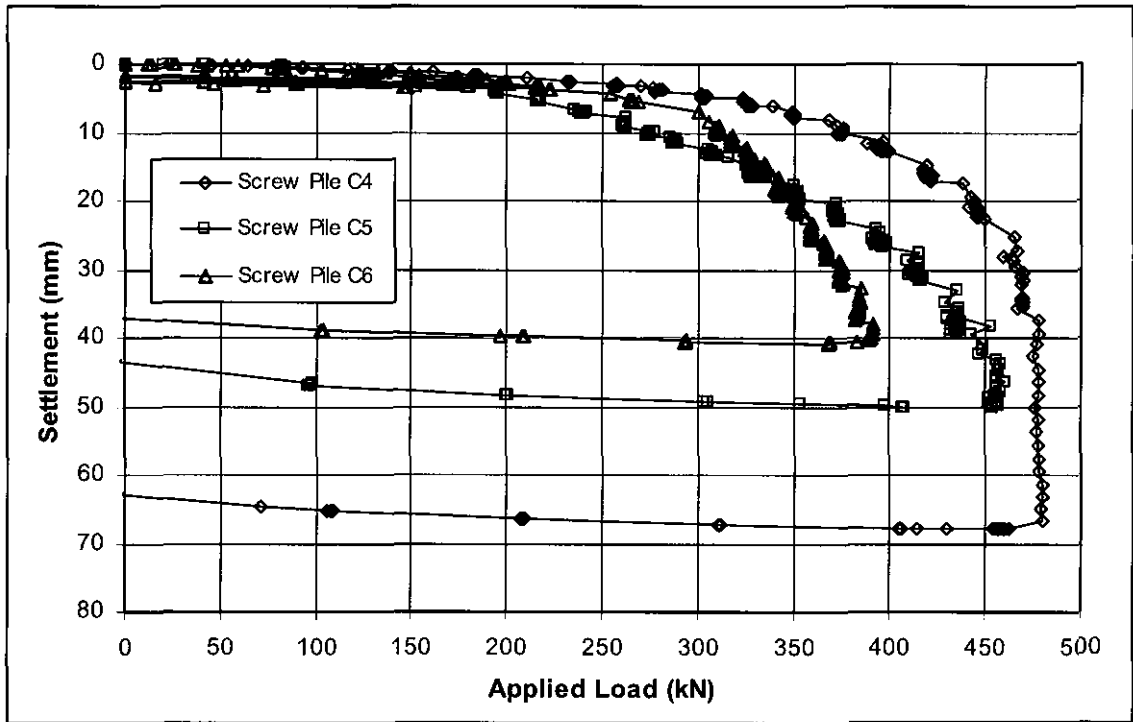
Figure 5-3: Load-Displacement Curves, Compression Tests at Bruderheim Site (after Zhang 1999)
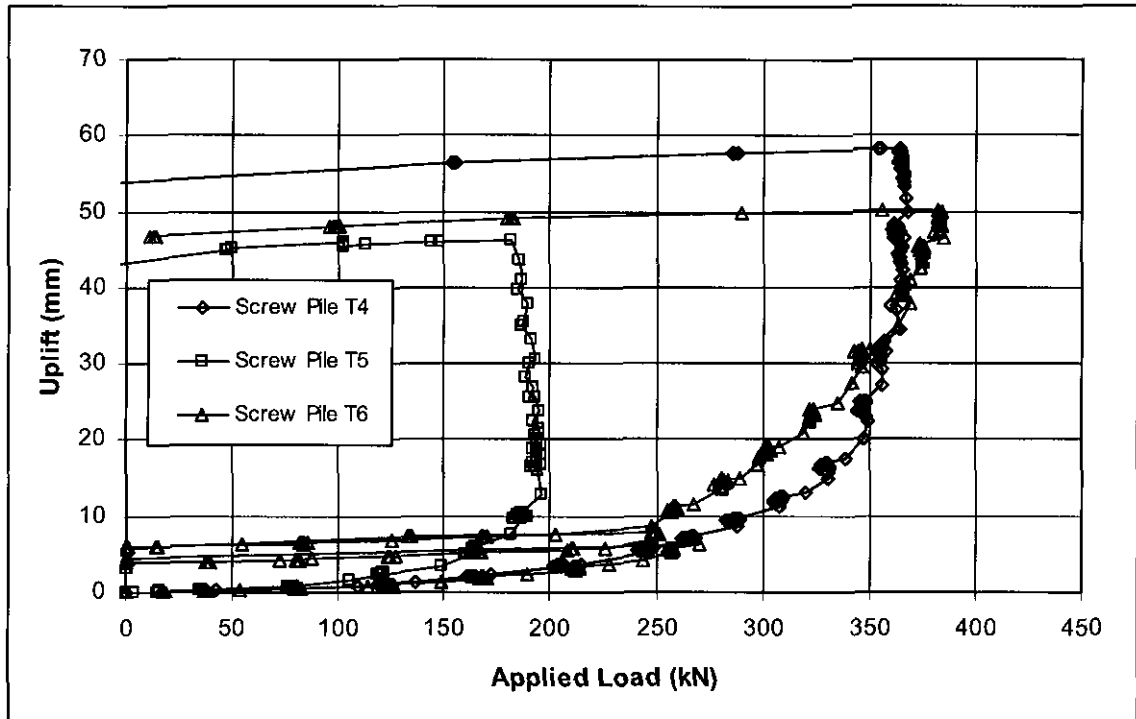
Figure 5-4: Load-Displacement Curves, Tension Tests at Bruderheim Site (after Zhang 1999)
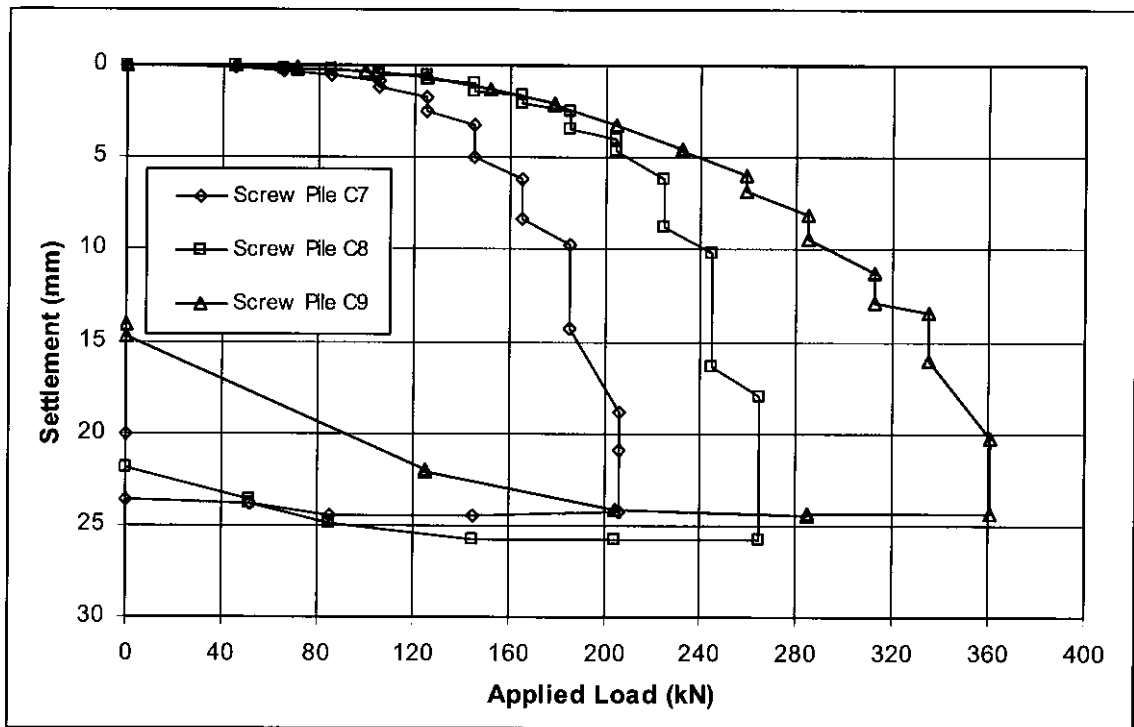
Figure 5-5: Load-Displacement Curves, Compression Tests at Ft. Saskatchewan Site
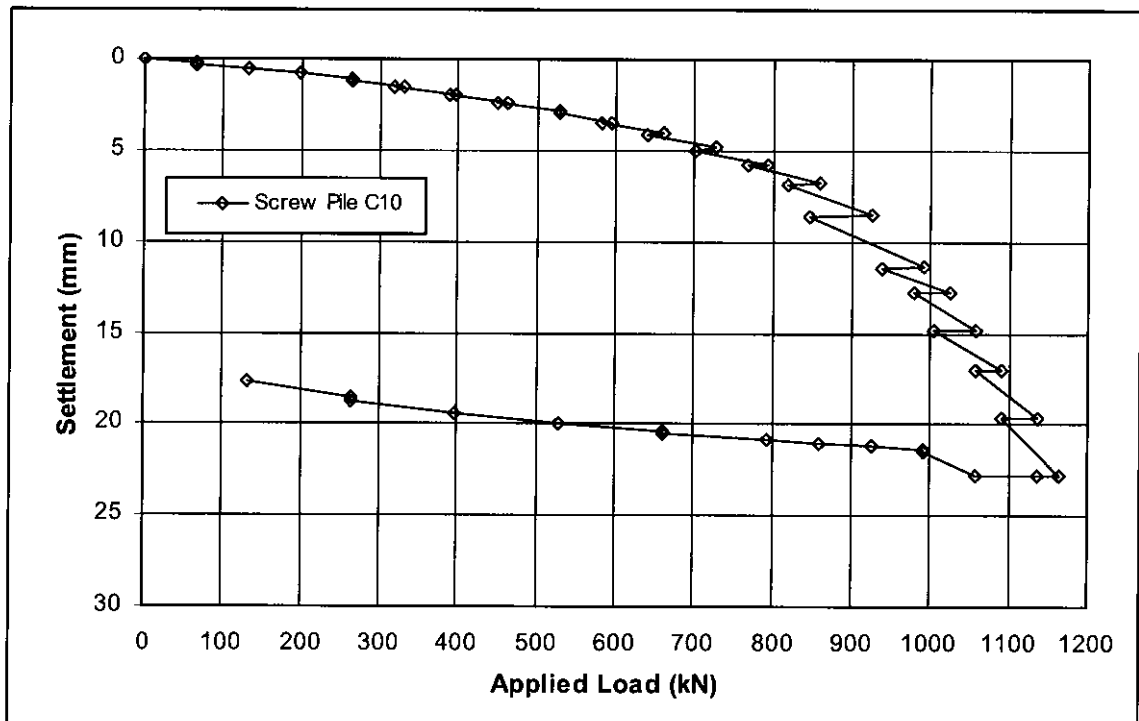
Figure 5-6: Load-Displacement Curve, Compression Test at Lamont Site
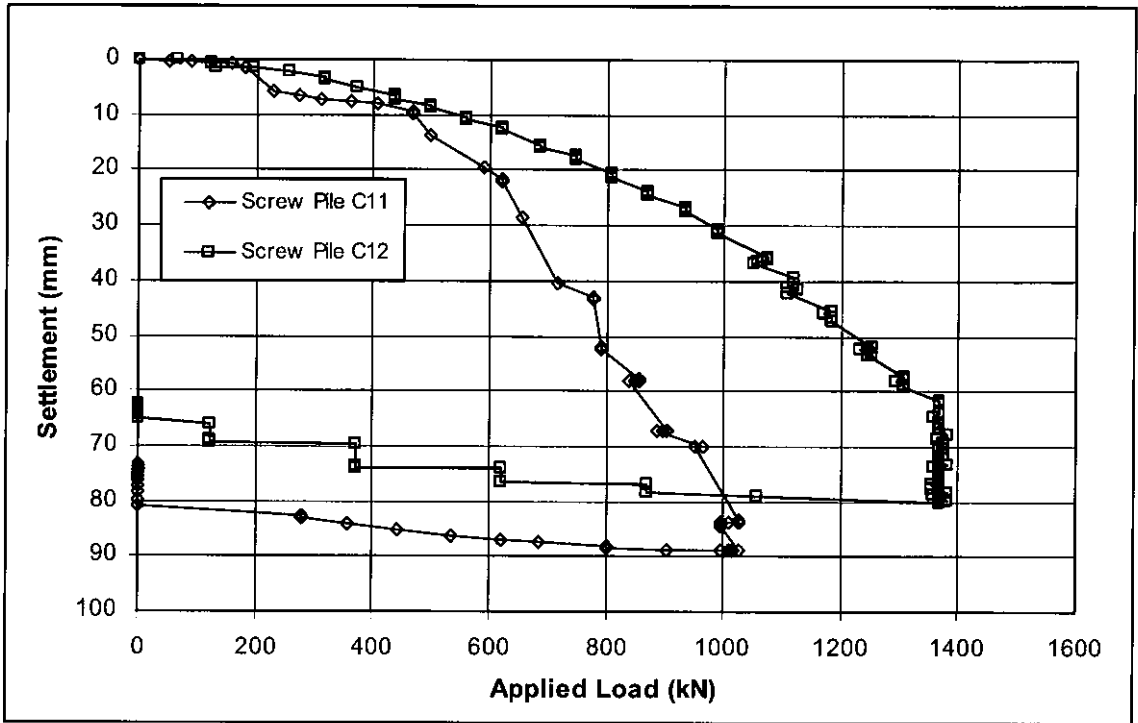
Figure 5-7: Load-Displacement Curves, Compression Tests at Ruth Lake Site
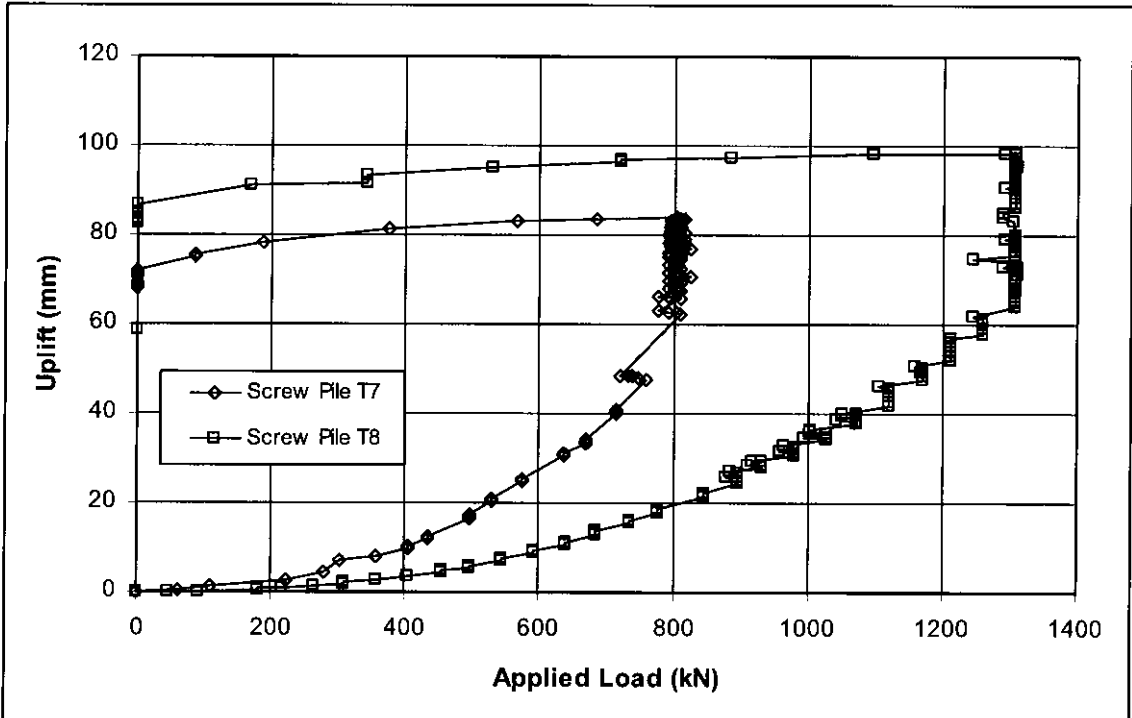
Figure 5-8: Load-Displacement Curves, Tension Tests at Ruth Lake Site
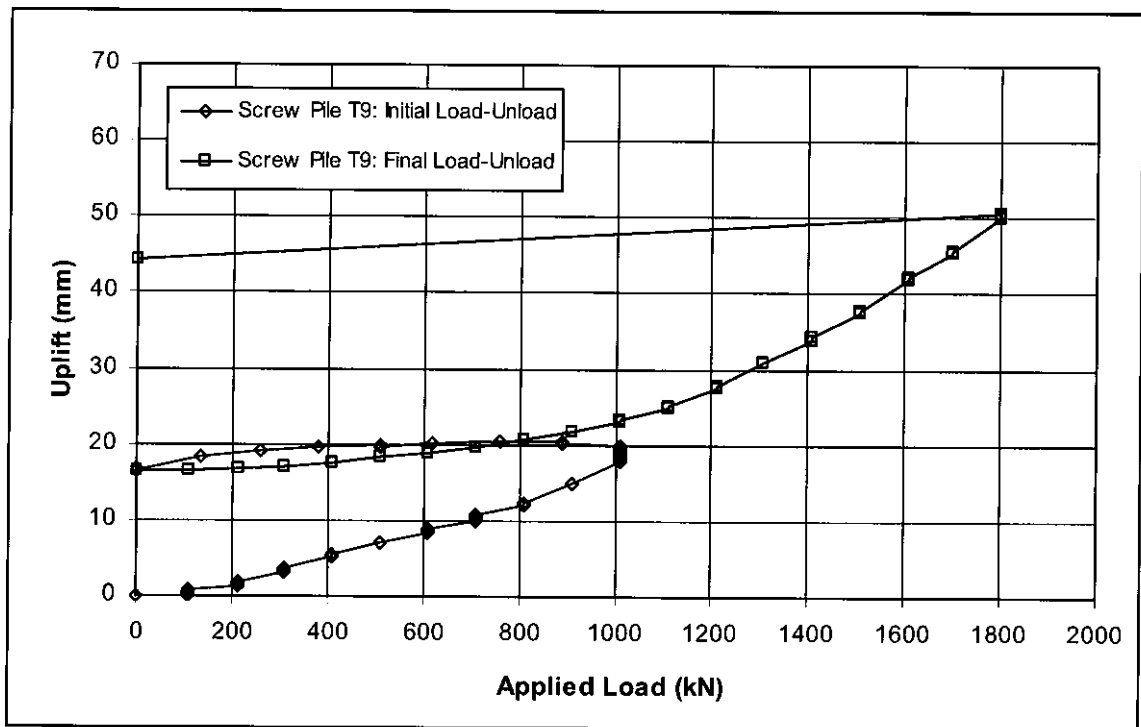
Figure 5-9: Load-Displacement Curve, Tension Test at Dover Site
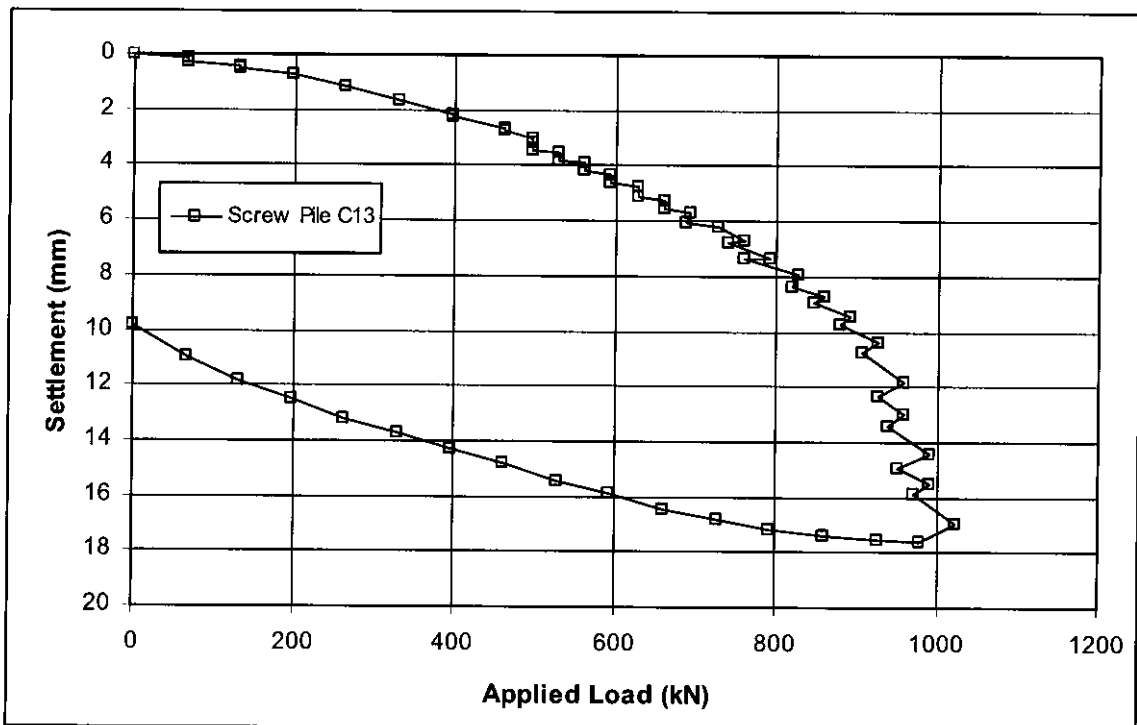
Figure 5-10: Load Displacement Curve, Compression Test at Hythe Site

102
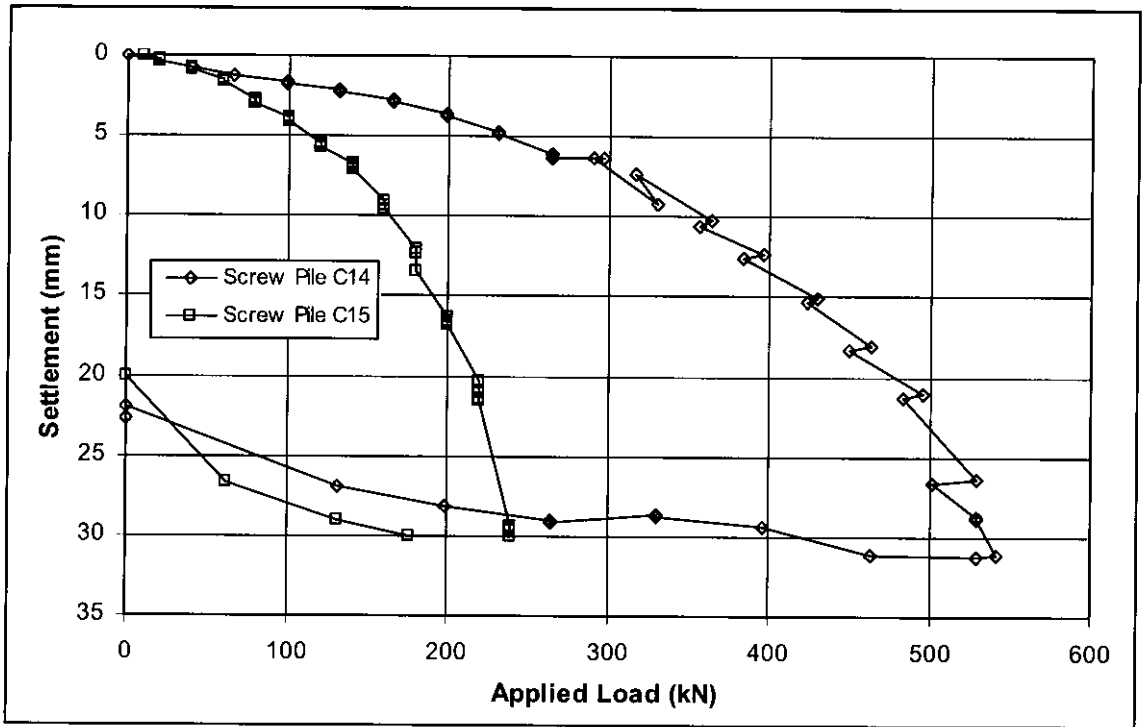
Figure 5-11: Load-Displacement Curves, Compression Tests at Ft. St. John Town Site
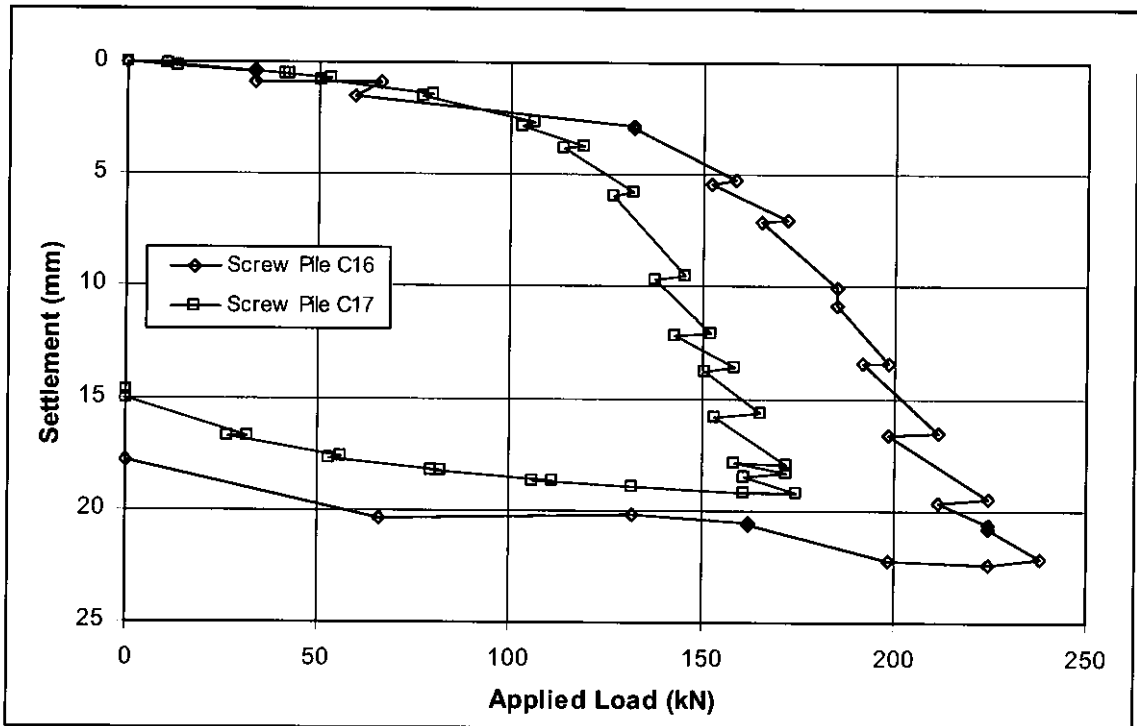
Figure 5-12: Load-Displacement Curves, Compression Tests at Ft. St. John Farm Site
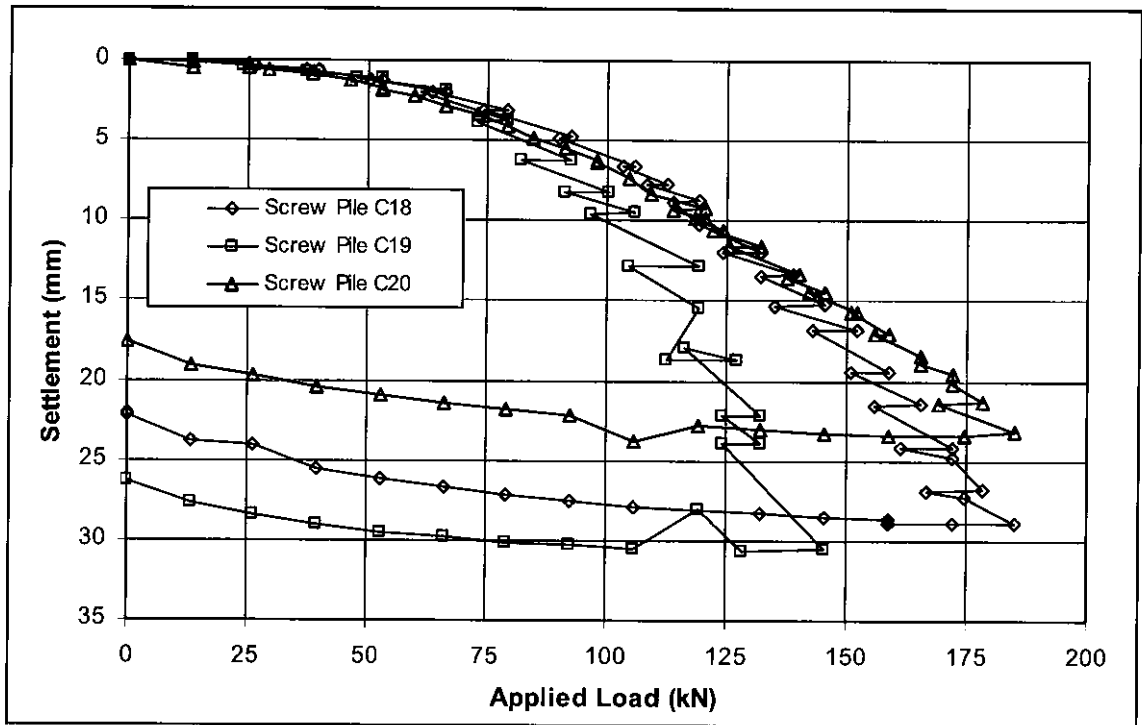
Figure 5-13: Load-Displacement Curves, Compression Tests at Saskatoon Site

5.4 References

ASTM Designation: D1143 1981. Standard test method for piles under static axial compressive load. American Society for Testing and Materials.

ASTM Designation: D3689 1990. Standard test method for individual piles under static axial tensile load. American Society for Testing and Materials.

Fellenius, B.H. 1990. Guidelines for the interpretation and analysis of the static loading test. Deep Foundations Institute, Sparta, New Jersey.

Zhang, D. 1999. Predicting capacity of helical screw piles in Alberta soils. M.Sc. thesis, Department of Civil and Environmental Engineering, University of Alberta, Edmonton, Alberta.

6 Screw Pile Capacity Predictions and Discussion

6.1 Introduction

The previous chapter supplied load test results for 29 screw piles that were tested in static axial compression and tension at scattered sites across Western Canada. Chapter 4 of this thesis presented cone penetration profiles for seven of the 10 sites where the aforementioned screw pile load tests were conducted. This chapter will focus on determining the accuracy with which the axial capacity of the screw piles tested may be predicted using the cone penetration tip resistance profiles, and the installation torque records. In order to predict the ultimate pile capacity using the tip resistance profiles, the well-known LCPC direct pile design method of Bustamante and Gianeselli (1982) will be used, in conjunction with either or both of the applicable cylindrical shear or individual plate bearing failure models. The final torque values required to install each of the test piles to their finished depths have also been reported in the previous chapter. This information will be used to formulate a possible direct relationship between the respective screw pile installation torques and the ultimate axial capacities in the spirit of Hoyt and Clemence (1989), as well as within the non-dimensional torque-capacity relationship formulated by Ghaly and Hanna (1991) for screw piles loaded in uplift in sand.

6.2 Capacity Predictions using the LCPC Method

6.2.1 Introduction

As detailed in Chapter 2, the only information required by the LCPC method to formulate a prediction of axial capacity for a pile of given geometry is a representative profile of the cone penetration tip resistance at the site. Based on the geometry of the screw pile installed, the suitable failure model(s) can be used to define the shape of the failure surface, and the appropriate frictional and end-bearing components of the ultimate axial capacity calculated by the LCPC approach. The advantage of the LCPC method is that it may be used to predict the capacity of a pile of any geometry, installed to any depth at the site, whether loaded tension or in compression, based on the results of a single representative cone penetration test. The LCPC method forgoes the need for intermediate laboratory testing and strength analysis of soil samples,

as required by theoretical capacity prediction methods, and the need to actually install a pile of given geometry and record the required torque value, as necessitated by empirical torque correlations.

6.2.2 Capacity Predictions with Depth

For the seven screw pile load test sites at which cone penetration testing was carried out, using either commercial CPT equipment or the modified cone penetration equipment described in Chapter 3, capacity predictions can be made using the LCPC method for all of the screw piles which were load tested at the sites in previous years. Commercial cone penetration tests were conducted at the University Farm, Bruderheim, Lamont, Ruth Lake, and Dover test sites, while modified cone penetration tests were carried out at the University Farm, Ft. Saskatchewan, and Ft. St. John Farm sites. Therefore, capacity predictions were calculated using the LCPC method for the screw piles designated C1 through C12, C16 and C17, and T1 through T9, the geometries of which were described in detail in the previous chapter. Because the cone penetration test provides a continuous record of tip resistance with depth, it is possible to calculate the screw pile capacity at any depth for the given site using the LCPC method. For illustrative purposes, it was decided to calculate the screw pile capacities at each site at intermittent depths up to the final depth of installation, and to plot the results as a record of estimated capacity with depth. The LCPC calculations being rather involved, this process was made easier by the creation of a computer program, designed to calculate the capacity of a screw pile of any geometry at intermittent intervals up to the installed depth, based on the input of near-continuous cone penetration tip resistance values and the corresponding depths. The program, labelled *LCPCmethod.exe*, is included in the electronic Appendix A (on compact disc) accompanying this thesis, with the corresponding source code (*LCPCmethod.rb*). The open-source programming language *Ruby* was used to create the *LCPCmethod* program, and is available at http://www.ruby-lang.org/en/. A full description of the *LCPCmethod* program is given in Appendix E.

The LCPC results of axial capacity prediction with depth for each of the screw piles installed at the seven sites where cone penetration testing was carried out are plotted in Figure 6-1 through Figure 6-23. The graphs are composed to show the contribution of point resistance from the helix or helices, Q_L^P, in relation to the predicted ultimate capacity, Q_L, with depth; the distance between Q_L and Q_L^P represents the frictional component of the ultimate capacity, contributed by shaft friction and friction on the cylinder formed between multiple helices (if applicable).

When using the LCPC method to predict the ultimate capacities of the screw piles, it is necessary to select the appropriate failure model(s) to be used, based on the geometry of the particular pile. For all single-helix piles, the individual plate bearing model was applied to calculate the ultimate capacity in tension or in compression. For the multi-helix piles, the individual plate bearing model was only applied to those piles with inter-helix spacing ratios greater than 2.0, as recommended by Narasimha Rao et al. (1993). In addition, the cylindrical shear model was applied to all of the multi-helix screw piles, with and without the correction proposed by Narasimha Rao et al. (1993) for capturing the effect of inter-helix spacing ratios greater than 1.5 (equations [2-1] [2-2] [2-3]). In terms of calculating the effective shaft length, H_{eff}, along which friction could be considered to act during loading of the piles, H_{eff} was taken to be equal to the length of shaft above the top helix (embedment depth) minus the diameter of the upper helix, as recommended by Zhang (1999). For the cases where the individual plate bearing model was used for multi-helix piles, an additional portion of shaft friction equal to the length of shaft between adjacent helices minus twice the average helix diameter was added to the frictional component of capacity. No shaft friction was calculated for the piles loaded in tension at depths for which their failure would be classified as "shallow" (Mitsch and Clemence 1985; Narasimha Rao et al. 1993), i.e., embedment less that twice the upper helix diameter in clay, or less than 5 times the upper helix diameter in sand.

6.2.3 Accuracy of LCPC Capacity Predictions

A summary of the axial capacity predictions calculated for the screw piles at their final depths of installation using the LCPC method in conjunction with each of the applicable failure models are summarized in Table 6-1. The ratio of Q_L/Q_U, being the ratio of the capacity predicted by the LCPC method to the actual measured capacity of the pile, is of particular interest. This ratio, also shown in Table 6-1, concisely displays the accuracy with which the capacity of each screw pile was predicted by each of the relevant failure models within the context of the LCPC method. Figure 6-24 visually displays the Q_L/Q_U ratios achieved using the LCPC method. The red line at a Q_L/Q_U value of 1.0 in Figure 6-24 indicates perfect agreement between the predicted and the measured screw pile capacities. Due to the amount of uncertainty and limited understanding which exists regarding the engineering prediction of axial capacity for any type of pile, an agreement within 20 percent of the actual value may still be considered a very good result (Bustamante and Gianeselli 1982). It may be observed from the Q_L/Q_U ratios of Figure 6-24 that both the cylindrical shear and the individual plate bearing models generally provide reasonable predictions of axial capacity when fittingly applied to the particular pile geometries, with many of the predicted capacities falling within 20 percent of the actual measured capacities.

However, there are several instances worth noting for which the predicted pile capacity is significantly higher than the actual measured capacity; in particular, piles T5, T7, T8, T9, C11, and C12 all exhibit Q_L/Q_U ratios greater than 2.0. In the case of test pile T5, installed at the Bruderheim site in Alberta, it was suggested by Zhang (1999) that the cone penetration tip resistance readings near the ground surface may have been unrepresentatively high due to the dessicated, lightly cemented nature of the sand crust at the test site. Because of the soil's desiccated state, tip resistance readings of approximately 10,000 kPa were achieved at a depth of only 2 m (6.6 ft), which may have, in turn, produced an unrealistically high prediction of capacity for the 3 m deep (9.8 ft) pile, T5. However, the capacity predicted by the LCPC method for an identical 3 m deep (9.8 ft) screw pile, C5, loaded in compression at the Bruderheim site was much closer to the actual value, with only a 60 percent overestimation. Previous research

has determined that the installation of a screw pile into cohesionless soil causes the lateral displacement of in-situ material, loosening the sand within the cylinder circumscribed by the helices while densifying the sand surrounding the disturbed zone (Mitsch and Clemence 1985). Therefore, it is suggested that the strength of the desiccated soil near the surface of the Bruderheim site may have been significantly compromised by the disturbance incurred during installation of the test pile. This destructuring effect would in turn account for the much lower-than-expected capacity for the 3 m deep (9.8 ft) pile bearing in tension on the disturbed, relatively unconfined near-surface sand.

As regards the significant overestimation of the capacities of piles T7, T8, T9, C11 and C12 using the LCPC method, it should be noted that all of these piles were installed in glacial till material, which appears to lie beyond the current scope of the LCPC method itself. In particular, the scaling coefficients developed for use within the LCPC method (Table 2-1) are grouped into categories based on the soil stiffness, as indicated by the measured cone penetration tip resistance within each layer, and the basic soil type, described simply as clay, silt, sand, or chalk. The scaling coefficients are used for translating the CPT tip resistance profile over an interval of depth into suitable components of sleeve friction and pile tip resistance. For clay soils, as concerns piles T7, T8, C11, and C12, installed in clay till, the values of the coefficients available are for "compact to stiff clay and compact silt" (Bustamante and Gianeselli 1982) having tip resistance readings greater than 5000 kPa. The clay till material at the Ruth Lake Substation site near Ft. McMurray where piles T7, T8, C11, and C12 were installed, exhibited tip resistance readings in the order of 10,000 to 20,000 kPa at the depth of the piles. Test pile T9 was installed at the Dover Substation site near Ft. McMurray, where the subsoil conditions were described as very dense sand or possible sand till. Again, no provisions are made for till materials within the LCPC method, and the coefficients used were those for "compact to very compact sand and gravel" (Bustamante and Gianeselli 1982), having corresponding tip resistance values of 12,000 kPa or greater. Tip resistance values of 15,000 to 60,000 kPa were recorded at the Dover

Substation site, indicating that the nature of the subsoil probably lies beyond the scope of the constants defined within the LCPC method.

It is therefore suggested that the LCPC method, as it currently stands, is not applicable for use in glacial till soils, as the method only defines constants for deposits that may be simply described as clay, silt, sand, or chalk, and open-endedly defines stiff clay materials as those producing tip resistance readings greater than 5000 kPa, and dense sand materials as exhibiting tip resistance readings greater than 12,000 kPa, with no explicit consideration of glacial deposits whose nature may greatly exceed these defined tip resistance values. More research is required involving load testing of instrumented screw piles installed in glacial till materials to establish suitable scaling coefficients for use within the LCPC method.

If the capacity predictions made for piles T7, T8, T9, C11 and C12 using the LCPC method are excluded from the set of results due to the fact that the glacial till into which they were installed lies beyond the scope of the method, the remaining 18 capacity predictions may be analyzed to determine how well the LCPC method applies to screw pile axial capacity prediction. When the LCPC method was used in conjunction with the cylindrical shear model, applicable to 14 of the remaining 18 screw piles, nine of the 14 axial capacity predictions made were within 30 percent of the actual capacities, whether or not the correction (equations [2-1], [2-2], and [2-3]) proposed by Narasimha Rao et al. (1993) was employed. The spread of the LCPC capacity predictions using the cylindrical shear model produced an average Q_L/Q_U ratio of 1.14 without the Narasimha Rao et al. (1993) correction, and 1.13 with the correction. The maximum Q_L/Q_U value produced under the cylindrical shear model, with and without the Narasimha Rao et al. (1993) correction was 2.53; the minimum Q_L/Q_U value was 0.74 without the Narasimha Rao et al. (1993) correction, and 0.72 with the correction. The standard deviation for the cylindrical shear model predictions made by the LCPC method was 0.48, regardless of whether or not the Narasimha Rao et al. (1993) correction was applied. As for the individual plate bearing model, which was applicable to 10 of the remaining 18 screw piles, seven of the 10 capacity predictions made in conjunction with the

111

LCPC method were within 30 percent of the measured axial capacities. The average Q_L/Q_U ratio produced using the individual plate bearing model in combination with the LCPC method was 1.23. The maximum Q_L/Q_U ratio produced by the LCPC method when using the individual plate bearing model was 1.99, and the minimum, 0.84. The standard deviation of the Q_L/Q_U ratios was 0.40 under the individual plate bearing model.

6.3 Relationship of Installation Torque to Ultimate Pile Capacity

6.3.1 Introduction

Several authors (Ghaly and Hanna 1991; Hoyt and Clemence 1989; Narasimha Rao et al. 1989; Perko 2000) have suggested the existence of a relationship between the torque required to install a given screw pile at a site, and the ultimate axial capacity which the pile can be expected to attain. Two torque-capacity relationships were discussed in detail in Chapter 2 of this thesis—the direct relationship proposed by Hoyt and Clemence (1989), and the non-dimensional relationship proposed by Ghaly and Hanna (1991). The following section will examine the accuracy with which these two torque relationships may be used to predict the capacities of the screw piles documented in this thesis.

6.3.2 Direct Correlation of Torque to Ultimate Capacity

In the spirit of Hoyt and Clemence's (1989) direct torque-to-capacity relationship (equation [2-6]), the installation torque versus axial capacity data for the screw piles documented in this thesis is plotted in Figure 6-25. The proposed direct relationship correlates the ultimate axial pile capacity to the installation torque by means of an empirical factor, K_t. Hoyt and Clemence (1989) suggest that the value of the installation torque used in equation [2-6] represent the average torque required for installation over the final three helix diameters of pile penetration. However, continuous torque records were not available for the test piles considered under the current investigation, so the final value of the installation torque, as recorded at the finished pile depth, was plotted against the ultimate axial pile capacity, with no distinction made between piles loaded in tension and those loaded in compression (Figure 6-25). Although the distribution of the data points does not warrant a full statistical analysis, a linear relationship is evident between the

ultimate axial pile capacity and the final installation torque. By linear regression of the whole

dataset, the best-fit value of K_t was determined to be 9.22 m^{-1}, as shown by the trend line plotted

in Figure 6-25. Upper and lower bounds are also suggested for the linear relationship, based on

the scatter of the data set, as having the same slope as the trend line, 9.22 m^{-1}, but with an

intercept of 475 kN for the upper bound, and -350 kN for the lower bound. It is also interesting to

note that the value of K_t suggested by the current data set, 9.22 m^{-1}, is very similar to the K_t

value of 9.8 m^{-1} recommended by Hoyt and Clemence (1989) for multi-helix, 8.9 cm (3 ½ in)

round-shaft screw piles with 21.9 cm (8 ⅝ in) extension shafts. The shaft diameters of the screw

piles considered under the current investigation range in size from 11.4 cm (4 ½ in) to 40.6 cm

(16 in), but have an average value of 21.4 cm (8.4 in). Hoyt and Clemence's (1989) relationship

using K_t equal to 9.8 m^{-1} is also plotted on Figure 6-25.

Using the value of K_t equal to 9.22 m^{-1} in equation [2-6], capacity predictions can be made for all

of the 29 test piles documented in this report, based solely on the final torque readings recorded

at the time of their installation. Table 6-2 summarizes the capacity predictions made using the

torque correlation, and compares the predicted capacities, Q_T, to the measured ultimate

capacities, Q_U, by way of the ratio Q_T/Q_U. Considering that a perfectly accurate prediction of

capacity yields a Q_T/Q_U of 1.0, the capacity predictions made using the K_t value of 9.22 m^{-1} are

within 30 percent of the actual axial capacity for all of the test piles, with the exception of piles T5,

and C16 through C20. Regarding the overestimation of pile T5's tensile capacity by 110 percent,

this may again be attributed to the fact that the pile was embedded in the dessicated, lightly

cemented sand crust at the Bruderheim test site in Alberta, and that although the torque required

to install the pile was very high, much of the strength of the dessicated sand may have been

compromised due to destructuring effects resulting from the installation of the test pile, which,

when loaded in tension, was bearing upon the disturbed material.

As for the capacity predictions made for piles C16 through C20, the predicted values are 40 to 60

percent lower than the measured values. However, it may be noted that all of these piles are

constructed of the smallest shaft diameter used for the documented test piles, 11.4 cm (4 ½ in). Therefore, the capacity predictions made using the direct torque correlation may be improved by selecting a second value of K_t to be used in equation [2-6] for screw piles with 11.4 cm (4 ½ in) diameter shafts. This move is in keeping with the findings of Hoyt and Clemence (1989), who suggested different K_t factors be used depending on the diameter of the screw pile shaft, with a value of K_t equal to 33 m^{-1} for screw piles with shaft diameters less than 8.9 cm (3 ½ in), a K_t value of 23 m^{-1} for screw piles with shaft diameters equal to 8.9 cm (3 ½ in), and a value of K_t equal to 9.8 m^{-1} for 8.9 cm (3 ½ in) diameter shaft piles affixed with 21.9 cm (8 ⅝ in) extension shafts (located between the upper helix and the ground surface). For the 11.4 cm (4 ½ in) shaft diameter screw piles considered within the current project (C16 through C20), a value of K_t equal to 16.9 m^{-1} was determined to yield the best predictions of axial capacity based on the final installation torques. For the remaining 24 piles, linear regression of the ultimate capacity versus torque data yields a K_t value equal to 9.19 m^{-1}. Figure 6-26 showcases the two direct linear relationships which best correlate the final installation torques to the ultimate screw pile axial capacities. The first linear relationship uses K_t equal to 16.9 m^{-1}, and applies to screw piles with 11.4 cm (4 ½ in) diameter shafts. The second linear relationship shown in Figure 6-26 uses K_t equal to 9.19 m^{-1}, and applies to all other test piles considered within this research program, having shaft diameters ranging from 14.0 cm (5 ½ in) to 40.6 cm (16 in). The capacity predictions made based on the correlations of installation torque to ultimate pile capacity are improved using the two separate K_t values, 16.9 m^{-1} and 9.19 m^{-1}, that are dependant on the pile shaft diameters.

Table 6-3 summarizes the axial capacity predictions made for the 29 test piles using the two different K_t values as appropriate. With the exception of pile T5, all of the capacity predictions based on the installation torques now lie within 30 percent of the actual ultimate pile capacities. Figure 6-27 depicts a bar chart of the Q_T/Q_U ratios attained using the torque correlation based on the screw pile shaft diameter. It may be observed from the figure that 23 of the 29 pile capacity predictions made using the torque correlation lie within 20 percent of the actual measured pile

capacity, which is a very good result. The capacity predictions made using the direct torque correlation factors are evenly distributed above and below the actual measured capacities, producing an average Q_T/Q_U ratio of 1.01, with a standard deviation of 0.27. All in all, the prediction of axial screw pile capacity using K_t values of 16.9 m^{-1} and 9.2 m^{-1} for piles with shaft diameters of 11.4 cm (4 ½ in) and 14.0 cm (5 ½ in) to 40.6 cm (16 in), respectively, is very promising.

6.3.3   Non-Dimensionalized Torque to Capacity Relationship

Ghaly and Hanna (1991) published a non-dimensional relationship between the uplift capacity of screw piles installed in sand and the final installation torque achieved. The torque factor, F_t, was used to express the torque required to install the screw pile in a non-dimensional form, as per equation [2-7], and the ultimate tensile capacity of the screw pile was expressed in the non-dimensional parameter N_u, which is the uplift capacity factor (equation [2-8]). Ghaly and Hanna (1991) presented a unique relationship between N_u and F_t for single and multi-helix screw piles installed in sand, approximated by the logarithmic equation [2-9], which can be rearranged to explicitly solve for the ultimate uplift capacity of the screw pile, as per equation [2-10].

Assuming a unit weight of 19 kN/m^3 for the sand deposits at the Bruderheim, Dover, and Saskatoon sites, the geometry and torque records for the test piles loaded in tension at the sites were inserted into equation [2-10] to obtain predictions of the ultimate uplift capacities, denoted Q_P. The ratios comparing the tensile capacity predictions made by Ghaly and Hanna's (1991) relationship to the actual measured capacities for the piles T4, T5, T6, and T9 are shown graphically in Figure 6-28. As evidenced by the chart, the agreement between the predicted and the measured capacities is not very good, with Ghaly and Hanna's (1991) relationship severely overestimating the uplift capacities, as summarized by the ratios of predicted to measured capacity, Q_P/Q_U, in Table 6-4, which vary from 2.32 to 9.58.

Table 6-1: Summary of LCPC Axial Capacity Predictions for Available Screw Piles

Load Test Designation (Tension, T, or Compression, C)	Predominant Soil Type	Installation Depth (m)	No. of Helices	Inter-Helix Spacing Ratio S/D	Ultimate Measured Capacity, Qu (kN)	Predicted Capacity, QL (kN) LCPC Method			Ratio of QL/Qu		
						Cylindrical Shear	Cylindrical Shear with Correction	Individual Plate Bearing	Cylindrical Shear	Cylindrical Shear with Correction	Individual Plate Bearing
C1	Clay	5.0	3	1.5	180	185	185	--	1.0	1.0	--
C2	Clay	3.0	3	1.5	160	139	139	--	0.9	0.9	--
C3	Clay	5.0	2	3.0	210	185	181	204	0.9	0.9	1.0
T1	Clay	5.0	3	1.5	210	155	155	--	0.7	0.7	--
T2	Clay	3.0	3	1.5	140	112	112	--	0.8	0.8	--
T3	Clay	5.0	2	3.0	210	155	151	176	0.7	0.7	0.8
C4	Sand	5.0	3	1.5	470	515	515	--	1.1	1.1	--
C5	Sand	3.0	3	1.5	420	672	672	--	1.6	1.6	--
C6	Sand	5.0	2	3.0	380	515	507	756	1.4	1.3	2.0
T4	Sand	5.0	3	1.5	360	526	526	--	1.5	1.5	--
T5	Sand	3.0	3	1.5	190	481	481	--	2.5	2.5	--
T6	Sand	5.0	2	3.0	360	526	518	654	1.5	1.4	1.8
C7	Clay	4.6	1	--	212	--	--	242	--	--	1.1
C8	Clay	4.6	1	--	268	--	--	261	--	--	1.0
C9	Clay	5.5	2	3.1	372	308	299	408	0.8	0.8	1.1
C10	Clay Shale	9.3	2	3.2	1177	1008	999	1764	0.9	0.8	1.5
C11	Clay Till	5.9	1	--	1094	--	--	3505	--	--	3.2
C12	Clay Till	6.0	2	3.0	1375	3681	3661	6516	2.7	2.7	4.7
T7	Clay Till	5.9	1	--	800	--	--	3075	--	--	3.8
T8	Clay Till	6.0	2	3.0	1325	3261	3242	6080	2.5	2.4	4.6
T9	Sand Till	4.9	1	--	2025	--	--	4533	--	--	2.2
C13	Clay Till, Clay Shale	7.5	1	--	1075	--	--	--	--	--	--
C14	Clay	10.4	2	1.8	634	--	--	--	--	--	--
C15	Clay	6.1	3	3.0	270	--	--	--	--	--	--
C16	Clay	5.0	2	3.3	245	224	215	262	0.9	0.9	1.1
C17	Clay	4.0	1	--	169	--	--	154	--	--	0.9
C18	Sand	5.0	1	--	203	--	--	--	--	--	--
C19	Sand	5.0	1	--	148	--	--	--	--	--	--
C20	Sand	5.9	2	3.4	200	--	--	--	--	--	--

Table 6-2: Summary of Screw Pile Axial Capacity Predictions Based on Torque

Load Test Designation (Tension, T, or Compression, C)	Predominant Soil Type	Installation Depth (m)	No. of Helices	Inter-Helix Spacing Ratio S/D	Shaft Diameter d (cm)	Installation Torque, T (kN·m)	Ultimate Measured Capacity, Qu (kN)	Predicted Capacity Torque Correlation, QT (kN) $K_t = 9.22$ m^{-1}	Ratio of QT/Qu
C1	Clay	5.0	3	1.5	21.9	20.3	180	188	1.0
C2	Clay	3.0	3	1.5	21.9	15.6	160	144	0.9
C3	Clay	5.0	2	3.0	21.9	19.5	210	180	0.9
T1	Clay	5.0	3	1.5	21.9	22.1	210	204	1.0
T2	Clay	3.0	3	1.5	21.9	20.3	140	188	1.3
T3	Clay	5.0	2	3.0	21.9	22.9	210	211	1.0
C4	Sand	5.0	3	1.5	21.9	44.7	470	413	0.9
C5	Sand	3.0	3	1.5	21.9	40.7	420	375	0.9
C6	Sand	5.0	2	3.0	21.9	44.7	380	413	1.1
T4	Sand	5.0	3	1.5	21.9	50.8	360	469	1.3
T5	Sand	3.0	3	1.5	21.9	42.7	190	394	2.1
T6	Sand	5.0	2	3.0	21.9	47.9	360	441	1.2
C7	Clay	4.6	1	--	17.8	25.6	212	236	1.1
C8	Clay	4.6	1	--	21.9	34.8	268	321	1.2
C9	Clay	5.5	2	3.1	17.8	31.5	372	290	0.8
C10	Clay Shale	9.3	2	3.2	24.4	118.6	1177	1094	0.9
C11	Clay Till	5.9	1	--	27.3	85.4	1094	788	0.7
C12	Clay Till	6.0	2	3.0	27.3	97.6	1375	900	0.7
T7	Clay Till	5.9	1	--	27.3	81.3	800	750	0.9
T8	Clay Till	6.0	2	3.0	27.3	122.0	1325	1125	0.8
T9	Sand Till	4.9	1	--	40.6	257.6	2025	2375	1.2
C13	Clay Till, Clay Shale	7.5	1	--	21.9	120.9	1075	1115	1.0
C14	Clay	10.4	2	1.8	32.4	79.0	634	729	1.1
C15	Clay	6.1	3	3.0	14.0	19.7	270	181	0.7
C16	Clay	5.0	2	3.3	11.4	13.5	245	125	0.5
C17	Clay	4.0	1	--	11.4	8.0	169	74	0.4
C18	Sand	5.0	1	--	11.4	11.0	203	102	0.5
C19	Sand	5.0	1	--	11.4	9.5	148	88	0.6
C20	Sand	5.9	2	3.4	11.4	9.5	200	88	0.4

Table 6-3: Summary of Screw Pile Axial Capacity Predictions Based on Torque and Shaft Diameter

Load Test Designation (Tension, T, or Compression, C)	Predominant Soil Type	No. of Helices	Inter-Helix Spacing Ratio S/D	Shaft Diameter d (cm)	Installation Torque (kN·m)	Ultimate Measured Capacity, Q_u (kN)	Predicted Capacity, Q_T (kN) Torque Correlation		Ratio of Q_T/Q_u	
							$K_I = 9.19\,m^{-1}$	$K_I = 16.9\,m^{-1}$	$K_I = 9.19\,m^{-1}$	$K_I = 16.9\,m^{-1}$
C1	Clay	3	1.5	21.9	20.3	180	187	--	1.04	--
C2	Clay	3	1.5	21.9	15.6	160	143	--	0.90	--
C3	Clay	2	3.0	21.9	19.5	210	179	--	0.85	--
T1	Clay	3	1.5	21.9	22.1	210	203	--	0.97	--
T2	Clay	3	1.5	21.9	20.3	140	187	--	1.33	--
T3	Clay	2	3.0	21.9	22.9	210	211	--	1.00	--
C4	Sand	3	1.5	21.9	44.7	470	411	--	0.87	--
C5	Sand	3	1.5	21.9	40.7	420	374	--	0.89	--
C6	Sand	2	3.0	21.9	44.7	380	411	--	1.08	--
T4	Sand	3	1.5	21.9	50.8	360	467	--	1.30	--
T5	Sand	3	1.5	21.9	42.7	190	392	--	2.07	--
T6	Sand	2	3.0	21.9	47.9	360	440	--	1.22	--
C7	Clay	1	--	17.8	25.6	212	235	--	1.11	--
C8	Clay	1	--	21.9	34.8	268	320	--	1.19	--
C9	Clay	2	3.1	17.8	31.5	372	289	--	0.78	--
C10	Clay Shale	2	3.2	24.4	118.6	1177	1090	--	0.93	--
C11	Clay Till	1	--	27.3	85.4	1094	785	--	0.72	--
C12	Clay Till	2	3.0	27.3	97.6	1375	897	--	0.65	--
T7	Clay Till	1	--	27.3	81.3	800	747	--	0.93	--
T8	Clay Till	2	3.0	27.3	122.0	1325	1121	--	0.85	--
T9	Sand Till	1	--	40.6	257.6	2025	2367	--	1.17	--
C13	Clay Till, Clay Shale	1	--	21.9	120.9	1075	1111	--	1.03	--
C14	Clay	2	1.8	32.4	79.0	634	726	--	1.15	--
C15	Clay	3	3.0	14.0	19.7	270	181	--	0.67	--
C16	Clay	2	3.3	11.4	13.5	245	--	229	--	0.93
C17	Clay	1	--	11.4	8.0	169	--	136	--	0.80
C18	Sand	1	--	11.4	11.0	203	--	186	--	0.92
C19	Sand	1	--	11.4	9.5	148	--	161	--	1.09
C20	Sand	2	3.4	11.4	9.5	200	--	161	--	0.80

Table 6-4: Summary of Screw Pile Uplift Capacity Predictions In Sand Based on Ghaly and Hanna's (1991) Non-Dimensional Torque Relationship

Load Test Designation (Tension, T, or Compression, C)	Embedment Depth H (m)	Helix Pitch p (m)	Surface Area of Blade A (m^2)	Unit Weight of Sand γ (kN/m^3)	Installation Torque (kN·m)	Ultimate Capacity Measured Q_u (kN)	Torque Factor, T	Ultimate Predicted Capacity, Ghaly and Hanna (1991) Relationship, Q_p (kN)	Ratio of Predicted to Measured Capacity Q_p/Q_u
T4	3.9	0.076	0.1237	19	50.8	360	111.0	2053	5.70
T5	1.9	0.076	0.1237	19	42.7	190	200.1	1819	9.58
T6	3.9	0.076	0.1237	19	47.8	360	103.7	1918	5.33
T9	4.9	0.152	0.6526	19	257.0	2025	38.7	4703	2.32

117
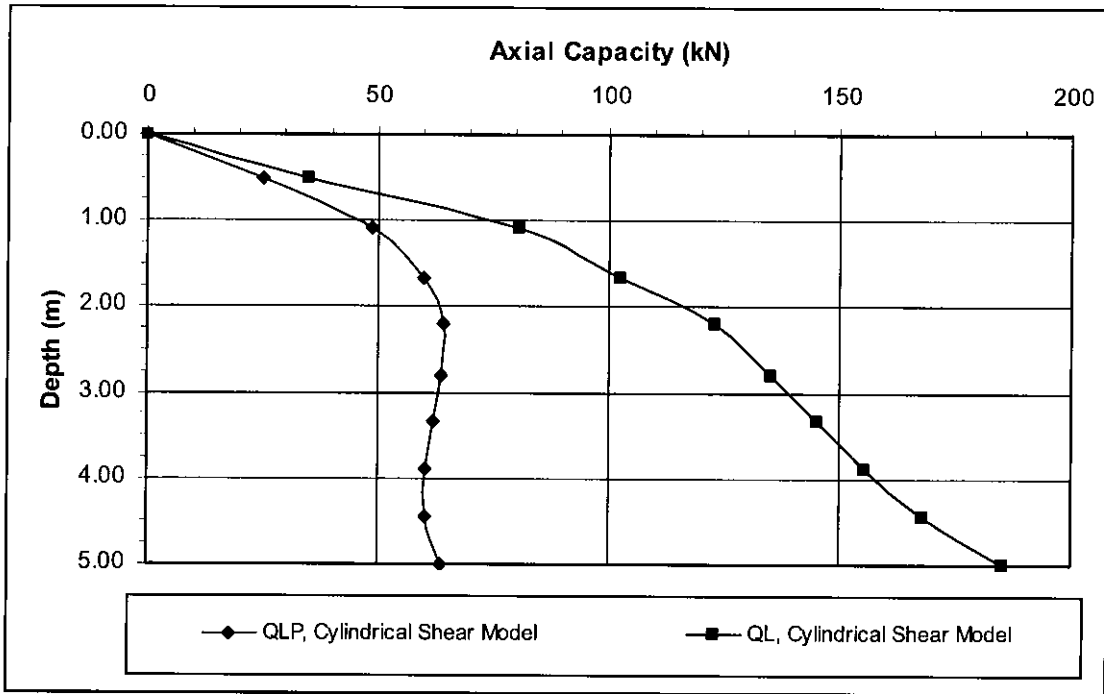
Figure 6-1: LCPC Capacity Predictions with Depth for Pile C1 in Compression; Point Resistance, QLP, and Total Capacity, QL.
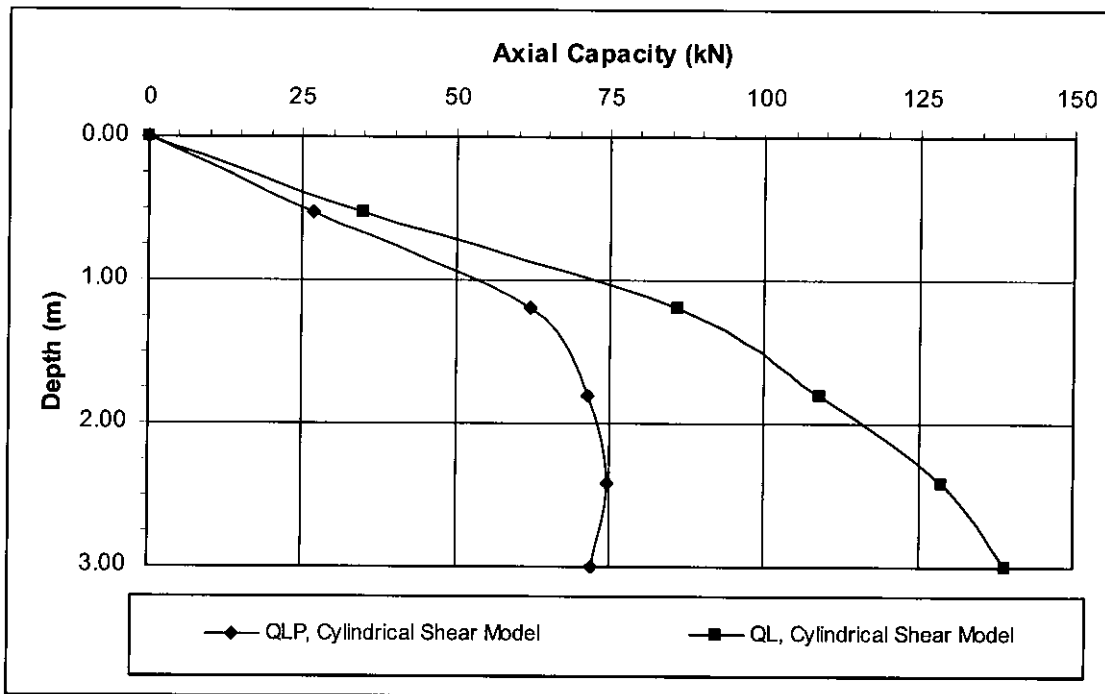
Figure 6-2: LCPC Capacity Predictions with Depth for Pile C2 in Compression; Point Resistance, QLP, and Total Capacity, QL.

118
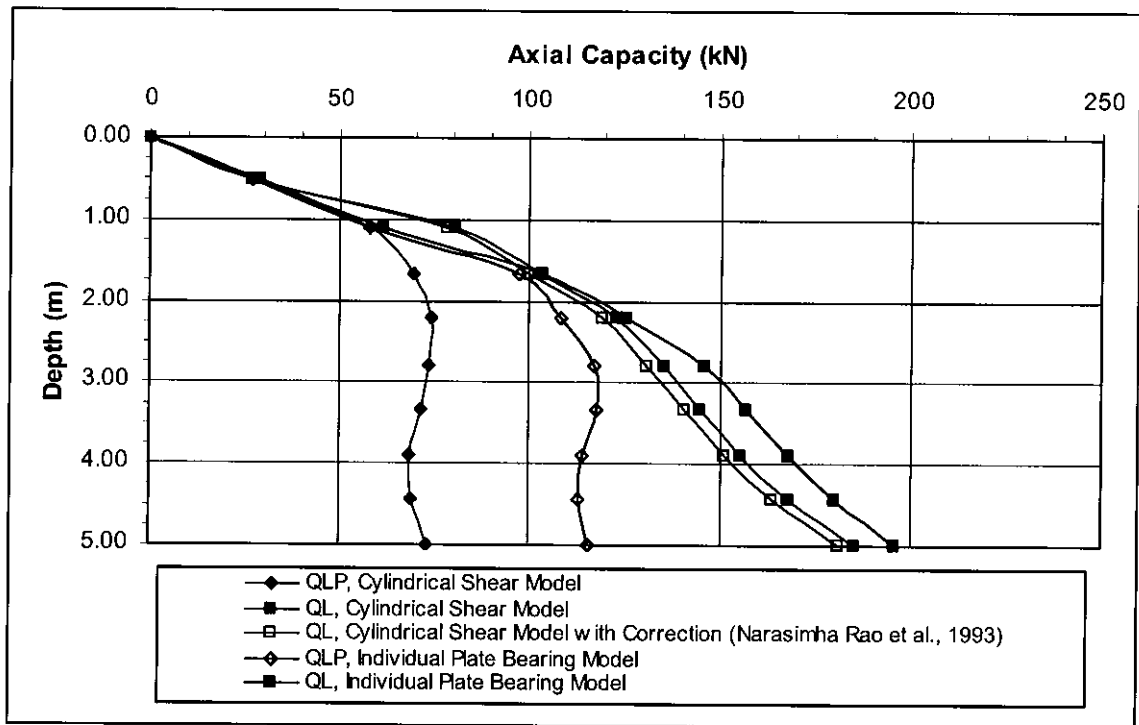
Figure 6-3: LCPC Capacity Predictions with Depth for Pile C3 in Compression; Point Resistance, QLP, and Total Capacity, QL.
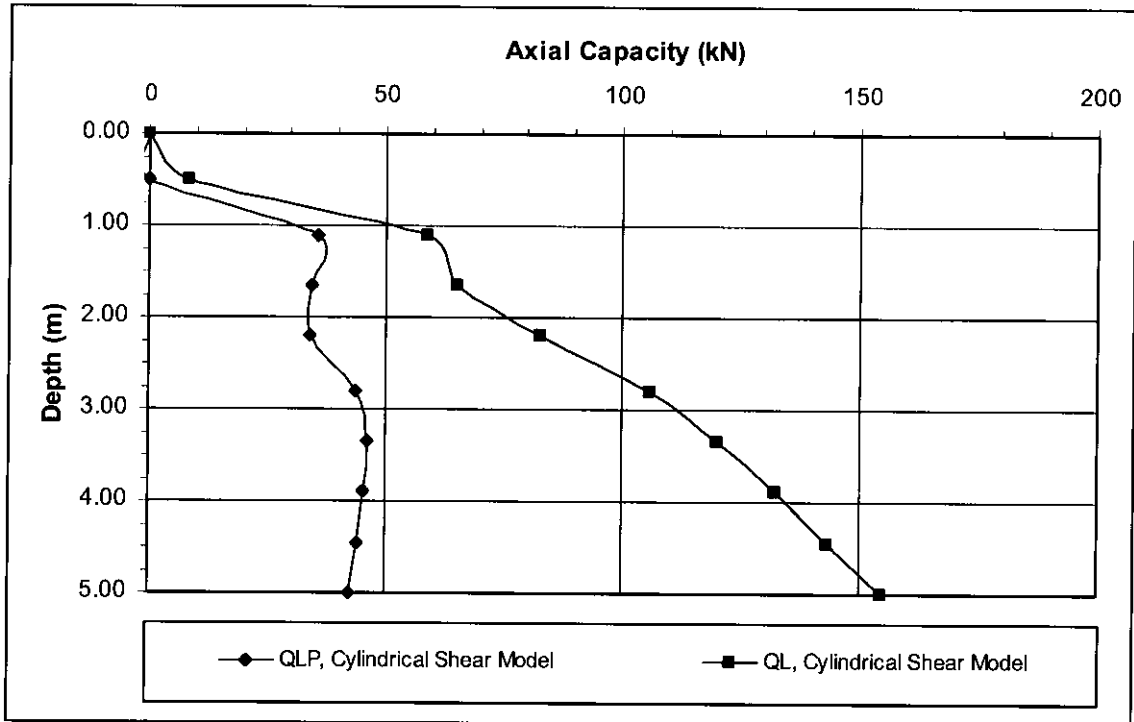
Figure 6-4: LCPC Capacity Predictions with Depth for Pile T1 in Tension; Point Resistance, QLP, and Total Capacity, QL.

119
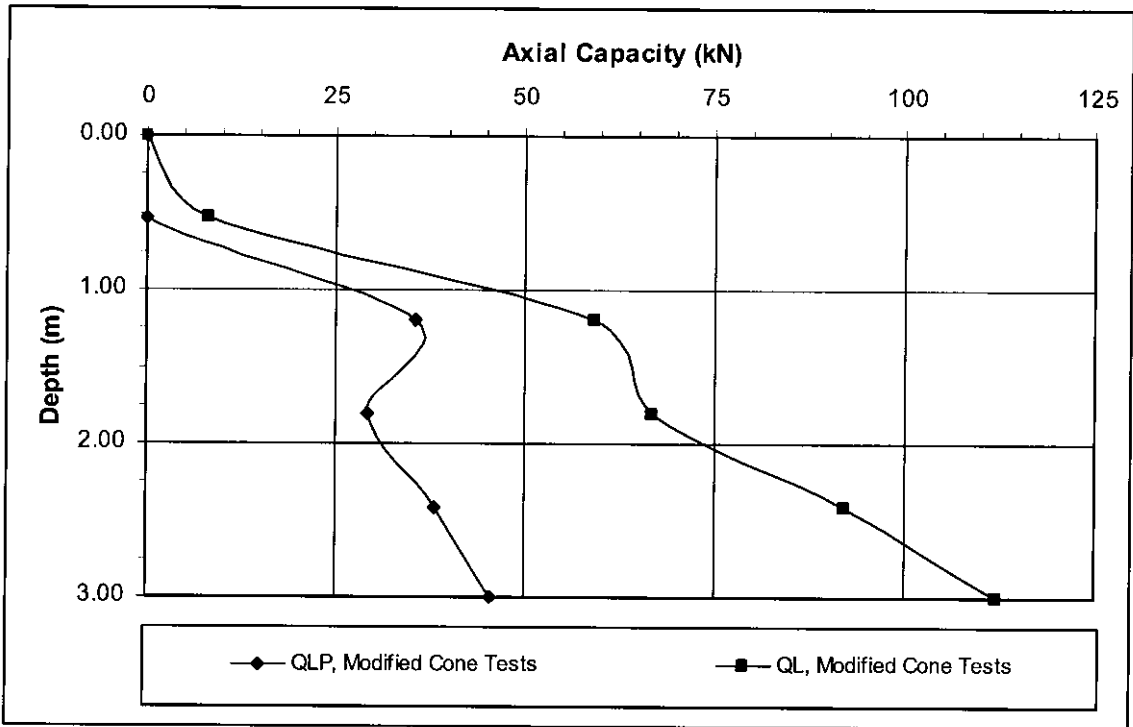
Figure 6-5: LCPC Capacity Predictions with Depth for Pile T2 in Tension; Point Resistance, QLP, and Total Capacity, QL.
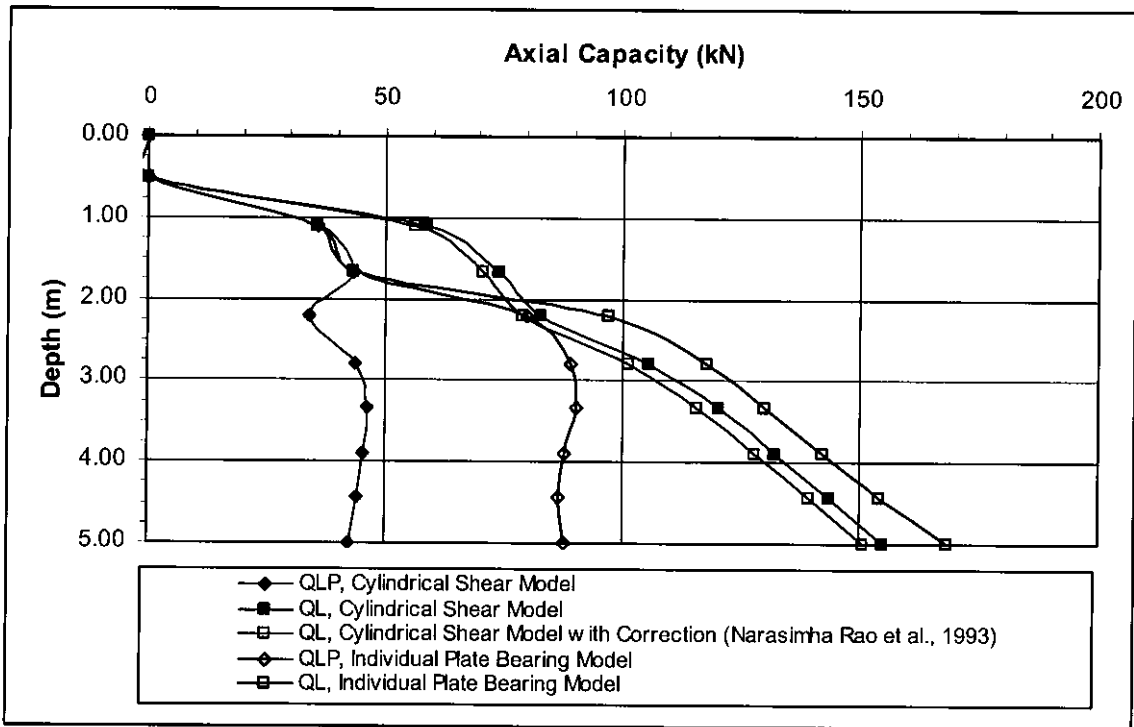
Figure 6-6: LCPC Capacity Predictions with Depth for Pile T3 in Tension; Point Resistance, QLP, and Total Capacity, QL.
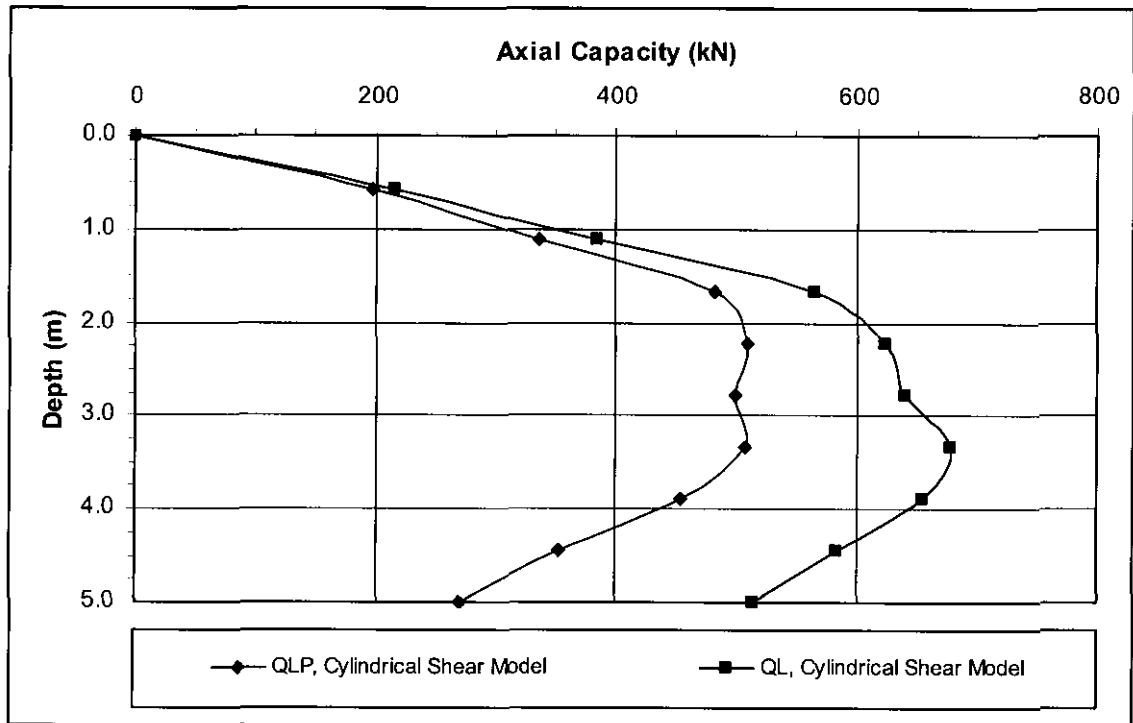
Figure 6-7: LCPC Capacity Predictions with Depth for Pile C4 in Compression; Point Resistance, QLP, and Total Capacity, QL.
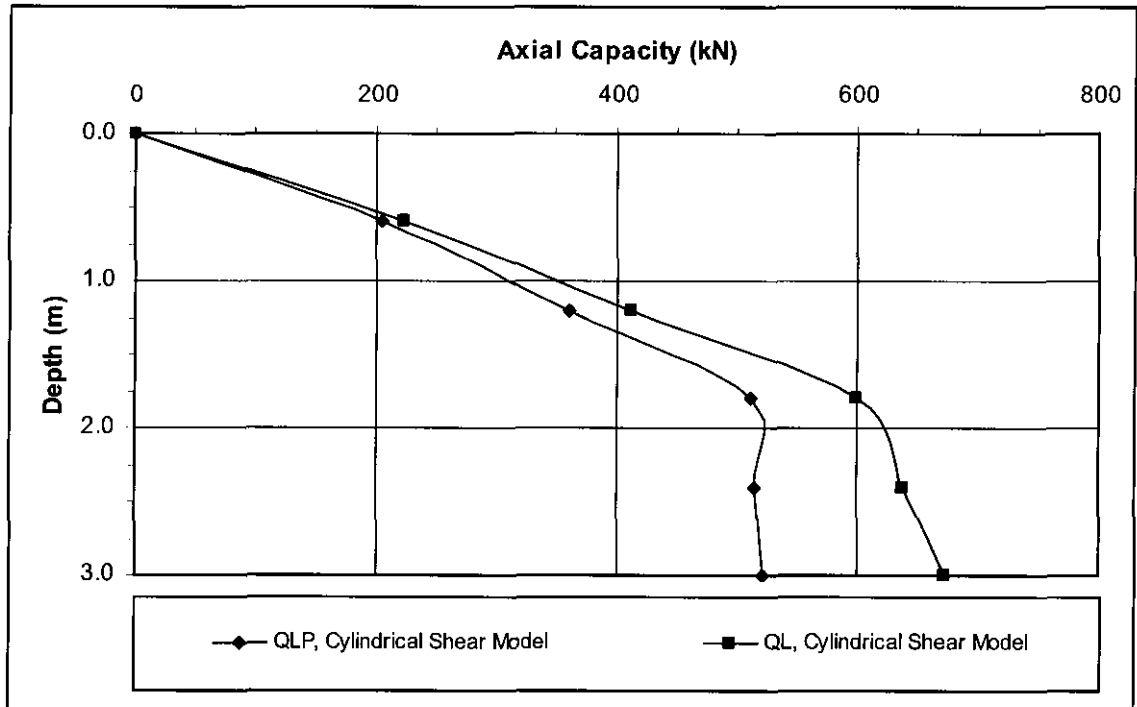
Figure 6-8: LCPC Capacity Predictions with Depth for Pile C5 in Compression; Point Resistance, QLP, and Total Capacity, QL.

121
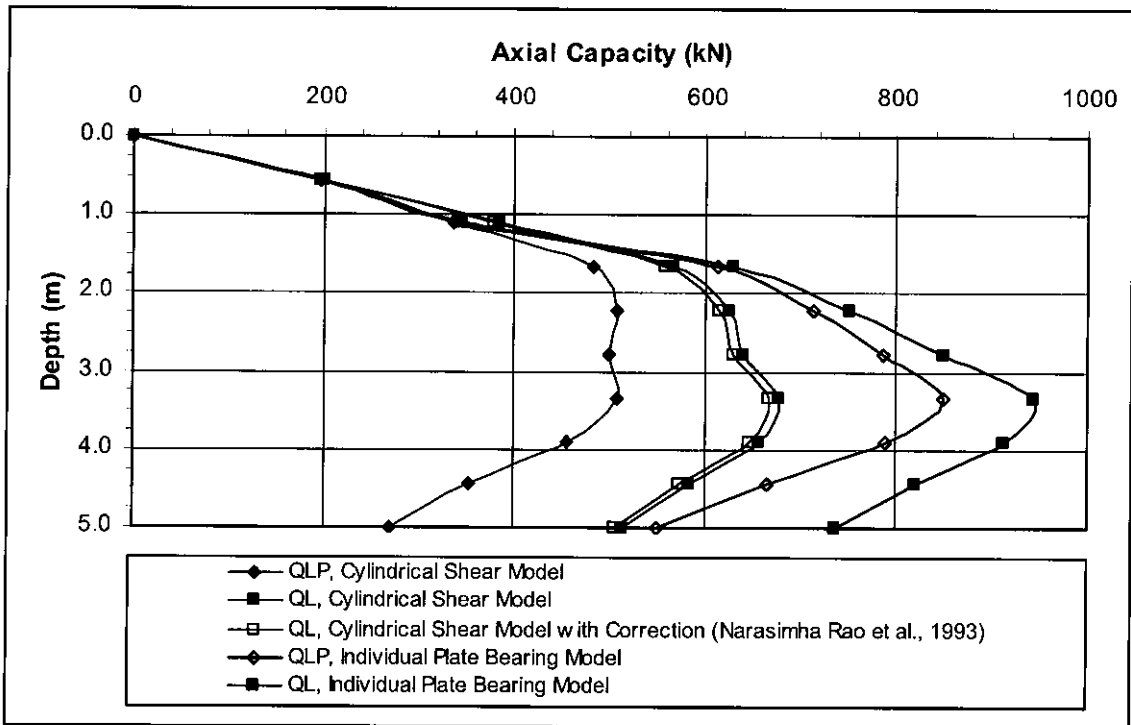
Figure 6-9: LCPC Capacity Predictions with Depth for Pile C6 in Compression; Point Resistance, QLP, and Total Capacity, QL.
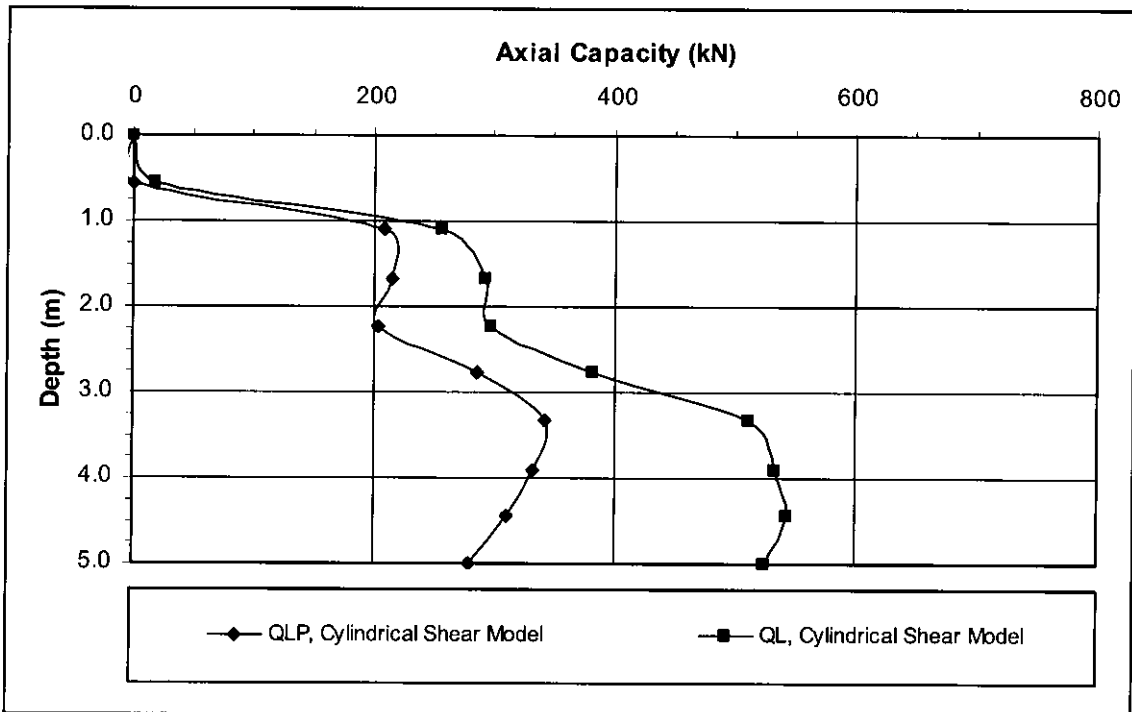
Figure 6-10: LCPC Capacity Predictions with Depth for Pile T4 in Tension; Point Resistance, QLP, and Total Capacity, QL.

122
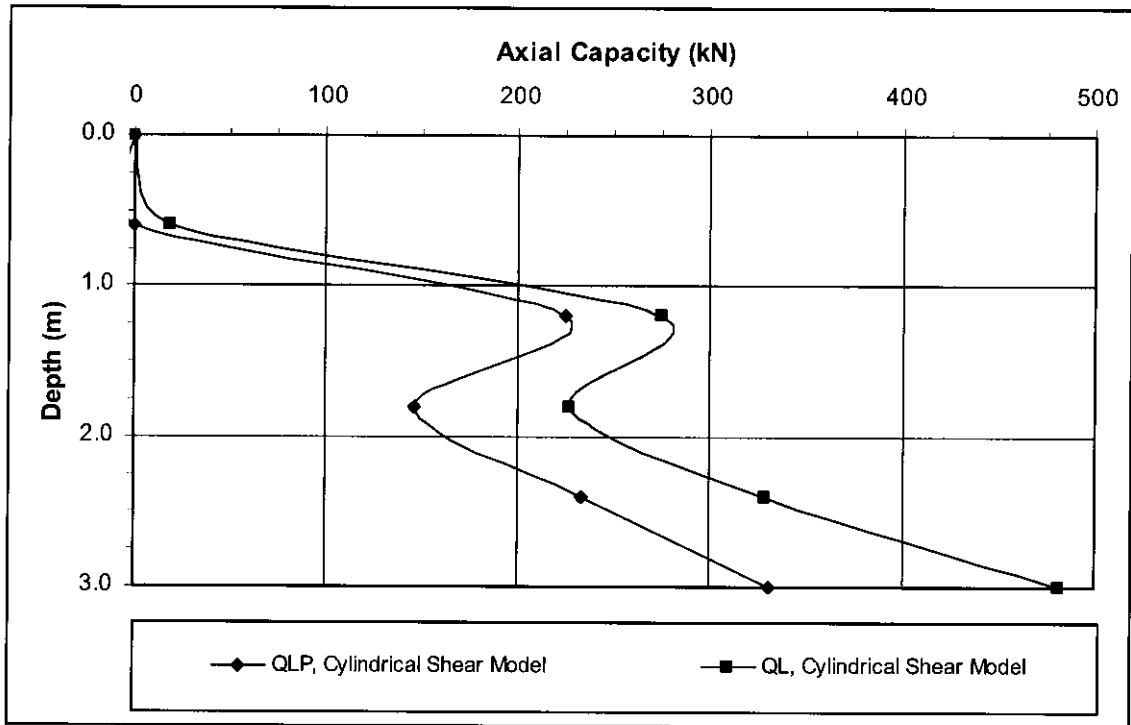
Figure 6-11: LCPC Capacity Predictions with Depth for Pile T5 in Tension; Point Resistance, QLP, and Total Capacity, QL.
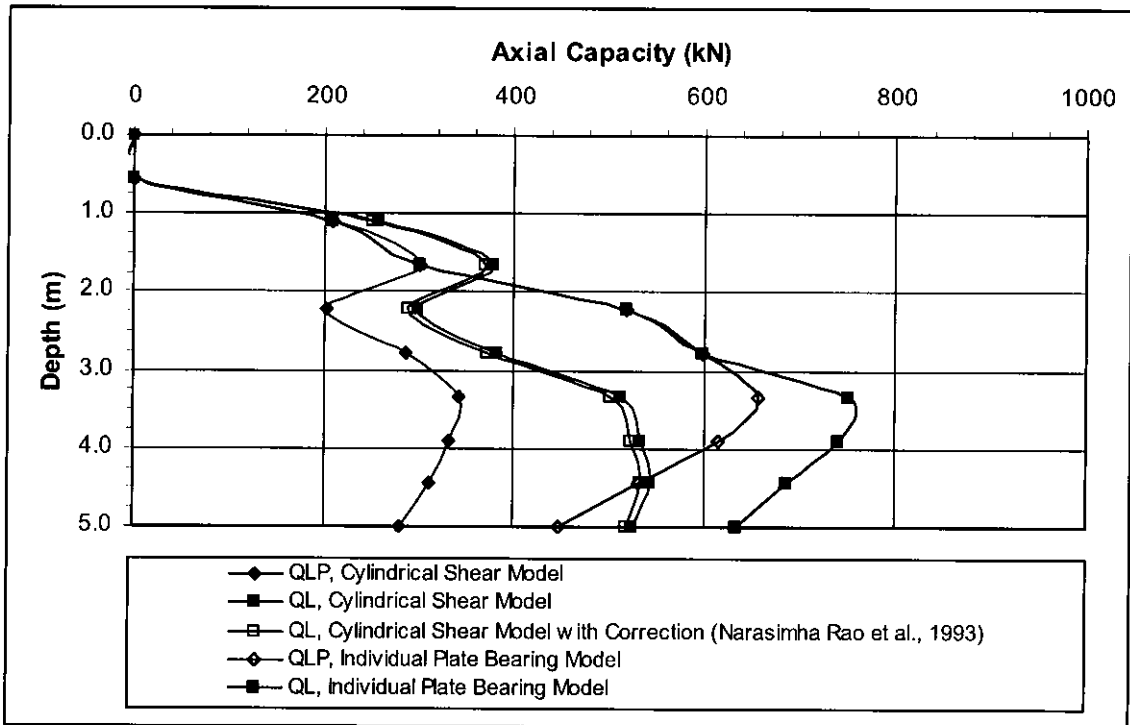
Figure 6-12: LCPC Capacity Predictions with Depth for Pile T6 in Tension; Point Resistance, QLP, and Total Capacity, QL.
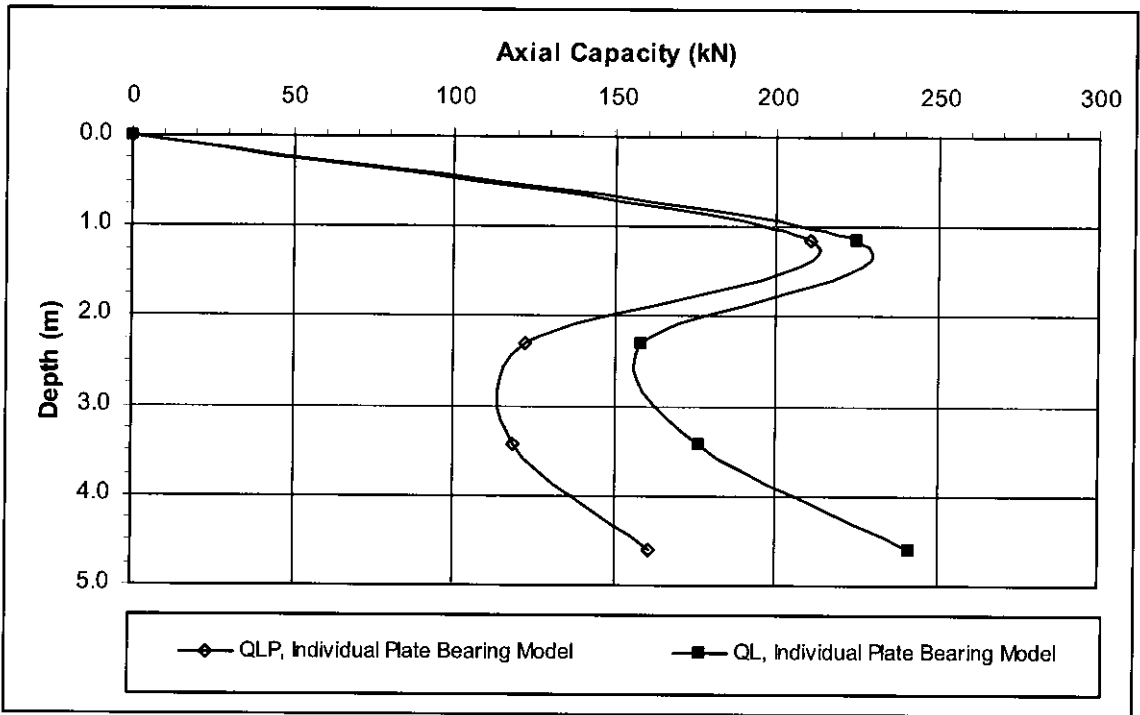
Figure 6-13: LCPC Capacity Predictions with Depth for Pile C7 in Compression; Point Resistance, QLP, and Total Capacity, QL.
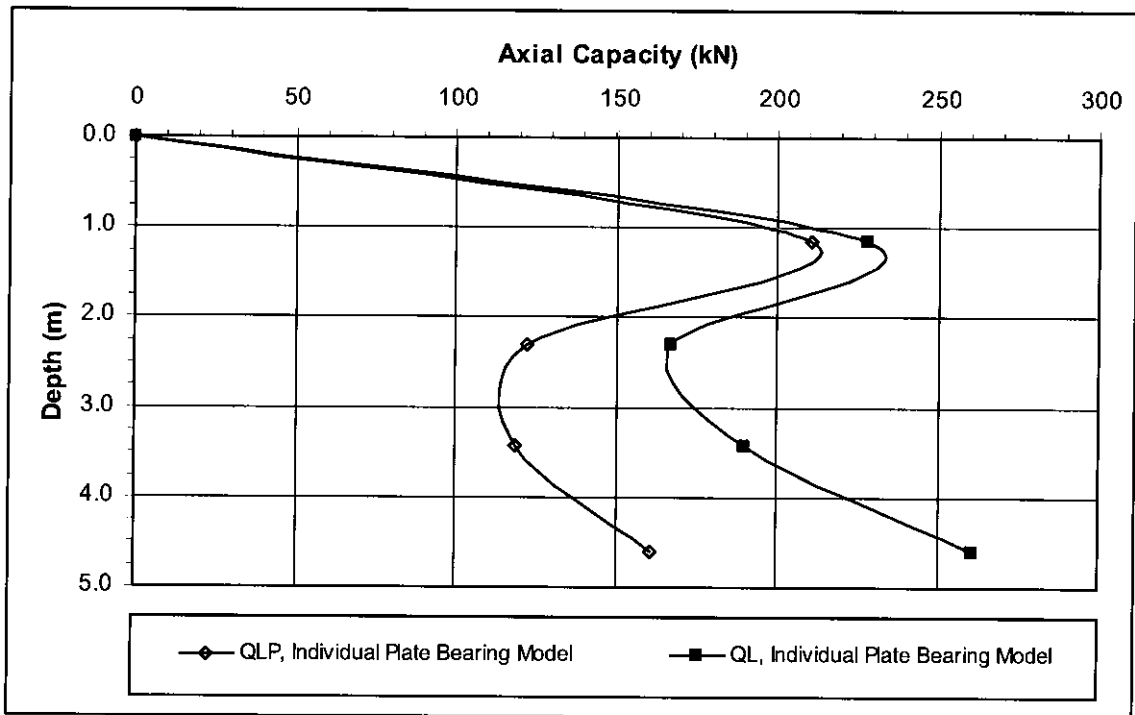
Figure 6-14: LCPC Capacity Predictions with Depth for Pile C8 in Compression; Point Resistance, QLP, and Total Capacity, QL.

124
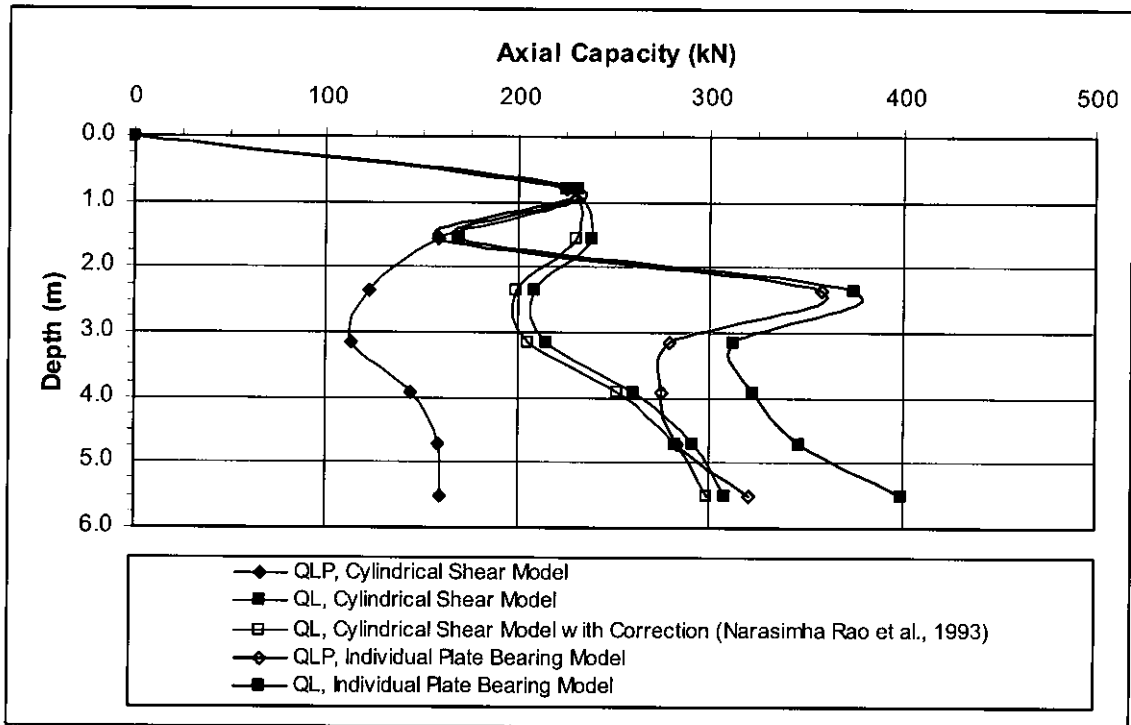
Figure 6-15: LCPC Capacity Predictions with Depth for Pile C9 in Compression; Point Resistance, QLP, and Total Capacity, QL.
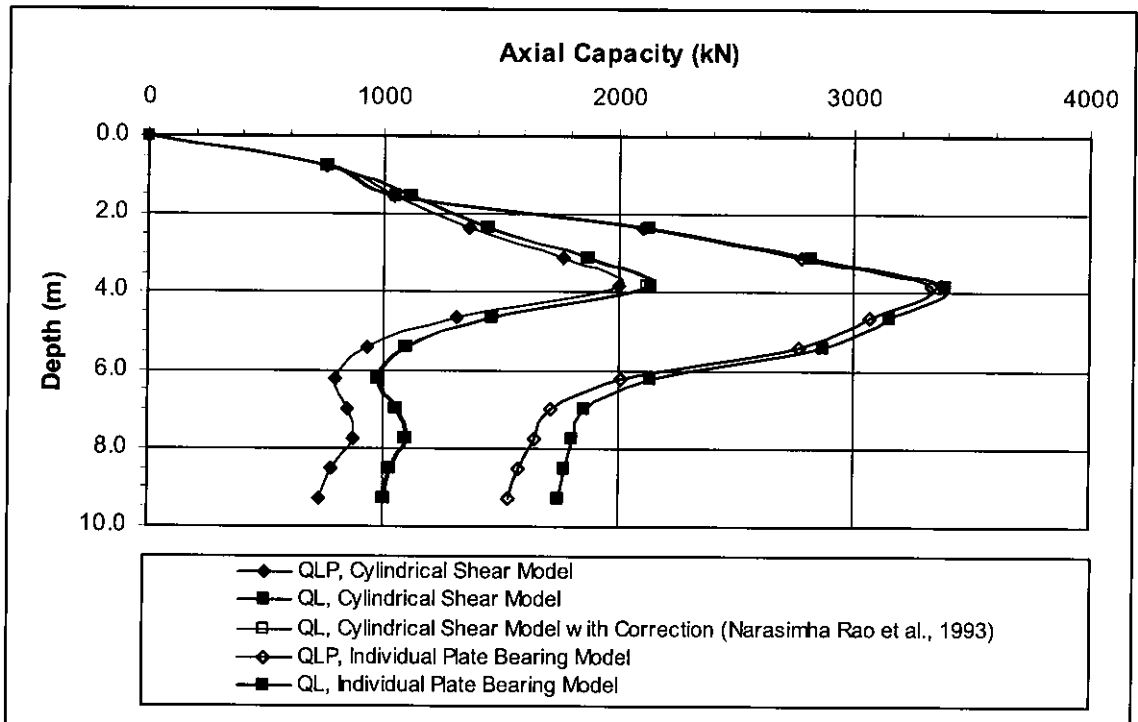
Figure 6-16: LCPC Capacity Predictions with Depth for Pile C10 in Compression; Point Resistance, QLP, and Total Capacity, QL.
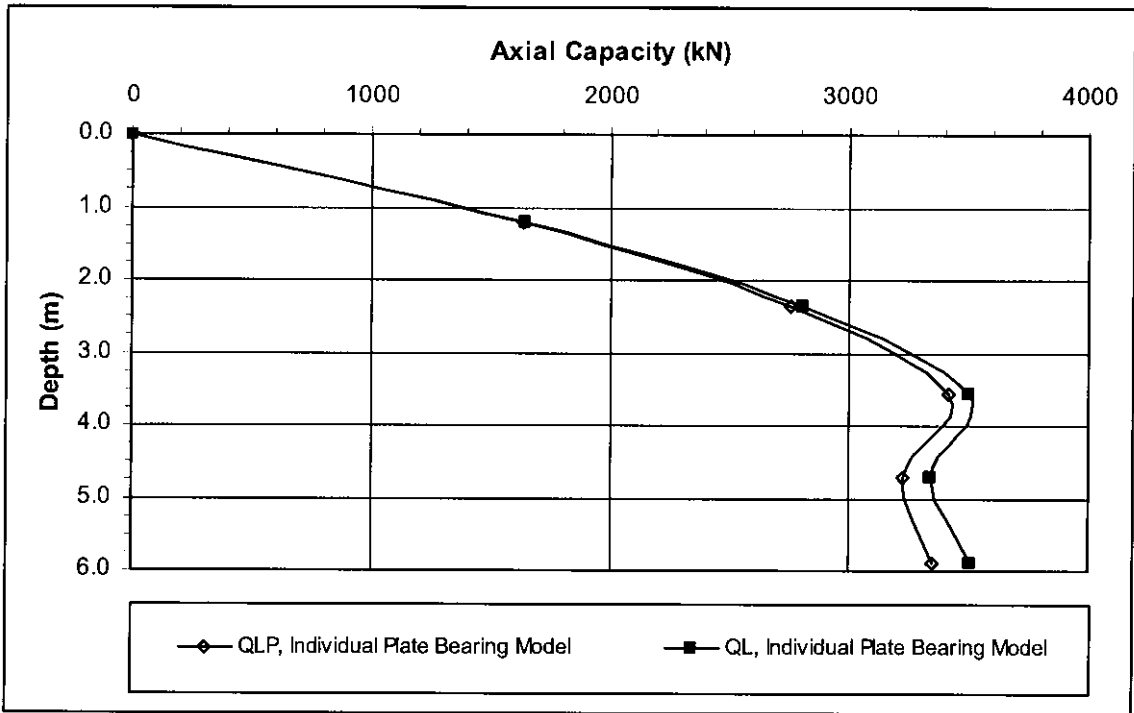
Figure 6-17: LCPC Capacity Predictions with Depth for Pile C11 in Compression; Point Resistance, QLP, and Total Capacity, QL.
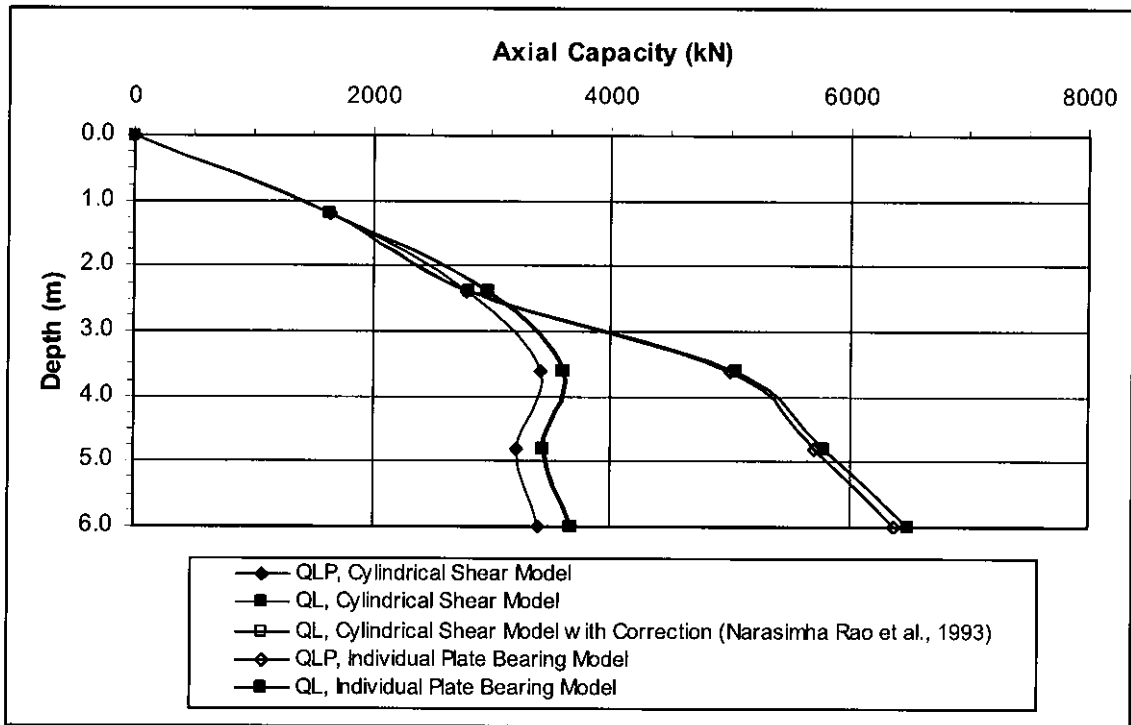
Figure 6-18: LCPC Capacity Predictions with Depth for Pile C12 in Compression; Point Resistance, QLP, and Total Capacity, QL.
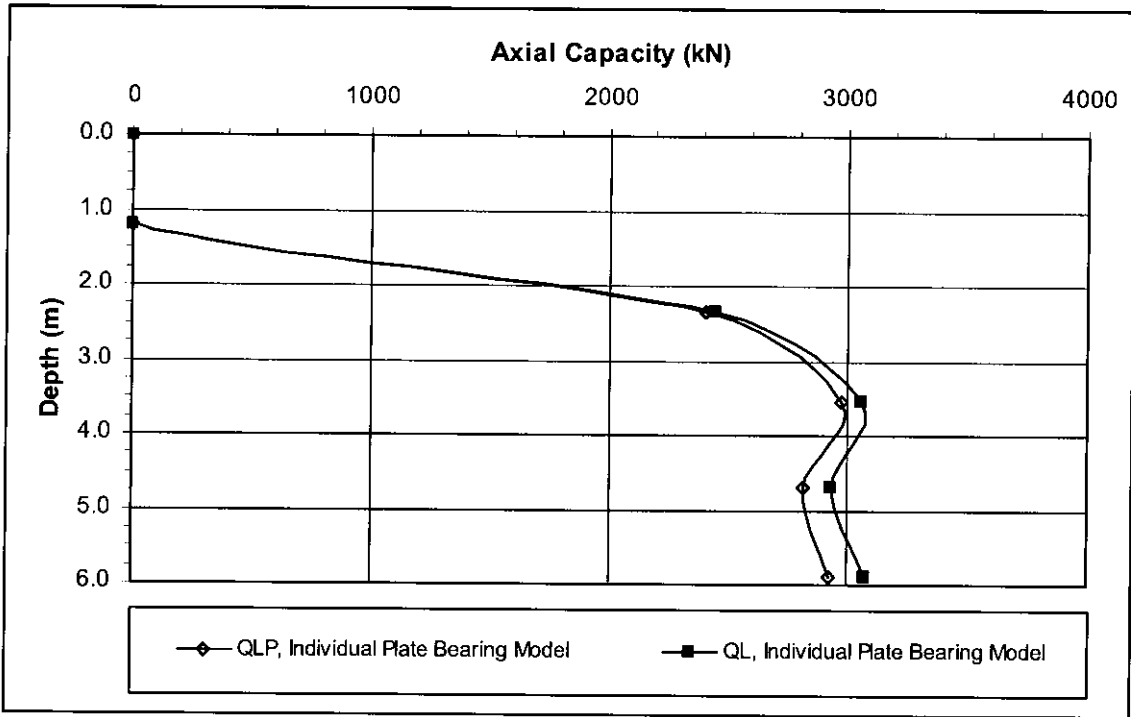
Figure 6-19: LCPC Capacity Predictions with Depth for Pile T7 in Tension; Point Resistance, QLP, and Total Capacity, QL.
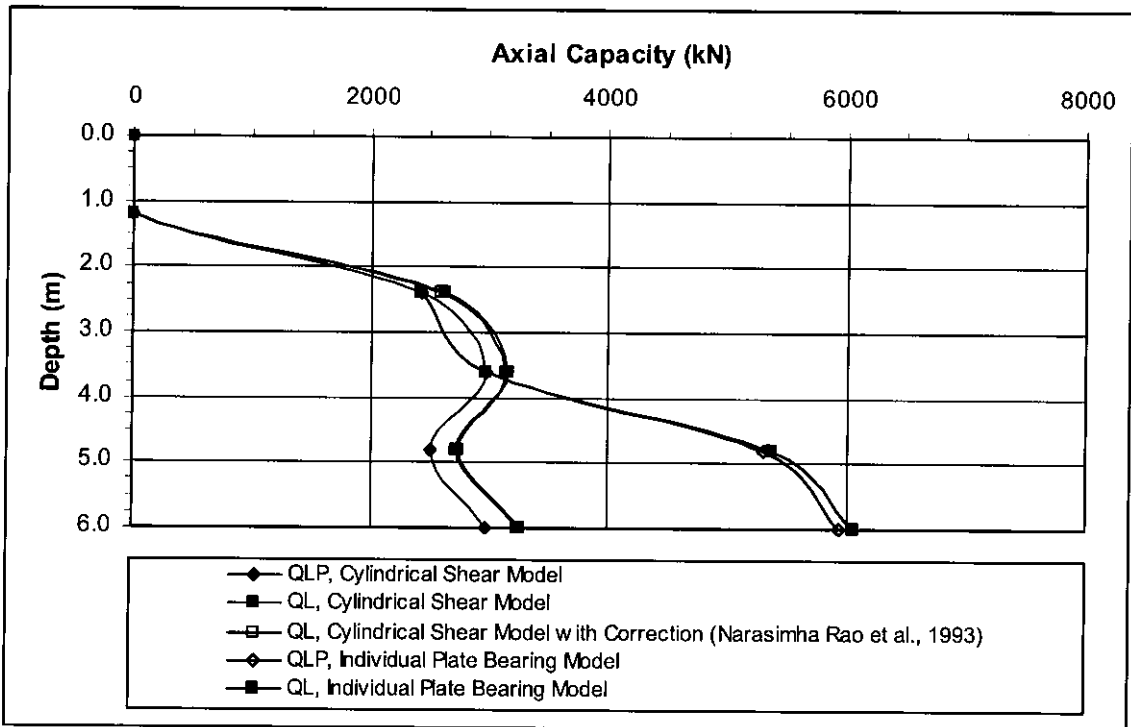
Figure 6-20: LCPC Capacity Predictions with Depth for Pile T8 in Tension; Point Resistance, QLP, and Total Capacity, QL.
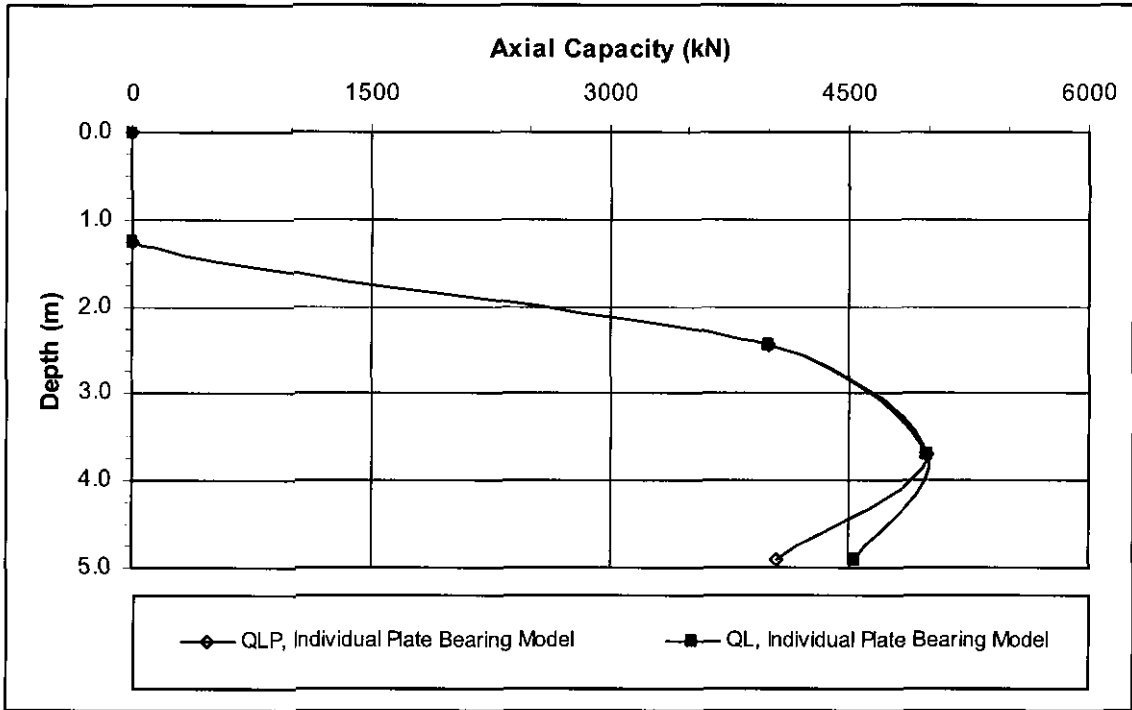
Figure 6-21: LCPC Capacity Predictions with Depth for Pile T9 in Tension; Point Resistance, QLP, and Total Capacity, QL.
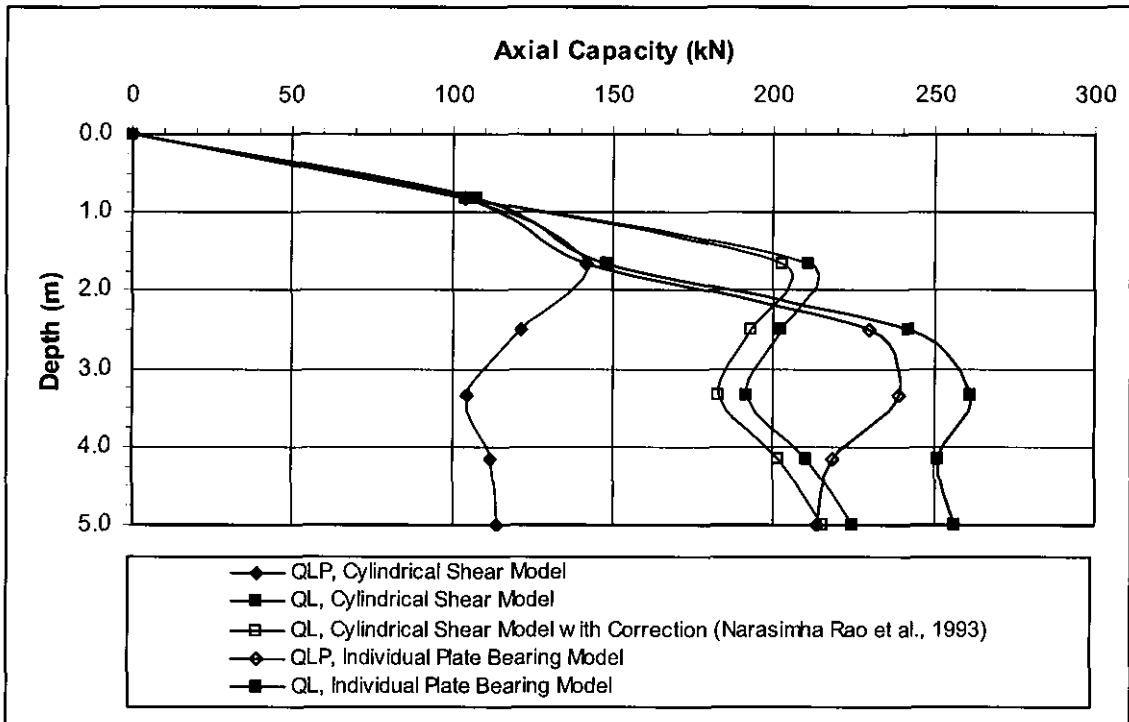
Figure 6-22: LCPC Capacity Predictions with Depth for Pile C16 in Compression; Point Resistance, QLP, and Total Capacity, QL.
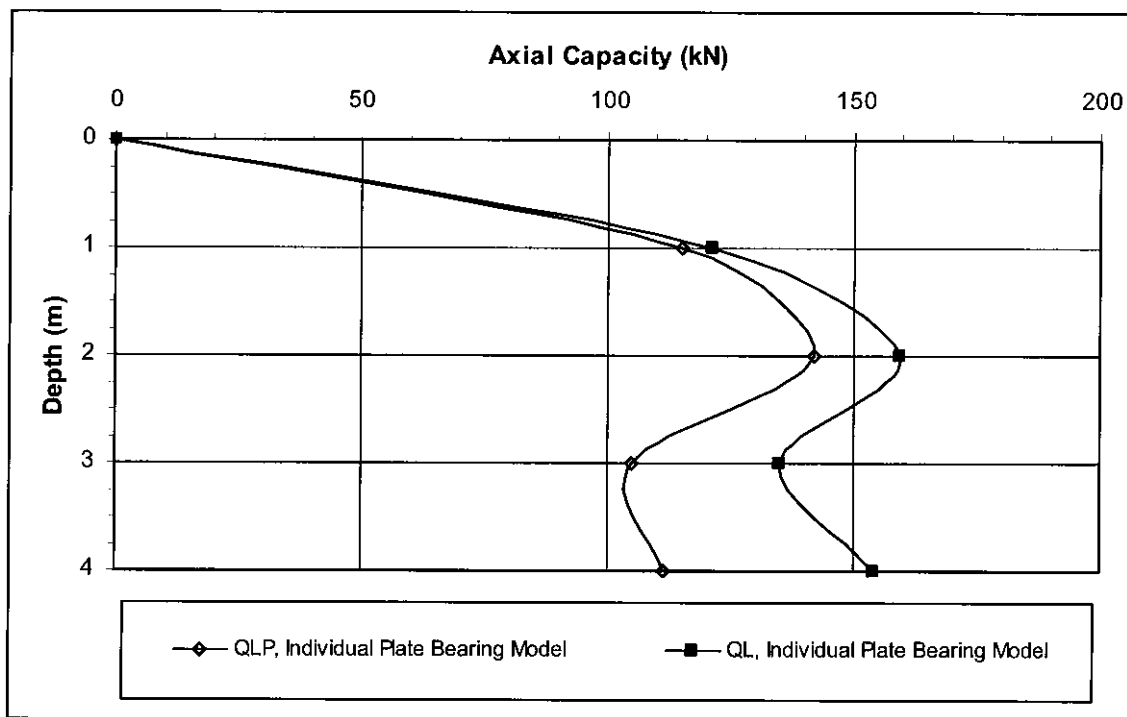
Figure 6-23: LCPC Capacity Predictions with Depth for Pile C17 in Compression; Point Resistance, QLP, and Total Capacity, QL.
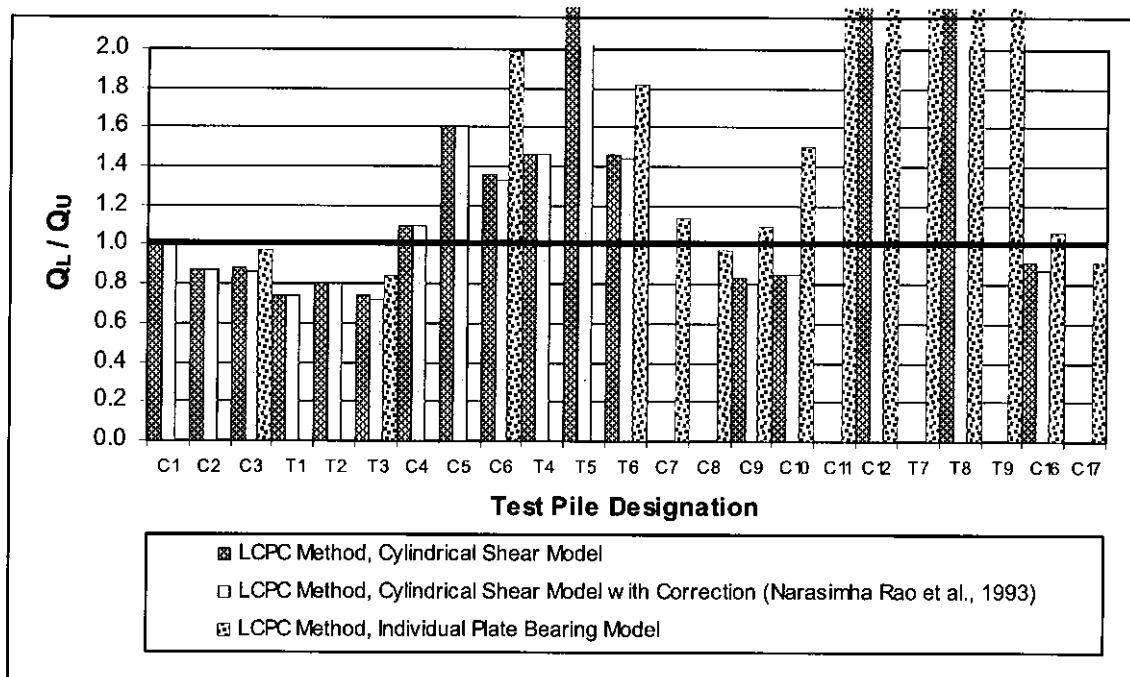
Figure 6-24: Ratios of Predicted Ultimate Capacity, Q_L, to Measured Ultimate Capacity, Q_U, Using LCPC Method
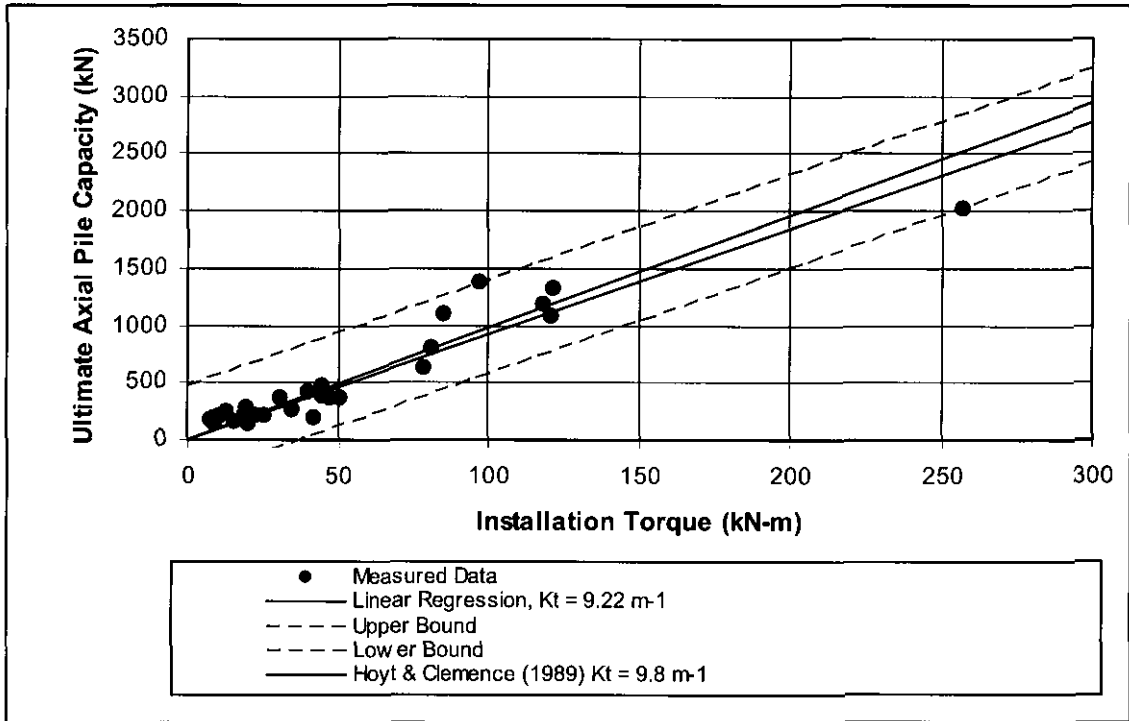
Figure 6-25: Correlation Between Measured Axial Pile Capacities and Required Installation Torque
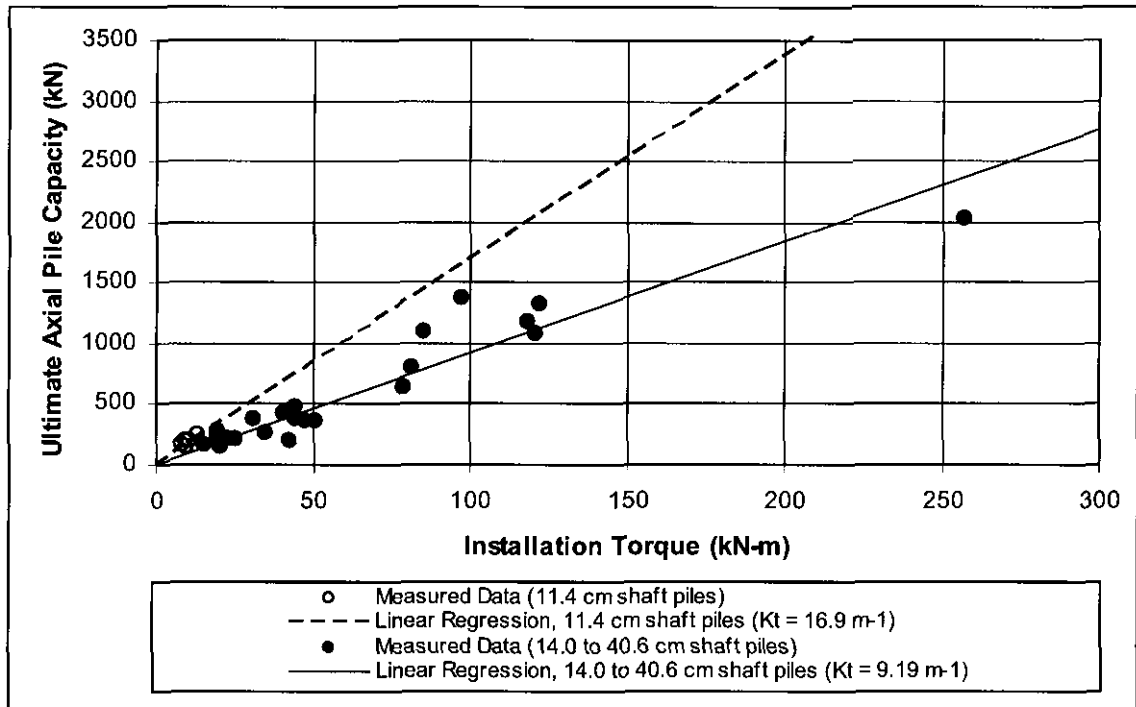
Figure 6-26: Refined Correlations Between Measured Axial Pile Capacities and Required Installation Torque, Based on Pile Shaft Diameter
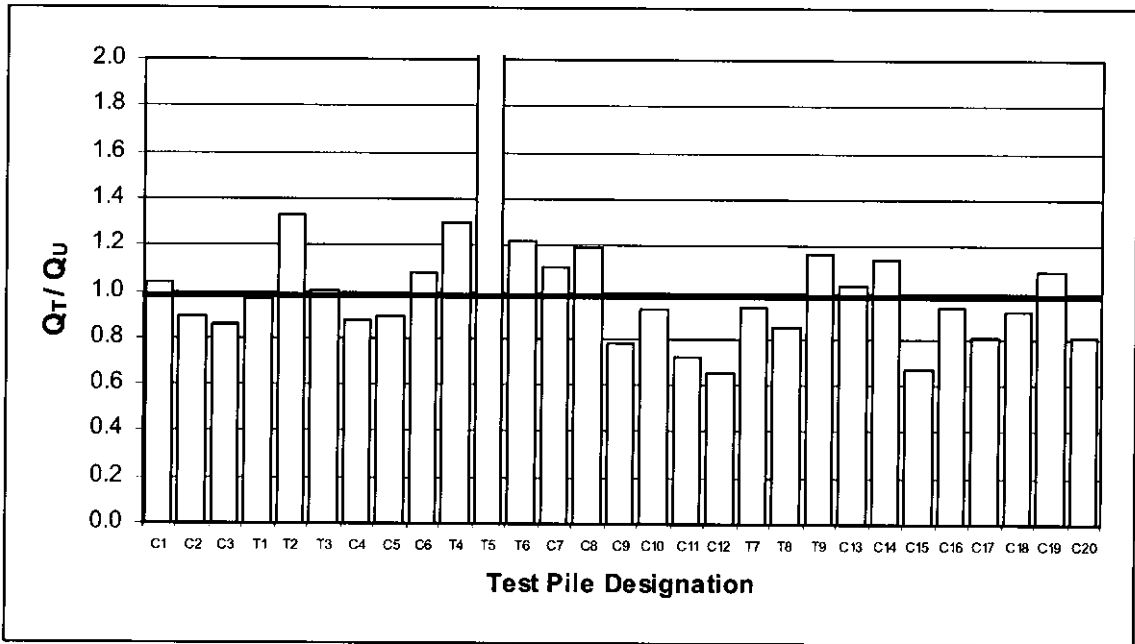
Figure 6-27: Ratios of Predicted Ultimate Capacity, Q_T, to Measured Ultimate Capacity, Q_U, Using Refined Torque Correlation Based on Diameter of Screw Pile Shaft
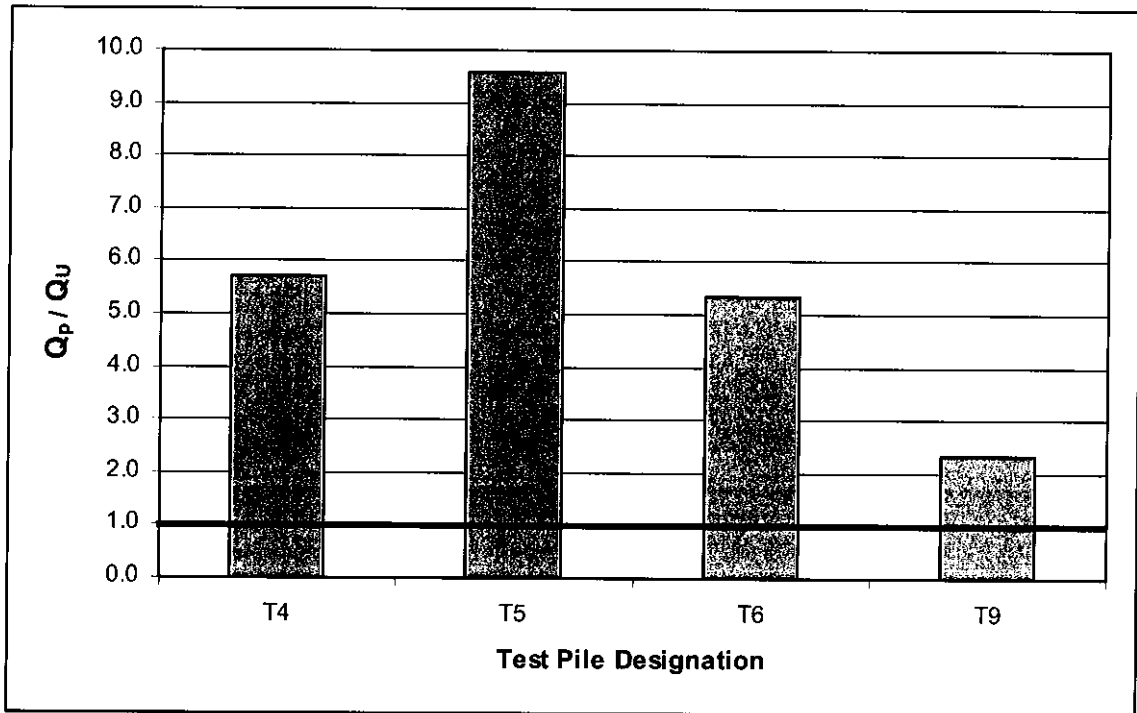
Figure 6-28: Ratios of Predicted Ultimate Capacity, Q_P, to Measured Ultimate Capacity, Q_U, Using Ghaly and Hanna's (1991) Non-Dimensional Torque Correlation for Uplift Capacity in Sand

6.4 References

Bustamante, M., and Gianeselli, L. 1982. Pile bearing capacity prediction by means of static penetrometer CPT. *In* Proceedings of the 2nd European Symposium on Penetration Testing, ESOPT-II. Amsterdam. Balkema Publisher, Rotterdam, Vol.2, pp. 493-500.

Ghaly, A., and Hanna, A. 1991. Experimental and theoretical studies on installation torque of screw anchors. Canadian Geotechnical Journal, **28**(3): 353-364.

Hoyt, R.M., and Clemence, S.P. 1989. Uplift capacity of helical anchors in soil. *In* Proceedings of the 12th International Conference on Soil Mechanics and Foundation Engineering. Rio de Janeiro, Brazil, Vol.2, pp. 1019-1022.

Mitsch, M.P., and Clemence, S.P. 1985. The uplift capacity of helix anchors in sand. *In* Uplift Behaviour of Anchor Foundations in Soil: Proceedings of ASCE. New York, New York, pp. 26-47.

Narasimha Rao, S., Prasad, Y.V.S.N., and Veeresh, C. 1993. Behaviour of embedded model screw anchors in soft clays. Geotechnique, **43**: 605-614.

Narasimha Rao, S., Prasad, Y.V.S.N., Shetty, M.D., and Joshi, V.V. 1989. Uplift capacity of screw pile anchors. Geotechnical Engineering, **20**(2): 139-159.

Perko, H.A. 2000. Energy method for predicting installation torque of helical foundations and anchors. *In* New technological and design developments in deep foundations. ASCE, Special Publication no. 100, Denver, Colorado. p. 490.

Zhang, D. 1999. Predicting capacity of helical screw piles in Alberta soils. M.Sc. thesis, Department of Civil and Environmental Engineering, University of Alberta, Edmonton, Alberta.

7 Conclusions and Recommendations

7.1 Project Summary

The objective of this thesis project was to investigate the effectiveness of using a CPT-based direct design method and empirical torque correlations to predict the axial capacities of screw piles installed in Western Canadian soils. Towards this end, a database was compiled of the results of 29 axial load tests performed on commercially-manufactured screw piles installed in the provinces of Alberta, Saskatchewan, and British Columbia since 1998. The load test results were used to verify the applicability of the two separate approaches to screw pile design—the LCPC direct pile design method (Bustamante and Gianeselli 1982), used in conjunction with a CPT profile and the cylindrical shear and individual plate bearing failure models, and the empirical methods of torque correlation proposed by Hoyt and Clemence (1989) and Ghaly and Hanna (1991).

The 29 screw piles included in the database of load test results vary in shaft diameter from 11.4 cm (4 ½ in) to 40.6 cm (16 in), affixed with one, two, or three helices ranging from 35.6 cm (14 in) to 91.4 cm (36 in) in diameter. The piles were installed to depths of 3.0 m to 10.4 m below the surface at 10 different test sites comprising a variety of soil conditions, including sand, clay, glacial till, and clay shale. Nine of the 29 screw piles tested were loaded in tension, and the remaining 20 piles loaded in compression in accordance with the ASTM "Quick Test" procedure (ASTM Designation: D1143 1981; ASTM Designation: D3689 1990) for determination of the load-settlement curves.

As required for use with the LCPC direct design method, cone penetration profiles were obtained and presented for seven of the 10 sites where the screw pile load tests had been previously performed. An inexpensive, portable apparatus was developed for conducting some of the required cone penetration tests in softer soils, and termed the modified cone penetration equipment. Commercial, rig-mounted cone penetration test results were presented for five of the

seven test sites, and profiles of tip resistance and sleeve friction obtained using the modified cone penetration equipment were presented for three of the seven test sites. Based on a comparison of results obtained at the University Farm site in Edmonton, Alberta, it was verified that the modified cone penetration equipment provided equivalent profiles of tip resistance and sleeve friction when compared to full-scale, commercial CPT results.

Capacity predictions made using the LCPC direct design method and empirical torque correlations were compared to the actual measured capacities of the screw piles tested, and the degree of discrepancy discussed. In light of the results, recommendations regarding the prediction of the ultimate capacities for screw piles loaded in axial tension and compression in Western Canadian soils will be outlined in the following section.

7.2 Design Recommendations

7.2.1 Direct Design Approach: LCPC Method

The LCPC direct design method presented by Bustamante and Gianeselli (1982) was developed in France for predicting the ultimate axial capacity of various types of bored, driven, and grouted piles using the results of a site-specific cone penetration test, namely the profile of tip resistance with depth. Axial load tests conducted by Zhang (1999) on full-scale instrumented screw piles installed in Alberta soils showed promise for the use of the LCPC method in predicting screw pile capacities when loaded to failure in tension or compression. Under the current investigation, tip resistance profiles were obtained by cone penetration testing at seven of the 10 screw pile load test sites, allowing for the LCPC method to be used for predicting the ultimate axial capacities of 23 of the total 29 documented screw piles. The capacity predictions made using the LCPC method were based on applying the appropriate failure model(s) to the individual pile geometries. The cylindrical shear failure model was applied to all multi-helix piles, with and without the reduction factor recommended by Narasimha Rao et al. (1993) for addressing the effect of inter-helix spacing ratios greater than 1.5, and the individual plate bearing failure model was applied to all single-helix screw piles, and multi-helix screw piles having an inter-helix spacing ratio greater than 2.0.

After comparing the ultimate axial capacities predicted by the LCPC method with the measured capacities determined by the screw pile load tests, it was concluded that the LCPC method provided a reasonable approximation of capacity for most of the screw piles tested. However, the method was not deemed to be applicable to screw piles installed in glacial till soils, namely the clay till and sand till encountered in the vicinity of Ft. McMurray, Alberta, as the axial capacities of the piles installed in the till were significantly overestimated by up to 374 percent using the LCPC method. Although the scaling coefficients which are defined for use within the LCPC method (Table 2-1) are based on the measured cone tip resistance with depth, it appears that they may not be applied to soil types other than those for which they were explicitly defined, i.e., clay, silt, sand, and chalk. Screw piles installed into surficial glacial till soils therefore lie beyond the current scope of the LCPC method. Further research involving axial load testing of fully-instrumented screw piles installed into glacial till materials is required in order to determine representative coefficients for use within the LCPC method.

Concern was also raised by the 153 percent overestimation of capacity for the 3 m long screw pile, T5, loaded in tension at the Bruderheim test site northeast of Edmonton, Alberta. Screw pile T5 was installed into dessicated, lightly cemented sand which existed near the surface of the Bruderheim site. The pile, when loaded in tension, exhibited a much lower capacity than predicted by the LCPC method, based on the cone penetration profile. It was suggested that disturbance caused by the installation of the screw pile resulted in loosening and destructuring of the material within the circumscribed cylinder. Due to the lightly cemented nature of the sand in its original state, there may have been a significant loss in strength associated with the screw pile installation, which would account for the much lower-than-expected tensile capacity. As only the upper crust of the sand at the Bruderheim site was desiccated and lightly cemented, the screw piles installed to lower depths at the site performed as predicted by the LCPC method. More research is required to determine the effects of installation disturbance in structured or lightly cemented materials; as regards the LCPC design method, the cone penetration tip resistance

profile performed on the in-situ material does not account for subsequent disturbance effects that may be caused by the screw pile installation.

Excepting the results for the screw piles installed into glacial till material, the LCPC method provided capacity predictions for single- and multi-helix screw piles that were, on average, 14 percent above the actual ultimate capacities when using the cylindrical shear model without the correction (equations [2-1], [2-2], and [2-3]) recommended by Narasimha Rao et al. (1993), 13 percent above the actual capacities when employing the cylindrical shear model with the Narasimha Rao et al. (1993) correction, and an average of 23 percent above the actual capacities when using the individual plate bearing model. Nine of the 14 capacity predictions made using the cylindrical shear model were within 30 percent of the actual capacities, regardless of whether the correction by Narasimha Rao et al. (1993) was employed. Seven of the 10 capacity predictions made using the LCPC method in conjunction with the individual plate bearing model were within 30 percent, in fact, within 16 percent, of the actual measured values.

Because the LCPC design method is based on a continuous cone penetration tip resistance profile, it is possible to calculate the theoretical capacity of any size pile installed to any depth at the given test location. The versatility of the LCPC method was exemplified by the incremental capacity calculations that were performed for each of the test piles considered, producing profiles of axial capacity with depth. In order to aid in the calculation process, a basic computer program was created to calculate the axial capacity of a screw pile of given geometry, based on an input file containing cone penetration tip resistance values and corresponding depth measurements for the proposed location.

7.2.2   Empirical Torque Methods for Estimating Ultimate Capacity

7.2.2.1   Direct Torque Correlation, Hoyt and Clemence (1989)

It was undertaken to determine whether the database of 29 screw pile load test results supported a correlation between the torque required to install each of the piles, and the ultimate axial capacities established. Hoyt and Clemence (1989) suggest a direct linear relationship whereby

the ultimate uplift capacity of a screw pile be estimated by multiplying the installation torque by an empirical factor, K_t. By plotting the ultimate axial pile capacities, in both tension and compression, against the final installation torques required for each of the screw piles documented in this report, a direct linear relationship was clearly established for the dataset. Based on linear regression, two best-fit lines were created to relate the installation torques to the ultimate axial capacities, based on the screw pile shaft diameters. For the five screw piles tested that had a shaft diameter of 11.4 cm (4 ½ in), a K_t factor of 16.9 m^{-1} was determined to provide a very good estimate of the ultimate axial capacity (kN), when multiplied by the final installation torque (kN·m). For the remaining 24 screw piles tested, having shaft diameters ranging from 14.0 cm (5 ½ in) to 40.6 cm (16 in), a K_t factor of 9.19 m^{-1} was found to accurately relate the ultimate axial capacity to the measured torque required for installation at the finished depth. The only severe discrepancy which resulted from using the appropriate K_t factor to predict the axial capacities of all 29 of the test piles was involving the 3 m deep tension pile, T5, installed at the Bruderheim test site northeast of Edmonton, Alberta. The capacity of the screw pile when loaded in tension was overestimated by 107 percent using the torque correlation factor, K_t = 9.19 m^{-1}. As previously mentioned, the upper crust of the sand material present at the Bruderheim site was described by Zhang (1999) at the time of the pile load test as being desiccated and lightly cemented in nature. It was therefore suggested that the overestimation of the screw pile's capacity when embedded in the desiccated crust may have been due to the in-situ strength of the sand being substantially compromised by disturbance resulting from the installation of the pile itself, which in turn was bearing up on the disturbed crust when loaded in tension.

Aside from the overestimation of the tensile capacity of pile T5, the suggested torque correlation factors provided very good predictions of the ultimate axial capacities for all of the remaining 28 screw piles, including those installed in glacial till materials. In fact, all of the 28 capacity predictions made fell within about 30 percent of the actual measured capacities in tension and compression. In addition, 21 of the total 29 capacity predictions made using the direct torque relationship fell within 20 percent of the actual measured capacities—this is a difficult mark to hit

in the design of any pile, because there exist many factors affecting the load transfer phenomena between a pile and the soil which are still not fully understood.

In conclusion, there appears to be some promise for the estimation of ultimate axial screw pile capacities using the respective K_t factors of 16.9 m^{-1} for screw piles with shaft diameters equal to 11.4 cm (4 ½ in), and 9.19 m^{-1} for screw piles with shaft diameters between 14.0 cm (5 ½ in) to 40.6 cm (16 in). The disadvantage of using the torque correlation method in isolation is that the capacity of the screw pile may not be designed in advance based on in-situ soil information, but can only be estimated after a pile of a certain geometry has been selected and installed at the site. The torque correlation therefore serves a valuable purpose in the field for checking that the torque achieved at the finished pile depth is within the range that should be expected for achieving the anticipated capacity under axial loading.

7.2.2.2   Non-Dimensional Torque Correlation, Ghaly and Hanna (1991)

Ghaly and Hanna (1991) conducted experimental and theoretical studies on the torque required to install model screw piles into sand, and suggested a non-dimensional relationship for relating the installation torque to the ultimate screw pile capacity in uplift. The installation torque for each model screw pile was normalized by the unit weight of the sand deposit, the surface area of the screw pile blade, the embedment depth, and the pitch of the screw blade, to produce the torque factor, F_t. The ultimate uplift capacity of the screw pile was incorporated into the non-dimensional uplift capacity factor, N_u, by dividing the capacity by the unit weight of the sand, the surface area of the blade, and the embedment depth. Ghaly and Hanna (1991) related the uplift capacity factor, N_u, to the torque factor, F_t, by means of the logarithmic relationship given in equation [2-9].

Ghaly and Hanna's (1991) relationship was applied, as part of the current investigation, to test piles T4, T5, T6, and T9, which were all installed in sand deposits and load-tested to failure in axial tension. The ultimate uplift capacities predicted by the relationship substantially overestimated the measured screw pile capacities, by amounts in the order of 132 to 858 percent. Based on the results obtained considering the four screw piles that were installed in sand and

load-tested in tension under the current project, the correlation developed by Ghaly and Hanna (1991) is not recommended for use in predicting the capacities of full-scale screw piles.

7.3 Modified Cone Penetration Equipment

In order to reduce the associated cost of conducting commercial cone penetration tests at the documented load test sites, as required for use with the LCPC method, an inexpensive, portable apparatus was developed for conducting some of the required cone penetration tests in softer soils, and termed the modified cone penetration equipment. A cone penetrometer was fabricated of steel to the standard dimensions of a commercial 10 cm^2 model, and was fitted with internal load cells for the measurement of tip resistance and sleeve friction with depth. The system for pushing the cone penetrometer into the soil was created from a steel frame assembled on the ground surface, to which two 6.35 cm (2 ½ in) bore, 1.22 m (48 in) stroke hydraulic cylinders were affixed. The cone penetrometer was threaded to 0.91 m (3 ft) segments of 3.49 cm (1 ⅜ in) diameter drill rod and pushed into the subsoil using a steel crossbar affixed to hydraulic cylinders. The frame was weighted at one end by the rear axle of a one-ton pickup truck, and at the other end by approximately 10 kN (2250 lbs) of steel weights. Due to the limited amount of ballast supplied to the system and the modest construction of the steel push frame, the modified cone penetration equipment was only useful for performing cone penetration tests in softer soils. Profiles of tip resistance and sleeve friction were successfully obtained using the modified cone penetration equipment at three of the 10 screw pile load test sites— the University Farm site in Edmonton, Alberta, the Ft. Saskatchewan site in Alberta, and the Ft. St. John Farm site in British Columbia. The upper stratigraphy of all of these sites was described as firm to stiff clay, and the modified cone penetration tests were pushed to depths of 8 m (26 ft), 9 m (29.5 ft), and 7 m (23 ft) at the respective sites.

Commercial CPT results were presented for five of the 10 screw pile load test sites documented, including the University Farm site in Edmonton, Alberta. A comparison was made between the cone penetration profiles obtained at the University Farm site using the modified equipment and those recorded by Zhang (1999) using commercial rig-mounted CPT equipment at the same site.

Based on the significant discrepancy observed between the two data sets, it was eventually determined that the load cells embedded in the modified cone penetrometer were sensitive to temperature fluctuations. As noted by Lunne et al. (1997), the output of load cells at zero load is often shifted due to changes in temperature. The zero load outputs of the load cells contained in the fabricated cone penetrometer were therefore monitored under controlled conditions, while subjecting the cone to incremental changes in ambient temperature. The zero load outputs of the penetrometer cells were found to vary linearly with change in ambient temperature, and this effect was quantified in mV/°C. Once the zero-shift was accounted for and corrected in the modified cone penetration data, very good agreement was achieved between the modified cone penetration results obtained at the University Farm site under the current investigation, and the commercial CPT results recorded by Zhang (1999) at the same location.

7.4 Recommendations for Future Research

Based on the results of this investigation, several related topics may be suggested as areas for future research. First, it is suggested that instrumented screw piles be installed and axially load-tested in Western Canadian glacial till soils, so that representative scaling coefficients may be established for use within the LCPC method for predicting screw pile capacity in tills. Load cells strategically placed along the screw pile shaft would provide an indication of the appropriate components of friction (along the shaft and along the cylindrical failure surface between helices, if applicable), and bearing (above or below each of the applicable helices) mobilized at the screw pile's ultimate load. These separated components of friction and bearing could then be used to back-calculate appropriate scaling factors (coefficients) to be applied to the CPT tip resistance profile in conjunction with the LCPC method. These coefficients may also depend on the level of tip resistance measured in the glacial till (that is, on the relative stiffness of the soil). Second, it is suggested that further tension tests be carried out on screw piles installed into highly dessicated materials, in order to quantify the effects of the installation disturbance on the ultimate axial pile capacity. The outcome of the load test performed on pile T5, installed in lightly cemented sand, suggests that the disturbance to the native material during the pile installation may severely reduce the expected tensile capacity for screw piles installed into structured soils. Finally, the

topic of calculating the lateral capacity of screw piles, including quantifying the effects of the pile geometry and the type of soil into which it is installed, was not touched upon in this thesis project, and with particular focus on Western Canadian soils would provide an excellent complementary study to this thesis work.

7.5 References

ASTM Designation: D1143 1981. Standard test method for piles under static axial compressive load. American Society for Testing and Materials.

ASTM Designation: D3689 1990. Standard test method for individual piles under static axial tensile load. American Society for Testing and Materials.

Bustamante, M., and Gianeselli, L. 1982. Pile bearing capacity prediction by means of static penetrometer CPT. In Proceedings of the 2nd European Symposium on Penetration Testing, ESOPT-II. Amsterdam. Balkema Publisher, Rotterdam, Vol.2, pp. 493-500.

Ghaly, A., and Hanna, A. 1991. Experimental and theoretical studies on installation torque of screw anchors. Canadian Geotechnical Journal, 28(3): 353-364.

Hoyt, R.M., and Clemence, S.P. 1989. Uplift capacity of helical anchors in soil. In Proceedings of the 12th International Conference on Soil Mechanics and Foundation Engineering. Rio de Janeiro, Brazil, Vol.2, pp. 1019-1022.

Lunne, T., Robertson, P.K., and Powell, J.J.M. 1997. Cone penetration testing in geotechnical practice. Blackie Academic & Professional.

Narasimha Rao, S., Prasad, Y.V.S.N., and Veeresh, C. 1993. Behaviour of embedded model screw anchors in soft clays. Geotechnique, 43: 605-614.

Zhang, D. 1999. Predicting capacity of helical screw piles in Alberta soils. M.Sc. thesis, Department of Civil and Environmental Engineering, University of Alberta, Edmonton, Alberta.

Appendix A: Compilation of Electronic Data

A.1 Introduction to Electronic Appendix

All of the data used in assembling this thesis report is included for the reader's reference in electronic format on the accompanying CD, entitled Appendix A. An electronic version of the thesis report is also included on the CD.

Appendix B: Temperature Calibration of Cone Penetrometers

B.1 Temperature Sensitivity of Load Cells

B.1.1 Cone No. 1: Used at University Farm Site

$$y = 0.0328x + 2.2428$$
$$R^2 = 0.9953$$

$$y = 0.0037x + 9.2105$$
$$R^2 = 0.7574$$
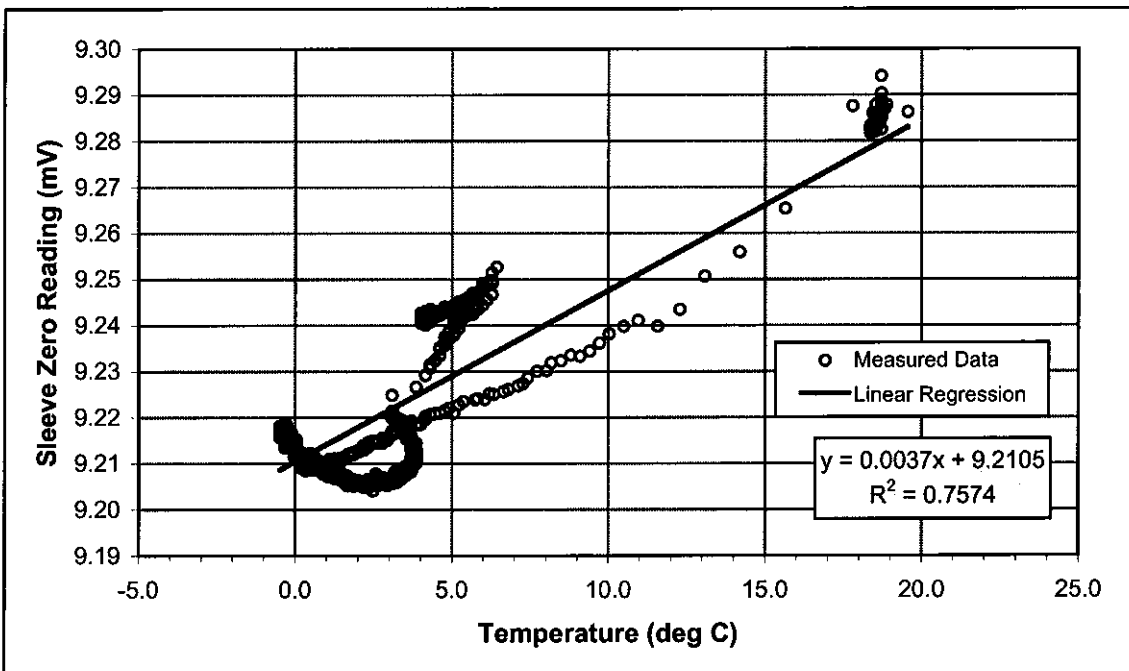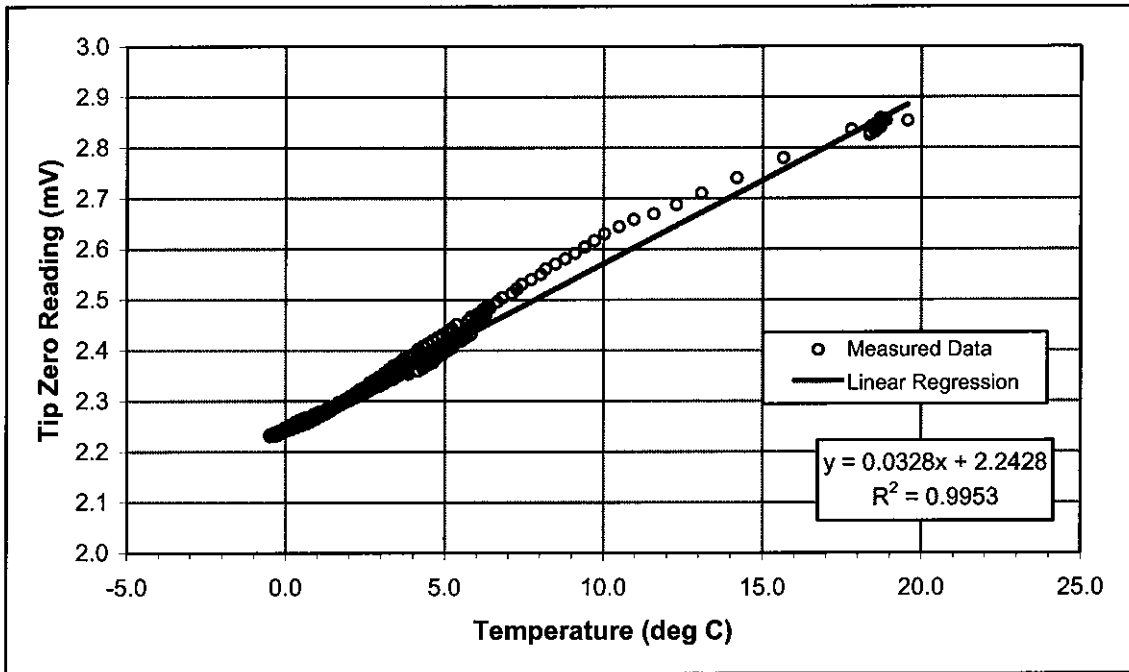
B.1.2   Cone No. 2: Used at Ft. St. John Farm Site
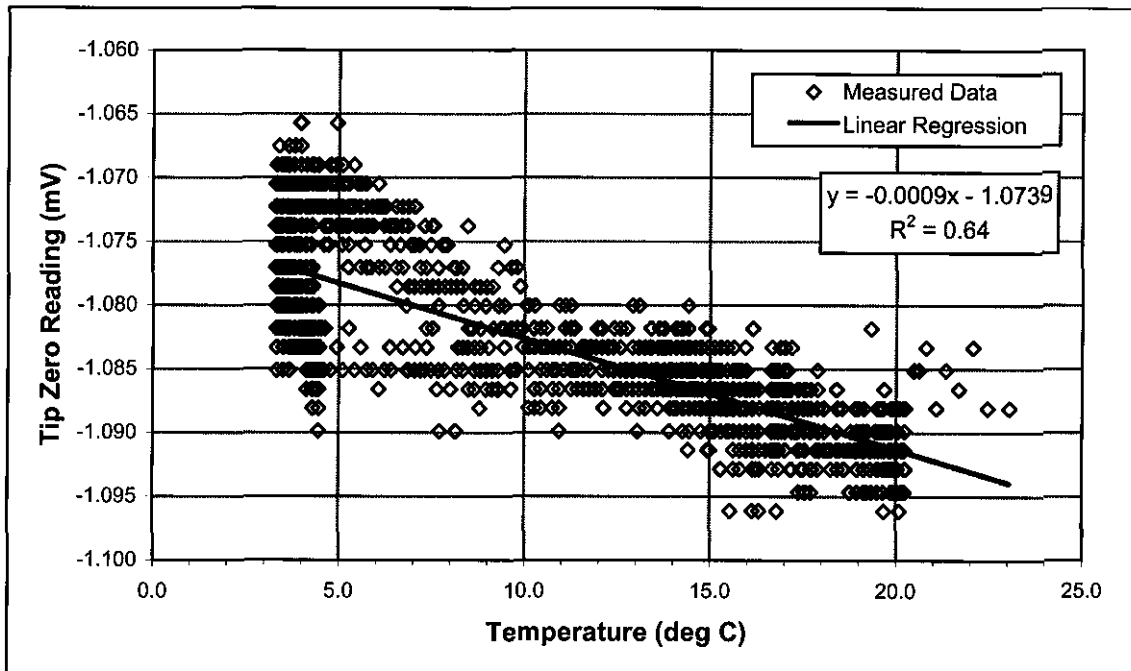
Note: There is no temperature sensitivity data available for the sleeve load cell on Cone No. 2, due to technical problems during the temperature sensitivity calibration and subsequent critical damage sustained by the cone during field testing.

B.1.3 Cone No. 3: Used at Ft. Saskatchewan Site
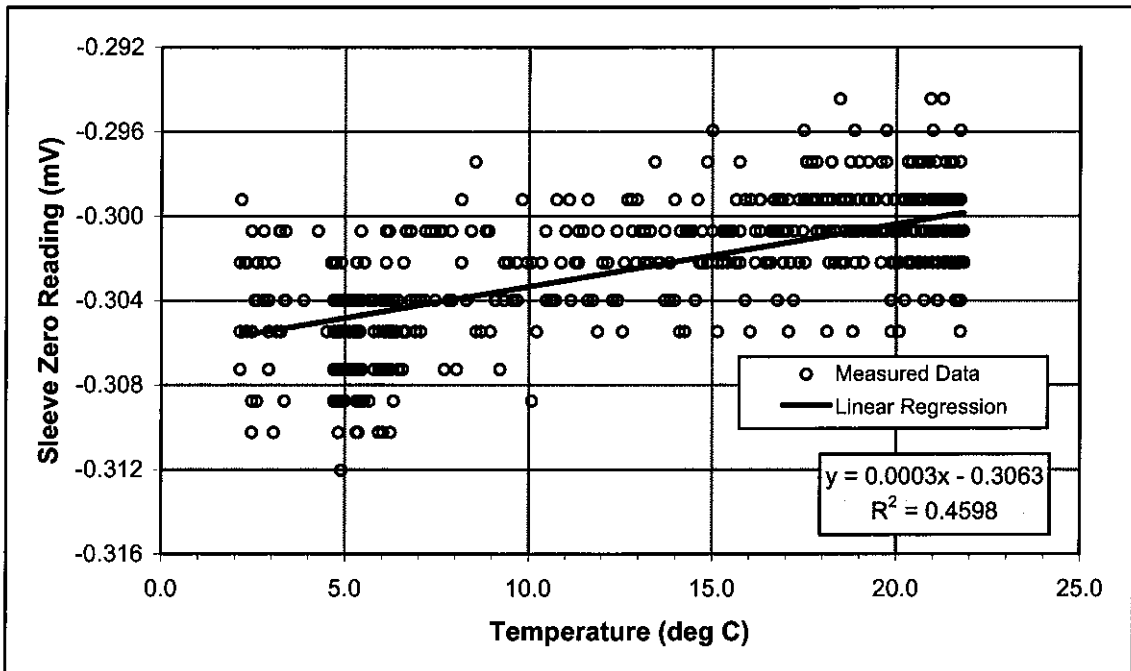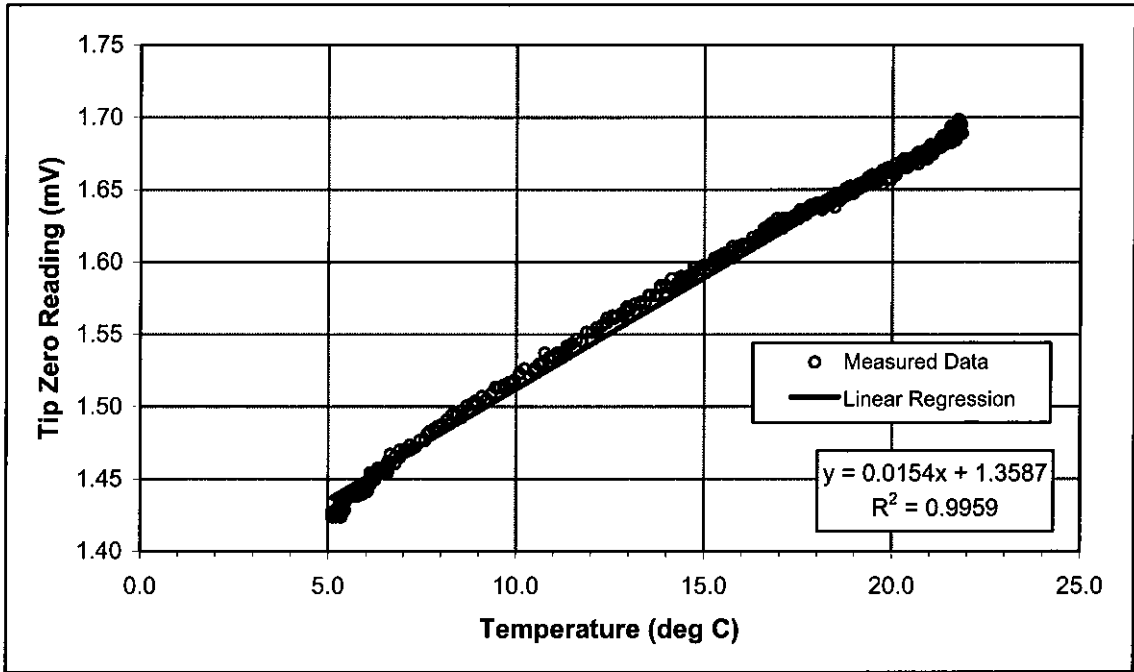
Appendix C: Borehole Logs

C.1 Edmonton Vicinity, Alberta:

C.1.1 Ft. Saskatchewan (First Borehole)

PROJECT:	Year 2001 Pile Load Test Program		
LOCATION:	Fort Saskatchewan, Alberta		TEST BORING
DATE:	July 26, 2001	TECH: MH	01-1

DRILL TYPE: B-58 Solid Stem Auger

SOIL PROFILE & DESCRIPTION

DATUM: --

SURFACE ELEVATION: --

FILL-TOPSOIL, silty, damp, stiff to very stiff, black

CLAY, silty, high plasticity, damp, stiff to very stiff, occasional slickensides surfaces, dark brown

-- very silty, firm consistency, medium plasticity, moist, uniform

-- soft to firm, dark brown

-- silty, medium plasticity, moist, brown

-- very stiff, medium plasticity, no evidence of groundwater seepage

-- no evidence of groundwater seepage

End of borehole at 10.5 m
Slough = 10.4 m, 0 hrs
Water = 10.4 m (dry), 0 hrs
Borehole covered with plywood

TEST RESULTS

PP = 210 kPa
PP = 170 kPa
PP = 160 kPa
PP = 270 kPa
PP = 220 kPa
PP = 230 kPa
PP = 210 kPa
PP = 90 kPa
PP = 100 kPa
PP = 170 kPa
PP = 180 kPa
PP = 160 kPa
PP = 170 kPa
PP = 180 kPa
PP = 190 kPa

MOISTURE CONDITIONS ATTERBERG LIMITS
MOISTURE CONTENT %
10 20 30 40 50 60

MOISTURE CONTENT ○
LIQUID LIMIT □
PLASTIC LIMIT △

Qu UNCONFINED COMPRESSION
γd DRY UNIT WEIGHT

SO₄ SULPHATE CONTENT
WATER TABLE
N PENETRATION RESISTANCE

STANDARD PENETRATION SAMPLE
UNDISTURBED SAMPLE (SHELBY)
BAG SAMPLE

PLATE No. 3

150

C.1.2 Ft. Saskatchewan (Second Borehole)

	PROJECT: Year 2001 Pile Load Test Program		
	LOCATION: Fort Saskatchewan, Alberta		TEST BORING
	DATE: July 26, 2001	TECH: MH	01-2

MOISTURE CONDITIONS ATTERBERG LIMITS

MOISTURE CONTENT %
10 20 30 40 50 60

DRILL TYPE B-56 Solid Stem Auger

SOIL PROFILE & DESCRIPTION

TEST RESULTS

DATUM: --

SURFACE ELEVATION: --

Depth in Feet / Depth (m)	Description	Tests
	FILL-TOPSOIL, some clay, damp, stiff, black	PP = 190 kPa
1		PP = 180 kPa
	CLAY, silty, high plasticity, damp, frequent slickensided surfaces, stiff to very stiff, brown	PP = 210 kPa
2	-- occasional CaCO₃ mottling from 1.6 to 1.9 m	PP = 210 kPa
3		PP = 230 kPa
4		PP = 170 kPa
5	-- medium plasticity, stiff to very stiff	PP = 210 kPa
		PP = 230 kPa
6		PP = 190 kPa
7		PP = 160 kPa
8	-- stiff consistency, medium plasticity	PP = 170 kPa
	-- siltier with depth, medium plasticity, moist	PP = 230 kPa
	-- no evidence of groundwater seepage	
9		PP = 240 kPa
	End of borehole at 9.0 m	
	Slough = 8.9 m, 0 hrs	
	Water = 8.9 m (dry), 0 hrs	
10	Borehole covered with plywood	

MOISTURE CONTENT ⊙	Qu UNCONFINED COMPRESSION	SO₄ SULPHATE CONTENT	⊠ STANDARD PENETRATION SAMPLE
LIQUID LIMIT ☐	Yd DRY UNIT WEIGHT	⊽ WATER TABLE	⊠ UNDISTURBED SAMPLE (SHELBY)
PLASTIC LIMIT △		N PENETRATION RESISTANCE	⊠ BAG SAMPLE

PLATE No. 4

151

C.1.3 Lamont (First Borehole)

C.1.4 Lamont (Second Borehole)

The borehole log shows the following layout with project information, moisture conditions/Atterberg limits chart, soil profile, and test results.

PROJECT: Proposed Industrial Site

LOCATION: Lot D, Plan 6121744, Hwy 637 & Hwy 15, Lamont, AB

DATE: April 15, 2008   TECH: MH

TEST BORING 06-1

DRILL TYPE: B-56 Solid Stem Auger

MOISTURE CONDITIONS ATTERBERG LIMITS	SOIL PROFILE & DESCRIPTION	TEST RESULTS

DATUM:

SURFACE ELEVATION:

Soil Profile & Description:

TOPSOIL, silty, trace of sand, compressible, black, 33 cm thick

CLAY TILL, silty, damp, medium plasticity, hard consistency, frequent calcium carbonate mottling from 0.6 to 1.5 m, light brown

— very hard consistency, dry, sandy

BEDROCK (Clay Shale), silty, highly weathered bedrock, hard consistency soil, medium plasticity, moist, bluish-grey

— dark brown, silty

— very hard soil

— occasional sandstone lenses

— occasional siltstone lenses

— no evidence of groundwater seepage

End of Borehole = 9.0 m
Slough = 8.8 m, 0 hours
Water level = 8.8 m (dry), 0 hours
Water level = 7.6 m (dry), 29 days later

Test Results (Miscellaneous Tests):

PP = 410 kPa

PP = 510 kPa
SO$_4$ = 0.03 %

PP = 560 kPa

PP = 510 kPa
SO$_4$ = 0.01 %

PP = 310 kPa

PP = 500 kPa

PP = 300 kPa

PP = 420 kPa

PP = 560 kPa

PP = 460 kPa
29 days later (Dry)

PP = 300 kPa

PP = 600 kPa

Legend:

⊙ MOISTURE CONTENT   Q$_u$ UNCONFINED COMPRESSION   SO$_4$ SULPHATE CONTENT   ⊠ STANDARD PENETRATION SAMPLE

▣ LIQUID LIMIT   Ɣ DRY UNIT WEIGHT   ∑ WATER TABLE   ⊠ UNDISTURBED SAMPLE (SHELBY)

△ PLASTIC LIMIT   N PENETRATION RESISTANCE   ⊠ BAG SAMPLE

PLATE No. 3

153

C.2 Ft. McMurray Vicinity, Alberta:

C.2.1 Ruth Lake Substation (First Borehole)

RUTH LAKE – MACKAY TRANSMISSION PROJECT				
RUTH LAKE SUBSTATION				
TRUCK–MOUNTED, SOLID STEM AUGER	PILE LOAD TEST SITE		ELEVATION:	
SAMPLE TYPE ■ Shelby Tube	▨ No Recovery	⊠ SPT Test (N)	▤ Grab Sample	⊞ Spit–Pen ▯ Core
BACKFILL TYPE ■ BENTONITE	▨ PEA GRAVEL	▥ SLOUGH	▨ GROUT	▨ DRILL CUTTINGS ▦ SAND

Depth(m)	SPT BLOW COUNTS / PLASTIC M.C. LIQUID	SOIL SYMBOL	SOIL DESCRIPTION	SAMPLE TYPE	SAMPLE NO	SPT(N)	INSTRUMENTATION DATA	OTHER TESTS COMMENTS	Depth(m)
0.0			TOPSOIL, silty, sandy, black, fine roots						0.0
			SAND, fine grained, poorly graded, loose to compact, light brown, moist		G1			pp = 20 kPa	
1.0			CLAY, sandy, silty, firm, low plastic, brown		D1	22		pp = 20 kPa	1.0
			SAND, fine to medium grained, silty, clayey, poorly graded, brown, moist		G2			pp = 50 kPa	
2.0			CLAY, silty, sandy, low plastic, very stiff, dark brown, random sand lenses						2.0
			CLAY TILL, silty, sandy, very stiff to hard, low plastic, dark brown, random sand		D2	36		pp > 450 kPa	
3.0			lenses, scattered gravel sizes		G3			pp = 100 kPa	3.0
			... FREEWATER at 2.6 m						
			... distinct bitumen odour at 2.7 m						
4.0			... sand layers below 3.9 m		D3	18		pp > 450 kPa	4.0
			... large cobble or boulder obstructing auger at 4.5 m; borehole re–drilled		G4			pp = 200 kPa	
5.0			... very sandy below 5.2 m						5.0
					D4	28		Note: SPT sampler bouncing on cobble at 5.5 m	
6.0					G5			pp = 200 kPa	6.0
7.0			SAND, silty, fine to medium grained, compact, grey, clay till inclusions, wet		D5	53		pp = 200 kPa	7.0
			CLEARWATER CLAY, sandy, silty, very stiff to hard, medium to high plastic, greyish–brown		G6			pp = 250 kPa	
8.0									8.0
9.0									9.0
10.0									10.0
			End of Borehole at 10.2 m						
			Borehole Sloughed–in to 3.0 m						
11.0			Water Level at 2.4 m upon Completion						11.0
			Borehole Backfilled with Drill Cuttings						
12.0									12.0

COMPLETION DEPTH: 10.2 m
COMPLETE: 06/11/01
Page 1 of 1

C.2.2 Ruth Lake (Second Borehole)

	RUTH LAKE – MACKAY TRANSMISSION PROJECT		
	RUTH LAKE SUBSTATION		
TRUCK–MOUNTED, SOLID STEM AUGER	PILE LOAD TEST SITE		ELEVATION:

SAMPLE TYPE	■ Shelby Tube	▨ No Recovery	⊠ SPT Test (N)	▤ Grab Sample	▥ Split–Pen	▉ Core
BACKFILL TYPE	■ BENTONITE	⊡ PEA GRAVEL	▥ SLOUGH	GROUT	▨ DRILL CUTTINGS	SAND

Depth(m)	SPT BLOW COUNTS / PLASTIC M.C. LIQUID	SOIL SYMBOL	SOIL DESCRIPTION	SAMPLE TYPE	SAMPLE NO	SPT(N)	OTHER TESTS COMMENTS	Depth(m)
0.0			SAND, fine grained, clayey, silty, loose to compact, light brown, random clay lumps, scattered gravel sizes		G1		pp = 50 kPa	0.0
1.0					D1	16	pp = 20 kPa	1.0
					G2		pp = 30 kPa	
2.0			CLAY TILL, silty, sandy, low plastic, very stiff, dark brown, random sand lenses, scattered gravel sizes		D2	25	pp = 350 kPa	2.0
3.0			... FREEWATER at 2.7 m ... distinct bitumen odour at 3.1 m ... sand layers below 3.4 m		G3		pp = 300 kPa	3.0
4.0					D3	28	pp = 350 kPa	4.0
					G4		pp = 300 kPa	
5.0					D4	23	pp > 450 kPa	5.0
6.0			... very silty, fine sandy, below 6.1 m		G5		pp = 300 kPa	6.0
7.0			OILSAND (RAFTED), lean to medium rich, fine grained, dense, clay till inclusions, fine gravel sizes, moist to wet		D5	26	pp = 50 kPa	7.0
8.0			CLEARWATER CLAY, silty, very stiff to hard, medium to high plastic, grey, thin light grey sand partings, trace glauconitic sand pockets		G6		pp = 300 kPa	8.0
9.0					D6	32	pp = 350 kPa	9.0
					G7			
10.0			End of Borehole at 9.3 m Borehole Sloughed–in to 9.1 m Water Level at 2.7 m upon Completion Water Level at 1.1 m after 17 days 25 mm PVC Standpipe Installed to 6.1 m					10.0
11.0								11.0
12.0								12.0

COMPLETION DEPTH: 10.2 m
COMPLETE: 06/11/01
Page 1 of 1

C.2.3 Dover Substation (One Borehole)

DOVER TO WHITEFISH TRANSMISSION LINE		
DOVER SUBSTATION		
DRILL/METHOD: SOLID STEM AUGER	NE 1/4 31-92-12 W4M	ELEVATION:

SAMPLE TYPE	■ Shelby Tube	▨ No Recovery	⊠ SPT Test (N)	▤ Grab Sample	▥ Split-Pen	▦ Core
BACKFILL TYPE	■ Bentonite	Pea Gravel	▥ Slough	Grout	▨ Drill Cuttings	Sand

Depth (m)	STANDARD PEN (N) 20 40 60 80 / PLASTIC M.C. LIQUID 20 40 60 80	SOIL SYMBOL	SOIL DESCRIPTION	SAMPLE TYPE	SAMPLE NO	SPT (N)	OTHER TESTS COMMENTS	Depth (m)
0			SAND, medium grained, brown, dry				Note: Borehole was drilled and logged by Sun-Alta Drilling	
1							Borehole log was prepared by AMEC from data provided by Sun-Alta Drilling	1
			CLAY TILL, brown, very stiff to hard, dry					
2	■			⊠	D1	30		2
	■		SAND (possible sand till), medium grained, very dense, brown, dry	⊠	D2	49		
3	■			⊠	D3	50/75		3
4								4
5	■			⊠	D5	69/150		5
6	■			⊠	D6	75		6
			End of Borehole at 6.4 m Dry on Completion No Sloughing Observed Drill Cuttings Backfilled					
7								7
8								8
9								9
10								

COMPLETION DEPTH: 6.40 m
COMPLETION DATE: 11/1/04
Page 1 of 1

156

C.3   Hythe, Alberta:

C.3.1   Hythe Warehouse Site (First Borehole)

	Project: Proposed Shop Facility	TEST HOLE NO: 05-1
	Location: Lots C&D, Blk 12, Plan 1398KS	
Method: 150mm diameter solid stem auger	Lot 1, Blk. 1, Plan 032 4625	ELEVATION:
SAMPLE TYPE ■ DISTURBED ⊘ SPT ⊠ SHELBY TUBE ▦ BULK SAMPLE ▥ A-CASING ▥ CORE

DEPTH (m)	PLASTIC M.C. LIQUID 20 40 60 80	USC	SOIL SYMBOL	SOIL DESCRIPTION	SAMPLE TYPE	SPT(N)	TEST RESULTS	INSTRUMENTATION DATA	ELEVATION(m)
0.0		GW		GRAVEL; 75mm crush 175mm					0.0
		FI		CLAY FILL; some organics intermixed, brown stiff, compact, medium plastic					
1.0				0.6m					-1.0
		CI		SILTY CLAY (rafted clay till); greenish brown, slight sandy texture, odd pebble, few stones and weathered coal, firm	⊘	11	[SO4] = low to moderate		
2.0				– seepage developing at 2.1m BGS					-2.0
▽				2.1m					▽
		CI		CLAY TILL; brown, moist, stiff, occ. pebble to gravel size stone, weathered coal fragments					
3.0					⊘	19			-3.0
				3.6m					
4.0				CLAY SHALE; brown, bentonitic to 4.0m, stiff to very stiff					-4.0
		SH		– sandstone ledges embedded below 4.6m					
5.0				– seepage ingressing at 4.9m	⊘	33			-5.0
6.0				6.0m	⊘	50/75			-6.0
		SS		SANDSTONE; brown, fine moderately cemented					
				– becoming hard, auger refusal @ 6.8m					
7.0				TESTHOLE TERMINATED @ 6.8m Seepage ingressing at 2.0m Depth to W.L. = 2.4m after drilling Hole Backfilled at completion.					-7.0
8.0									-8.0
9.0									-9.0
10.0									-10.0
11.0									-11.0

| COMPLETION DEPTH: 6.8 m |
| COMPLETE: 05/25/05 |
| Page 1 of 1 |

157

C.3.2 Hythe Warehouse Site (Second Borehole)

Project: Proposed Shop Facility	TEST HOLE NO: 05-2
Location: Lots C&D, Blk 12, Plan 1396KS	
Method: 150mm diameter solid stem auger	Lot 1, Blk. 1, Plan 032 4625	ELEVATION:

SAMPLE TYPE	▓ DISTURBED	☑ SPT	☒ SHELBY TUBE	▤ BULK SAMPLE	⫼ A-CASING	⫿ CORE

DEPTH (m)	PLASTIC M.C. LIQUID 20 40 60 80	USC	SOIL SYMBOL	SOIL DESCRIPTION	SAMPLE TYPE	SPT(N)	TEST RESULTS	INSTRUMENTATION DATA	ELEVATION(m)
0.0		TS		TOPSOIL 270mm					0.0
		CH		CLAY; brown, moist, stiff 0.75m			[SO4] = moderate		
1.0		CI		SILTY CLAY (rafted clay till); brown moist, slight sandy texture, odd pebble, few stones and weathered coal, firm	/	15			-1.0
2.0		CH		- clay (CH) seam @ 1.8m to 2.1m					-2.0
3.0 ▽		CI		- seepage developing at 3.0m BGS	/	14			-3.0 ▽
				3.6m					
4.0		CI		CLAY TILL; brown, moist, stiff, occ. pebble to gravel size stone, weathered coal fragments 4.3m					-4.0
		SS		SANDSTONE; brown, wet, dense, weathered 4.6m	/	45			
5.0		SH		CLAY SHALE; brown, weathered, moist, stiff to very stiff 5.5m					-5.0
6.0		SP		SAND; brown, dense, water bearing, hard sandstone legde @ 5.3m to 5.6m, poor auger recovery - hard ledge at 6.1m	/	50/100			-6.0
				TESTHOLE TERMINATED @ 6.2m Seepage ingressing at 3.0m, immediate sloughing below 5.5m					
7.0				Depth to W.L. = 3.0m after drilling Hole Backfilled at completion. sloughing below 5.3m					-7.0
8.0									-8.0
9.0									-9.0
10.0									-10.0
11.0									-11.0

COMPLETION DEPTH: 6.2 m
COMPLETE: 05/25/05
Page 1 of 1

C.3.3   Hythe Warehouse Site (Third Borehole)

Project: Proposed Shop Facility			TEST HOLE NO: 05-3	
Location: Lots C&D, Blk 12, Plan 1396KS				
Method: 150mm diameter solid stem auger	Lot 1, Blk. 1, Plan 032 4625		ELEVATION:	

SAMPLE TYPE ▓ DISTURBED   ▨ SPT   ⊠ SHELBY TUBE   ⊟ BULK SAMPLE   ▥ A-CASING   ▥ CORE

DEPTH (m)	PLASTIC / M.C. / LIQUID (20 40 60 80)	USC	SOIL SYMBOL	SOIL DESCRIPTION	SAMPLE TYPE	SPT (N)	TEST RESULTS	INSTRUMENTATION DATA	ELEVATION (m)
0.0		CH		CLAY; brown, moist, stiff					0.0
1.0		CI		0.9m — SILTY CLAY (rafted clay till); brown moist, slight sandy texture, odd pebble, few stones and weathered coal, firm			[SO4] = moderate		-1.0
2.0		CH		— clay (CH) seam @ 1.8m to 2.3m — sandy and soft on auger below 2.3m		12			-2.0
		CI		— seepage developing at 2.6m BGS					
3.0				3.0m		18			-3.0
		CI		CLAY TILL; brown, moist, stiff, occ. pebble to gravel size stone, weathered coal fragments					
4.0									-4.0
		SP		4.3m — SAND; brown, dense, fine, immediate sloughing and rapid ingress of water, refusal drilling @ 5.2m		49			
5.0				TESTHOLE TERMINATED @ 5.2m					-5.0
				Seepage ingressing at 3.0m, immediate sloughing below 4.5m					
6.0				Depth to W.L. = 2.6m after drilling Hole Backfilled at completion.					-6.0
7.0									-7.0
8.0									-8.0
9.0									-9.0
10.0									-10.0
11.0									-11.0

COMPLETION DEPTH: 5.2 m
COMPLETE: 05/25/05
Page 1 of 1

159

C.4 Saskatoon, Saskatchewan:

C.4.1 Saskatoon Condominium Site (One Borehole Over Two Pages)

PAGE 1 OF 2

TEST HOLE 05-2

DEPTH (m)

N U γ_w Pw Lw w ELEV: 99.6 m

pp

FILL, sand, silty, trace clay, compact, poorly graded, fine grained, damp, mottled brown/black.

SAND, silty, compact, poorly graded, fine grained, moist, mottled brown/black.
—seepage, sloughing at 2.1 m.

8.1
8.8
18.1
22.4
31.4
30.2
29.7
30.5
29.6

—grey below 7.9 m.

—clay layer 11.5 to 11.6 m.

CONTINUED ON NEXT PAGE

LEGEND:

GRAVEL   SAND   GLACIAL TILL

TOPSOIL   SAND   CLAY   FILL

pp...POCKET PENETROMETER (kg/cm²)

w...WATER CONTENT (PERCENT OF DRY SOIL WEIGHT)

Lw...LIQUID LIMIT

Pw...PLASTIC LIMIT

γ_w...WET UNIT WEIGHT (kN/m³)

U...UNCONFINED COMPRESSIVE STRENGTH (kPa)

N...STANDARD PENETRATION TEST (ROPE–CATHEAD & DONUT HAMMER)

SO₄...SULPHATE CONTENT (PERCENT OF DRY SOIL)

I.A.D....IMMEDIATELY AFTER DRILLING

▽...RECORDED WATER LEVEL TEST HOLE (I.A.D.)

▼...RECORDED WATER LEVEL (PIEZO)

SHELBY TUBE   SPLIT SPOON   CUTTINGS

LIMITATIONS: THE FIELD DRILL LOG IS A SUMMARY OF THE SUBSURFACE CONDITIONS ENCOUNTERED AT THE SPECIFIC TEST HOLE LOCATION AT THE TIME OF TEST DRILLING. SUBSURFACE CONDITIONS MAY VARY AT OTHER LOCATIONS OF THIS SITE AND, IN TIME, MAY CHANGE AT THIS SPECIFIC TEST HOLE LOCATION.

FIELD DRILL LOG AND SOIL TEST RESULTS

PROJECT: PROPOSED WILLOWS MULTI-FAMILY HOUSING

LOCATION: 401 CARTWRIGHT ST, SASKATOON, SK

DATE DRILLED: APR 20/05

160

C.4.2 Saskatoon Condominium Site (Borehole Continued)

TEST HOLE 05-2

DEPTH
(m)

N U γ_w Pw Lw w

pp

SAND, silty, compact, poorly graded, fine grained, wet, grey, sloughing.

CLAY, trace silt, stiff, medium to highly plastic, moist, grey.

26.9

NOTE:
1. Test Hole sloughed to 2.3 m I.A.D.

LEGEND:

GRAVEL   GLACIAL TILL

TOPSOIL   SAND   CLAY   FILL

pp...POCKET PENETROMETER (kg/cm²)

w.....WATER CONTENT (PERCENT OF DRY SOIL WEIGHT)

Lw...LIQUID LIMIT

Pw...PLASTIC LIMIT

γ_w...WET UNIT WEIGHT (kN/m³)

U.....UNCONFINED COMPRESSIVE STRENGTH (kPa)

N.....STANDARD PENETRATION TEST (ROPE-CATHEAD & DONUT HAMMER)

SO₄...SULPHATE CONTENT (PERCENT OF DRY SOIL)

I.A.D....IMMEDIATELY AFTER DRILLING

▽...RECORDED WATER LEVEL TEST HOLE (I.A.D.)

▼.....RECORDED WATER LEVEL (PIEZO)

SHELBY TUBE   SPLIT SPOON   CUTTINGS

LIMITATIONS: THE FIELD DRILL LOG IS A SUMMARY OF THE SUBSURFACE CONDITIONS ENCOUNTERED AT THE SPECIFIC TEST HOLE LOCATION AT THE TIME OF TEST DRILLING. SUBSURFACE CONDITIONS MAY VARY AT OTHER LOCATIONS OF THIS SITE AND, IN TIME, MAY CHANGE AT THIS SPECIFIC TEST HOLE LOCATION.

FIELD DRILL LOG AND SOIL TEST RESULTS

PROJECT: PROPOSED WILLOWS MULTI-FAMILY HOUSING

LOCATION: 401 CARTWRIGHT ST, SASKATOON, SK

DATE DRILLED: APR 20/05

161

Appendix D: Ultimate Pile Capacity Determinations

D.1   Ft. Saskatchewan Site, Alberta

D.1.1   Screw Pile C7

D.1.1.1   Brinch-Hansen Failure Criterion
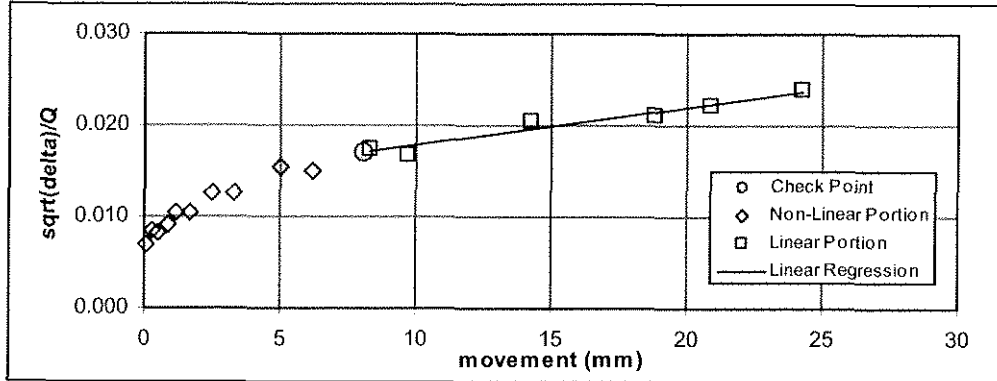
Brinch-Hansen Method:								
slope	0.000419275							
y-Intercept	0.013588369							
r²	0.952199868							
Q_u	209 kN							
Δ_u	32 mm							
Check that this point lies on or near plotted test data:								
$Q' = 0.80\ Q_u$	168							
$\Delta' = 0.25\ \Delta_u$	8							
$\sqrt{\Delta'/Q'}$	0.016985461							
Is it okay ? (Y/N)	Y							

D.1.1.2   Mazurkiewicz Method

163
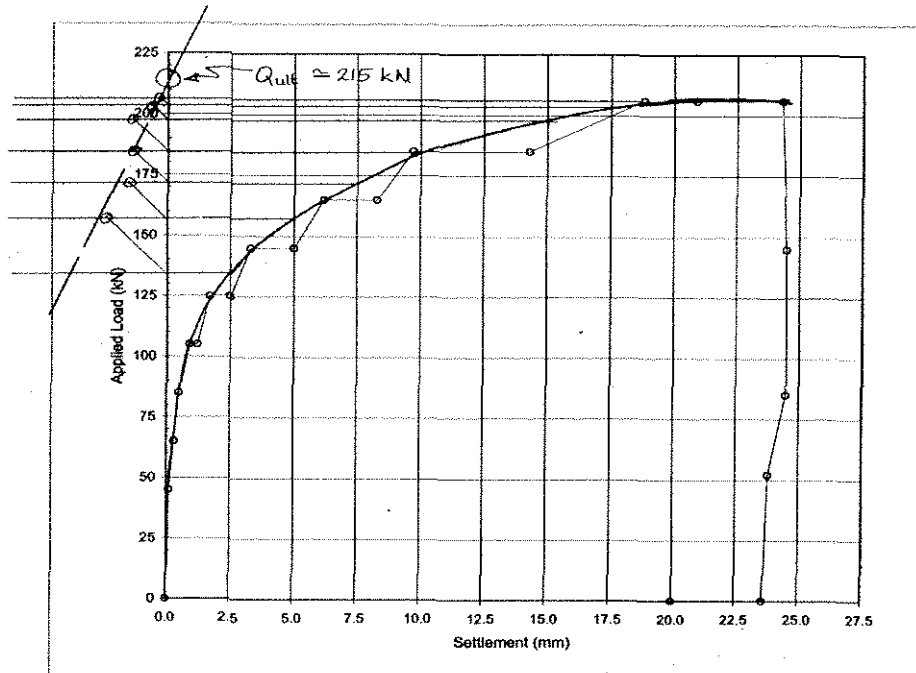
D.1.2   Screw Pile C8

D.1.2.1   Brinch-Hansen Failure Criterion
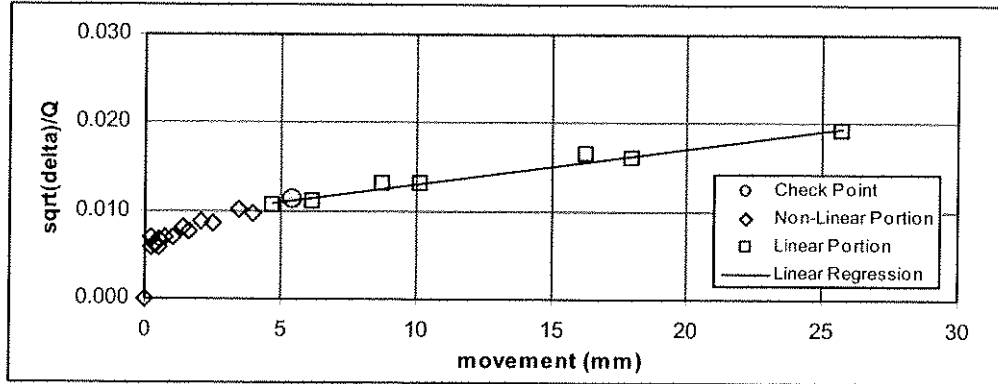
Brinch-Hansen Method:	
slope	0.000409079
y-intercept	0.008955135
r²	0.972619289
Q_u	261 kN
Δ_u	22 mm

Check that this point lies on or near plotted test data:

Check		
Q' = 0.80 Q_u	209	
Δ' = 0.25 Δ_u	5	
√Δ'/Q'	0.011193918	
Is it okay ? (Y/N)	Y	

D.1.2.2   Mazurkiewicz Method
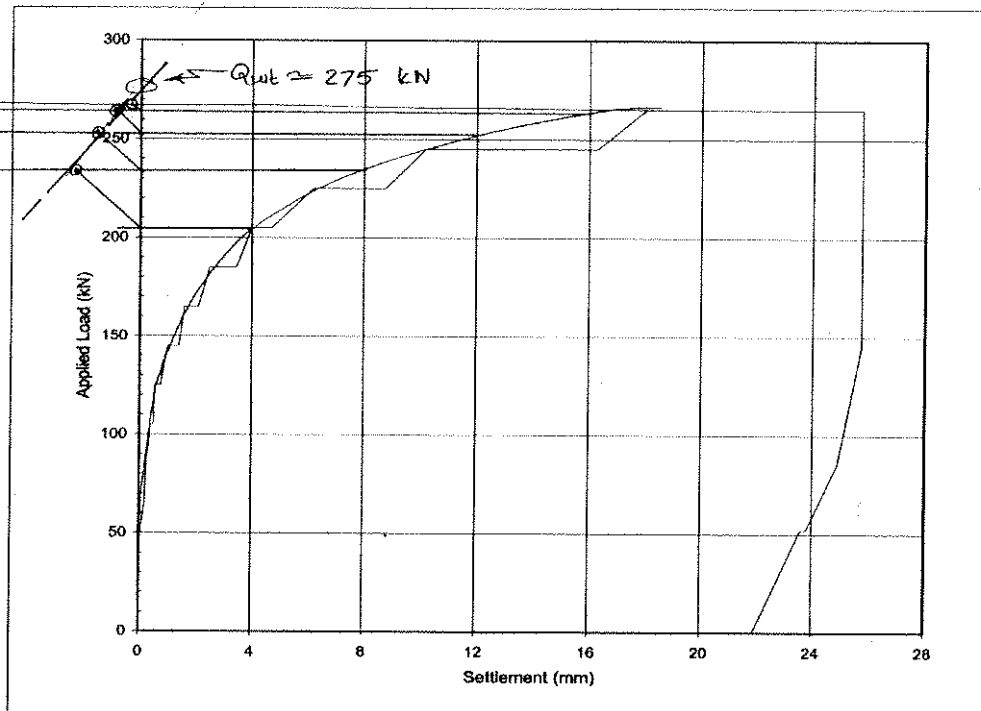
D.1.3 Screw Pile C9

D.1.3.1 Brinch-Hansen Failure Criterion
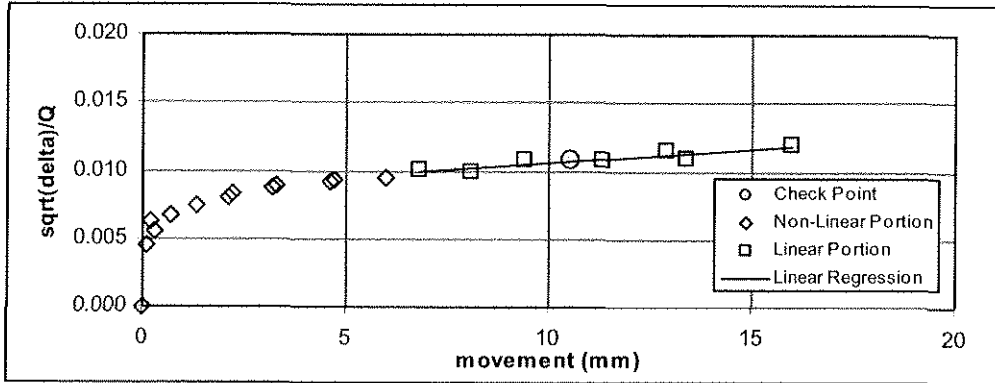
Brinch-Hansen Method:	
slope	0.000203408
y-intercept	0.008588571
r²	0.867033184
Q_u	378 kN
Δ_u	42 mm

Check that this point lies on or near plotted test data:

$Q' = 0.80\ Q_u$	303
$\Delta' = 0.25\ \Delta_u$	11
$\sqrt{\Delta'}/Q'$	0.010735713
Is it okay ? (Y/N)	Y

D.1.3.2 Mazurkiewicz Method
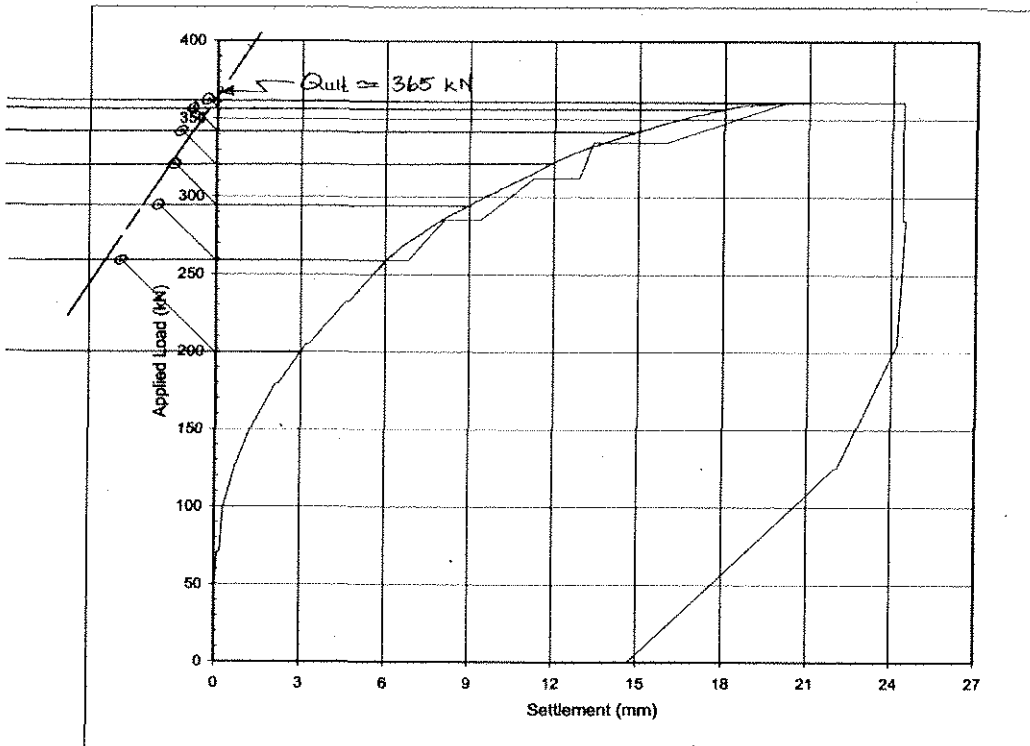
D.2   Lamont Site, Alberta

D.2.1   Screw Pile C10

D.2.1.1   Brinch-Hansen Failure Criterion
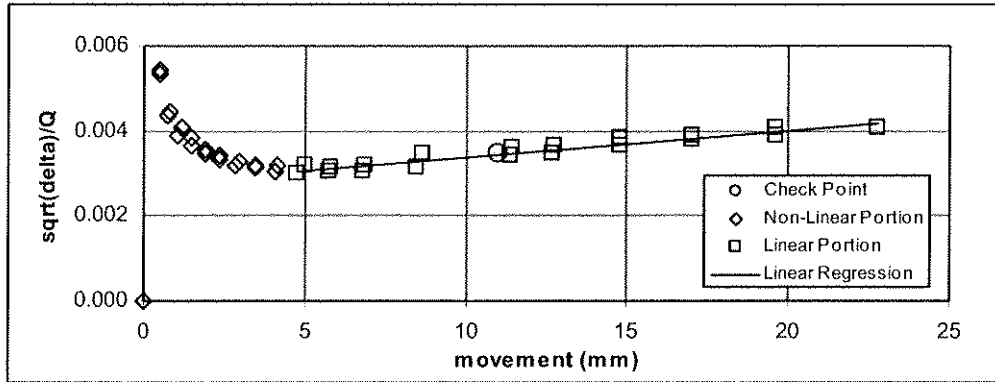
Brinch-Hansen Method:	
slope	0.000062702
y-intercept	0.002756773
r^2	0.921158676
Q_u	1203 kN
Δ_u	44 mm
Check that this point lies on or near plotted test data:	
$Q' = 0.80\ Q_u$	962
$\Delta' = 0.25\ \Delta_u$	11
$\sqrt{\Delta'/Q'}$	0.003445967
Is it okay ? (Y/N)	Y

D.2.1.2   Mazurkiewicz Method

166
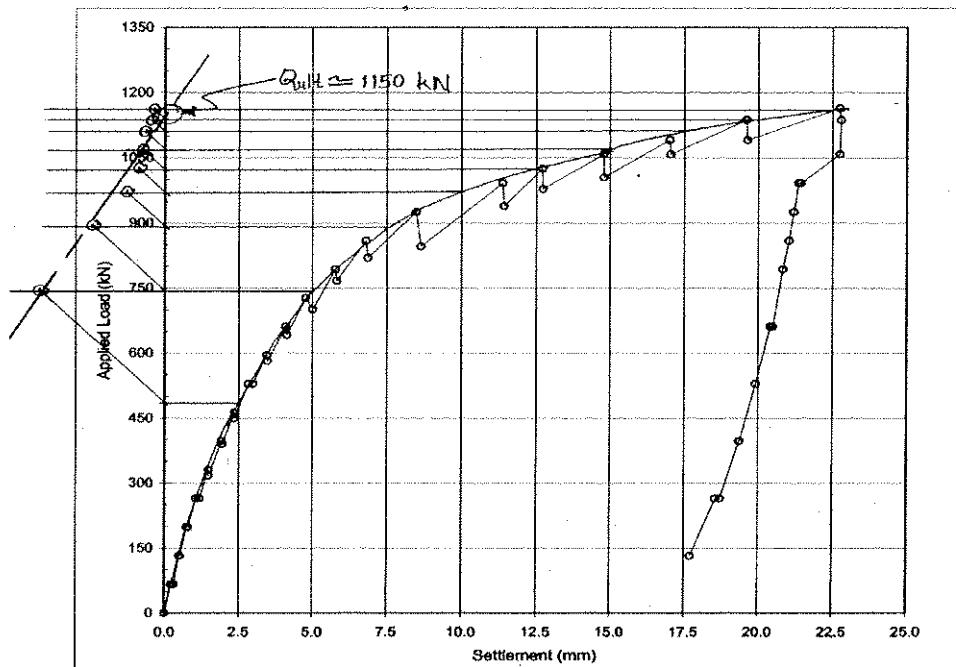
D.3 Dover Site, Alberta

D.3.1 Screw Pile T9

D.3.1.1 Brinch-Hansen Failure Criterion
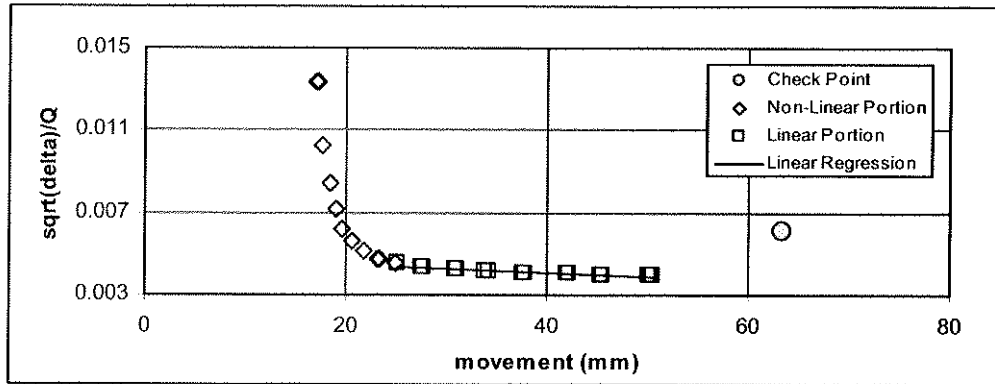
Brinch-Hansen Method:	
slope	-1.91932E-05
y-intercept	0.004857959
r^2	0.895335961
Q_u	1637 kN
Δ_u	-253 mm

Check that this point lies on or near plotted test data:	
$Q' = 0.80\ Q_u$	1310
$\Delta' = 0.25\ \Delta_u$	63
$\sqrt{\Delta'}/Q'$	0.006072449
Is it okay ? (Y/N)	N

D.3.1.2 Mazurkiewicz Method

167
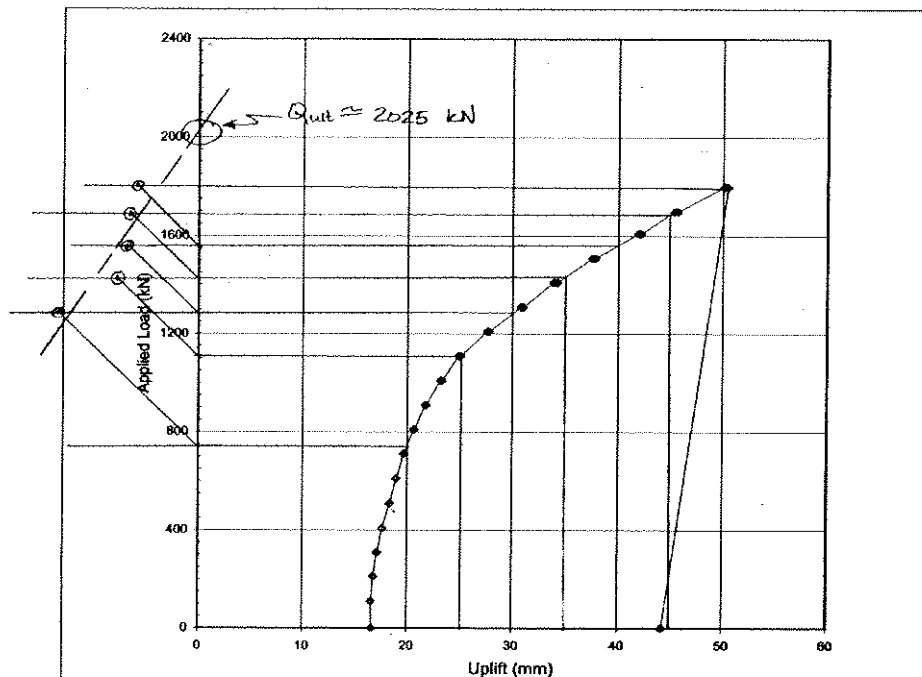
D.4   Hythe Site, Alberta

D.4.1   Screw Pile C13

D.4.1.1   Brinch-Hansen Failure Criterion
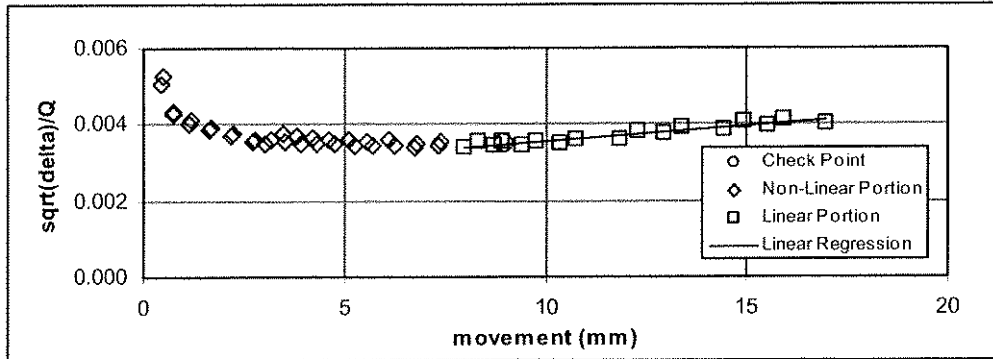
Brinch-Hansen Method:	
slope	7.75679E-05
y-intercept	0.002784192
r^2	0.905844504
Q_u	1076 kN
Δ_u	36 mm
Check that this point lies on or near plotted test data:	
Q' = 0.80 Q_u	861
Δ' = 0.25 Δ_u	9
$\sqrt{\Delta'}$/Q'	0.003480239
is it okay ? (Y/N)	Y

D.4.1.2   Mazurkiewicz Method
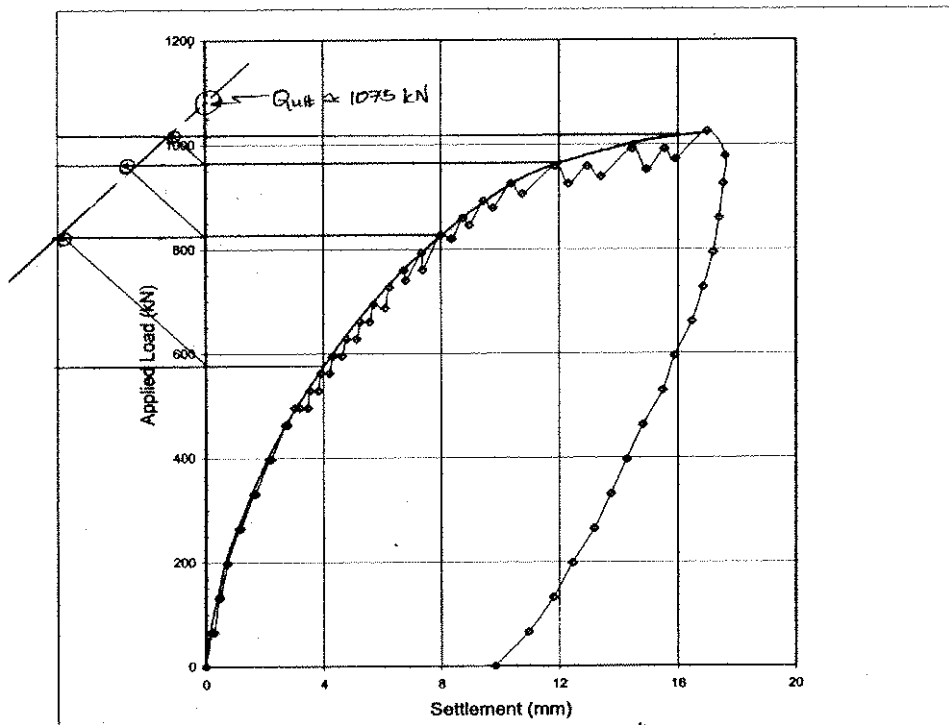
D.5 Ft. St. John Town Site, British Columbia

D.5.1 Screw Pile C14

D.5.1.1 Brinch-Hansen Failure Criterion
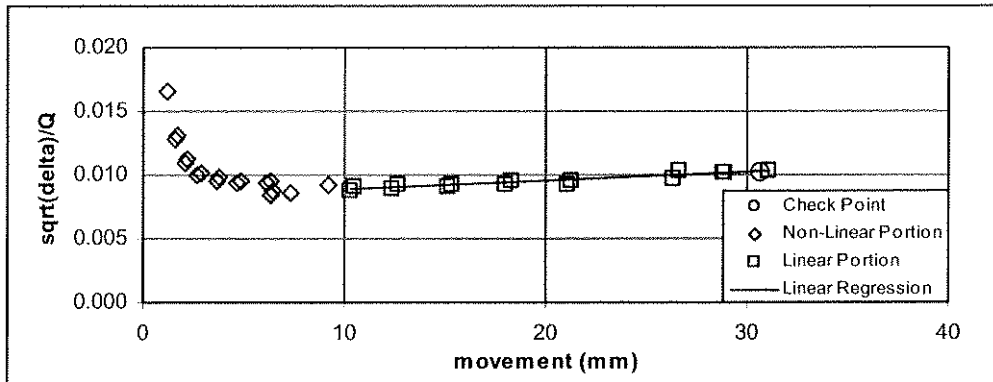
Brinch-Hansen Method:	
slope	6.65919E-05
y-intercept	0.008178743
r^2	0.869575808
Q_u	678 kN
Δ_u	123 mm

Check that this point lies on or near plotted test data:

$Q' = 0.80\ Q_u$	542
$\Delta' = 0.25\ \Delta_u$	31
$\sqrt{\Delta'}/Q'$	0.010223429
Is it okay ? (Y/N)	Y

D.5.1.2 Mazurkiewicz Method
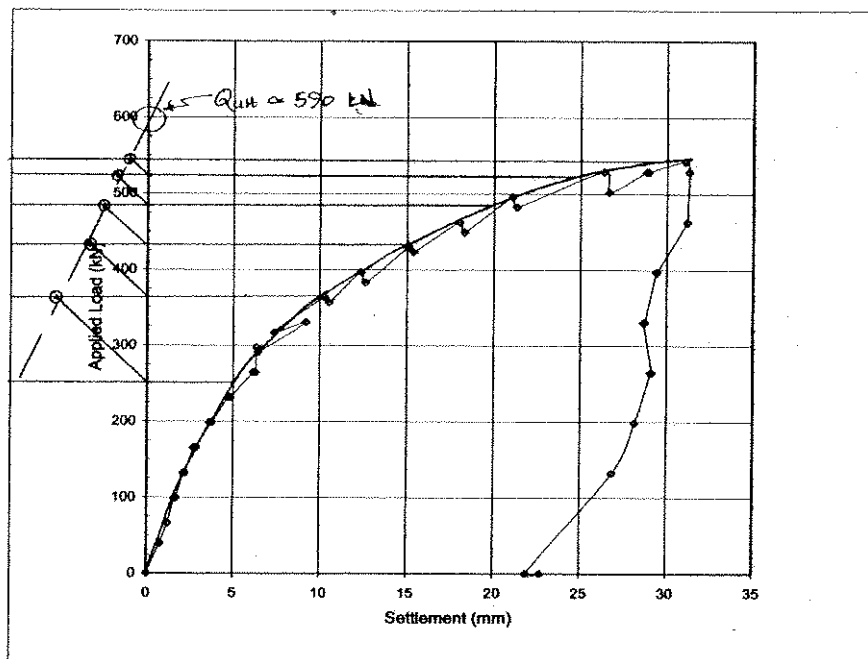
D.5.2   Screw Pile C15

D.5.2.1   Brinch-Hansen Failure Criterion

Brinch-Hansen Method:

slope	0.000169068
y-intercept	0.017542965
r^2	0.971906749
Q_u	290 kN
Δ_u	104 mm

Check that this point lies on or near plotted test data:

$Q' = 0.80\ Q_u$	232
$\Delta' = 0.25\ \Delta_u$	26
$\sqrt{\Delta'}/Q'$	0.021928707
Is it okay? (Y/N)	Y
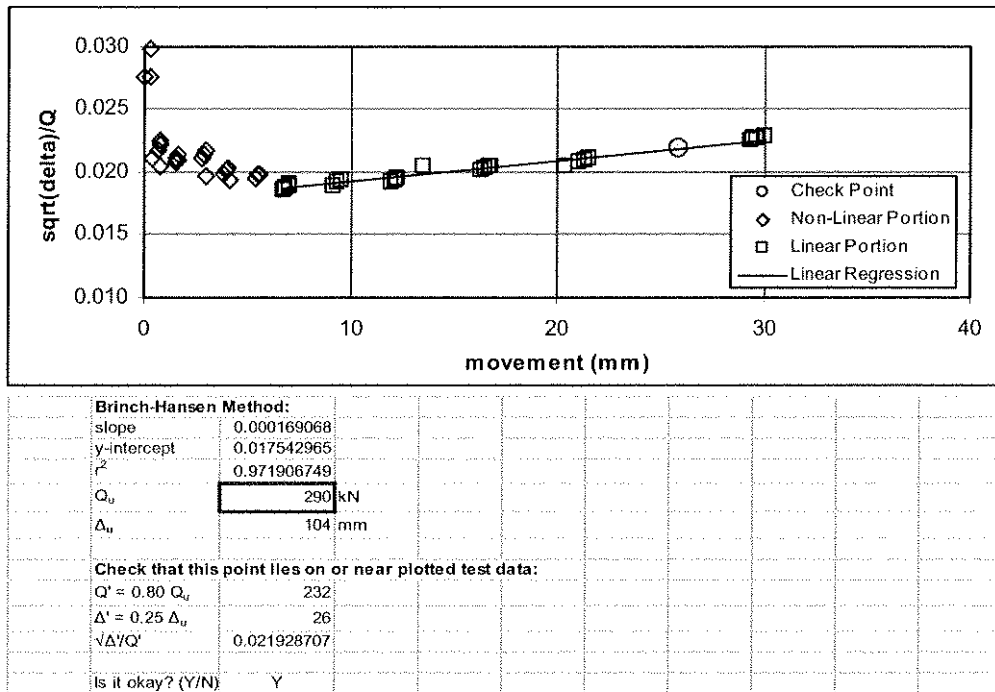
D.5.2.2   Mazurkiewicz Method
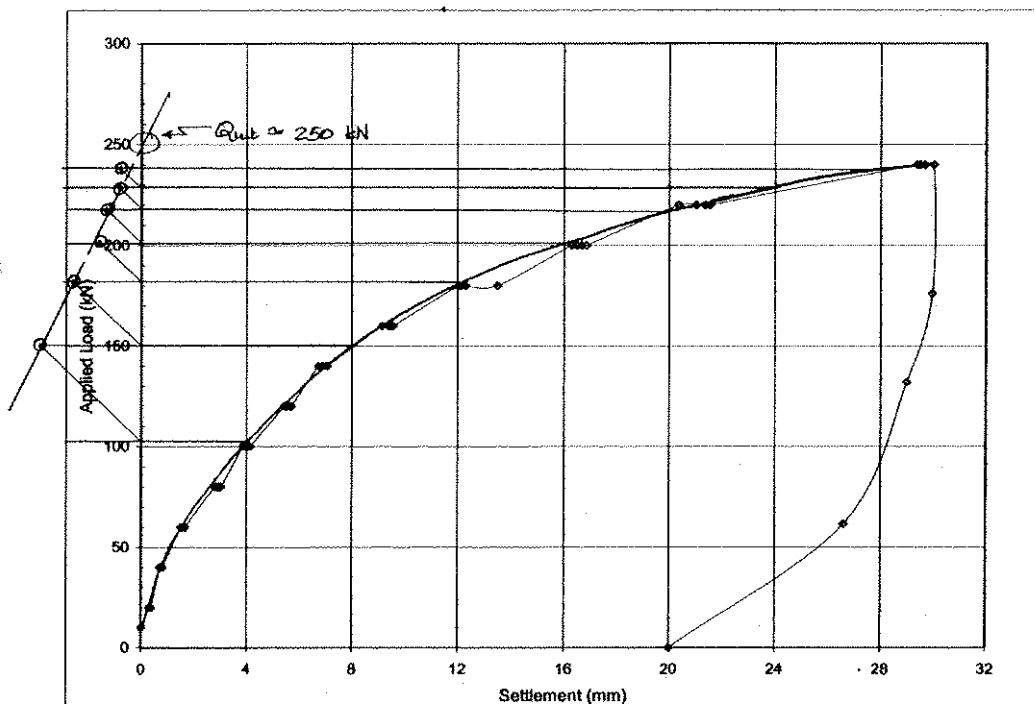
D.6 Ft. St. John Farm Site, British Columbia

D.6.1 Screw Pile C16

D.6.1.1 Brinch-Hansen Failure Criterion
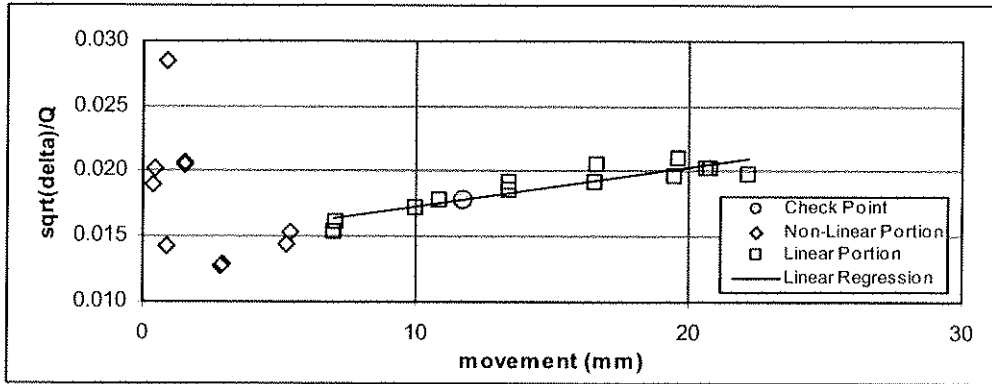
Brinch-Hansen Method:	
slope	0.000302985
y-intercept	0.014213235
r^2	0.842546793
Q_u	241 kN
Δ_u	47 mm

Check that this point lies on or near plotted test data:

$Q' = 0.80\ Q_u$	193
$\Delta' = 0.25\ \Delta_u$	12
$\sqrt{\Delta'}/Q'$	0.017766544
Is it okay ? (Y/N)	Y

D.6.1.2 Mazurkiewicz Method
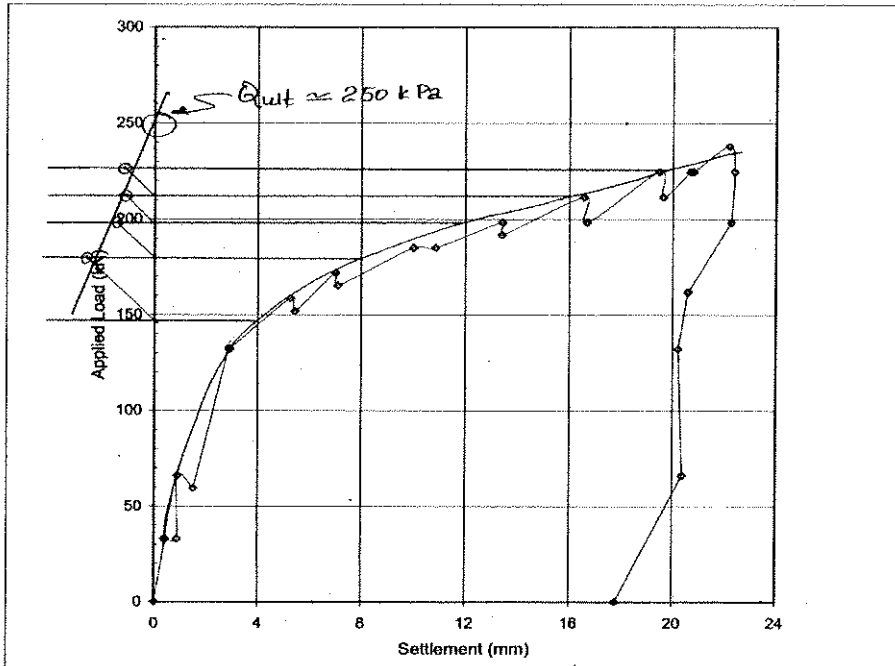
D.6.2   Screw Pile C17

D.6.2.1   Brinch-Hansen Failure Criterion
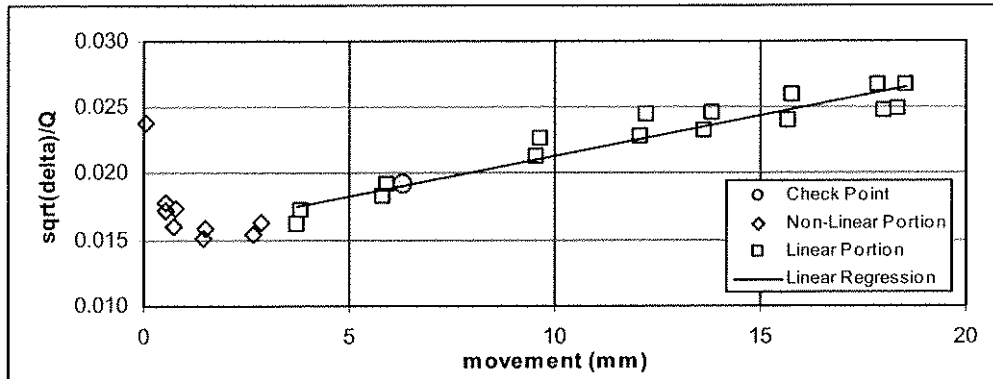
Brinch-Hansen Method:

slope	0.000606849	
y-intercept	0.015297264	
r^2	0.907099047	
Q_u	164	kN
Δ_u	25	mm

Check that this point lies on or near plotted test data:

$Q' = 0.80\ Q_u$	131	
$\Delta' = 0.25\ \Delta_u$	6	
$\sqrt{\Delta'/Q'}$	0.01912158	
Is it okay ? (Y/N)	Y	

D.6.2.2   Mazurkiewicz Method

$Q_{ult} \simeq 173\ kN$

172
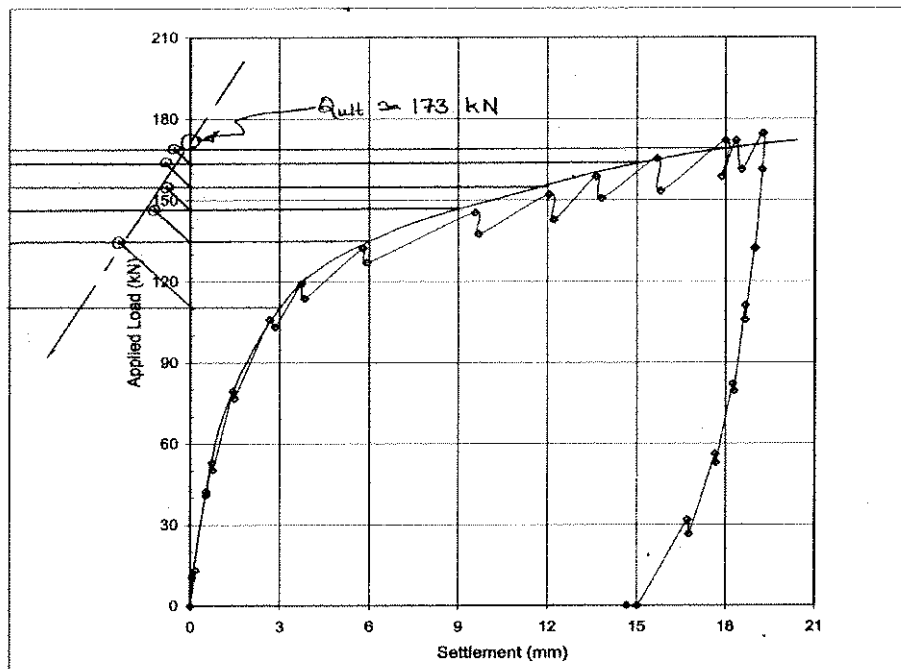
D.7 Saskatoon Site, Saskatchewan

D.7.1 Screw Pile C18

D.7.1.1 Brinch-Hansen Failure Criterion
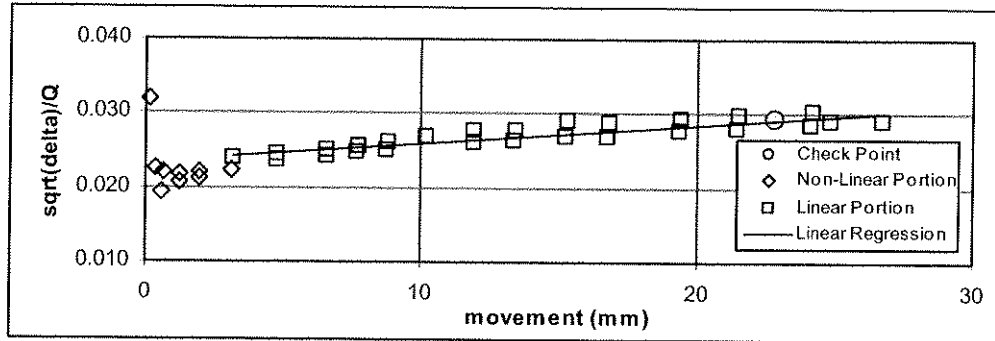
Brinch-Hansen Method:	
slope	0.000255542
y-intercept	0.02334358
r^2	0.818448209
Q_u	205 kN
Δ_u	91 mm

Check that this point lies on or near plotted test data:

Q' = 0.80 Q_u	164
Δ' = 0.25 Δ_u	23
√Δ'/Q'	0.029179475
Is it okay ? (Y/N)	Y

D.7.1.2 Mazurkiewicz Method
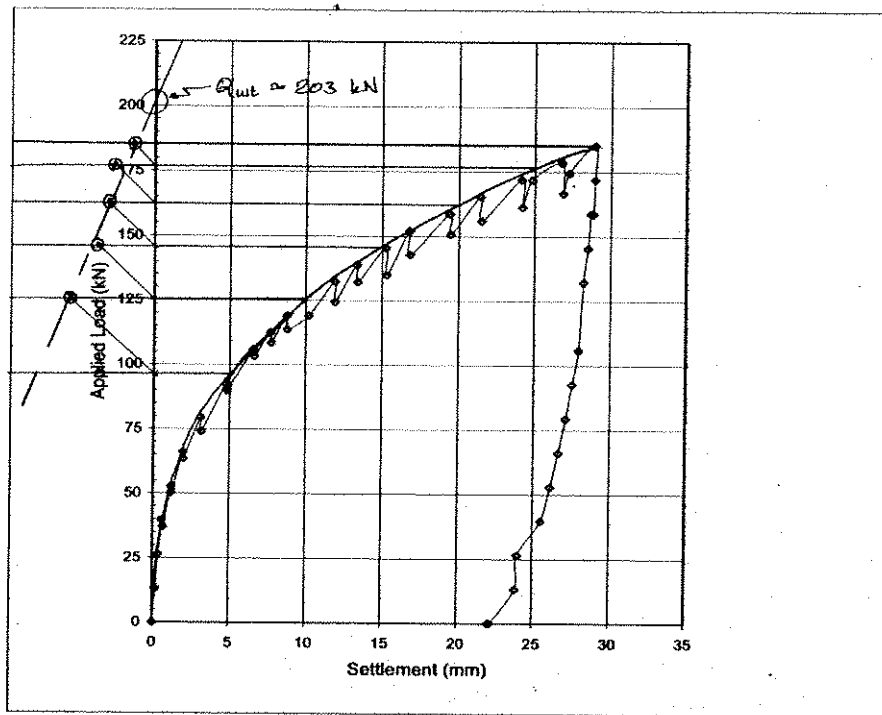
D.7.2 Screw Pile C19

D.7.2.1 Brinch-Hansen Failure Criterion
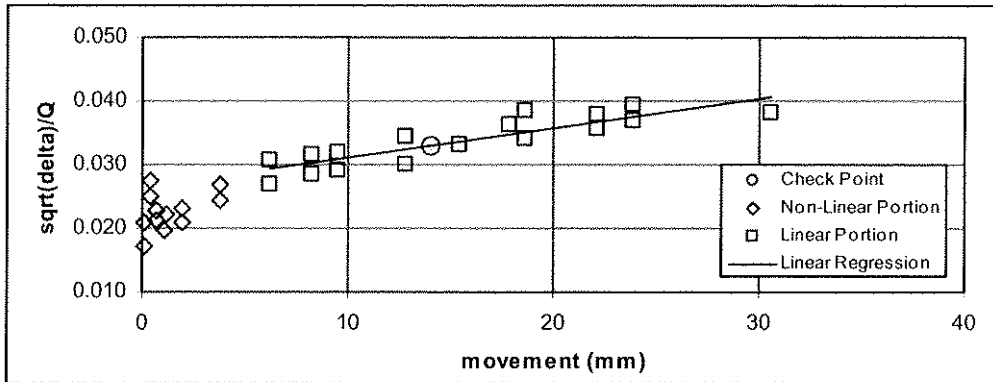
Brinch-Hansen Method:		
slope	0.000467685	
y-intercept	0.026334296	
r²	0.77816116	
Q_u	142	kN
Δ_u	56	mm
Check that this point lies on or near plotted test data:		
Q' = 0.80 Q_u	114	
Δ' = 0.25 Δ_u	14	
√Δ'/Q'	0.032917869	
Is it okay ? (Y/N)	Y	

D.7.2.2 Mazurkiewicz Method
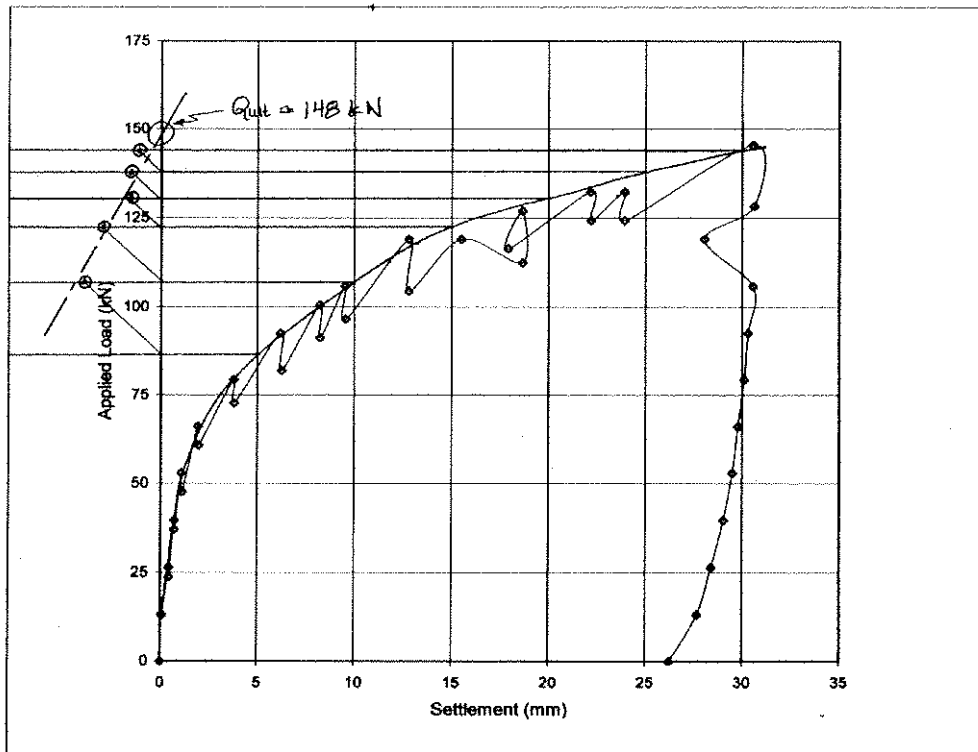
D.7.3 Screw Pile C20

D.7.3.1 Brinch-Hansen Failure Criterion
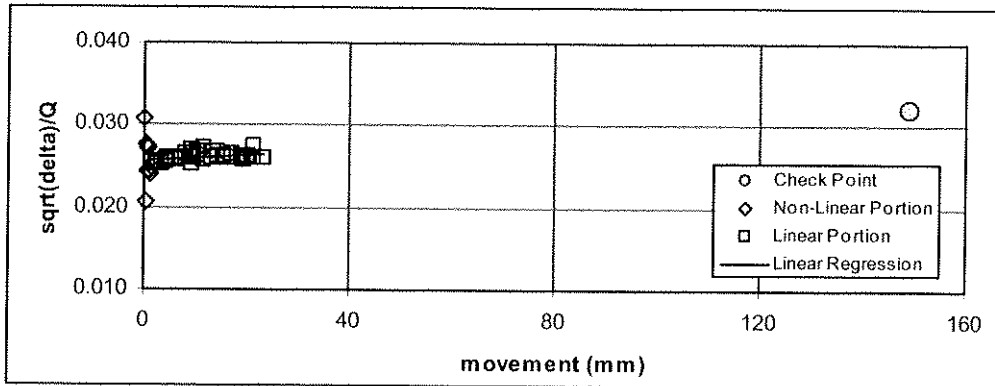
Brinch-Hansen Method:	
slope	4.28441E-05
y-intercept	0.025574411
r²	0.263150642
Q_u	478 kN
Δ_u	597 mm

Check that this point lies on or near plotted test data:	
Q' = 0.80 Q_u	382
Δ' = 0.25 Δ_u	149
√Δ'/Q'	0.031968014
Is it okay ? (Y/N)	N

D.7.3.2 Mazurkiewicz Method

175
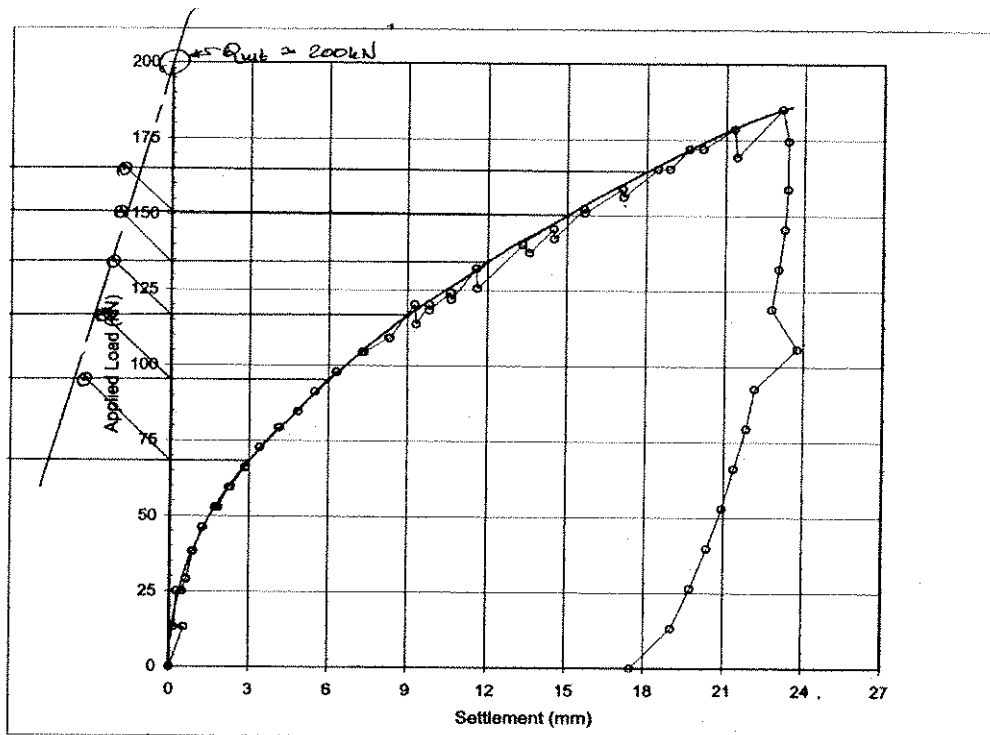
Appendix E: Computer Program, *LCPCmethod*

E.1 Introduction

The *LCPCmethod.exe* program was developed as part of this thesis project for the purpose of performing the required calculations related to the use of Bustamante and Gianeselli's (1982) LCPC direct pile design method. The geometry and depth of installation (length) of a screw pile is entered by the user. A profile of cone penetration tip resistance with depth, representing the site where the screw pile is to be installed, must also be inputted to the program. In order for the axial capacity calculations to be made, the profile must extend to a depth equal to the pile length, if the screw pile is to be loaded in tension, or to a depth equal to the pile length plus 1.5 times the diameter of the bottom helix, if the pile is to be loaded in compression. The program output is a comma-separated-values (csv) data file which may be opened in Microsoft *Excel*, reiterating the input parameters, and summarizing the axial capacity predictions for the screw pile at incremental depths up to and including the final user-specified pile length. The increments of depth are taken as approximately equal to 2/3 the inter-helix spacing for multi-helix piles, or approximately equal to 1 m for single-helix piles. Two sets of axial capacity calculations are included in the output file, one using the cylindrical shear failure model, with and without the correction to the cylindrical friction component recommended by Narasimha Rao et al. (1993), and the other using the individual plate bearing failure model. It is up to the user to decide which model is more applicable, based on the geometry of the specific screw pile. The source code for the *LCPCmethod.exe* computer program is included in Appendix A, as *LCPCmethod.rb*.

E.2 Assumptions of the LCPCmethod Program

- Screw pile under consideration has a circular shaft, affixed with 1, 2, or 3 helices.

- In the case where the lower helix of the screw pile is bearing in compression, it is assumed that a soil plug has formed in the bottom of the pile shaft to create an effectively closed-ended pile.

- Any helix must be buried to a depth greater than twice its diameter before its contribution of point resistance in tension, if any, is calculated, or to 1.5 times its diameter before its

contribution of point resistance in compression, if any, can be calculated by the LCPC method.

■ No shaft friction is calculated for tension piles buried to "shallow" depths, i.e. embedment less than twice the upper helix diameter in clay, or less than 5 times the upper helix diameter in sand.

■ In calculating shaft friction, the length of shaft between the upper helix and the ground surface, minus a length equal to the diameter of the upper helix is considered in the calculations to represent the "effective shaft length." The effective shaft length, over which shaft friction is considered to act, is a result of the shadow effect created above the upper helix when the screw pile is loaded in compression, and the effect of the bearing disturbance around the upper helix when the screw pile is loaded in tension.

■ Within the individual plate bearing failure model, additional lengths of shaft over which friction is considered to act are taken between the individual helices. A length equal to the average helix diameter is subtracted from above and below each helix that is considered to be contributing point resistance in tension or compression.

■ The soil deposit into which the screw pile is installed is considered to be uniform in nature. That is,. the user must specify whether the shaft of the helix is embedded in cohesive (clay/silt) material or cohesionless (sand) material, for the purpose of selecting the constants to be used in the LCPC calculations.

E.3 *Operating the LCPCmethod Program*

E.3.1 Case Study: Capacity Calculation for Screw Pile C9

1. Create a data file in *Excel* containing the relevant cone penetration tip resistance values (kPa) in the second column and the corresponding depth values (m) in the first column, with no headers. An example is shown in Figure E-1. Close the data file and save it in comma-separated values (csv) format, which can be selected from the pull-down list of file types (as shown in Figure E-2). The tip resistance compiled in "Cone Test #16.csv" is used in this example, found in the electronic Appendix A under "\LCPC Calculations\CSV Data Files."

2. Double-click on the *LCPCmethod.exe* icon to open the program.

3. Enter the full path and filename of the csv data file containing the cone penetration tip resistance and depth values. The name entered for the data file must include the full path and file name, ending with the extension ".csv", as shown in Figure E-3. Hit enter to continue.

4. Next, the user will be prompted to enter numerical information about the geometry of the screw pile under consideration. The first prompt will ask how many helices are affixed to the screw pile (Figure E-4). Enter the number of helices, 1, 2, or 3, (Figure E-5) and hit the enter key to receive the next prompt. Continue to describe the relevant geometry of the screw pile by typing the numerical answers to each of the subsequent prompts, pushing the enter key after each response (Figure E-6). The geometry of screw pile C9, installed at the Ft. Saskatchewan site where Cone Test #16 was obtained, is used in this example.

5. The user will then be prompted to enter whether the screw pile under consideration is to be loaded in tension or in compression. Type "t" for tension, or "c" for compression (Figure E-7), and hit enter.

6. Finally, the user must specify whether the soil into which the screw pile is installed, i.e. the soil described by the cone penetration data file, may be characterized as sand or clay/silt. This information will be used by the program to select the appropriate constants specified for use within the LCPC method, which are based on soil type and measured cone penetration tip resistance. Type "s" for sand or "c" for clay/silt (Figure E-8) and press enter.

7. At this point, the capacity predictions for the specified screw pile will be instantaneously displayed inside of the program window, which may be resized to show all of the results as seen in Figure E-9. In addition, a data file entitled "out.csv" will be automatically created by the program at this point, containing all of the results in a comma-separated-values format. Double-click on the "out.csv" icon to open the summary of results in *Excel*, as illustrated in Figure E-10.

8. Save the out.csv file under a different name, and in the ".xls" (*Excel* spreadsheet) format before closing. The out.csv data file must be closed or saved under a different name before attempting to re-run the *LCPCmethod* program. Re-run the program using the "Cone Test

#15.csv" data file included electronically in Appendix A of this report (Appendix A\LCPC Calculations\CSV Data Files). The results obtained can then be averaged with those from the "Cone Test #16.csv" run—this is the result presented in the main thesis report for test pile C9, because Cone Test #15 and Cone Test #16 represent the two penetration tests conducted at the Ft. Saskatchewan site.
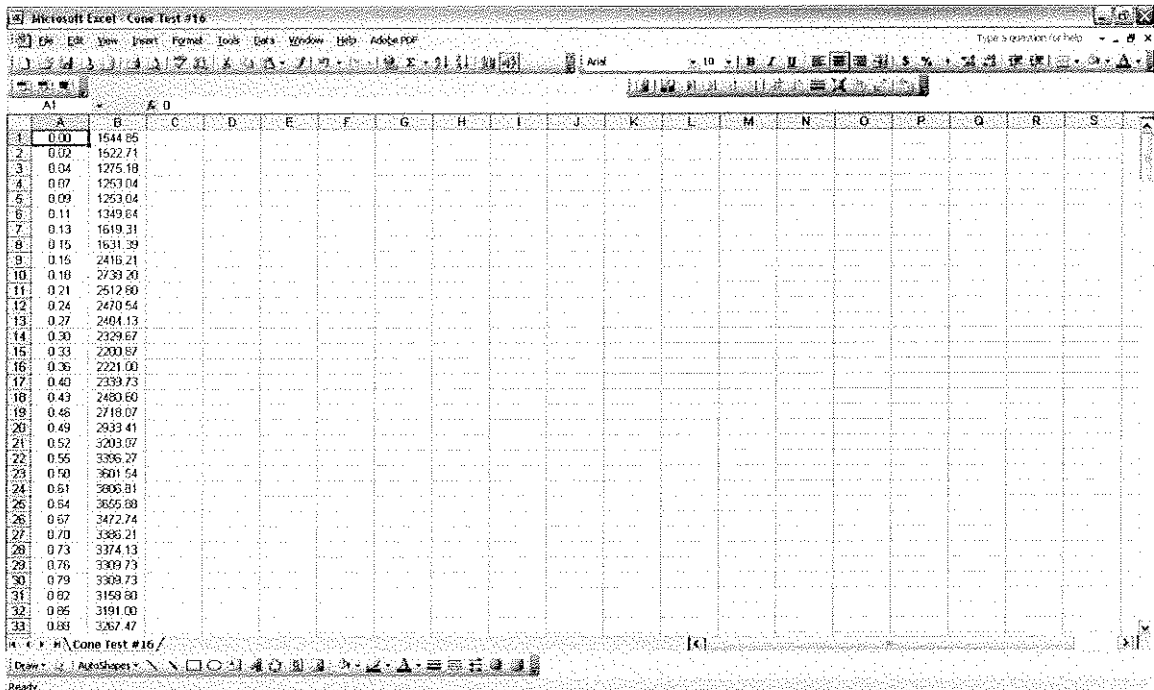
Figure E-1: Example Data File Created in Excel, Containing Cone Penetration Tip Resistance Values in kPa (Column B) and Corresponding Depth Values in Meters (Column A)
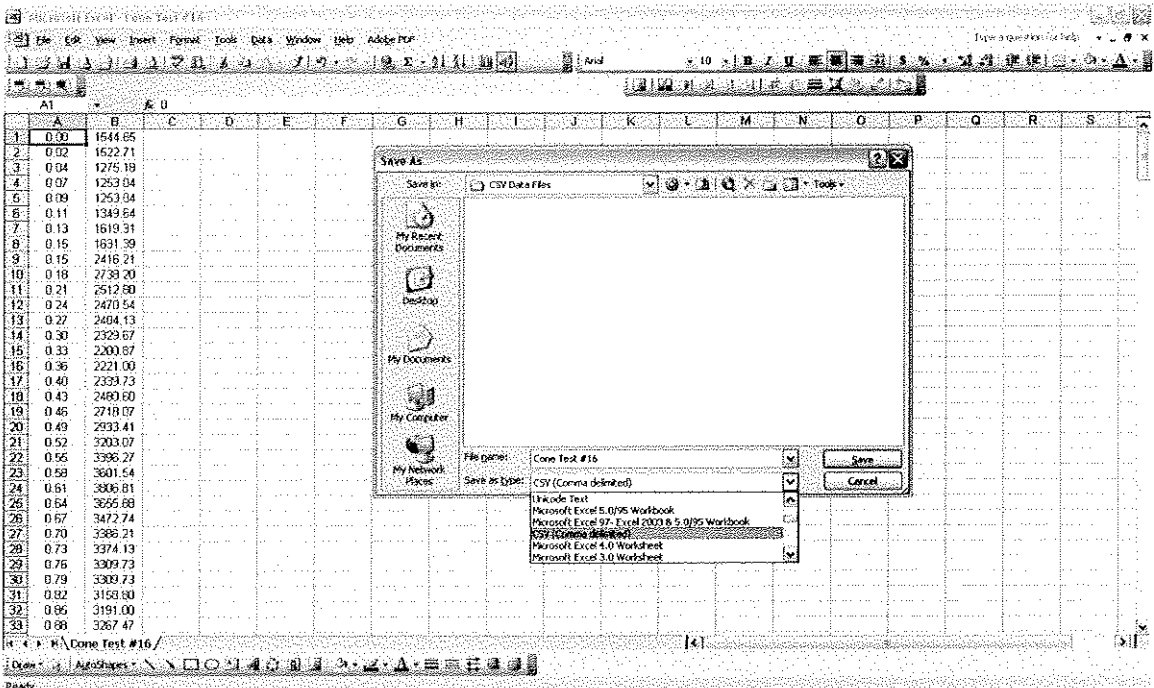
Figure E-2: Saving the Data File in Comma-Separated Values Format
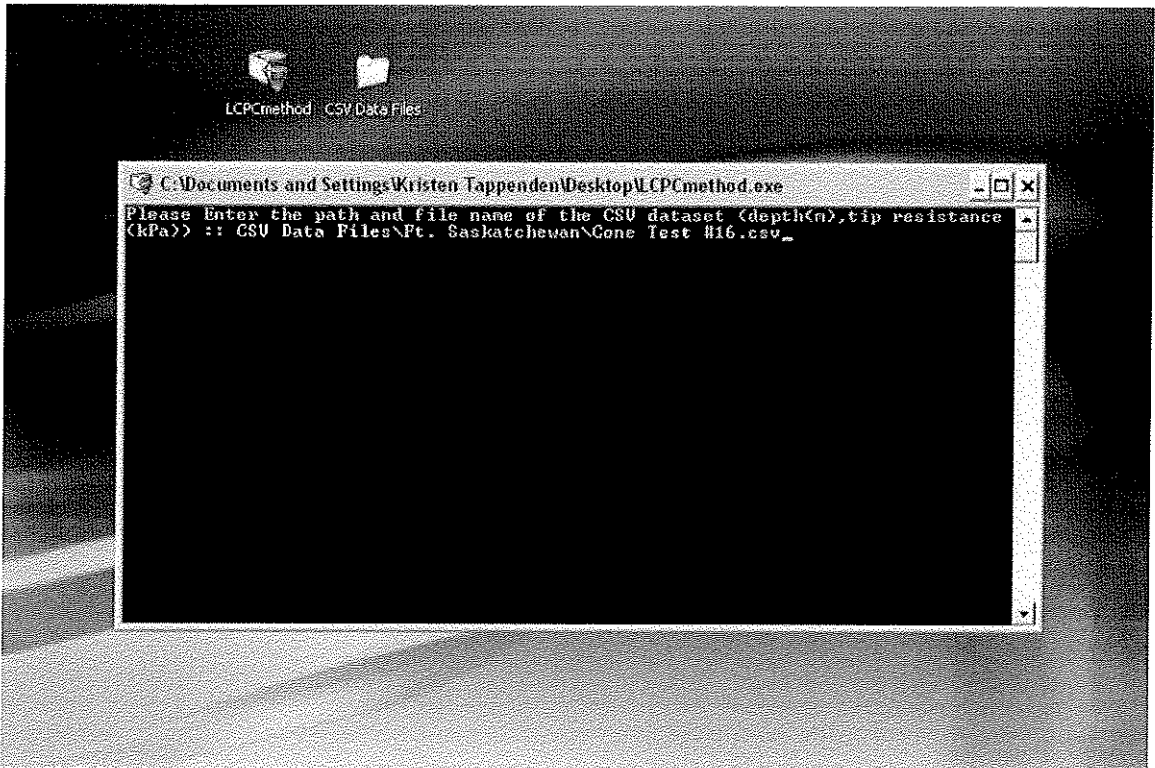
Figure E-3: Example Entry for Referring the *LCPCmethod* Program to the Relevant Tip Resistance Data File
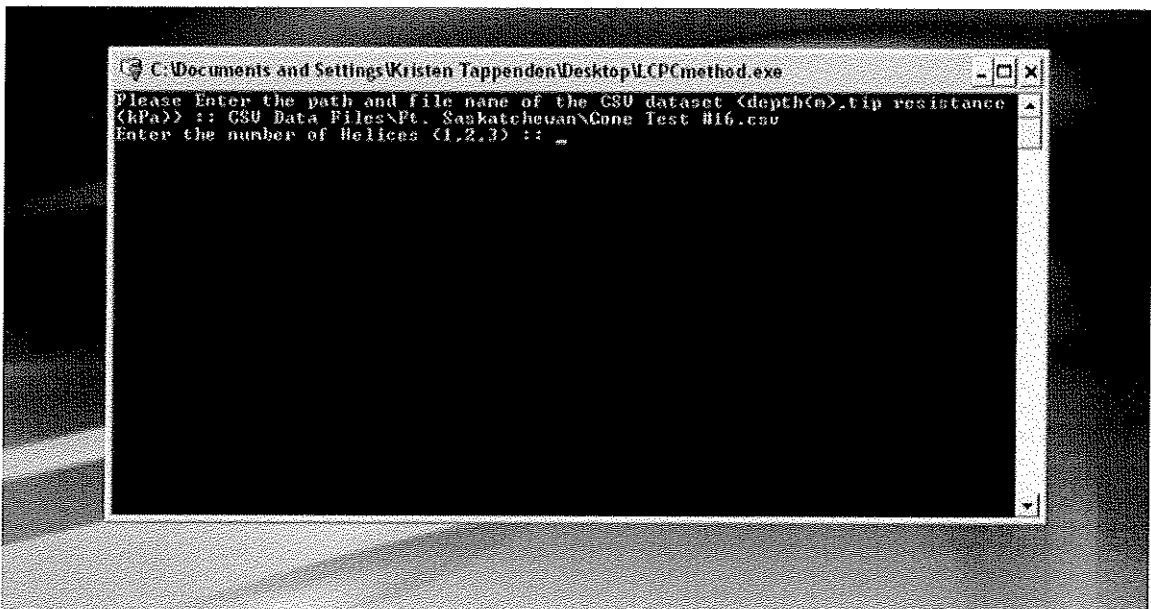
Figure E-4: Prompt to Enter the Number of Helices Affixed to the Screw Pile
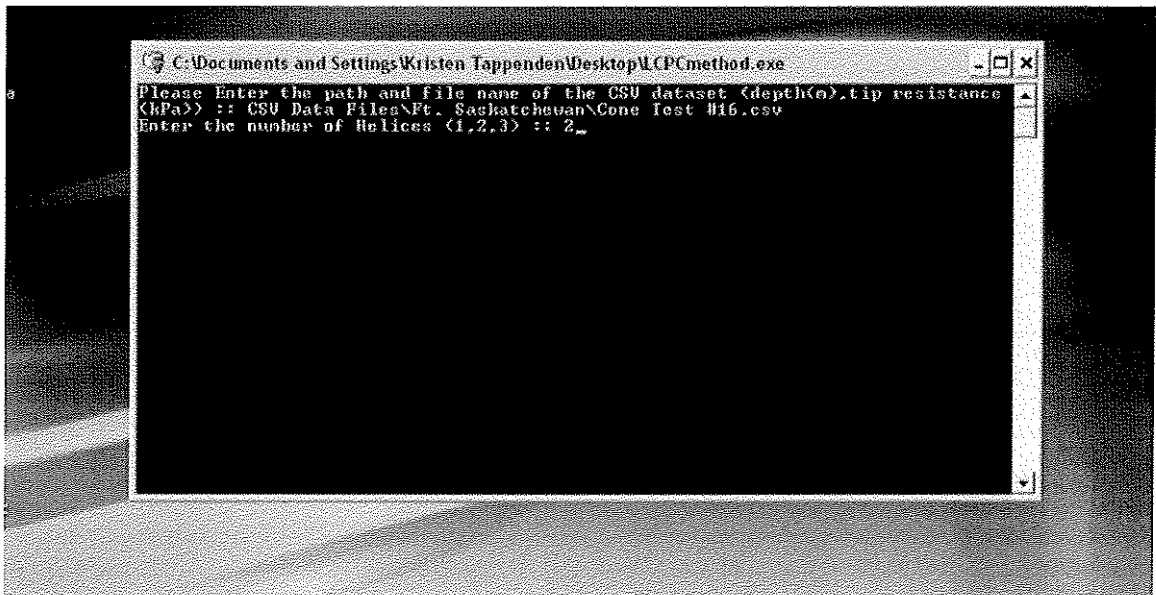
Figure E-5: Valid Numerical Response to the Question of the Number of Helices Affixed to the Screw Pile Shaft
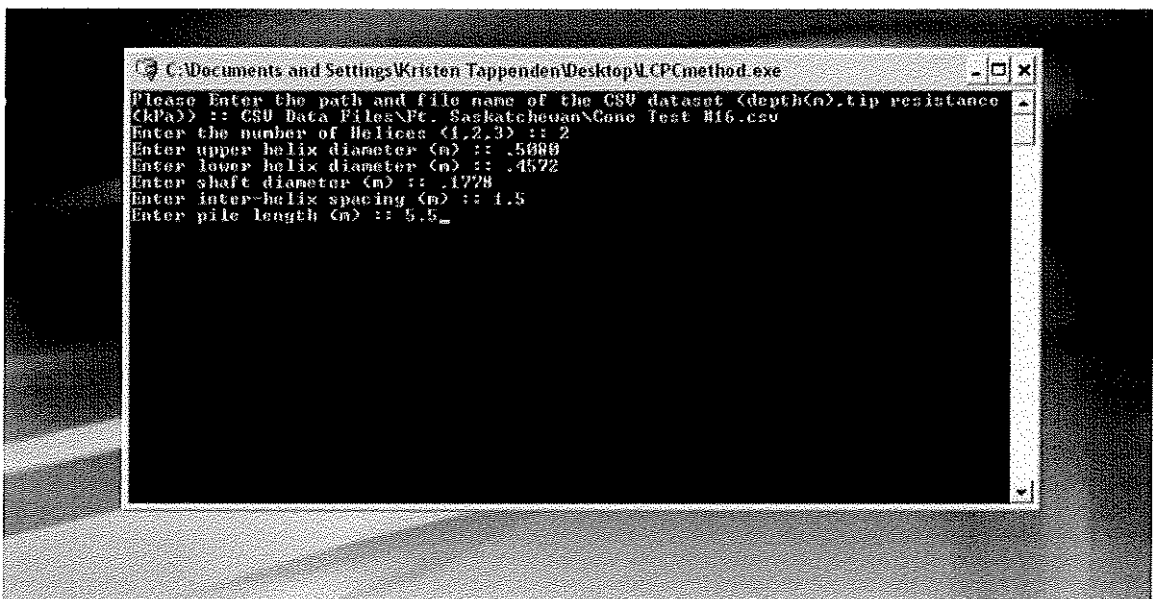
Figure E-6: Entries Describing the Screw Pile Geometry as Prompted
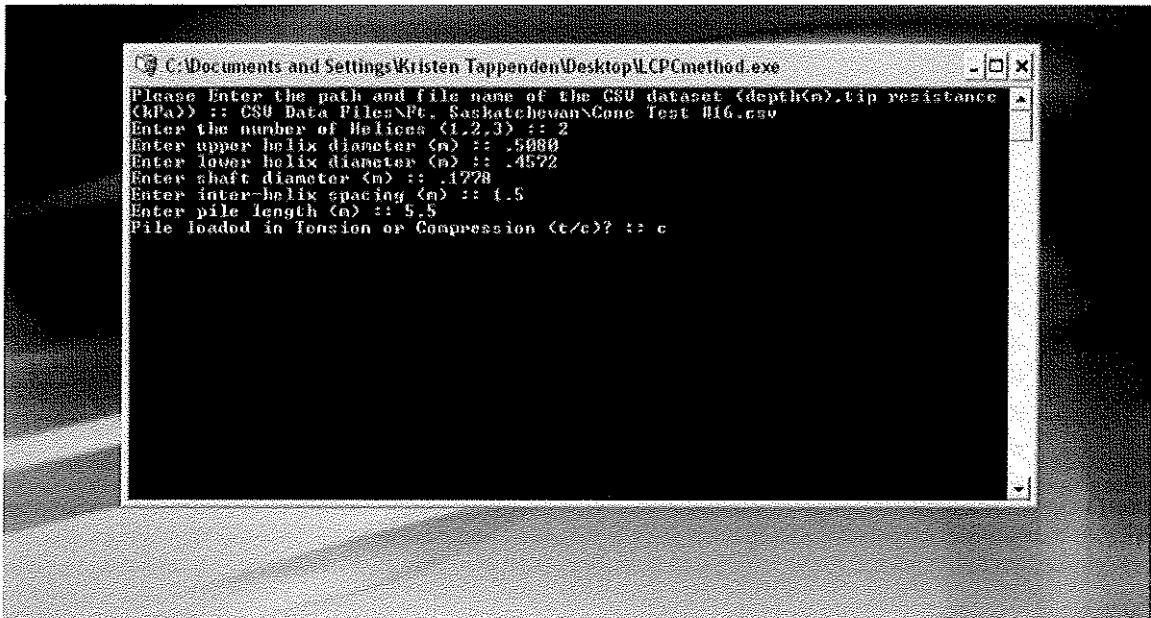
Figure E-7: Entry of "c" to Indicate that the Ultimate Axial Capacity of the Screw Pile in Question Should be Calculated Under Compression Loading
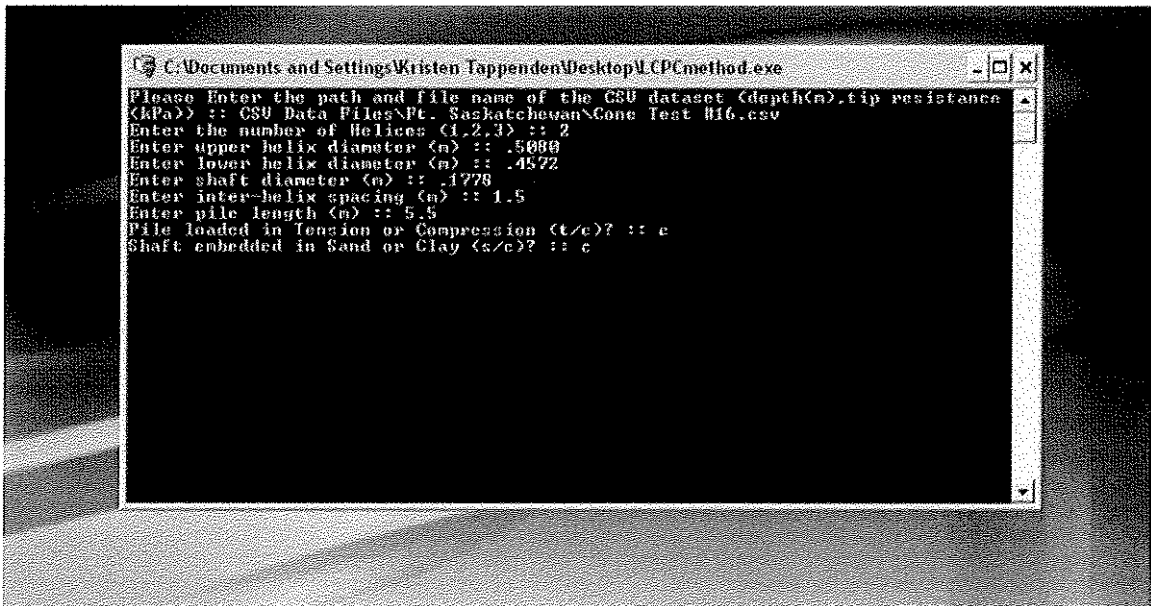
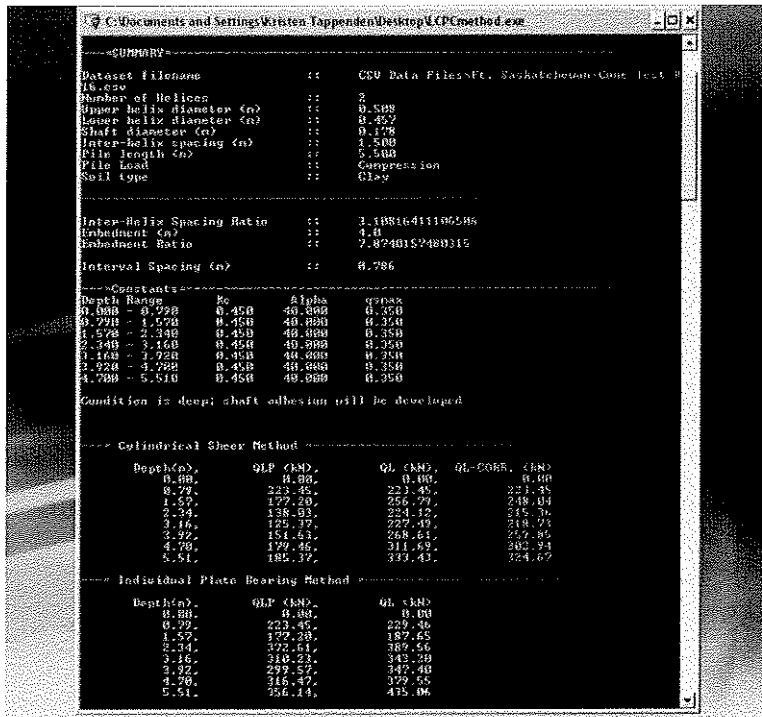**Figure E-8: Entry of "c" to Indicate that the Subsurface into which the Screw Pile will be Installed Consists of Clay/Silt (Cohesive) Material**

Figure E-9: Output Generated to the Screen by *LCPCmethod* Program, Indicating Predicted Screw Pile Capacity with Depth, Using Both the Cylindrical Shear Model and the Individual Plate Bearing Model in Conjunction with the LCPC Direct Design Method
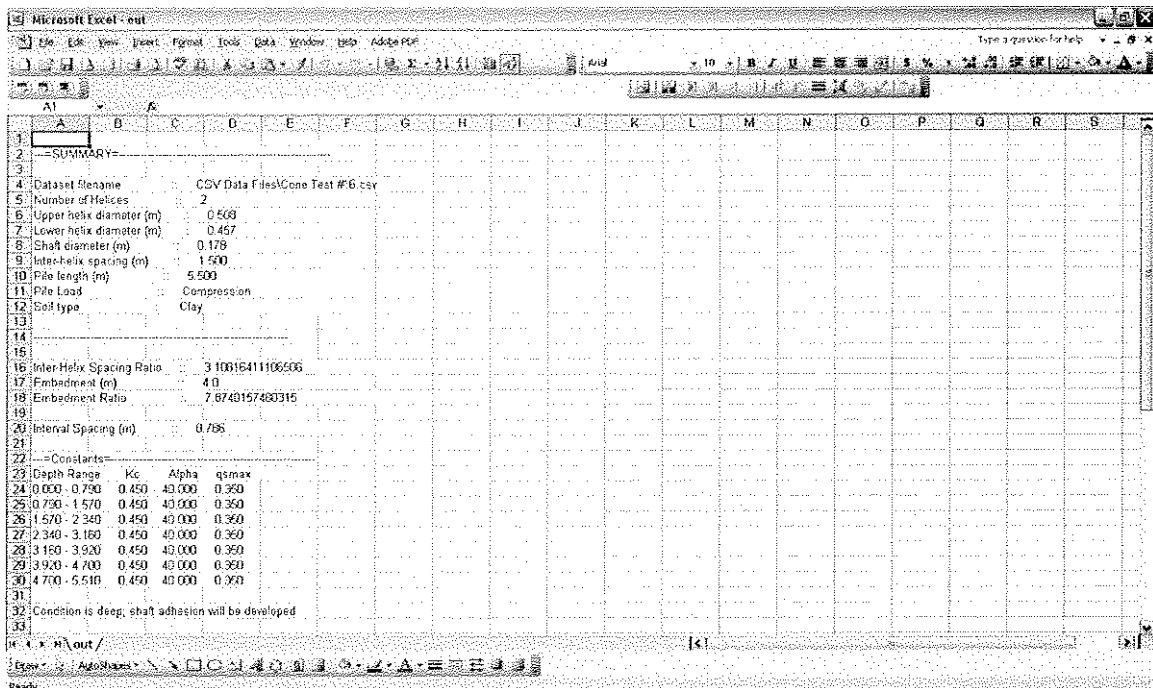

Figure E-10: Data File Automatically Generated by the *LCPCmethod* Program, Opened in *Excel*. File Contains Summary of Input Parameters and All Capacity Predictions with Depth

Appendix F: Sample Calculations, LCPC Method

F.1   Introduction

Sample calculations of axial screw pile capacity with depth using the LCPC method (Bustamante and Gianeselli 1982) are included in the electronic Appendix A accompanying this report (\LCPC Calculations\Spreadsheet Calculations).   The sample calculations are displayed in *Excel* spreadsheets under the pathname "LCPC Calculations\Spreadsheet Calculations." The method for performing LCPC capacity calculations at incremental depths was inspired by a worked example for a conventional concrete pile provided by Robertson and Campanella (1988). For added clarification of the LCPC calculation process for screw piles, hand drawings and two worked examples are included in the following section of this Appendix. The worked examples apply to test pile C9; using the results of the Cone Test #16, performed at the Ft. Saskatchewan site. Sample calculations are made of pile C9's capacity in compression at a depth of 1.57 m using the cylindrical shear model, and at the final depth of 5.51 m using the individual plate bearing model. It should be noted that the reader must still simultaneously refer to the spreadsheet calculations made for pile C9, as certain parameters used in the LCPC method, such as q'_{ca} and q_{ca}, should be calculated electronically in the interest of efficiency.

F.2   Worked Examples

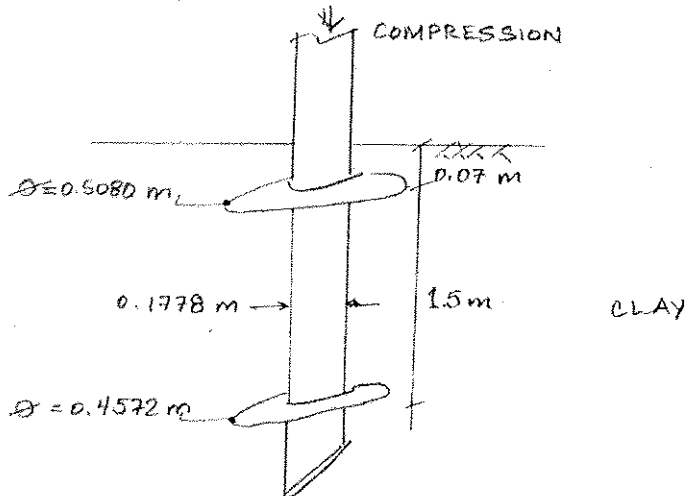### F.2.1   Compression Capacity of Screw Pile C9, Depth 1.57 Meters

SAMPLE CALCULATIONS
L.C.P.C.   METHOD

CONE TEST #16

PILE C9, Ft. Saskatchewan Site

At depth 1.57 m :

COMPRESSION

$\varnothing = 0.5080$ m   0.07 m

0.1778 m →   1.5 m   CLAY

$\varnothing = 0.4572$ m

⊙   CYLINDRICAL SHEAR MODEL :

Subsoil is divided into layers, arbitrarily set to
approx. 2/3 × interhelix spacing in height.
Exact height of each interval depends on the
spacing of the tip resistance readings .

Qshaft

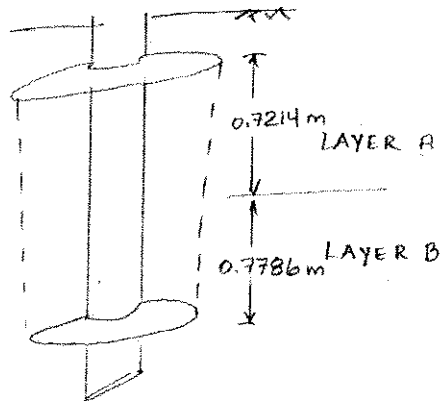Qcyl   0.7894 m

Qbearing   1.5680 m
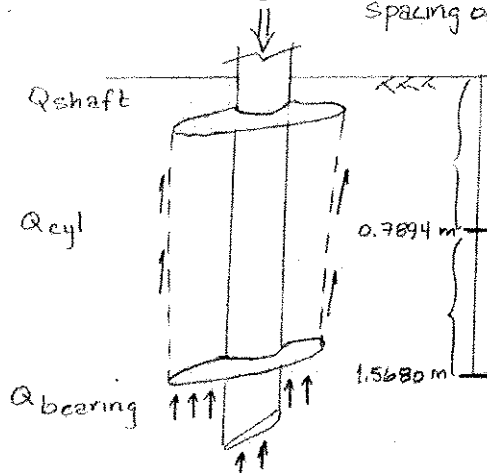
LAYER A: avg $q_c = 26.32$ bar
$k_c = 0.45$
$\alpha = 40$
$q_{si} = 26.32/40 = 0.66$ bar
     max $q_s = 0.35$ bar

LAYER B: avg $q_c = 30.70$ bar
$k_c = 0.45$
$\alpha = 40$ $q_{si} = 30.70/40 = 0.77$ bar
     max $q_c = 0.35$ bar
     $q'_{ca} = 24.52$ bar
     $q_{ca} = 23.97$ bar

188

- $Q_{shaft} = 0$ due to shadow effect above top helix

- Q_{cyl} :

$$Q_{cyl} = 0.7214\,m * \left(\frac{0.5080 + 0.4572}{2}\right)m * \pi * 0.35\,bar * 100\,\frac{kPa}{bar}$$

$$+ \; 0.7786\,m * \left(\frac{0.5080 + 0.4572}{2}\right)m * \pi * 0.35\,bar * 100\,\frac{kPa}{bar}$$

$$= 79.60\;kN$$

- $Q_{bearing} = k_c * q_{ca} * \pi * \dfrac{(0.4572\,m)^2}{4}$

$$= 0.45 * 23.97\,bar * \frac{100\,kPa}{bar} * \pi * \frac{(0.4572\,m)^2}{4}$$

$$= 177.1\;kN$$

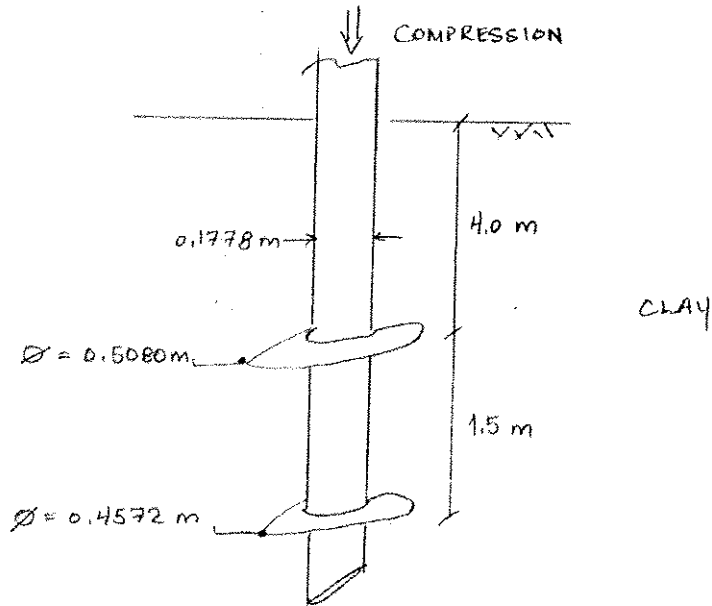- $Q_{ultimate} = Q_{shaft} + Q_{cyl} + Q_{bearing} = \boxed{256.7\;kN}$

189

F.2.2 Compression Capacity of Screw Pile C9, Depth 5.5 Meters

CONE TEST #16
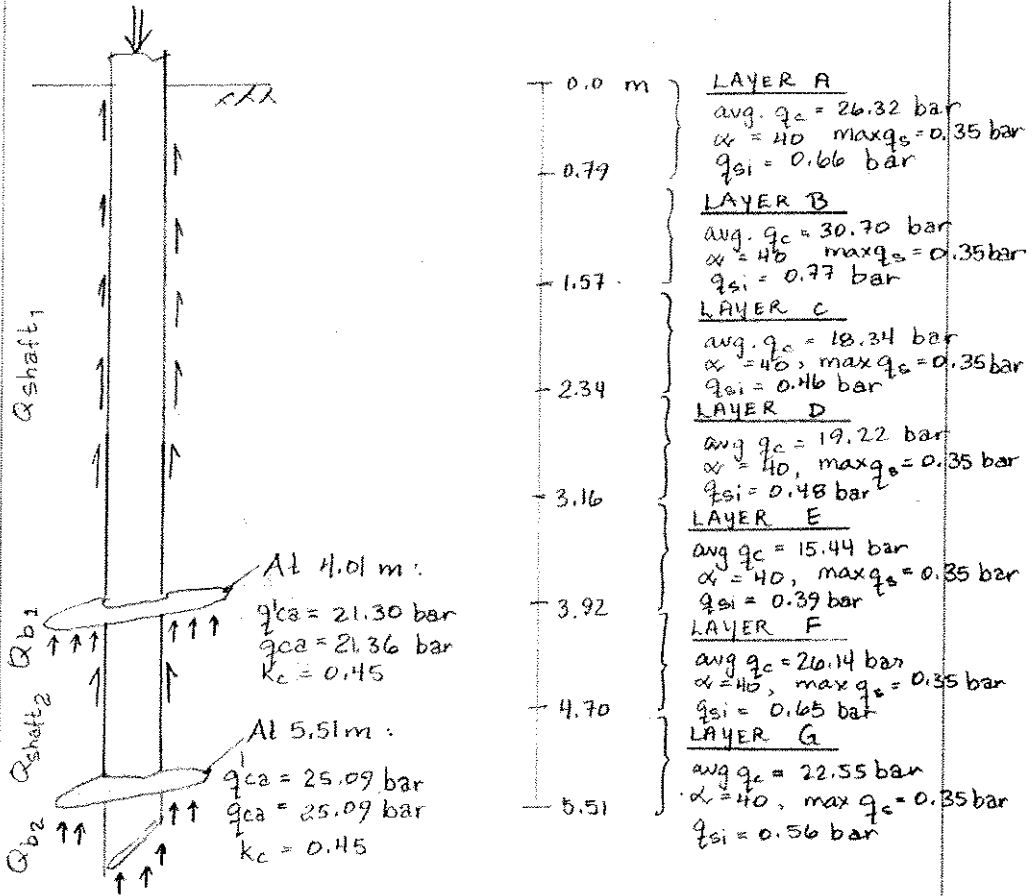
PILE C9, Ft. Saskatchewan Site

At final depth, 5.5 m :

⊙ INDIVIDUAL PLATE BEARING MODEL :

Subsoil is divided into layers, arbitrarily set
to approx. 2/3 × inter helix spacing in
height. Exact height of each interval depends
on the spacing of tip resistance readings.

At 4.01 m :
q'_{ca} = 21.30 bar
q_{ca} = 21.36 bar
k_c = 0.45

At 5.51 m :
q'_{ca} = 25.09 bar
q_{ca} = 25.09 bar
k_c = 0.45

0.0 m

LAYER A
avg. q_c = 26.32 bar
α = 40   max q_s = 0.35 bar
q_{si} = 0.66 bar

0.79

LAYER B
avg. q_c = 30.70 bar
α = 40   max q_s = 0.35 bar
q_{si} = 0.77 bar

1.57

LAYER C
avg. q_c = 18.34 bar
α = 40, max q_s = 0.35 bar
q_{si} = 0.46 bar

2.34

LAYER D
avg q_c = 19.22 bar
α = 40, max q_s = 0.35 bar
q_{si} = 0.48 bar

3.16

LAYER E
avg q_c = 15.44 bar
α = 40, max q_s = 0.35 bar
q_{si} = 0.39 bar

3.92

LAYER F
avg q_c = 26.14 bar
α = 40, max q_s = 0.35 bar
q_{si} = 0.65 bar

4.70

LAYER G
avg q_c = 22.55 bar
α = 40, max q_c = 0.35 bar
q_{si} = 0.56 bar

5.51

191

▸ Q_{shaft_1} : Use length of shaft between upper helix and ground surface minus upper helix diameter, ie from ground surface down to 3.50 m. This accounts for the shadow effect above the upper helix.

Calculate Q_{shaft_1} in layers:

$$Q_{shaft_1} = 0.79 \, m * \pi * 0.1778 \, m \times 0.35 \, bar \times \frac{100 \, kPa}{bar}$$

$$+ (1.57 - 0.79 \, m) \times \pi \times 0.1778 \, m \times 0.35 \, bar \times \frac{100 \, kPa}{bar}$$

$$+ (2.34 - 1.57 \, m) \times \pi \times 0.1778 \, m \times 0.35 \, bar \times \frac{100 \, kPa}{bar}$$

$$+ (3.16 - 2.34 \, m) \times \pi \times 0.1778 \, m \times 0.35 \, bar \times \frac{100 \, kPa}{bar}$$

$$+ (3.50 - 3.16 \, m) \, \pi \times 0.1778 \, m \times 0.35 \, bar \times \frac{100 \, kPa}{bar}$$

∴ Q_{shaft_1} = 68.43 kN

▸ Q_{shaft_2} : The friction acting on the length of shaft between the two helices. The length of shaft to be considered is the interhelix spacing, 1.50 m, minus two times the average helix diameter. This accounts for the shadow effect created above the lower helix, and the bearing interference created below the upper helix

$$Q_{shaft_2} = \left[1.50m - 2 \times \left(\frac{0.4572 + 0.5080}{2} \right) \right] \times \pi \times 0.1778m \times 0.35 \, bar \times \frac{100 \, kPa}{bar}$$

$$\therefore Q_{shaft_2} = 10.46 \, kN$$

▶ $Q_{b_1} = k_c \times q_{ca} \times \pi \times \dfrac{(0.5080m^2 - 0.1778m^2)}{4}$

$= 0.45 \times 21.36 \, bar \times \dfrac{100 \, kPa}{bar} \times \pi \times 0.0566 \, m^2$

$\therefore Q_{b_1} = 170.95 \, kN$

▶ $Q_{b_2} = k_c \times q_{ca} \times \pi \left(\dfrac{0.4572m}{4} \right)^2$ ← assumes formation of soil plug in shaft bottom

$= 0.45 \times 25.09 \, bar \times \dfrac{100 \, kPa}{bar} \times \pi \times 0.0523 \, m^2$

$\therefore Q_{b_2} = 185.36 \, kN$

▶ $Q_{ultimate} = Q_{shaft_1} + Q_{shaft_2} + Q_{b_1} + Q_{b_2}$

$= 68.43 + 10.46 + 170.95 + 185.36 \, kN$

$\therefore Q_{ultimate} = \boxed{435 \quad kN}$ ←